NOVEL POWER AMPLIFIER DESIGN USING NON-LINEAR MICROWAVE CHARACTERISATION AND MEASUREMENT TECHNIQUES

A thesis submitted to Cardiff University in candidature for the degree of Doctor of Philosophy

By

OGBOI FRIDAY LAWRENCE, MSc MBA

Centre for High Frequency Engineering
Cardiff School of Engineering
Cardiff University
United Kingdom

SEPTEMBER 2014

DECLARATION OF ORIGINALITY

This work has not previously been accepted in substance for any degree and is not concurrently submitted in candidature for any degree.

Signed …… (Candidate) Date……

STATEMENT 1

This thesis is being submitted in partial fulfilment of the requirements for the Degree of PhD

Signed …… (Candidate) Date……

STATEMENT 2

This thesis is the result of my own independent work/investigation except where otherwise stated. Other sources are acknowledged by explicit references.

Signed …… (Candidate) Date……

STATEMENT 3

I hereby give consent for my thesis, if accepted to be available for photocopying and for inter-library loan, and for the title and summary to be made available to outside organisations.

Signed …… (Candidate) Date……

ACKNOWLEDGEMENTS

First and foremost, I thank God, The Almighty for keeping my family healthy and alive all through my stay and work on this project at the Centre for High Frequency Engineering. I received different kinds of news from home at different times during this period but the good Lord helped me to remain focused and able to concentrate on my project. By the grace of the almighty God, all was well.

I thank Prof. P.J. Tasker, Prof. Johannes Benedikt and Dr. Jonny Lees for their help and support on this very complicated, complex and cutting edge research topic. I thank, Prof. Adrian Porch, Dr. Akmal. M, Dr. Choi. H for their support and encouragement.

Especially, I thank my main supervisor, Prof. Paul Tasker for all his support and excellent advice.

Finally, I thank all the research associates adviser and Dr. Carol Featherstone, all the staff in the workshops, such as Paul Ferrugia, Denley Slade and all the research staff in the research office for the unprecedented support I got from them during the duration of this project. May God bless them and their families. I like to thank the entire staff in the school of engineering research office, they are wonderful people.

I would also like to thank Engineering and Physical Science Research Council (EPSRC) for the financial support. This work would not have been possible without this support. This work is supported by EPSRC (grant EP/F033702/1).

During the period of this project, I have learnt a lot at the Centre for High Frequency Engineering while working in its state of the art laboratories and well knowledgeable research staff. To some other students we have spent learning time together such as Anoor Aldoumani, David Loescher, Zulhazmi Mokhti, Syalwani Kamarudin, Minghao Koh and Timothy Canning, I say thank you for your wonderful time.

More especially, I want to thank my wife, Mrs Chinwe Njideka Ogboi, my brothers and sisters and also my mother Mrs. Victoria Ogboi and my father Mr. Augustine Ogboi.

In addition, I thank all the members of the African Research Hub, such as Kess, Dan, Dr. Margaret Kadiri, and Dr. Akintude Babatunde.

Finally, I want to thank CREE for supplying devices and specifically Simon Wood, Ryan Baker and Ray Pengelly.

ABSTRACT

This thesis, addresses some aspects of the well-known, problem, experienced by designer of radio frequency power amplifiers (RFPA): the efficiency/linearity trade-off. The thesis is focused on finding and documenting solution to linearity problem than can be used to advance the performance of radio frequency (RF) and microwave systems used by the wireless communication industry. The research work, this was undertaken by performing a detailed investigation of the behaviour of transistors, under complex modulation, when subjected to time varying baseband signals at their output terminal: This is what in this thesis will be referred to as "baseband injection". To undertake this study a new approach to the characterisation of non-linear devices (NLD) in the radio frequency (RF) region, such as transistors, designated as device-under-test (DUT), subjected to time varying baseband signals at its output terminal, was implemented. The study was focused on transistors that are used in implementing RF power amplifiers (RFPA) for base station applications. The non-linear device under test (NL-DUT) is a generalisation to include transistors and other non-linear devices under test. Throughout this thesis, transistors will be referred to as 'device' or 'radio frequency power amplifier (RFPA) device'. During baseband injection investigations the device is perturbed by multi-tone modulated RF signals of different complexities. The wireless communication industry is very familiar with these kinds of devices and signals. Also familiar to the industry are the effects that arise when these kind of signal perturb these devices, such as inter-modulation distortion and linearity, power consumption/dissipation and efficiency, spectral re-growth and spectral efficiency, memory effects and trapping effects.

While the concept of using baseband injection to linearize RFPAs is not new the mathematical framework introduced and applied in this work is novel. This novel approach

has provided new insight to this very complex problem and highlighted solutions to how it could be a usable technique in practical amplifiers.

In this thesis a very rigorous and complex investigative mathematical and measurement analysis on RFPA response to applied complex stimulus in a special domain called the envelope domain was conducted. A novel generic formulation that can 'engineer' signal waveforms by using special control keys with which to provide solution to some of the problems highlighted above is presented.

The formulation is based on specific background principles, identified from the result of both mathematical theoretical analysis and detailed experimental device characterisation.

.

LIST OF PUBLICATIONS

1. **Ogboi, F.L**.; Tasker, P.J.; Akmal, M.; Lees, J.; Benedikt, J.; Bensmida, S.; Morris, K.; Beach, M.; McGeehan, J., "**A LSNA configured to perform baseband engineering for device linearity investigations under modulated excitations**," European Microwave Conference (EuMC), 2013 43rd, Nuremberg, Germany vol., no., pp.684,687, 6-10 Oct. 2013

Abstract - A Large Signal Network Analyzer (LSNA) system has been configured to automatically engineer specific baseband voltage waveforms that, when injected into the output of an active device enable novel device linearization investigations. This is achieved using a formulation, generalized in the envelope domain, to describe the required baseband injection voltage. The advantage of this formulation is that it can be used to compute and then engineer the required baseband injection voltage signals, for arbitrary amplitude modulated envelopes, in terms of a limited set of describing coefficients. Using this approach, it is possible to determine the optimum baseband signal coefficients necessary to linearize a 10W Cree GaN HEMT device using baseband injection techniques. The formulation is validated by experimental investigation, using a 3-tone modulated signal, where the optimum output baseband signal for third and fifth order IMD suppression is successfully identified. For the optimum case, the observed level of IM3 and IM5 distortion was reduced to less than -56dBc whilst driving into 1.5 dB of compression.

2. **Ogboi, F.L**.; Tasker, P.J.; Akmal, M.; Lees, J.; Benedikt, J.; Bensmida, S.; Morris, K.; Beach, M.; McGeehan, J., " **A Novel Formulation For Defining Linearising Baseband Injection Signals Of RF Power Amplifier Devices Under Arbitrary**

Modulation," Automated Radio Frequency and Microwave Measurement Society (ARMMS) Conference, The Oxford Belfry, Nr Thame UK, April. 2014

Abstract - A new formulation, in the envelope domain for linearising RF power amplifier devices is demonstrated. By applying this formulation, it is possible to linearise RF power amplifiers by signal injection using a time varying baseband voltage signal. The formulation defines the baseband inter-modulation distortion (IMD) envelope as a function of the input carrier signal envelope. Irrespective of the modulated RF signal, intermodulation distortion envelopes can always be defined as a finite sum of distortion-envelopes multiplied by their control coefficients.

These coefficients are the keys used to optimise the time varying baseband voltage signal. In this formulation, 'engineering' the optimized time-varying baseband voltage signal requires the determination of only a finite number of constant coefficients. This eases the optimization process. This formulation was validated in an open-loop active baseband loadpull exercise on a 3-tone amplitude modulated RF signal. The investigation and validation experiment was performed on a Cree 10W GaN HEMT device, biased into class AB at 1.5 dB of compression. When the optimum linearizing baseband voltage was described, computed, engineered and injected into the device, IM3 and IM5 distortions were simultaneously suppressed for the optimum case to less than -56dBc. An improvement of 42dBc over the reference classical short circuit case.

3. **Ogboi, F.L.**; Tasker, P.J.; Akmal, M.; Lees, J.; Benedikt, J.; Bensmida, S.; Morris, K.; Beach, M.; McGeehan, J., " **Sensitivity of AM/AM Linearizer to AM/PM distortion in Devices**," Automatic Radio Frequency Techniques Group 83rd, ARFTG Conference, Tampa Florida, USA, June 2014

Abstract - Baseband injection is a technique that can provide a cost-effective linearizing solution that can be combined with supply modulation techniques such as envelope tracking (ET), to minimize AM-AM distortion and potentially simplify the DSP linearization requirement and associated cost. Recently [8], a new approach for computing the baseband injection stimulus, formulated in the envelope domain, was introduced. The concept was originally demonstrated using a 10W Cree GaN-on-SiC HFET device. In this work its robustness with respect to alternative device technology is investigated using 25W Nitronex NPTB00025 GaN-on-Si HEMT depletion-mode and a 10W, high-voltage LD-MOS, enhancement-mode devices. Its effectiveness in dealing with AM-AM distortion is confirmed.

4. **Ogboi, F.L**.; Tasker, P.J.; Akmal, M.; Lees, J.; Benedikt, J.; Bensmida, S.; Morris, K.; Beach, M.; McGeehan, J., "**High Bandwidth Investigations of a Baseband Linearization Approach Formulated in the Envelope Domain Under Modulated Stimulus**," 44th, European Microwave Conference (EuMC), 2014 44th, European , Rome, Italy 5-10 Oct. 2014

Abstract - Baseband injection provides a useful approach for use in linearizing power amplifiers. The challenge is the determination of the required baseband signal. In [6] a generalized formulation quantifying the baseband voltage signal, injected at the output bias port, to linearize the device behaviour was introduced. This envelope domain based solution requires the determination of only a small number of linearizing coefficients. More importantly these coefficients should be stimulus, hence bandwidth independent. This property has been experimentally investigated using a 10W Cree GaN HEMT device under a

3-tone modulated stimulus at 1.5dB of compression. It will be shown that the linearization coefficients were invariant when varying the modulation bandwidth from 2MHz to 20MHz.

5. **Ogboi, F.L**.; Tasker, P.J.; Akmal, M.; Lees, J.; Benedikt, J.; Bensmida, S.; Morris, K.; Beach, M.; McGeehan, J., "**Investigation of various envelope complexity linearity under modulated stimulus using a new envelope formulation approach**," Compound Semiconductor Integrated Circuit Symposium (CSICS) Conference, 2014 San-Diego, California, USA, 19-22 Oct. 2014

Abstract - In [1] a new formulation for quantifying the linearizing baseband voltage signal, injected at the output bias port, to linearize a device behaviour was introduced. A key feature of this approach is that since it is formulated in the envelope domain the number of linearization coefficient required is independent of the envelope shape, complexity. This property is validated by performing baseband linearization investigations on a 10W Cree GaN HEMT device. Modulated signals with increasing complexity 3, 5, and 9-tone modulated stimulus, at 1.5dB of compression, were utilized. In all cases just two-linearization coefficients needed to be determined in order to compute the output baseband signal envelope necessary. Intermodulation distortion was reduced to around -50dBc, a value very close to the dynamic range limit of the measurement system.

JOINT PUBLICATIONS

1. Akmal, M.; **Ogboi, F.L**.; Yusoff, Z.; Lees, J.; Carrubba, V.; Choi, H.; Bensmida, S.; Morris, K.; Beach, M.; McGeehan, J.; Benedikt, J.; Tasker, P.J., "**Characterization of electrical memory effects for complex multi-tone excitations using broadband active baseband load-pull**," Microwave Conference (EuMC), 2012 42nd European , vol., no., pp.1265,1268, Oct. 29 2012-Nov. 1 2012

Abstract - This paper focuses on multi-tone characterization of baseband (IF) electrical memory effects and their reduction through the application of complex-signal, active baseband loadpull. This system has been implemented to allow the precise evaluation of intrinsic nonlinearity in high-power microwave devices for wideband applications. The developed active baseband load-pull capability allows a constant, frequency independent baseband load environment to be presented across wide modulation bandwidths, and this capability is important in allowing the effects of baseband impedance variation on the performance of nonlinear microwave devices, when driven by broadband multi-tone stimuli, to be fully understood. The experimental investigations were carried out using a 10 W GaN HEMT device, under 9-carrier complex modulated excitation. These confirmed that presenting a wideband baseband short circuit was essential for maximum ACPR suppression together with the minimization of ACPR asymmetry, confirming the importance of proper termination of baseband frequency components when designing DC bias networks.

LIST OF ACRONYMS

AC	Alternate Current
ACPR	Adjacent Channel Power Ratio
ADC	Analog to Digital Converter
ADS	Advanced Design System
AET	Auxiliary Envelope Tracking
ALG	Algorithm
AM	Amplitude Modulation
APD	Analog Predistortion
APP	A Posteriori Probability
ARFTG	Automatic Radio Frequency Techniques Group
ARMMS	Automatic Radio Frequency and Microwave Measurements Society
AWG	Arbitrary Waveform Generator
AWGN	Additive White Gaussian Noise
BB	Baseband
BE	Baseband Envelope
BEE	Baseband Envelope Engineering
BEL	Baseband Envelope Linearisation
BER	Bit Error Rate
BIE	Baseband Impedance Engineering
BIL	Baseband Impedance Linearisation
BPSK	Binary Phase Shift Keying
CAD	Computer-Aided-Design
CCDF	Complementary Cumulative Distribution Function

CN(0,1)	Complex Gaussian distribution with Zero Mean and Unity Variance
CO_2	Carbon Dioxide
CSA	Communication Signal Analyser
CSI	Channel State Information
CSICS	Compound Semiconductor Integrated Circuit Symposium
CW	Continuous Wave
dB	decibel
dBc	decibel relative to carrier (decibel-carrier, with respect to carrier)
DC	Direct Current
DPD	Digital Predistortion
DSP	Digital Signal Processing
DUT	Device Under Test
EA	Envelope Amplifier
ED	Envelope Detector
EDA	Envelope Domain Analysis
EDGE	Enhanced Data for Global Evolution
EER	Envelope Elimination and Restoration
EL	Envelope Lineariser
EM	Electromagnetic
EMA	Envelope Mathematic Analysis
ESG	Economy Signal Generator
ET	Envelope Tracking
EUMC	European Microwave Conference
EVM	Error Vector Magnitude
FBK	Feedback

FDD	Frequency Division Duplexing
FDM	Frequency Division Multiplex
Fe2O3	Iron Oxide
FEC	Forward Error Correction
FET	Field Effect Transistor
FFT	Fast Fourier Transform
G	Transposition Weighting Matrix
GaAs	Gallium Arsenide
GaN	Gallium Nitride
GHz	Gigahertz
GPIB	General Purpose Instrument Bus
GUI	Graphic User Interface
HBT	Heterojunction Bipolar Transistor
HD	Harmonic Distortion
HEMT	High Electron Mobility Transistor
HFET	Heterojunction Field Effect Transistor
HF	High Frequency
I	Current
IF	Intermediate Frequency
IFFT	Inverse Fast Fourier Transform
IL	Insertion Loss
IM	Inter-Modulation
IMD	Inter-Modulation Distortion
IM3	Third-Order Intermodulation
IM5	Fifth-Order Intermodulation

IMN	Input Matching Network
I&Q	In-phase and Quadrature
ISI	Inter-Symbol Interference
K	Number of Symbols in a Frame
LDMOS	Laterally Diffused Metal Oxide Semiconductor
LF	Low Frequency
LINC	Linear Amplification using Nonlinear Components
LSNA	Large Signal Network Analyser
LTE	Long Term Evolution
LUT	Look Up Table
Mbps	Megabits per Second
MBps	Megabytes per Second
MESFET	Metal Semiconductor FET
MHz	Megahertz
MIMO	Multiple Input Multiple Output
ML	Maximum Likelihood
MLSE	Maximum Likelihood Sequence Estimator
MMSE	Minimum Mean Square Error
MnO	Manganese Oxide
MnZn	Manganese Zinc
MSE	Mean Squared Error
NiO	Nickel Oxide
NiZn	Nickel_Zinc
NMMSE	Normalised Minimum Mean Squared Error
NMSE	Normalised Mean Squared Error

OFDM	Orthogonal frequency-division multiplexing
OFDM A	Orthogonal Frequency Division Multiple Access
OMN	Output Matching Network
PA	Power Amplifier
PAPR	Peak-to-Average-Power-Ratio
PAR	Peak-to-Average Ratio
PBO	Power Back Off
PEP	Peak Envelope Power
P-I	Performance Improvement
PLL	Phase-Locked Loop
PM	Phase Modulation
PSG	Performance Signal Generator
PSK	Phase Shift Keying
Q	Quadrature
QAM	Quadrature Amplitude Modulation
QPSK	Quaternary Phase Shift Keying
RF	Radio Frequency
RFPA	Radio Frequency Power Amplifier
SD	Sphere Decoder
Si	Silicon
SiC	Silicon Carbide
SiGe	Silicon Germanium
SINR	Signal to Interference and Noise Ration
SNR	Signal to Noise Ratio
SOLT	Short Open Load Thru

TETRA	Terrestrial Trunked Radio
TRL	Thru Reflect Line
TRM	Thru Reflect Match
TV	Television
UMB	Ultra Mobile Broadband
UMTS	Universal Mobile Telecommunication System
V	Voltage
VCO	Voltage-Controlled Oscillator
VHF	Very High Frequency
VNA	Vector Network Analyser
VSA	Vector Signal Analyser
WCDMA	Wideband Code Division Multiple Access
WiMAX	Worldwide Interoperability for Microwave Access
WLAN	Wireless Local Area Network
3GPP	Third generation partnership program
3GPP2	Third generation partnership program - 2
4G	Fourth generation mobile communications system
5G	Fifth generation mobile communication system

LIST OF SYMBOLS

α	Distortion Coefficient
β	Linearisation Coefficient
χ_{2n+1}	Iterative Function
†	Hermitian Matrix
h_j	j-th, column of Channel Matrix H
σ^2	Noise Variance
$\hat{s}$	Envelope of s
C	Capacity of a Wireless Channel
det(A)	Determinant of Matrix A
H	N × M Channel Matrix
H^+	Pseudoinverse of Matrix H
H^H	Hermitian of Matrix H
i	Iteration Number
j	Iteration Number
K	Number of Symbols in a Frame
k	Iteration number maximum
l	Iteration number maximum
m	Iteration number maximum
N	Model coefficient matrix
n	Iteration Number
N_0	Noise Power Spectral Density at Reception
R	N × K Matrix of Received Symbols

r	N-Vector of Received Symbols
R_{ss}	M × M Covariance Matrix of
S	M × K Matrix_of_Transmitted_Symbols
#	Conjugate
$\hat{V}_{1,rf}$	Envelope of input voltage signal

TABLE OF CONTENTS

Contents

CHAPTER ONE

INTRODUCTION

1.1 Research Motivation

Radio frequency power amplifier (RFPA) devices such as transistors, are the main fundamental building block of all modern wireless communication systems. In operation these devices can be used in either a non-linear and efficient mode or linear and non-efficient mode. The design of an efficient and linear radio frequency power amplifier (RFPA) is [1], [2], an extremely complex process, and subject of continuous research. Over the years, wireless communication industries have lived with the problem of "trading-off" RFPA efficiency for linearity or vice-versa, thus leading to increasing the overall system power consumption and complexity [6]. Efficient and linear RFPAs are not only required by wireless communication systems, but also in other areas like medicine, aviation, telecommunication and environmental sensors where waste power dissipation impacts on battery life and environmental pollution. For instance, in patient low-power head-injury treatment in medicine, battery power wastage in mobile phones, transmitter power consumption in aviation and general environmental degradation due to heat, which adds to global warming. Hence, it is important that RFPAs are efficient and linear while supporting all communication platforms. However, in real life, this is not the case. RFPA operation [8], is a compromise, a situation where neither the required efficiency nor linearity is achieved. In doing so, the modulated signal complexity must also be considered, such as the bandwidth of the modulation or the number of tones in the modulation. Hence, signal complexity can be

viewed as going from a simple two-tone modulation to “real” communication signals. Key is that certain varying complexity results in signals that have significantly different Peak to Average Power Ratio (PAPR).

Addressing these issues has driven a process of continual modification of existing techniques [4][5][6], including the birth of new techniques or [14] – [25] both. One of these new techniques involves the use of a baseband modulated signal, derived from the RF input signal and fed into the output bias line to linearize the Power Amplifier. This thesis will focus on this approach. In particular the thesis aims to contribute to this area of research by presenting and investigating a more structured approach to formulating and utilizing baseband injection to linearise RFPAs. Central to this investigation is a formulation, described in the envelope domain, to quantifying the required baseband injection signals to linearize the RFPA.

Baseband injection is not a new technique but the presented formulation for quantifying the required baseband injection signal is the novel part of this approach. The utilization of baseband injection offers the possibility of reducing both (RFPA) and associated digital signal processing (DSP) power consumption. This could be particularly useful in emerging small-cell mobile communications network architectures. The approach is based on an improved understanding and hence modelling of the transistor’s non-linear behaviour, achieved via the application and further development of advanced non-linear measurement systems. The results of this research investigation is documented in this thesis.

1.2 Why Linearization is necessary

1.2.1 Distortion

Distortion is the unwanted signal component in the output signal response of RFPA and devices when they respond to different kinds of stimulus.

RF power amplifiers and devices experience distortion in their output signal response when excited by an applied signal at its input port. For this discussion, the input port is considered as port1 (P1) while the output port is considered port2 (P2). When such an excitation is applied and device driven into compression, a complex response is generated by the device. Consider the terminal response of the device, it can be described in either the voltage – current (I-V) domain or the input-output traveling wave (a-b) domain, as shown in figure 1.2.1.1.

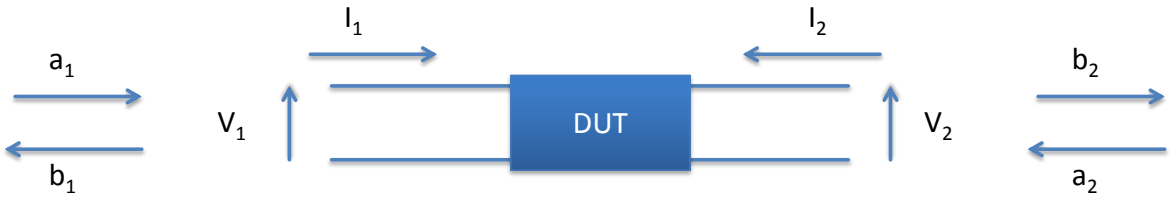

Figure 1.2.1.1 showing a simple model representation of a device with its excitation and response signals.

The (a-b) domain defines the small signal scattering S-Parameters for the two port network as follows:-

$S_{11} = \frac{b_1}{a_1}$ With a_2=0 (1.2.1.1)

Input reflection coefficient with the output port terminated in a matched load Z_L equal to the characteristic impedance Z_0 of the network

$S_{22} = \frac{b_2}{a_2}$ With a_1=0 (1.2.1.2)

Output reflection coefficient with the input port terminated in a matched load Z_{in} equal to the characteristic impedance Z_0 of the network

$S_{21} = \frac{b_2}{a_1}$ With a_2=0 (1.2.1.3)

Forward transmission (insertion) gain with the output port terminated in a matched load Z_L equal to the characteristic impedance Z_0 of the network

$S_{12} = \frac{b_1}{a_2}$ With a_1=0 (1.2.1.4)

Reverse transmission (insertion) gain with the input port terminated in a matched load Z_{in} equal to the characteristic impedance Z_0 of the network. Conjugately matched for maximum power.

And the characteristic impedance of the network Z_0 defined as

$Z_0 = \sqrt{Z_L Z_{in}^*}$ (1.2.1.5)

If the system is linear, the output signal (b_2 or I_2) should only be a scaled version of the input signal (a_1 or V_1) ignoring phase shift at this time. This is shown in figure 1.2.1.2 and figure 1.2.1.3 respectively. If the system is non-linear, the resulting output response signal is usually a scaled and distorted version of the input signal. This can be represented in figure 1.2.1.4. In this state a number of parameters affect the level of distortion such as temperature, input signal drive level, complexity of input signal, number of signals and the device operating point.

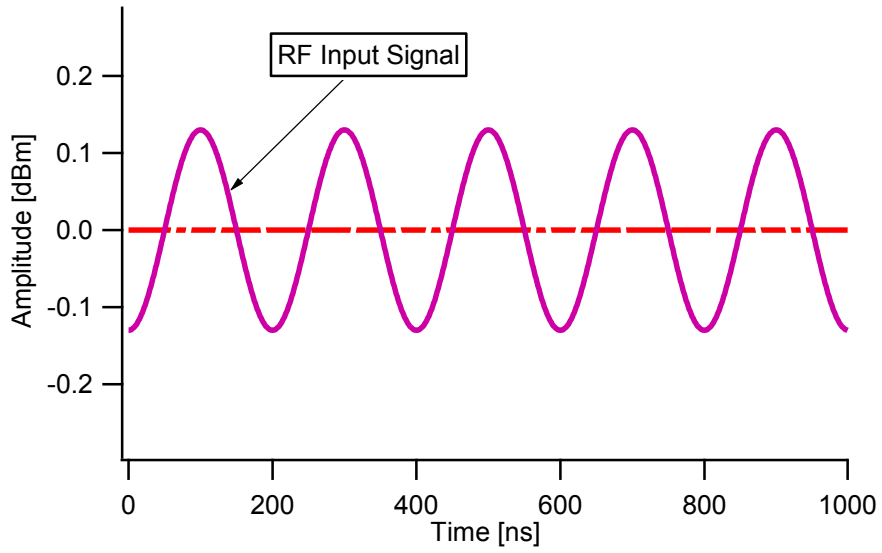

Figure 1.2.1.2 showing RF excitation signal (applied stimulus)

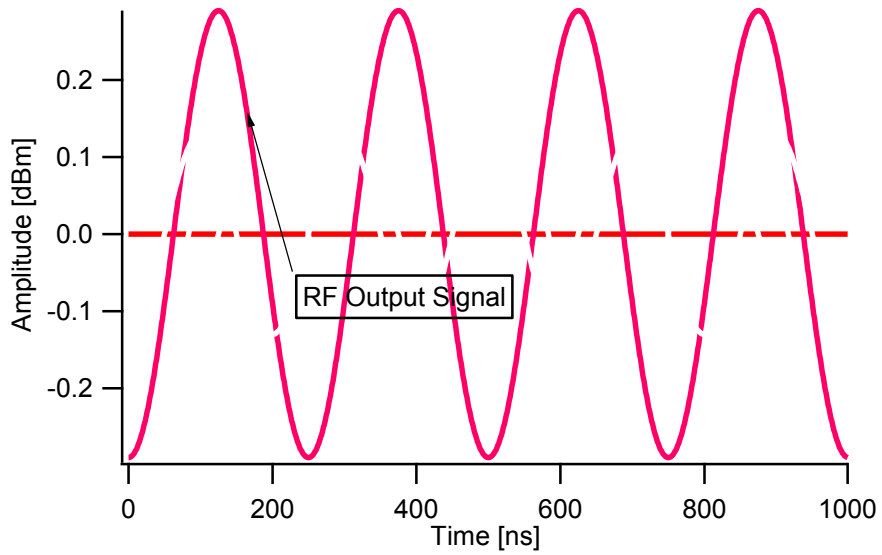

Figure 1.2.1.3 showing device amplified and un-distorted response to applied stimulus.

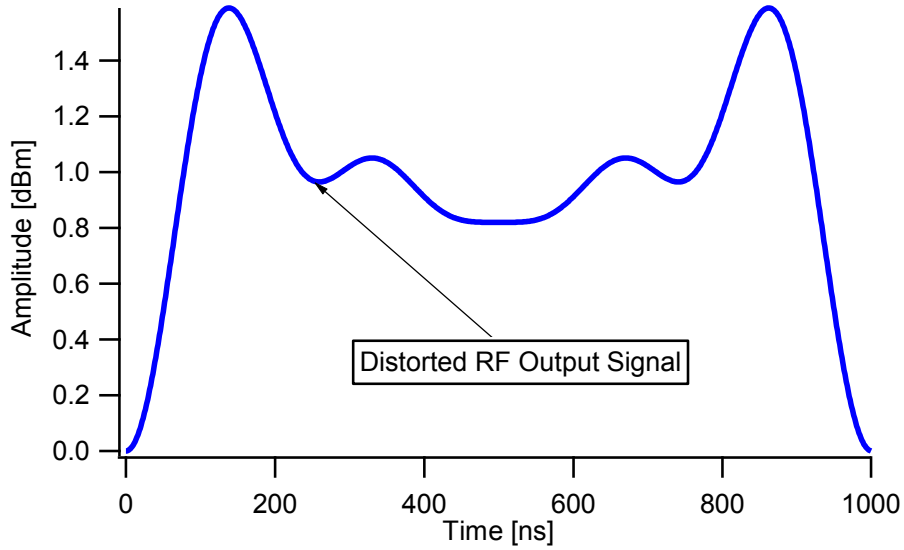

Figure 1.2.1.4 showing device amplified and distorted response to applied stimulus

1.3 Types of Distortion

Distortion can be broadly classified into two types. They are inter-modulation distortion (IMD) and harmonic distortion (HD).

1.3.1 Inter-modulation distortion (IMD)

Inter-modulation distortion (IMD) is very important in communication systems since it produces distortion at and around the carrier-band. It can be defined as the non-linear

contribution to the output signal that was originally not present in the input signal but shares the same frequency-band as the ideal and undistorted output signal [9]. Getting rid of this kind of component of distortion by filtering can be difficult because of its position in respect to the signal of interest and hence other means of removal have to be sought. One figure of merit for measuring this kind of distortion is to measure the level of distortion occurring very close to the carrier fundamental frequency of interest. This is called the inter-modulation distortion (IMD). The main focus of this research is to propose a solution for suppressing/eliminating IMD.

Of the IMD's terms, the most disturbing to the device and the communication channel are the third (IM3) and fifth (IM5) order intermodulation distortions terms [33]. Their elimination for instance, will reduce the impact of those distortions occurring within the main carriers usually quantified by EVM (error vector magnitude). Hence it is essential to eliminate IMD. Generally speaking, all distortion types are vector components. This means they exhibit both amplitude and phase distortion components.

a). AM/AM distortion

The unwanted amplitude modulation (AM) distortion, of the modulated output RF carrier envelope, caused by the conversion of the amplitude of the modulated input RF carrier envelope as a result of the gain of the RFPA or device, is called amplitude modulation – amplitude modulation distortion (AM/AM distortion) [34– 44]

b). AM/PM distortion

The unwanted phase modulation (PM) distortion of the modulated output RF carrier envelope, caused by the conversion of the amplitude/phase of the modulated input RF carrier envelope as a result of the gain of the RFPA or device, is called amplitude modulation - phase modulation distortion (AM/PM distortion) [45] – [52].

Quantifying the AM/AM and AM/PM is a basic way of characterizing an RFPA's non-linear behavior. The AM/AM and AM/PM non-linear behavior of any RFPA can be measured, calculated and represented in plots in many ways [53] – [54]. One such representation of a measured sample is shown in figure 1.3.1 (a) and (b) using a 3 tone input signal with the device output response in an undistorted state usually referred to as linear state.

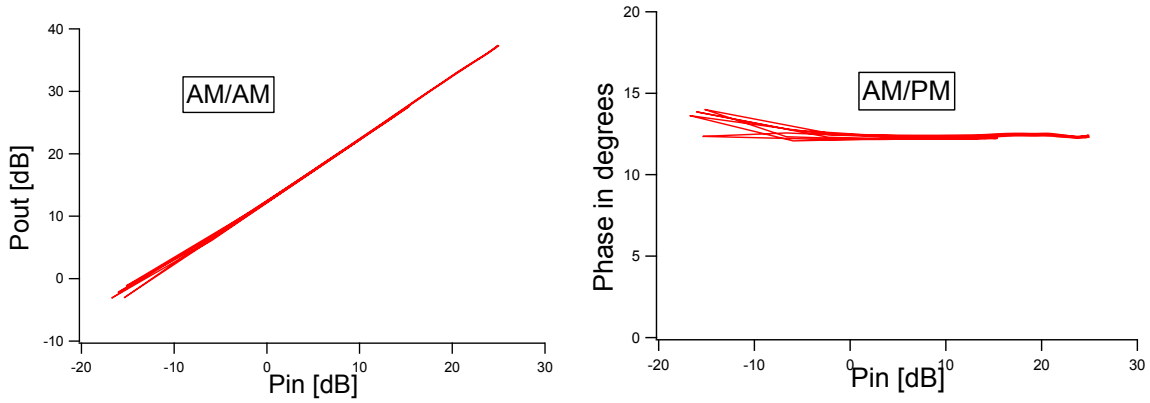

(a). Measured AM/AM curve (b). Measured AM/PM curve

Figure 1.3.1 Showing measured AM/AM and AM/PM curves of a 3tone excitation of a linear system.

Other ways of representing these include the envelope dynamic transfer characteristics. This is shown in subsequent chapters of this thesis.

From these plots, it is possible to describe the linearity behavior of the measured device. The focus of this work is to investigate the linearity behavior of RFPA devices using baseband envelope linearization.

1.3.2 Harmonic distortion (HD)

This has components that occur at the harmonics of the fundamental carrier frequency and hence called harmonic distortion (HD). Since HD occurs at the harmonics of the fundamental frequency, they can and are usually removed by filtering. This is because they

are far from the frequency of interest and filters can be designed that will have good cut-off frequencies to be able to remove HD components.

1.4 Role of baseband linearization

(a). Definition of Baseband Linearization:- A linearization technique that utilizes the even order non-linearities generated by a transistor in its output current to generate additional (ideally cancelling), in-band intermodulation distortion, to cancel the odd-order non-linearities generated by the same transistor in its resulting output current. This means: - that the **baseband** (**DC**) formed by the even order non-linearities is used to cancel the distortion around the carrier formed by the odd order non-linearities generated by the same device. This concept is shown in the Figure 1.4.

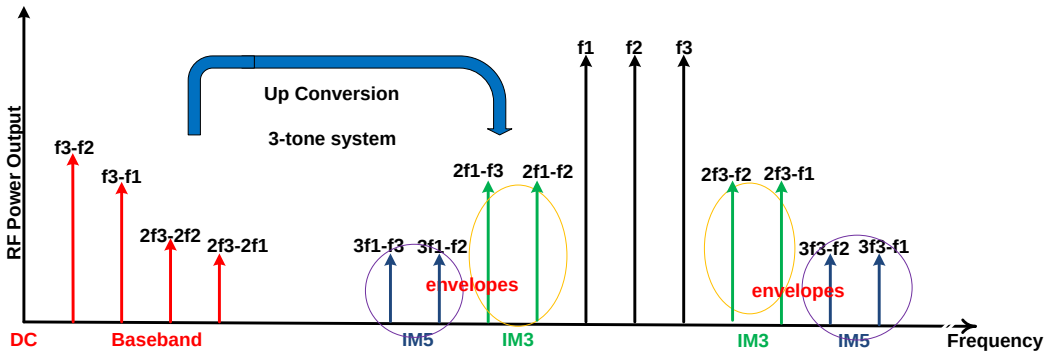

Figure 1.4 Showing the basic concept of baseband linearization principle.

Baseband injection is a technique that can provide a cost-effective linearizing solution that can be combined with supply modulation techniques such as envelope tracking (ET), to minimize AM/AM distortion and potentially simplify the Digital Signal Processing (DSP) linearization cost requirement associated with digital pre-distortion (DPD).

Typically, RFPAs are linearized using digital pre-distortion (DPD). Any technique that can help reduce DPD complexity could lead to reduction in its power consumption. Such a technique can help DPD power consumption to scale-down even as device RF power scales-

down. This will be potentially useful in small cell base stations. Secondly, DPD is a process that occurs at the PA input port hence input signal remodulation and increased PAPR. This will increase both the input bandwidth requirement of the linearizer and the device. A technique whose focus is to reduce the complexity of the performance improvement signal such as the one used to pre-distort (DPD) the device input port will lead to reduced input signal bandwidth expansion and also indirectly improve PA spectral efficiency. Thirdly, DPD can be combined with very linearly efficient technology that can help in its power scale-down. Fourthly, improving device linearity while satisfying the three points listed above will go a long way in improving design techniques. Lastly, investing in a technique compatible with emerging architectures is the bedrock of pure scientific engineering. This means improvement does not mean discarding already existing entire infrastructure or architecture. The advantage of this is cost reduction. Baseband injection is one such technique. The technique introduced and researched in this thesis is based on baseband and injection satisfies these 5 important points.

1.4.1 Problem definition: - The AM/AM distortion component exhibited by RFPA devices in their non-linear state needs to be suppressed to improve their linearity performance. A novel linearization technique based on baseband envelope mathematics and measurements need to be formed and then used to suppress AM/AM distortion.

1.4.2 Research Objective: - The novel technique should be able to suppress AM/AM distortion when using input signals of different complexities and devices of different technologies. Possible integration with existing and emerging linearization techniques should be considered.

1.5 Advanced utilization of non-linear microwave characterisation and measurement techniques

1.5.1 Formulation: in this thesis refer to a special, mathematically formed baseband envelope signal voltage, formed in the envelope domain. This baseband signal, controlled by a set of coefficients which are used to 'shape' (engineer) it is injected into an active device output port. The aim is to use the engineered baseband signal to suppress the distortion present in the device output response to an applied input stimulus. This process is called 'linearization'. The process of using this so formed baseband signal to linearize the device output response is called **baseband envelope linearization** (**BEL**). The solution documented in this thesis is as a result of the investigation carried out when BEL was used to linearize real active devices output response.

BEL was the result of responding to the research objective in this chapter, by carrying out a very detailed analysis of the response of an RFPA device to a specially and specifically formulated baseband injection signal when subjected to both previously and presently applied stimulus in a special domain called the envelope domain. The detailed investigation of the response of RFPA devices to various applied input stimulus using this new formulation was undertaken in the following steps;

- Build and test a measurement system to measure and work with the specific formulation
- Test of the formulation was required and to know how the formulation works
- Application of the formulation to envelope complexity
- Application of the formulation to frequency complexity
- Application of the formulation for device technology complexity
- Application of formulation for verification of a-priori knowledge

The formulation was found to function successfully in each case of its test and application. This thesis is documented evidence of the intensive investigation of this technique.

1.6 Principle of baseband linearisation

It takes a mathematical approach in the envelope domain, based on a certain background principle.

1.6.1 Principle which states that:-

The transistor (RFPA) even-order non-linearities, present in its output current, can be used to generate additional ideally cancelling, in-band inter-modulation distortion used to suppress the odd-order inter-modulation distortion in its resulting output current.

It was experimentally observed that when the ***RFPA input and output signals are studied and compared in the envelope domain, a quasi-static-relationship is observed such that any IMD current waveform envelope*** (IMD_k) ***can be defined as a function of the modulated input RF signal voltage waveform envelope and hence, its linearizing baseband signal can also be defined in terms of the same input RF signal voltage waveform envelope.***

A distortion environment is created in a RFPA device when the device is driven into compression. When this happens, the device generates a lot of mixing terms in its response to the applied stimulus. The terms so generated are a result of the non-linear behaviour of the device. These terms are called – mixing terms. The level of compression determines how many mixing terms are generated. In a severe distortion environment, such as having the RFPA device driven deep into compression, more mixing terms are generated, and more distortion contributions are formed. These distortion contributions are called distortion components.

The distortion components add-up both constructively and destructively causing ensemble of distortion signal envelopes. This will lead to a more distorted signal around the fundamental

frequency of interest. By defining the linearizing baseband envelope as a function of the input signal envelope, it becomes possible to cause suppression/elimination of these distortions. To achieve this it is important to correctly 'engineer' the required output baseband signal voltage waveform envelope to be injected into the device output port.

When this was carried out, it was possible to carry out novel investigations, results were collected and scientific deduction and conclusions were drawn. The knowledge so gathered was then applied to re-build/modify (software and hardware) an existing envelope measurement system to enable it to work with this baseband envelope lnearisation.

The remaining part of this thesis demonstrates the efficiency of this technique, measurements, findings and conclusions.

1.7 How this thesis is arranged

The investigation and application of BEL to device characterisation and measurements documented in this thesis involves sectioning this thesis into seven chapters. Each thesis chapter explores the motivation and objective of this work.

Chapter 1

This chapter explains the motivation for this present (new) research work. It gives an introduction to the problem that needs to be solved. It gives background knowledge into the problem and introduces some concepts and standards that this research work considered in solving the problem. It introduces the basic principle guiding the solution and why the research was necessary. It sets the framework for the research.

Chapter 2

This chapter reviews literature that have relevance to this research work. It compares this (new) work to previous and published work and draws attention to the similarities and

differences between this work and previous work. It further explain what is different between what has been (previous) done and present work. It then summarises the chapter.

Chapter 3

This chapter is the core part of this research work. It explains in detail the work called the baseband envelope linearization (BEL) which is the major work in this thesis. It explains what this research achieved. It also show the various mathematical relations between the parameters (voltage, current and IMD) used in this work and concludes with a summary. It shows the detail concept of envelope domain and analysis.

Chapter 4

This chapter deals with the verification experiment of BEL with complex modulation (3-tone multi-tone modulation). It shows the basic application of the novel technique in detail and the results achieved. It also shows the investigation that was carried out using this technique on this modulation type and the knowledge gained. It then summarises the chapter in a forward looking note to the various applications of the technique that have been developed.

Chapter 5

This chapter is the application of BEL.

It is divided into two sections. A section that deals with the application of the technique to wide bandwidth and a section that deal with more complex modulation than the one used in chapter 4. This was done by increasing the number of excitation tones in the modulation of the excitation signal with a bandwidth from 2MHz to 20MHz. This part is called ‘section one’ of the chapter. The second section of the chapter, deals with the application BEL to excitation signal complexity by variation of peak-to-average-power-ratio (PAPR) of the excitation signal. The reason for this is that in real-life, signals are complex and in their complexity, they exhibit varying peak-to-average-power (PAPR) which was emulated by varying the number of tones in the modulation and varying bandwidth.

Chapter 6

This chapter investigates additional knowledge gained from the research and how this knowledge can be used in combination with other techniques and what can be gained from such integration when applied to future systems.

It also looks at the limitations of the novel technique.

Chapter 7

This chapter gives the conclusion and offer potential future paths for the developments of BEL and suggest its possible future application It also concludes the thesis.

1.8 Contribution

The goal was to investigate a solution that can be applied to RFPA devices for the purpose of improving their performance. The approach taken is supported by detailed measurements on a real RFPA device. It will address the issue of minimizing intermodulation distortion using baseband injection, but formulated in the way that has not been previously experimentally investigated. The idea was to realise an approach that can be both easily integrated into existing infrastructures and be compatible with emerging architectures. The goal was to find out the mathematical relationship between the device response when a complex signal is applied to RFPA devices and the baseband injected signal. Both considered in the envelope domain. This was undertaken experimentally by performing measurements to achieve a deeper understanding of RFPA devices responses. It was required to:-

Build and test a measurement system to measure found formulation

Test of formulation required and how formulation works

Application of formulation to envelope complexity

Application of formulation to frequency complexity

Application of formulation for technology independence

Application of formulation for verification of a priori knowledge

Each of the above project steps have been published and presented in a conference.

For this project, the input main signal types chosen for investigating this formulation include.

Main multi-tone modulation:-

2-tone modulation with peak-to-average power ration (PAPR) of 3dB

3-tone modulation with peak-to-average power ratio (PAPR) of 4.77dB

5-tone modulation with peak-to-average power ratio (PAPR) of 6.99dB

9-tone modulation with peak-to-average power ratio (PAPR) of 9.54dB

Other additional measured signal types (Appendix E, pg., 205)

11-tone modulation with peak-to-average power ratio (PAPR) of 10.41dB

13-tone modulation with peak-to-average power ratio (PAPR) of 11.14dB

17-tone modulation with peak-to-average power ratio (PAPR) of 12.3dB

For all the modulation types, the RF carrier signal was centred at 2GHz.

The modulation bandwidth investigated was between 2MHz to 20MHz in steps of 2MHz. For all the devices used, the compression level was between 1.5dB compression and 2.5dB compression and the peak-envelope-power (PEP) ranged between approximately 38dBm and 40dBm. The level of distortion to be studied was up to the 5th order (IM3 and IM5).

To be able to carry out this research the “port of operation” on the device was considered. The technique is an output port injection technique. This means that the technique will cause the drain bias to modulate. To support such drain supply voltage modulation, due to signal injection on its output bias port, a power device that can accommodate a high breakdown voltage is required. This device property is basically found in RFPA devices with a technology based on wide-band-gap semiconductors from elements found in group III and V of the periodic table such as Gallium (Ga), Aluminium (Al), and Nitrogen (N). These include GaN-on-Si, (Gallium Nitride on Silicon) [30], [31], [32], GaN-on-SiC (Gallium Nitride on

Silicon Carbide). Silicon Carbide (SiC) [28], [29], has high breakdown voltage and GaN exhibit high gain, when combined with SiC, the result is a high power, high frequency, high breakdown voltage and thermal friendly device that can be used with architectures that support supply modulation experiments. Hence, devices used were GaN-on-Si, GaN-on-SiC and Silicon (Si) devices.

Class AB was chosen for the power amplifier device because of its flexibility to maintain linearity even as the drain supply voltage modulates.

Choice of 3-tone starting base modulation. Although, a 2-tone measurement was also carried out, 3-tones modulation was chosen as base modulation from which higher number of tone modulations was measured because of the ability to vary peak-to-average-power ratio (PAPR) and hence modulation of up to 17-tones was measured.

Results of the measurements were documented and very important conclusions were drawn from the results.

The conclusions address solutions to some of the well-known problem of the wireless communication industry such as spectrum efficiency, linearity improvement and power efficiency.

1.9 References

[1] Raab, F.H., "High-efficiency linear amplification by dynamic load modulation," *Microwave Symposium Digest, 2003 IEEE MTT-S International* , vol.3, no., pp.1717,1720 vol.3,8-13June2003doi:10.1109/MWSYM.2003.1210470.

[2] Parsons, K.J.; Wilkinson, R.J.; Kenington, P.B., "A highly-efficient linear amplifier for satellite and cellular applications,"*GlobalTelecommunicationsConference,1995. GLOBECOM'95.,IEEE*,vol.1,no.,pp.203,207vol.1,14-16Nov1995 doi: 10.1109/GLOCOM.1995.500352. Available online, accessed 07th, July, 2014

[3] Wilkinson, R.J.; Kenington, P.B.; Marvill, J. D., "Power amplification techniques for linear TDMA base stations," Global Telecommunications Conference, 1992. Conference Record., GLOBECOM '92. Communication for Global Users., IEEE , vol., no., pp.74,78 vol.1, 6-9 Dec 1992 doi: 10.1109/GLOCOM.1992.276516.

[4] Raab, F.H.; Asbeck, P.; Cripps, S.; Kenington, P.B.; Popovic, Z.B.; Pothecary, N.; Sevic, J.F.; Sokal, N.O., "Power amplifiers and transmitters for RF and microwave," Microwave Theory and Techniques, IEEE Transactions on , vol.50, no.3, pp.814,826, Mar 2002 doi: 10.1109/22.989965.

[5] Kenington, P.B., "Electronic tracking systems for space communications," *Electronics & Communication Engineering Journal* , vol.2, no.3, pp.95,101, Jun 1990.

[6] Kenington, P.B.; Astier, L., "Power consumption of A/D converters for software radio applications," *Vehicular Technology, IEEE Transactions on* , vol.49, no.2, pp.643,650, Mar 2000 doi: 10.1109/25.832996.

[7] Parsons, K.J.; Kenington, P.B.; McGeehan, J.P., "EFFICIENT LINEARISATION OF RF POWER AMPLIFIERS FOR WIDEBAND APPLICATIONS," *Linear RF Amplifiers and Transmitters,IEEColloquiumon*,vol.,no.,pp.7/1,,11Apr1994.

[8] Bennett, D.W.; Kenington, P.B.; Wilkinson, R. J., "Distortion effects of multicarrier envelope limiting," Communications, IEE Proceedings- , vol.144, no.5, pp.349,356, Oct 1997, doi: 10.1049/ip-com:19971502.

[9] Larson, L.; Kimball, D.; Asbeck, P.; Draxler, P.; Junxiong Deng; Ming Li, "Digital predistortion techniques for linearized power amplifiers," Microwave Conference, 2006. APMC 2006. Asia-Pacific , vol., no., pp.1048,1051, 12-15 Dec. 2006 doi: 10.1109/APMC.2006.4429590.

[10] Draxler, P.; Deng, J.; Kimball, D.; Langmore, I; Asbeck, P.M., "Memory effect evaluation and predistortion of power amplifiers," Microwave Symposium Digest, 2005 IEEE MTT-S International , vol., no., pp.4 pp.,, 12-17 June 2005 doi: 10.1109/MWSYM.2005.1516993.

[11] Jinseong Jeong; Kimball, D.F.; Myoungbo Kwak; Chin Hsia; Draxler, P.; Asbeck, P.M., "Modeling and Design of RF Amplifiers for Envelope Tracking WCDMA Base-Station Applications," Microwave Theory and Techniques, IEEE Transactions on , vol.57, no.9, pp.2148,2159, Sept. 2009 doi: 10.1109/TMTT.2009.2027075.

[12] Grotzbach, Manfred; Draxler, B., "Effect of DC ripple and commutation on the line harmonics of current-controlled AC/DC converters," Industry Applications, IEEE Transactions on , vol.29, no.5, pp.997,1005, Sep/Oct 1993 doi: 10.1109/28.245725

[13] Draxler, M.; Biermann, T.; Karl, H.; Kellerer, W., "Cooperating base station set selection and network reconfiguration in limited backhaul networks," *Personal Indoor and Mobile Radio Communications (PIMRC), 2012 IEEE 23rd International Symposium;on*,vol.,no.,pp.1383,1389,9-12Sept.2012doi: 10.1109/PIMRC.2012.6362563.

[14] Shastry, P.N.; Ibrahim, AS., "Design Guidelines for a Novel Tapered Drain Line Distributed Power Amplifier," *Microwave Conference, 2006. 36th European* , vol., no., pp.1274,1277,10-15Sept.2006doi: 10.1109/EUMC.2006.281228.

[15] Rong Zeng; Tao Cao; YouJiang Liu; Jie Zhou, "A novel design technique of Doherty power amplifier," Microwave Conference Proceedings (CJMW), 2011 China-Japan Joint , vol., no., pp.1,3, 20-22 April 2011.

[16] Kuran, S.; Huang, C.-W.P.; Xu, S., "A novel integrated design simulation method for linear cellular and WLAN power amplifiers," *Electronics, Circuits and Systems, 2003. ICECS 2003. Proceedings of the 2003 10th IEEE International Conference on* , vol.3, no., pp.1256,1259Vol.3,14-17Dec.2003doi: 10.1109/ICECS.2003.1301742.

[17] Rui Ma; Kompa, G.; Bangert, A, "A novel concept for first-pass design of RF Power amplifiers for wireless communications," *Wireless Technology and Applications (ISWTA),2011IEEESymposiumon*,vol.,no.,pp.13,16,25-28Sept.2011
doi: 10.1109/ISWTA.2011.6089542.

[18] Winslow, T.A, "A novel in-situ impedance probing method for multistage power amplifier analysis and design," *Microwave Conference (EuMC), 2010 European* , vol., no., pp.1150,1153, 28-30 Sept. 2010.

[19] Jangheon Kim; Junghwan Moon; Jungjoon Kim; Boumaiza, S.; Kim, Bumman, "A novel design method of highly efficient saturated power amplifier based on self-generated harmonic currents," *Microwave Conference, 2009. EuMC 2009. European* , vol., no., pp.1082,1085, Sept. 29 2009-Oct. 1 2009.

[20] Maziere, C.; Reveyrand, T.; Mons, S.; Barataud, D.; Nebus, J. M.; Quere, R.; Mallet, A; Lapierre, L.; Sombrin, J., "A novel behavioural model of power amplifier based on a dynamic envelope gain approach for the system level simulation and design,"

Microwave Symposium Digest, 2003 IEEE MTT-S International , vol.2, no., pp.769,772 vol.2, 8-13 June 2003 doi: 10.1109/MWSYM.2003.1212484.

[21] Cha, Yong-Sung; Kang, Byeong-Gwon; Kim, Young-Tae; Kim, Sun-Hyeong; Jun-Seok Park; Lim, Jae-Bong, "A New Design Method for Performance Improvement of High Power Amplifier by Using the Matching Circuit of Defected Ground Structure," *Microwave Conference, 2003. 33rd European* , vol., no., pp.1341,1344, Oct. 2003 doi: 10.1109/EUMA.2003.340868.

[22] Lian, J.; Roblin, P.; Pla, Jaime, "Novel B-spline behavioural model extracted and verified using vectorial harmonic and multitone data," *ARFTG Microwave Measurements Conference, 2003. Fall 2003. 62nd* , vol., no., pp.291,300, 4-5 Dec. 2003, doi: 10.1109/ARFTGF.2003.1459793.

[23] Haitao Zhang; Huai Gao; Yintat Ma; Forbes, A; Pavio, R.; Guann-Pyng Li, "A Novel High Efficiency and Linearity Power Amplifier with Over-Voltage Protection," *Microwave Symposium, 2007. IEEE/MTT-S International* , vol., no., pp.147,150, 3-8 June,2007, doi: 10.1109/MWSYM.2007.380311.

[24] Dennler, P.; Quay, R.; Ambacher, O., "Novel semi-reactively-matched multistage broadband power amplifier architecture for monolithic ICs in GaN technology," *Microwave Symposium Digest (IMS), 2013 IEEE MTT-S International* , vol., no., pp.1,4,2-7June,2013 doi: 10.1109/MWSYM.2013.6697403.

[25] Sewiolo, B.; Waldmann, B.; Fischer, G.; Weigel, R., "A novel cascode power matching approach for high efficiency tapered traveling wave power amplifiers in SiGe BiCMOS," Ultra-Wideband, 2009. ICUWB 2009. IEEE International Conference on , vol., no., pp.98,101, 9-11 Sept. 2009 doi: 10.1109/ICUWB.2009.5288710.

[26] Shameli, A; Safarian, A; Rofougaran, A; Rofougaran, M.; De Flaviis, F., "A Novel DAC Based Switching Power Amplifier for Polar Transmitter," *Custom Integrated Circuits Conference, 2006. CICC '06. IEEE* , vol., no., pp.137,140, 10-13 Sept. 2006 doi: 10.1109/CICC.2006.320851.

[27] Meshkin, R.; Saberkari, A; Niaboli-Guilani, M., "A novel 2.4 GHz CMOS class-E power amplifier with efficient power control for wireless communications," Electronics, Circuits, and Systems (ICECS), 2010 17th IEEE International Conference on , vol., no., pp.599,602, 12-15 Dec. 2010, doi: 10.1109/ICECS.2010.5724583.

[28] Ikeda, N.; Kaya, S.; Jiang Li; Sato, Y.; Kato, S.; Yoshida, S., "High power AlGaN/GaN HFET with a high breakdown voltage of over 1.8 kV on 4 inch Si substrates and the suppression of current collapse," Power Semiconductor Devices and IC's, 2008. ISPSD '08. 20th International Symposium on , vol., no., pp.287,290, 18-22 May 2008, doi: 10.1109/ISPSD.2008.4538955.

[29] Pengelly, R.S.; Wood, S.M.; Milligan, J.W.; Sheppard, S.T.; Pribble, W.L., "A Review of GaN on SiC High Electron-Mobility Power Transistors and MMICs," Microwave Theory and Techniques, IEEE Transactions on , vol.60, no.6, pp.1764,1783, June 2012, doi: 10.1109/TMTT.2012.2187535.

[30] Marcon, D.; Viaene, J.; Vanaverbeke, F.; Kang, X.; Lenci, S.; Stoffels, S.; Venegas, R.; Srivastava, P.; Decoutere, S., "GAN-on-Si HEMTs for 50V RF applications," Microwave Integrated Circuits Conference (EuMIC), 2012 7th European , vol., no., pp.325,328, 29-30 Oct. 2012.

[31] Germain, M.; Derluyn, J.; Van Hove, M.; Medjdoub, F.; Das, J.; Cheng, S.D.K.; Leys, M.; Visalli, D.; Marcon, D.; Geens, K.; Viaene, J.; Sijmus, B.; Decoutere, S.; Cartuyvels, R.; Borghs, G., "GaN-on-Si power field effect transistors," VLSI

Technology Systems and Applications (VLSI-TSA), 2010 International Symposium on , vol., no., pp.171,172, 26-28 April 2010, doi: 10.1109/VTSA.2010.5488899.

[32] Takenaka, I; Ishikura, K.; Asano, K.; Takahashi, S.; Murase, Y.; Ando, Y.; Takahashi, H.; Sasaoka, C., "High-Efficiency and High-Power Microwave Amplifier Using GaN-on-Si FET With Improved High-Temperature Operation Characteristics," Microwave Theory and Techniques, IEEE Transactions on , vol.62, no.3, pp.502,512, March 2014 doi: 10.1109/TMTT.2014.2298381

[33] Chunming Liu; Heng Xiao; Qiang Wu; Fu Li; Tam, K.W., "Nonlinear distortion analysis of RF power amplifiers for wireless signals," Signal Processing, 2002 6th International Conference on , vol.2, no., pp.1282,1285 vol.2, 26-30 Aug. 2002 doi: 10.1109/ICOSP.2002.1180026.

[34] Cotimos Nunes, L.; Cabral, P.M.; Pedro, J.C., "AM/AM and AM/PM Distortion Generation Mechanisms in Si LDMOS and GaN HEMT Based RF Power Amplifiers," Microwave Theory and Techniques, IEEE Transactions on , vol.62, no.4, pp.799,809, April 2014, doi: 10.1109/TMTT.2014.2305806.

[35] Cabral, P.M.; Pedro, J.C.; Carvalho, N.B., "Dynamic AM-AM and AM-PM behavior in microwave PA circuits," Microwave Conference Proceedings, 2005. APMC 2005. Asia-Pacific Conference Proceedings , vol.4, no., pp.4 pp.,, 4-7 Dec. 2005 doi: 10.1109/APMC.2005.1606809.

[36] Nunes, L.C.; Cabral, P.M.; Pedro, J.C., "AM/PM distortion in GaN Doherty power amplifiers," Microwave Symposium (IMS), 2014 IEEE MTT-S International , vol., no., pp.1,4, 1-6 June 2014, doi: 10.1109/MWSYM.2014.6848333.

[37] Lavrador, P.; Cunha, T.R.; Cabral, P.; Pedro, J.C., "The Linearity-Efficiency Compromise," Microwave Magazine, IEEE , vol.11, no.5, pp.44,58, Aug. 2010 doi: 10.1109/MMM.2010.937100.

[38] Cabral, P.M.; Pedro, J.C.; Carvalho, N.B., "Bias Networks Impact on the Dynamic AM/AM Contours in Microwave Power Amplifiers," *Integrated Nonlinear Microwave and Millimeter-Wave Circuits, 2006 International Workshop on* , vol., no., pp.38,41, 30-31 Jan. 2006, doi: 10.1109/INMMIC.2006.283503.

[39] Marante, R.; Garciá, J.A; Cabria, L.; Aballo, T.; Cabral, P.M.; Pedro, J.C., "Nonlinear characterization techniques for improving accuracy of GaN HEMT model predictions in RF power amplifiers," Microwave Symposium Digest (MTT), 2010 IEEE MTT-S International , vol., no., pp.1680,1683, 23-28 May 2010, doi: 10.1109/MWSYM.2010.5517652.

[40] Pedro, J.C.; Martins, J.P.; Cabral, P.M., "New method for phase characterization of nonlinear distortion products," Microwave Symposium Digest, 2005 IEEE MTT-S International , vol., no., pp.4 pp.,, 12-17 June 2005, doi: 10.1109/MWSYM.2005.1516789.

[41] Marante, R.; Garcia, J.A; Cabral, P.M.; Pedro, J.C., "Impact of Ron(VDD) dependence on polar transmitter residual distortion," Integrated Nonlinear Microwave and Millimetre-Wave Circuits, 2008. INMMIC 2008. Workshop on , vol., no., pp.123,126, 24-25 Nov. 2008, doi: 10.1109/INMMIC.2008.4745732.

[42] Nunes, L.C.; Cabral, P.M.; Pedro, J.C., "A physical model of power amplifiers AM/AM and AM/PM distortions and their internal relationship," Microwave Symposium Digest (IMS), 2013 IEEE MTT-S International , vol., no., pp.1,4, 2-7 June 2013, doi: 10.1109/MWSYM.2013.6697497.

[43] Cabral, P.M.; Cabria, L.; Garcia, J.A; Pedro, J.C., "Polar transmitter architecture used in a Software Defined Radio context," RF Front-ends for Software Defined and Cognitive Radio Solutions (IMWS), 2010 IEEE International Microwave Workshop Series on , vol., no., pp.1,4, 22-23 Feb. 2010, doi: 10.1109/IMWS.2010.5440965.

[44] Pedro, J.C.; Garcia, J.A; Cabral, P.M., "Nonlinear Distortion Analysis of Polar Transmitters," Microwave Theory and Techniques, IEEE Transactions on , vol.55, no.12, pp.2757,2765, Dec. 2007,doi: 10.1109/TMTT.2007.909145.

[45] Ciccognani, W.; Colantonio, P.; Giannini, F.; Limiti, E.; Rossi, M., "AM/AM and AM/PM power amplifier characterisation technique," *Microwaves, Radar and Wireless Communications, 2004. MIKON-2004. 15th International Conference on* , vol.2, no., pp.678,681 Vol.2, 17-19 May 2004, doi: 10.1109/MIKON.2004.1357126.

[46] Zhiwen Zhu; Xinping Huang; Caron, M.; Leung, H., "A Blind AM/PM Estimation Method for Power Amplifier Linearization," *Signal Processing Letters, IEEE* , vol.20, no.11, pp.1042,1045, Nov. 2013, doi: 10.1109/LSP.2013.2280394. Available online, accessed 07th, July, 2014.

[47] Cunha, T.R.; Cabral, P.M.; Nunes, L.C., "Characterizing power amplifier static AM/PM with spectrum analyzer measurements," *Multi-Conference on Systems, Signals & Devices (SSD), 2014 11th International* , vol., no., pp.1,4, 11-14 Feb. 2014 doi: 10.1109/SSD.2014.6808883.

[48] Butel, Y.; Adam, T.; Cogo, B.; Soulard, M., "High efficiency LOW AM/PM 6W C-band MMIC power amplifier for a space radar program," *Microwave Conference, 2000. 30th European* , vol., no., pp.1,4, Oct. 2000, doi: 10.1109/EUMA.2000.338704.

[49] Sorace, R.; Reines, R.; Carlson, N.; Glasgow, M.; Novak, T.; Conte, K., "AM/PM distortion in nonlinear circuits [power amplifier applications]," *Vehicular Technology Conference, 2004. VTC2004-Fall. 2004 IEEE 60th* , vol.6, no., pp.3994,3996 Vol. 6, 26-29 Sept. 2004, doi: 10.1109/VETECF.2004.1404827.

[50] Piazzon, L.; Giofre, R.; Colantonio, P.; Giannini, F., "Investigation of the AM/pm distortion in Doherty Power Amplifiers," *Power Amplifiers for Wireless and Radio*

Applications (PAWR), 2014 IEEE Topical Conference on , vol., no., pp.7,9, 19-23 Jan. 2014, doi: 10.1109/PAWR.2014.6825729.

[51] Nunes, L.C.; Cabral, P.M.; Pedro, J.C., "AM/PM distortion in GaN Doherty power amplifiers," *Microwave Symposium (IMS), 2014 IEEE MTT-S International* , vol., no., pp.1,4, 1-6 June 2014, doi: 10.1109/MWSYM.2014.6848333.

[52] Sang-Min Han; Popov, O.; Sun-Ju Park; Dal Ahn; Jongsik Lim; Won-Sang Yoon; Seongmin Pyo; Young-Sik Kim, "Adaptive calibration method for AM/PM distortion in nonlinear devices," *Radio-Frequency Integration Technology, 2009. RFIT 2009. IEEE International Symposium on* , vol., no., pp.76,79, Jan. 9 2009-Dec. 11 2009 doi: 10.1109/RFIT.2009.5383748.

[53] Kim, J.H.; Jeong, J.H.; Kim, S.M.; Park, C.S.; Lee, K.C., "Prediction of error vector magnitude using AM/AM, AM/PM distortion of RF power amplifier for high order modulation OFDM system," *Microwave Symposium Digest, 2005 IEEE MTT-S International* , vol., no., pp.4 pp.,, 12-17 June 2005, doi: 10.1109/MWSYM.2005.1517143.

[54] Wang, A K.; Ligmanowski, R.; Castro, J.; Mazzara, A, "EVM Simulation and Analysis Techniques," *Military Communications Conference, 2006. MILCOM 2006. IEEE* , vol., no., pp.1,7, 23-25 Oct. 2006, doi: 10.1109/MILCOM.2006.302043.

CHAPTER TWO

LITERATURE REVIEW

2.1 Introduction

Researchers have studied and developed various techniques for suppressing distortion in RFPA. Some of these techniques are used to reduce radio frequency power amplifier (RFPA) power consumption, improve spectral efficiency and enhance RFPA and device linearity. A collective effort that will lead to enhanced battery life in portable devices, reduced CO_2 emission etc. A number of researchers have tried to analyse and document a device's output response signal by observation, mathematical-analysis, computer-simulation, device-emulation and even measurements, a process collectively called characterisation.

Characterization provides solutions that are aimed towards device performance improvement (P-I). One solution is the use of a baseband signal to improve device linearity, hence device performance. Techniques that use the baseband signal to improve device linearity are called baseband linearization techniques.

Baseband linearization technique have been used by researchers over the years. The baseband signal itself is the low frequency information signal. One attraction, is its cost effectiveness. To use baseband in linearization, a few points need consideration. Some of these points include; (i). The global motivation for its use, (ii). What the proposed baseband signal will be, (iii). How to formulate it, (iv). Where to apply it to the device, (v). How to control it and (vi). What its target is. These six points are of importance because they help characterize and identify the differences between the several baseband techniques in the baseband

linearization literature. Some previous work has been done with the baseband linearization signal, applied to the input port [P1], the output port [P2] or at both ports of an RFPA or device. This chapter takes a looks at some previous work, relevant to this (new) work, where the baseband linearization signal was used to linearize devices. In this (new) work (subject of this thesis), baseband linearization signal is applied at the output port [P2] of the device. In this thesis, the baseband linearization signal is applied at the RFPA device output port [P2] and will be referred to as output port injection. This (new) work called baseband envelope linearization (BEL) focuses on output port [P2] injection. The remaining part of this chapter will focus on previous published work, introduce this (new) work and summarize the chapter. Linearization techniques that have employed baseband linearization are now considered.

2.2 Output port baseband injection

In this case, the baseband signal or the performance improvement signal is applied at the output port [P2] of the device. One advantage of this is that it does not require an increase of the input bandwidth, of both the device and the input spectrum to improve the device performance: this leads to savings in input bandwidth. Another advantage is that since the technique is output port injection, the original input RF signal is not re-modulated. A situation which would have happened if input injection was used. Some approaches employing this technique include envelope elimination and restoration (EER), envelope tracking (ET) and a few others. A good example of this is in the use of the envelope tracking (ET) technique.

2.2.1 Envelope elimination and restoration (EER) technique

This technique (EER) has been applied and used in many ways and achieved good results. Its basic structure is shown in figure 2.2.1 It was first introduced by Kahn in 1952 [56]-[57]. It is

attractive due to its high efficiency performance improvement. It includes two amplifiers, one highly efficient envelope amplifier and one highly efficient non-linear (RFPA) amplifier. The idea of this is to have two separate paths, which separates the amplitude modulation from the phase modulation.

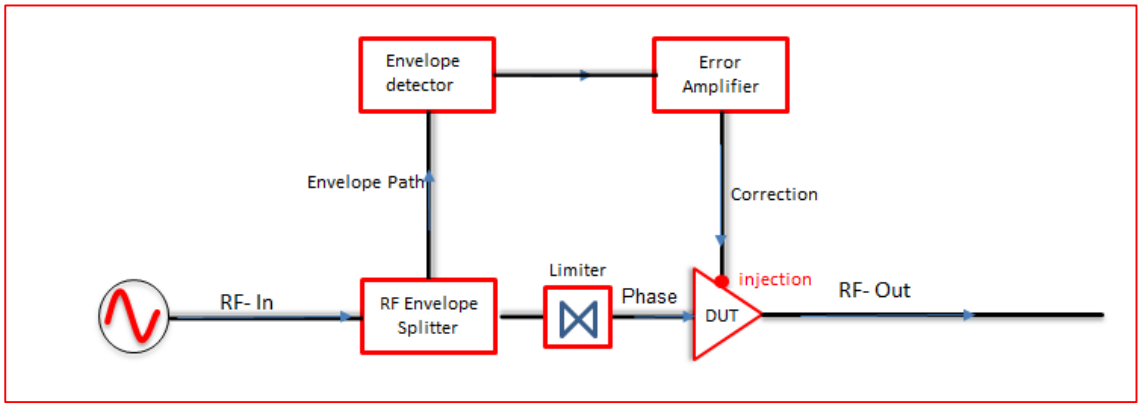

Figure 2.2.1 showing simplified EER structure. (Adapted from [56], [57])

The output signal from the device is a combination from the error amplifier and the phase limiter. The signal that is amplified by the error amplifier is a supply voltage modulated signal generated by the envelope detector stage. A phase limiter is used to produce the phase modulation signal which is also sent to the (RFPA) amplifier. Hence, the (RFPA) amplifier output signal is the signal from the error amplifier and the phase limiter. This technique has undergone modification where it is called the hybrid EER. The difference between the hybrid technique and its previous, non-hybrid version is that instead of a phase modulated signal sent to the (RFPA) amplifier (Previous version), an RF modulated signal is sent to the (RFPA) amplifier. The main disadvantage however is that the amplitude only signal which in essence is a baseband signal requires high power amplification which is done by the error amplifier. This causes a reduction of the entire system efficiency.

2.2.2 Envelope tracking (ET) technique

The envelope tracking technique [58] is a special emergence from EER. Its basic structure is shown in figure 2.2.2 below. This technique is a more modern improvement on the hybrid EER technique. An ET RF power amplifier [59]-[69] needs to work in the linear mode while the EER's work in the highly efficient but non-linear mode. Secondly, the ET RF power amplifier amplifies both amplitude and phase while its EER equivalent reconstruct only phase. ET's efficiency improvement and main advantage, is from the great reduction in power dissipation compared to the fixed drain bias modes of operation.

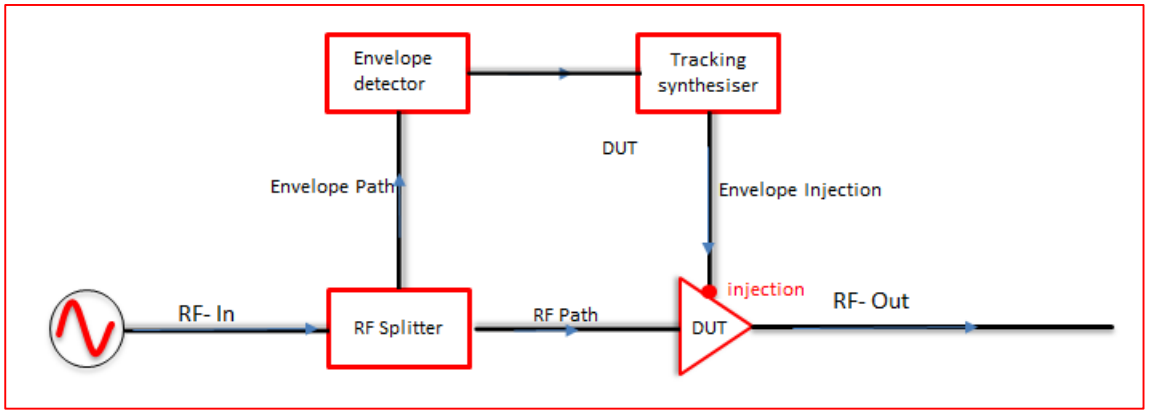

Figure 2.2.2 showing the basic structural of the ET technique. (Adapted from [58])

Another advantage of ET is that it can be used with pre-distortion techniques such as (DPD) technique. Hence it can work in conjunction with other techniques to greatly enhance RFPA/device performance.

2.2.3 Baseband linearization – impedance optimization

In recent work, baseband investigation focused on 'engineering' the output baseband impedance environment. In this case, the performance improvement signal (baseband signal) is applied at the device output port. This technique can be found in [10] – [26]. Such solutions involved presenting constant broadband baseband impedances, targeted at specific IMD components contained in the baseband IMD envelope. Such solution proved successful

for signals with a small number of tones and limited IMD components like the 2-tone case of figure 2.2.3(a).

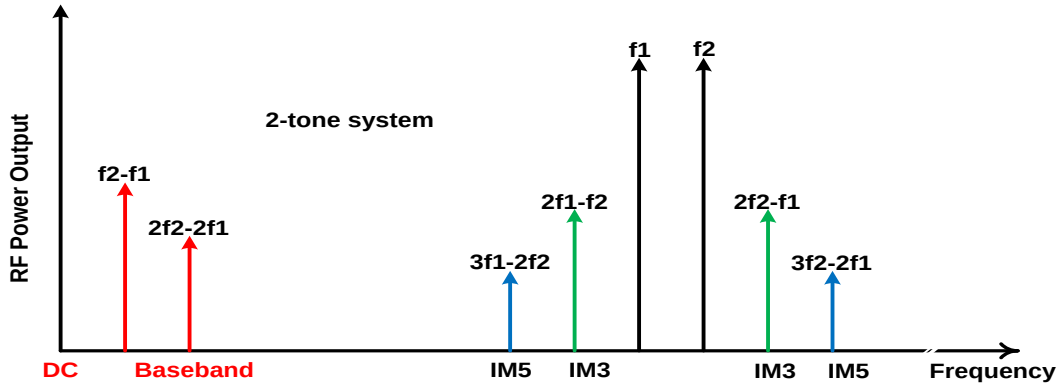

Fig. 2.2.3(a) two-tone case

However, as the number of tones in the modulation increase, like the 9-tone case shown in figure 2.2.3(b), so does the number of IMD components, contained in the baseband IMD envelope. Each of these IMD components require its own baseband impedance in order to suppress it. Resulting in an increasing number of impedance requirements, and hence on increasing number of variables to control. This was the constraint of the impedance approach. However, if the suppression targets were the IMD envelope rather than the IMD components contained inside the IMD envelopes, then the number of variables to control will greatly reduce.

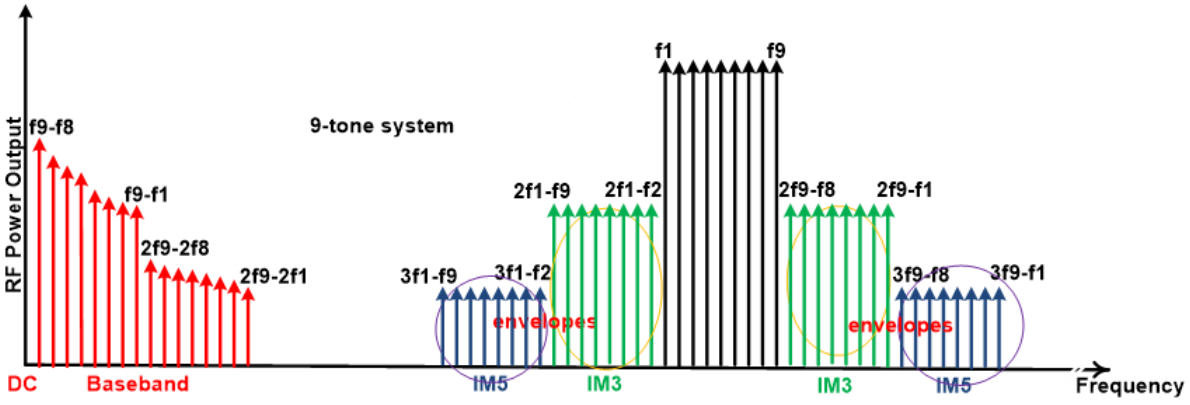

Fig. 2.2.3(b) nine-tone case showing IMD envelopes and IMD components

The major work to overcome this constraint lead to the development of this (*new*) work (BEL) documented in this thesis. BEL is introduced in this chapter. It is discussed in detail in subsequent chapters and used in the remaining parts of this thesis.

2.3 Input port baseband injection

In this case, the baseband signal or the performance improvement signal is applied at the input port [P1] of the device. Hence, the device is pre-distorted (input port perturbation). A good example of this is the pre-distortion technique. There are two ways to implement this, one is the analogue pre-distortion (APD) technique and the other is the digital pre-distortion (DPD) technique. Other techniques also apply their performance improvement signal at the input port but are called other names, some of these are considered in this section. The main idea is that their performance improvement signal is applied at the input port of the device. DPD however has un-officially gained the name for the pre-distortion technique because of its popularity.

2.3.1 Basic Pre-distortion technique

The basic pre-distorter block diagram is shown in figure 2.3.1. The pre-distortion technique, is basically a first RFPA (DPD) stage that provides an expansive behavioural characteristic as the input signal into a second RFPA/device/DUT stage that has a compressive behaviour characteristic. Eventually, the global output signal behavioural characteristic which is a combination of the two previous states is a linearized state.

There are 2 major types in this category which are (a) analogue pre-distortion and (b) digital pre-distortion techniques. In the figure below, DUT (Device Under Test), ALG (ALGorithm) and FBK (FeedBacK) respectively.

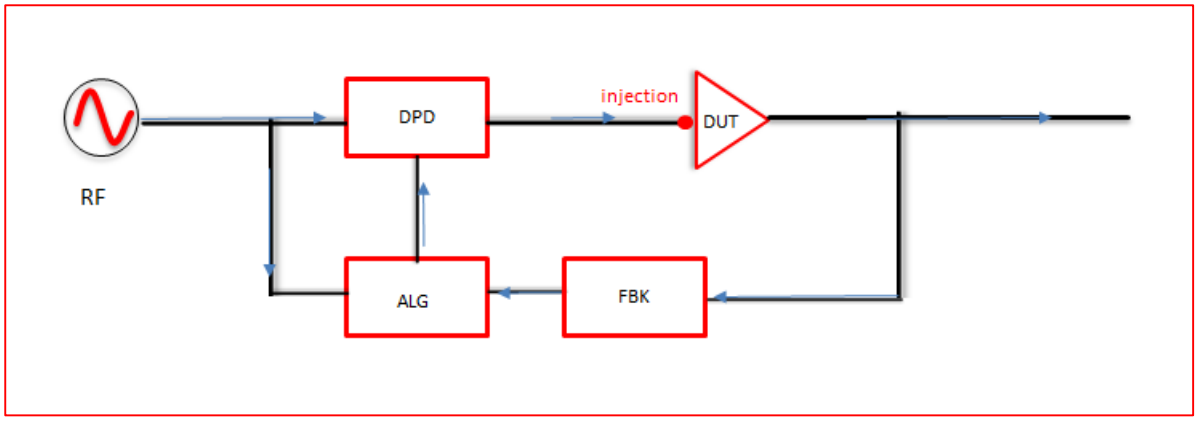

Figure 2.3.1. showing basic RFPA pre-distortion concept

2.3.1. (a) Analogue Pre-distortion (APD)

In the analogue pre-distortion technique, the expansive characteristics generated by the expansive amplifier output is an analogue signal synthesised by analogue processes.

2.3.1. (b) Digital Pre-distortion (DPD)

This is a further development of the analogue pre-distortion technique. This is brought about because of developments in digital signal processing technologies where the required signal input to each stage is synthesised by digital signal processors (DSP). The technique is therefore called digital pre-distortion (DPD) as a result. Hence is it possible to synthesise any type of signal from the analogue baseband to digital baseband, and analogue RF to digital RF signals.

DPD complexity is a concern. One such concern is discussed in [53]. Also, the complexity of the pre-distorter increases as the signal complexity increases. Another problem is the advent of small-cell transmitters for use in micro or femto cells. In general as transmitters get smaller, so does the RF power. DPD complexity does not follow this trend.

DPD is the technique of choice for the wireless communications industry, but its utilization begs for a technique that can be used in conjunction with it to help it scale down on its power complexity. There are two types of pre-distorter implementations which are pre-distorter

models for memory-less RFPAs and those for RFPAs with memory. For narrow-band applications, a simple memory-less digital pre-distorter is sufficient. In this case, the pre-distorter model is determined by characterizing the AM/AM and AM/PM of the required RFPA. For wideband applications however, where the RFPA is assumed to exhibit electrical and thermal memory effects, the digital pre-distorter used are those that model all kinds of non-linear effects, which can be modelled using Volterra series [64]&[65], Hammerstein model and Wiener models. However, the power scale-down problem is generic to all types of DPD. This DPD problem is another motivation for the development of the Baseband Envelope Linearization (BEL) technique described in detail in later chapters of this thesis.

2.3.2 Baseband pre-distortion Linearization

This is perhaps, one of the most popular baseband-Predistorter (PD) technique implementations. It is state of the art because of its use with the pre-distorter (DPD) [27]-[29]. Examples of it include baseband digital pre-distortion, baseband analogue pre-distortion, and many others. Various researchers have used this method. It can also be in the form of analogue pre-distortion [50] – [52] and digital [30] – [49] predistortion. In this case, the baseband signal is applied at the device input port. According to previous discussion, this widens the input linearization bandwidth, the device input bandwidth and increase the input signal PAPR.

2.4 Other envelope performance improvement techniques

2.4.1 Mis-tuned envelope injection

Youjiang Liu et'al in 2010 introduced miss-tuned envelope injection [4]. It linearizes the device by "injecting both envelope signal and faded two-tones with their IMD products into original two-tone signal" [4]. This method also is different from BEL both in envelope

formulation and application. The basic structures are shown in the figures 2.4.1(a) and 2.4.1(b) below. There are two types which are the (a) direct envelope (DE) injection and (b) forward miss–tuned envelope injection (FMTEI).

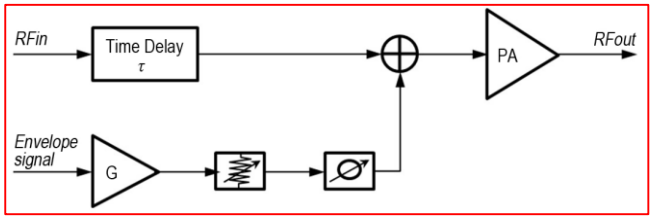

Figure 2.4.1 (a) Structure of Direct Envelope Injection (DEI) (Adapted from 4])

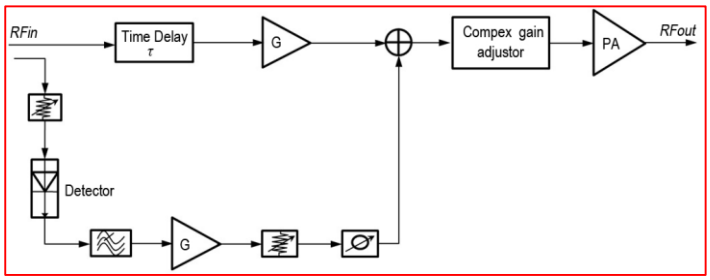

Fig. 2.4.1 (b) Structure of feed forward Mis-Tuned Envelope Injection (FMTEI)(Adapted from [4])

This technique shows a rapid decrease in IMD3 suppression after linearization when increasing the modulation frequency higher than 10MHz for FMTEI. This technique was tested on a 2-tone signal for distortion up to third order IMD.

BEL however formulates its baseband signal mathematically in the envelope domain, based on the envelope of the RF input carrier signal and formulated according to particular principle and effectively controlled by simple reduced number of control coefficients. BEL was also shown to be modulation envelope invariant.

2.4.2 Harmonic and baseband injection

This is also an input port technique [5], [6]. The experimental setup is shown in figure 2.4.2

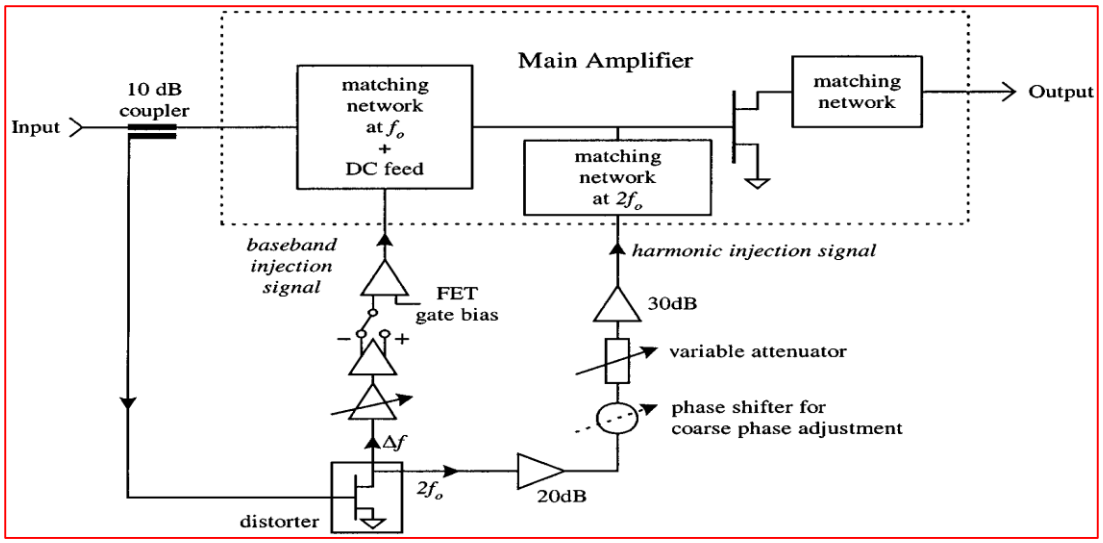

Figure 2.4.2 Experimental setup of harmonic and baseband injection (Adapted from [6])

"In this method, second-order frequency components generated by predistortion circuits are fed to the input of the main amplifier to mix with the fundamental signal for third-order intermodulation distortion (IMD) cancellation". The technique injects both baseband and second order terms with the second order terms formulated using Volterra-series and tested on a 2-tone signal for distortion up to the 3rd order IMD. According to the authors, "It is also observed that the IMD performance deteriorates as the output power increases toward the 1dB compression point. This phenomenon is believed to be due to the higher order mixing effect that has not been included above. Nevertheless, for a strongly nonlinear case, reduction of the higher order IMD such as IM5 is indeed important [8]." In [5] however, the carrier second harmonic signal and a baseband signal were simultaneously fed into the input port of the main amplifier to mix with the fundamental signal on a 2-tone system and a reduction of the 3rd order IMD of 27dB was achieved. BEL distortion suppression of any IMD is achieved by simple control of key coefficients which can easily be turned-on or off. It can also be applied to an arbitrary number of tones. Its highest level of simultaneous suppression in 3rd order and 5th order IMD was 56dBc.

2.4.3 3rd and 5th order baseband injection

This is an approach [7] used with pre-distortion technique. The block diagram is shown in figure 2.4.3.

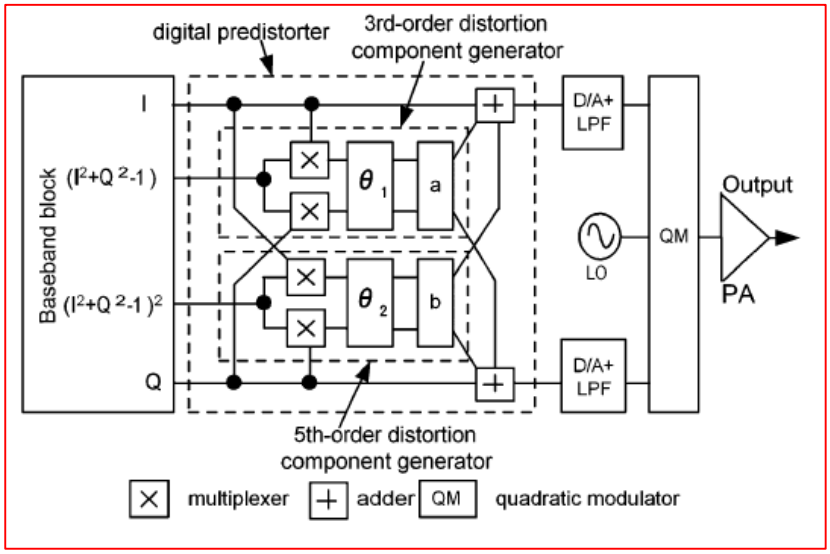

Figure 2.4.3 Block diagram of the 3rd & 5th order proposed predistorter (Adapted from [7]).

One of the differences between this approach and BEL is that it is a pre-distorter approach. This means the performance improvement signal is applied at the input port of the device. Secondly and most importantly, the major difference between this technique and BEL is in the baseband linearization signal formulation. While this approach injects "the third and fifth order distortion components in the baseband block", BEL injects the square and the fourth of the RF input carrier signal envelope with control coefficients.

2.4.4 Dual baseband injection

This is achieved in two ways. One method is to inject 2-signals into one port on the device simultaneously. The other is to inject 2-signals simultaneously into the 2-ports of the device. The third is to inject, a split-signal into the 2-ports of the device simultaneously. Examples of these are in [8] and [9] respectively. BEL is shown to be modulation bandwidth invariant in

chapter 5 section one. However, the techniques shown in [8] and [9] reported results for low modulation frequencies of 1MHz and 100 KHz respectively.

2.5 Present (new) work

2.5.1 Baseband envelope linearization technique (BEL)

The fundamental structure of the proposed baseband envelope linearization technique, is shown in Figure 2.5.1 and will be referred to as (BEL). In this architecture, the performance improvement signal, defined mathematically in the envelope domain is injected into the device output port. Its technique and architecture is important because of the advantages listed below:

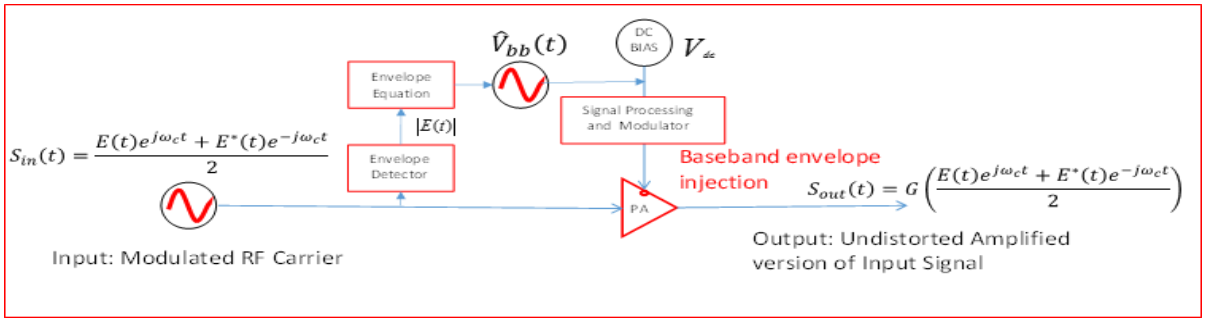

Figure 2.5.1 shows the fundamental concept of BEL technique

(i). This technique does not increase the device input bandwidth because it is output injection based.

(ii). The original input RF signal is not re-modulated as would have been the case if the technique were an input injection type. This means there is no additional distortion added at the device input port which would have happened in the case of input injection.

(iii). Re-modulating the input signal can increase the input signal complexity and PAPR.

(iv). Input injection will increase the input signal bandwidth leading to input signal spectrum inefficiency.

(v). It is assumed that in devices where input injection is used, the device begins to experience increase in thermal stress as a result of the injection being applied earlier than it would have.

(vi). Every RFPA device is also a mixer. With output injection, the resulting output port mixing is easier to control because the mixing can be controlled directly by the output injected signal.

(vii). The fundamental BEL structure is compatible with emerging technology architecture. One such technology is envelope tracking (ET). This means that to deploy BEL, there is no need to discard the entire existing ET architecture.

(viii). Usually, linearizing with baseband means using a small bandwidth. This also helps to reduce linearization spectrum requirement and cost.

(ix). Using this technique, as shall be shown in the later part of chapter 3, it is possible to target multiple distortion components and hence achieve an all-important simultaneous suppression.

(x). it requires the determination of only a few linearization coefficients to optimize hence there is reduced computation.

(xi). It is signal complexity invariant and device technology invariant.

(xii). No additional distortion in the linearized output response of the device as a result of the injected linearizing baseband signal.

With BEL, all signals are defined in the envelope domain. As a result of this, the number of variables required to control is small. This property is shown in chapters 4 and 5. This also makes it relatively easy to use and control this technique.

For instance, once the distortion order of the system is chosen, say a fifth order system, the number of coefficients to control is two and will remain two no matter any change in the complexity of the excitation signal.

In addition, for a particular device, and at a particular drive level, the values of these coefficients are stimulus invariant.

2.6 What makes BEL - different from other baseband linearization approach

BEL is a baseband voltage engineering linearization concept. As shown, a lot of previous work has been done using baseband to linearize RFPA and devices [1] – [69]. BEL is different. The differences are that, it is developed in the envelope domain. Its baseband voltage is formulated mathematically according to a particular fundamental principle [3]. The formulation relates the output current signal envelope, and the inter-modulation distortion envelope to the same quantity. This quantity is the input carrier signal envelope. It then mathematically formulates the baseband signal voltage with the same quantity according to a fundamental principle. Coefficients are used to control the formulated baseband voltage. The resulting formulated baseband signal is used to linearize the device. The linearization process is controlled by these control coefficients. The rest of this thesis will detail the aforementioned process.

2.6.1 BEL and ET

The main differences between BEL and ET are, firstly; the way their baseband signals are formulated. BEL defines its linearizing baseband injection signal envelope mathematically in the envelope domain, as a function of the modulated input RF carrier signal envelope (envelope squared and envelope to the power four) which is then ‘engineered’ or ‘shaped’ by a set of linearization coefficients. The BEL baseband signal formulation is described in detail in chapter 3. In the case of ET, its injected envelope is detected using physical detection techniques such as detectors from Analog Devices, Marconi, HP and others. Secondly, BEL is new and focused primarily at device linearity improvement. BEL still has a lot of

refinement before it will assume its full potential, while ET is further advanced in development and is used to improve the efficiency of the amplifier.

2.6.2 BEL and DPD

BEL is very effective at linearizing devices. This effectiveness is shown in chapters 3,4,5 and 6 of this thesis. It can be used with DPD. The goal of its integration with DPD is for it to suppress AM/AM distortion, while DPD suppresses AM/PM distortion. It is hoped that this idea will help DPD to scale down in its power complexity. The understanding is that if DPD is used to suppress only AM/PM distortion, its complexity can reduce. Some of the routes to DPD power complexity reduction are assumed to be, reduced number of calculations, reduced number of variables to control, reduced computation needed, reduced number of coefficients to calculate, reduced coefficient complexity and hence less power will be consumed. This has not been experimentally confirmed yet, but is the motivation for the combination.

2.6.3 BEL simplicity

BEL is a technique that uses a formulation defined in the envelope domain, to quantify the necessary baseband signal that should be applied to the output bias port of the RFPA. In practice, it can be implemented using an ET architecture and can combine with DPD. Experimentally, it can be investigated using an active-open-loop baseband envelope load-pull engineering system that will be discussed in chapter 3. The result are shown in chapters 3,4,5 and 6 respectively.

2.7 Chapter summary

In this chapter, the various related performance improvement techniques have been discussed.

The main topics considered were, envelope tracking, pre-distortion, BEL, impedance optimisation, envelope injection and envelope restoration & elimination, and output port injection. These are the main techniques that have relevance with BEL.

A pattern clearly shown is a continuous development from one technique to the other. A continuous development pattern could work better if used in conjunction with others. Such can be seen with DPD's usage with other techniques. A combination of techniques will favour the future of the wireless communication industry. In view of this, moving forward into the future of small cell designs, it is believed that combining BEL with DPD will help the scale-down of DPD power complexity in particular as RF power scales down.

BEL is aimed at improving the linearity performance of the RFPA device and the power amplifier (PA).

While a lot of work has been done by modifying the signals at both the input and the output ports of the DUT, most of the focus recently has been on DPD. In this thesis, the BEL approach is investigated using baseband injection at the output bias port of the device for improvement of linearity.

2.8 References

[1] Suk Keun Myoung; Xian Cui; Chaillot, D.; Roblin, P.; Verbeyst, F.; Bossche, M.V.; Seok Joo Doo; Wenhua Dai, "Large signal network analyzer with trigger for baseband & RF system characterization with application to K-modeling & output baseband modulation linearization," ARFTG Microwave Measurements Conference, Fall 2004. 64th , vol., no., pp.189,195, 2-3 Dec. 2004, doi: 10.1109/ARFTGF.2004.1427596.

[2] Yusoff, Z.; Lees, J.; Benedikt, J.; Tasker, P.J.; Cripps, S.C., "Linearity improvement in RF power amplifier system using integrated Auxiliary Envelope Tracking system," Microwave Symposium Digest (MTT), 2011 IEEE MTT-S International , vol., no., pp.1,4, 5-10 June 2011, doi: 10.1109/MWSYM.2011.5972769.

[3] Ogboi, F.L.; Tasker, P.J.; Akmal, M.; Lees, J.; Benedikt, J.; Bensmida, S.; Morris, K.; Beach, M.; McGeehan, J., "A LSNA configured to perform baseband engineering for device linearity investigations under modulated excitations," Microwave Conference (EuMC), 2013 European , vol., no., pp.684,687, 6-10 Oct. 2013.

[4] Youjiang Liu; Yinong Liu; Banghua Zhou, "Miss-Tuned Envelope Injection for 2.1GHz HPA Based on Polynomial Model," Wireless Communications Networking and Mobile Computing (WiCOM), 2010 6th International Conference on , vol., no., pp.1,5, 23-25 Sept. 2010, doi: 10.1109/WICOM.2010.5600782.

[5] Chun-Wah Fan; Cheng, K.-K.M., "Theoretical and experimental study of amplifier linearization based on harmonic and baseband signal injection technique," Microwave Theory and Techniques, IEEE Transactions on , vol.50, no.7, pp.1801,1806, Jul 2002 doi: 10.1109/TMTT.2002.800441.

[6] Chun-Wah Fan; Cheng, K.-K.M., "Amplifier linearization using simultaneous harmonic and baseband injection," Microwave and Wireless Components Letters, IEEE , vol.11, no.10, pp.404,406, Oct. 2001, doi: 10.1109/7260.959309.

[7] Mizusawa, N.; Kusunoki, S., "Third- and fifth-order baseband component injection for linearization of the power amplifier in a cellular phone," Microwave Theory and Techniques, IEEE Transactions on , vol.53, no.11, pp.3327,3334, Nov. 2005 doi: 10.1109/TMTT.2005.855747.

[8] Cheng, K.-K.M.; Chung-Fai Au-Yeung, "Novel difference-frequency dual-signal injection method for CMOS mixer linearization," Microwave and Wireless Components Letters, IEEE , vol.14, no.7, pp.358,360, July 2004, doi: 10.1109/LMWC.2004.828017.

[9] Pui Ching Chun; Chi-Hou Chan; Quan Xue, "Dual Baseband Injection Method for Amplifier Linearization," Microwave Conference, 2007. APMC 2007. Asia-Pacific , vol., no., pp.1,3, 11-14 Dec. 2007, doi: 10.1109/APMC.2007.4554590.

[10] Akmal, M.; Carrubba, V.; Lees, J.; Bensmida, S.; Benedikt, J.; Morris, K.; Beach, M.; McGeehan, J.; Tasker, P.J., "Linearity enhancement of GaN HEMTs under complex modulated excitation by optimizing the baseband impedance environment," Microwave Symposium Digest (MTT), 2011 IEEE MTT-S International , vol., no., pp.1,4, 5-10 June 2011, doi: 10.1109/MWSYM.2011.5972833.

[11] Brinkhoff, J.; Parker, A.E.; Leung, M., "Baseband impedance and linearization of FET circuits," Microwave Theory and Techniques, IEEE Transactions on , vol.51, no.12, pp.2523,2530, Dec. 2003, doi: 10.1109/TMTT.2003.819208.

[12] Richards, A.; Morris, K.A.; McGeehan, J.P., "Removing the effects of baseband impedance on distortion in FET amplifiers," Microwaves, Antennas and Propagation, IEE Proceedings , vol.153, no.5, pp.401,406, Oct. 2006, doi: 10.1049/ip-map:20060005.

[13] Brinkhoff, J.; Parker, A.E., "Implication of baseband impedance and bias for FET amplifier linearization," Microwave Symposium Digest, 2003 IEEE MTT-S International , vol.2, no., pp.781,784 vol.2, 8-13 June 2003
doi: 10.1109/MWSYM.2003.1212487.

[14] Akmal, M.; Lees, J.; Bensmida, S.; Woodington, S.; Carrubba, V.; Cripps, S.; Benedikt, J.; Morris, K.; Beach, M.; McGeehan, J.; Tasker, P.J., "The effect of baseband impedance termination on the linearity of GaN HEMTs," Microwave Conference (EuMC), 2010 European , vol., no., pp.1046,1049, 28-30 Sept. 2010.

[15] Brinkhoff, J.; Parker, A.E., "Effect of baseband impedance on FET intermodulation," Microwave Theory and Techniques, IEEE Transactions on , vol.51, no.3, pp.1045,1051, Mar 2003, doi: 10.1109/TMTT.2003.808704.

[16] Akmal, M.; Carrubba, V.; Lees, J.; Smida, S.B.; Morris, K.; McGeehan, J.; Beach, M.; Benedikt, J.; Tasker, P.J., "Linearity enhancement of GaN HEMTs under complex modulated excitations by optimizing the baseband impedance environment," Microwave Symposium Digest (MTT), 2011 IEEE MTT-S International , vol., no., pp.1,1, 5-10 June 2011, doi: 10.1109/MWSYM.2011.5973183.

[17] Manjanna, A.K.; Marchetti, M.; Buisman, K.; Spirito, M.; Pelk, M.J.; de Vreede, L.C.N., "Device characterization for LTE applications with wideband baseband, fundamental and harmonic impedance control," Microwave Conference (EuMC), 2013 European , vol., no., pp.255,258, 6-10 Oct. 2013.

[18] Andrews, C.; Molnar, A.C., "A passive-mixer-first receiver with baseband-controlled RF impedance matching, ≪ 6dB NF, and ≫ 27dBm wideband IIP3," Solid-State Circuits Conference Digest of Technical Papers (ISSCC), 2010 IEEE International , vol., no., pp.46,47, 7-11 Feb. 2010, doi: 10.1109/ISSCC.2010.5434056.

[19] Akmal, M.; Ogboi, F.L.; Yusoff, Z.; Lees, J.; Carrubba, V.; Choi, H.; Bensmida, S.; Morris, K.; Beach, M.; McGeehan, J.; Benedikt, J.; Tasker, P.J., "Characterization of electrical memory effects for complex multi-tone excitations using broadband active baseband load-pull," Microwave Integrated Circuits Conference (EuMIC), 2012 7th European , vol., no., pp.885,888, 29-30 Oct. 2012.

[20] Alghanim, A.; Lees, J.; Williams, T.; Benedikt, J.; Tasker, P.J., "Sensitivity of electrical baseband memory effects to higher-order IF components for high-power LDMOS power amplifiers," Electronics Letters , vol.44, no.5, pp.358,359, Feb. 28 2008, doi: 10.1049/el:20083348.

[21] Akmal, M.; Lees, J.; Bensmida, S.; Woodington, S.; Benedikt, J.; Morris, K.; Beach, M.; McGeehan, J.; Tasker, P.J., "The impact of baseband electrical memory effects on the dynamic transfer characteristics of microwave power transistors," Integrated Nonlinear Microwave and Millimeter-Wave Circuits (INMMIC), 2010 Workshop on , vol., no., pp.148,151, 26-27 April 2010, doi: 10.1109/INMMIC.2010.5480111.

[22] Akmal, M.; Lees, J.; Jiangtao, S.; Carrubba, V.; Yusoff, Z.; Woodington, S.; Benedikt, J.; Tasker, P.J.; Bensmida, S.; Morris, K.; Beach, M.; McGeehan, J., "An enhanced modulated waveform measurement system for the robust characterization of microwave devices under modulated excitation," Microwave Integrated Circuits Conference (EuMIC), 2011 European , vol., no., pp.180,183, 10-11 Oct. 2011.

[23] Akmal, M.; Lees, J.; Carrubba, V.; Bensmida, S.; Woodington, S.; Benedikt, J.; Morris, K.; Beach, M.; McGeehan, J.; Tasker, P.J., "Minimization of baseband electrical memory effects in GaN HEMTs using active IF load-pull," Microwave Conference Proceedings (APMC), 2010 Asia-Pacific , vol., no., pp.5,8, 7-10 Dec. 2010.

[24] Alghanim, Abdulrahman; Lees, J.; Williams, Tudor; Benedikt, J.; Tasker, P.J., "Using active IF load-pull to investigate electrical base-band induced memory effects in high-power LDMOS transistors," Microwave Conference, 2007. APMC 2007. Asia-Pacific , vol., no., pp.1,4, 11-14 Dec. 2007, doi: 10.1109/APMC.2007.4554737.

[25] Lees, J.; Haczewski, A.; Benedikt, J.; Tasker, P.J., "An automated multiple-stimulus measurement system for characterising multiple-device amplifiers," Microwave Conference, 2004. 34th European , vol.1, no., pp.435,438, 12-14 Oct. 2004.

[26] Kheirkhahi, A.; Yan, J.J.; Asbeck, P.M.; Larson, L.E., "RF Power Amplifier Efficiency Enhancement by Envelope Injection and Termination for Mobile Terminal Applications," Microwave Theory and Techniques, IEEE Transactions on , vol.61, no.2, pp.878,889, Feb. 2013, doi: 10.1109/TMTT.2012.2234475.

[27] Wangmyong Woo; Ding, Lei; Kenney, J.S.; Zhou, G.T., "An RF/DSP Test Bed for Baseband Pre-Distortion of RF Power Amplifiers," ARFTG Conference Digest-Spring, 57th , vol.39, no., pp.1,7, May 2001, doi: 10.1109/ARFTG.2001.327464.

[28] Feipeng Wang; Ojo, A.; Kimball, D.; Asbeck, P.; Larson, L., "Envelope tracking power amplifier with pre-distortion linearization for WLAN 802.11g," Microwave Symposium Digest, 2004 IEEE MTT-S International , vol.3, no., pp.1543,1546 Vol.3, 6-11 June 2004, doi: 10.1109/MWSYM.2004.1338872.

[29] Sardrood, P.S.; Solat, G.R.; Vakili, V.T.T., "Improvement eye diagram opening by base band pre-distortion over nonlinear channel in DVB-RCS transmitter," Ultra Modern Telecommunications and Control Systems and Workshops (ICUMT), 2010 International Congress on , vol., no., pp.26,30, 18-20 Oct. 2010
doi: 10.1109/ICUMT.2010.5676663.

[30] Hammi, O.; Carichner, S.; Vassilakis, B.; Ghannouchi, F.M., "Synergetic Crest Factor Reduction and Baseband Digital Predistortion for Adaptive 3G Doherty Power Amplifier Linearizer Design," Microwave Theory and Techniques, IEEE Transactions on , vol.56, no.11, pp.2602,2608, Nov. 2008, doi: 10.1109/TMTT.2008.2004899.

[31] Boumaiza, S.; Ghannouchi, F.M., "Realistic power-amplifiers characterization with application to baseband digital predistortion for 3G base stations," Microwave Theory and Techniques, IEEE Transactions on , vol.50, no.12, pp.3016,3021, Dec 2002
doi: 10.1109/TMTT.2002.805139.

[32] Bondar, D.; Budimir, D., "Digital baseband predistortion of wideband power amplifiers with improved memory effects," Radio and Wireless Symposium, 2009. RWS '09. IEEE , vol., no., pp.284,287, 18-22 Jan. 2009
doi: 10.1109/RWS.2009.4957334.

[33] Madero-Ayora, M.J.; Barataud, D.; Dine, M.S.E.; Neveux, G.; Nebus, J.M.; Reina-Tosina, J.; Allegue-Martinez, M.; Crespo-Cadenas, C., "Baseband digital predistortion of a 10 W GaN power amplifier," Microwave Conference (EuMC), 2011 41st European , vol., no., pp.341,344, 10-13 Oct. 2011.

[34] Bondar, D.; Lopez, N.D.; Popovic, Z.; Budimir, D., "Linearization of high-efficiency power amplifiers using digital baseband predistortion with iterative injection," Radio and Wireless Symposium (RWS), 2010 IEEE , vol., no., pp.148,151, 10-14 Jan. 2010
doi: 10.1109/RWS.2010.5434184.

[35] Bondar, D.; Budimir, D.; Shelkovnikov, B., "Linearization of power amplifiers by baseband digital predistortion for OFDM transmitters," Microwave & Telecommunication Technology, 2008. CriMiCo 2008. 2008 18th International Crimean Conference , vol., no., pp.270,271, 8-12 Sept. 2008
doi: 10.1109/CRMICO.2008.4676376.

[36] Thian, M.; Ming Xiao; Gardner, P., "Digital Baseband Predistortion Based Linearized Broadband Inverse Class-E Power Amplifier," Microwave Theory and Techniques, IEEE Transactions on , vol.57, no.2, pp.323,328, Feb. 2009
doi: 10.1109/TMTT.2008.2011164.

[37] Coviello, G.; Cannone, F.; Avitabile, G., "Robust behavioral non uniform look-up table spacing in adaptive digital baseband predistortion technique for RF power amplifier," AFRICON, 2013 , vol., no., pp.1,5, 9-12 Sept. 2013
doi: 10.1109/AFRCON.2013.6757706.

[38] Chi-Tsan Chen; Chien-Jung Li; Du, J.-Y.; Tzyy-Sheng Horng; Je-Kuan Jau; Jian-Yu Li; Horng, P.-K.; Deng, D.-S., "Power amplifier linearization using baseband digital predistortion for WiMAX applications," Microwave Conference, 2008. APMC 2008. Asia-Pacific , vol., no., pp.1,4, 16-20 Dec. 2008
doi: 10.1109/APMC.2008.4958286.

[39] Fehri, B.; Boumaiza, S., "Baseband Equivalent Volterra Series for Digital Predistortion of Dual-Band Power Amplifiers," Microwave Theory and Techniques, IEEE Transactions on , vol.62, no.3, pp.700,714, March 2014
doi: 10.1109/TMTT.2014.2303944.

[40] Cottais, E.; Wang, Y.; Toutain, S., "Experimental results of power amplifiers linearization using adaptive baseband digital predistortion," Microwave Conference, 2005 European , vol.3, no., pp.4 pp.,, 4-6 Oct. 2005
doi: 10.1109/EUMC.2005.1610307.

[41] Fehri, B.; Boumaiza, S., "Baseband Equivalent Volterra Series for Behavioral Modeling and Digital Predistortion of Power Amplifiers Driven With Wideband Carrier Aggregated Signals," Microwave Theory and Techniques, IEEE Transactions on , vol.PP, no.99, pp.1,10, doi: 10.1109/TMTT.2014.2360387.

[42] Raich, R.; Hua Qian; Zhou, G.T., "Digital baseband predistortion of nonlinear power amplifiers using orthogonal polynomials," Acoustics, Speech, and Signal Processing, 2003. Proceedings. (ICASSP '03). 2003 IEEE International Conference on , vol.6, no., pp.VI,689-92 vol.6, 6-10 April 2003, doi: 10.1109/ICASSP.2003.1201775.

[43] Cottais, E.; Wang, Y.; Toutain, S., "Experimental results of power amplifiers linearization using adaptive baseband digital predistortion," Wireless Technology, 2005. The European Conference on , vol., no., pp.329,332, 3-4 Oct. 2005 doi: 10.1109/ECWT.2005.1617724.

[44] Gotthans, T.; Baudoin, G.; Mbaye, A., "Influence of delay mismatch on digital predistortion for power amplifiers," Mixed Design of Integrated Circuits and Systems (MIXDES), 2013 Proceedings of the 20th International Conference , vol., no., pp.490,493, 20-22 June 2013.

[45] Bin Fu; Zhaowu Chen, "A digital baseband predistorter based on power series model," Microwave and Millimeter Wave Technology, 2004. ICMMT 4th International Conference on, Proceedings , vol., no., pp.804,807, 18-21 Aug. 2004 doi: 10.1109/ICMMT.2004.1411652.

[46] Peng Zhang; Fei Yang; Gang Yang; Changyin Liu, "Effects of digital baseband predistortion on linearized transmitter design," Power Electronics and Intelligent Transportation System (PEITS), 2009 2nd International Conference on , vol.1, no., pp.60,63, 19-20 Dec. 2009, doi: 10.1109/PEITS.2009.5406964.

[47] Hammi, O.; Boumaiza, S.; Jaidane, M.; Ghannouchi, F.M., "Baseband digital predistortion using subband filtering technique," Microwave Symposium Digest, 2003 IEEE MTT-S International , vol.3, no., pp.1699,1702 vol.3, 8-13 June 2003 doi: 10.1109/MWSYM.2003.1210466.

[48] de Mingo, J.; Valdovinos, A., "Performance of a new digital baseband predistorter using calibration memory," Vehicular Technology, IEEE Transactions on , vol.50, no.4, pp.1169,1176, Jul 2001, doi: 10.1109/25.938591.

[49] Ding, Lei; Zhou, G.T.; Morgan, D.R.; Zhengxiang Ma; Kenney, J.S.; Jaehyeong Kim; Giardina, C.R., "A robust digital baseband predistorter constructed using memory polynomials," Communications, IEEE Transactions on , vol.52, no.1, pp.159,165, Jan. 2004, doi: 10.1109/TCOMM.2003.822188.

[50] Korol, V.; Larson, L.E., "A UWB CMOS SoC RF transmitter with analog baseband predistortion and on-package printed balun," Silicon Monolithic Integrated Circuits in RF Systems (SiRF), 2011 IEEE 11th Topical Meeting on , vol., no., pp.45,48, 17-19 Jan. 2011, doi: 10.1109/SIRF.2011.5719302.

[51] Lianqing Ji; Jianyi Zhou; Jianfeng Zhai; Ke Zhou, "Design of a FPGA-based baseband for MIMO TD-LTE BTS," Wireless Symposium (IWS), 2013 IEEE International , vol., no., pp.1,3, 14-18 April 2013
doi: 10.1109/IEEE-IWS.2013.6616806.

[52] Banelli, P.; Baruffa, G., "Mixed BB-IF predistortion of OFDM signals in non-linear channels," Broadcasting, IEEE Transactions on , vol.47, no.2, pp.137,146, Jun 2001
doi: 10.1109/11.948266.

[53] Yang, Tingxiao; Zenteno, Efrain; Bjorsell, Niclas, "Measurement imperfections impact on the performance of digitally predistorted power amplifiers," Instrumentation and Measurement Technology Conference (I2MTC) Proceedings, 2014 IEEE International , vol., no., pp.230,233, 12-15 May 2014 doi: 10.1109/I2MTC.2014.6860742.

[54] Changsoo Eun; Powers, E.J., "A new Volterra predistorter based on the indirect learning architecture," Signal Processing, IEEE Transactions on , vol.45, no.1, pp.223,227, Jan 1997 doi: 10.1109/78.552219.

[55] You Li; Xiaolin Zhang, "Adaptive digital predistortion based on MC-FQRD-RLS algorithm using indirect learning architecture," Advanced Computer Control (ICACC), 2010 2nd International Conference on , vol.4, no., pp.240,242, 27-29 March 2010, doi: 10.1109/ICACC.2010.5486962.

[56] Kahn, L.R., "Comparison of Linear Single-Sideband Transmitters with Envelope Elimination and Restoration Single-Sideband Transmitters," Proceedings of the IRE , vol.44, no.12, pp.1706,1712, Dec. 1956, doi: 10.1109/JRPROC.1956.275062.

[57] Kahn, L.R., "Single-Sideband Transmission by Envelope Elimination and Restoration," Proceedings of the IRE , vol.40, no.7, pp.803,806, July 1952 doi: 10.1109/JRPROC.1952.273844.

[58] Saleh, A A M; Cox, D.C., "Improving the Power-Added Efficiency of FET Amplifiers Operating with Varying-Envelope Signals," Microwave Theory and Techniques, IEEE Transactions on , vol.31, no.1, pp.51,56, Jan. 1983 doi: 10.1109/TMTT.1983.1131428.

[59] Anding Zhu; Draxler, P.J.; Chin Hsia; Brazil, T.J.; Kimball, D.F.; Asbeck, P.M., "Digital Predistortion for Envelope-Tracking Power Amplifiers Using Decomposed Piecewise Volterra Series," Microwave Theory and Techniques, IEEE Transactions on , vol.56, no.10, pp.2237,2247, Oct. 2008 doi: 10.1109/TMTT.2008.2003529.

[60] Huan Xi; Qian Jin; Xinbo Ruan, "Feed-Forward Scheme Considering Bandwidth Limitation of Operational Amplifiers for Envelope Tracking Power Supply Using Series-Connected Composite Configuration," Industrial Electronics, IEEE

Transactions on , vol.60, no.9, pp.3915,3926, Sept. 2013 doi: 10.1109/TIE.2012.2206342.

[61] Kim, Bumman; Jinsung Choi; Kang, Daehyun; Dongsu Kim, "Optimized envelope tracking operation of Doherty power amplifier," Signals, Circuits and Systems (SCS), 2009 3rd International Conference on , vol., no., pp.1,5, 6-8 Nov. 2009 doi: 10.1109/ICSCS.2009.5412541.

[62] Yusoff, Z.; Lees, J.; Chaudhary, M.A; Carrubba, V.; Heungjae Choi; Tasker, P.; Cripps, S.C., "Simple and low-cost tracking generator design in envelope tracking radio frequency power amplifier system for WCDMA applications," Microwaves, Antennas & Propagation, IET , vol.7, no.10, pp.802,808, July 16 2013 doi: 10.1049/iet-map.2013.0091.

[63] Yusoff, Z.; Lees, J.; Benedikt, J.; Tasker, P.J.; Cripps, S.C., "Linearity improvement in RF power amplifier system using integrated Auxiliary Envelope Tracking system," Microwave Symposium Digest (MTT), 2011 IEEE MTT-S International , vol., no., pp.1,4, 5-10 June 2011 doi: 10.1109/MWSYM.2011.5972769.

[64] Jinsung Choi; Kang, Daehyun; Dongsu Kim; Kim, Bumman, "Optimized Envelope Tracking Operation of Doherty Power Amplifier for High Efficiency Over an Extended Dynamic Range," Microwave Theory and Techniques, IEEE Transactions on , vol.57, no.6, pp.1508,1515, June 2009 doi: 10.1109/TMTT.2009.2020674.

[65] Yan Li; Lopez, J.; Schecht, C.; Ruili Wu; Lie, D.Y.-C., "Design of High Efficiency Monolithic Power Amplifier With Envelope-Tracking and Transistor Resizing for Broadband Wireless Applications," Solid-State Circuits, IEEE Journal of , vol.47, no.9, pp.2007,2018, Sept. 2012 doi: 10.1109/JSSC.2012.2201289.

[66] Jooseung Kim; Dongsu Kim; Yunsung Cho; Daehyun Kang; Byungjoon Park; Kyunghoon Moon; Bumman Kim, "Supply modulator for envelope-tracking operation of dual-mode handset power amplifier," Microwave Integrated Circuits Conference (EuMIC), 2013 European , vol., no., pp.344,347, 6-8 Oct. 2013.

[67] Draxler, P.; Lanfranco, S.; Kimball, D.; Hsia, C.; Jeong, J.; van de Sluis, J.; Asbeck, P.M., "High Efficiency Envelope Tracking LDMOS Power Amplifier for W-CDMA," Microwave Symposium Digest, 2006. IEEE MTT-S International, vol., no., pp.1534, 1537, 11-16 June 2006 doi: 10.1109/MWSYM.2006.249605.

[68] Young, J.P.; Ripley, D.; Lehtola, P., "Envelope Tracking power amplifier optimization for mobile applications," SOI-3D-Subthreshold Microelectronics Technology Unified Conference (S3S), 2013 IEEE , vol., no., pp.1,4, 7-10 Oct. 2013 doi: 10.1109/S3S.2013.6716534.

[69] Zhancang Wang; Li Wang; Rui Ma; Lanfranco, S., "A GaN MOSFET supply modulator compatible with feed forward loop for wideband envelope tracking power amplifier," Silicon Monolithic Integrated Circuits in RF Systems (SiRF), 2013 IEEE 13th Topical Meeting on , vol., no., pp.42,44, 21-23 Jan. 2013 doi: 10.1109/SiRF.2013.6489426.

CHAPTER THREE

BASEBAND ENVELOPE LINEARIZATION (BEL)

3.1 Reason for baseband envelope linearization

In recent work baseband investigation focused on 'engineering' the output baseband impedance environment. Such solutions involved presenting constant broadband baseband impedances, targeted at specific IMD components contained in the baseband IMD envelope. Such solution proved successful for signals with a small number of tones and limited IMD components like the 2-tone case, shown in Fig. 3.1(a)

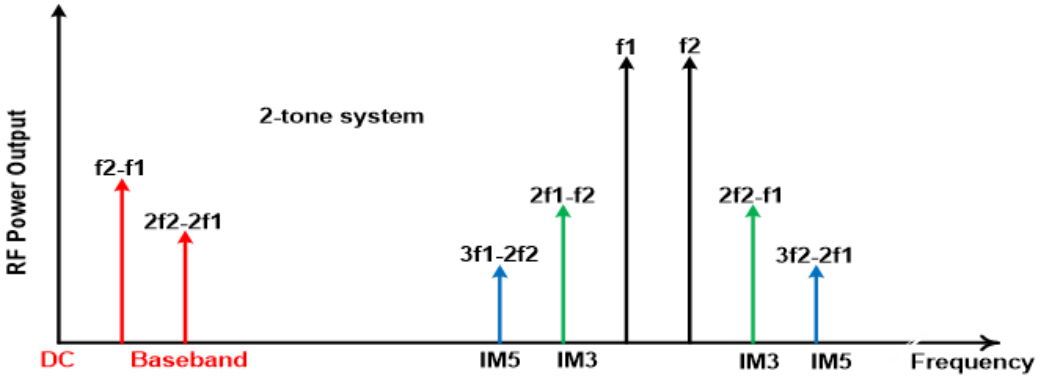

Figure. 3.1(a) A 2-tone system

However, as the number of tones in the modulation scale up, as in the 3-tone and 9-tone case shown in Fig. 3.1 (b) and Fig. 3.1 (c) respectively, so does the number of baseband and IMD components with each component resulting in an increasing number of impedance requirements, and hence increasing number of variables to control. This is a major constraint because, a point will be reached in development where the number of variables to control will

become too many and impractical to use. An alternative, based on reduction of the number of control variables was sought.

A new and alternative approach was developed, defined in the envelope domain. It uses a mathematical formulation, formulated in the envelope domain.

The formulation defines the baseband inter-modulation distortion (IMD) envelope as a function of the input carrier signal envelope. Irrespective of the modulated RF signal, intermodulation distortion envelopes can always be defined as a finite sum of distortion-envelopes multiplied by their control coefficients.

Shown below is an example comparing few number of tones to an increased number of tones

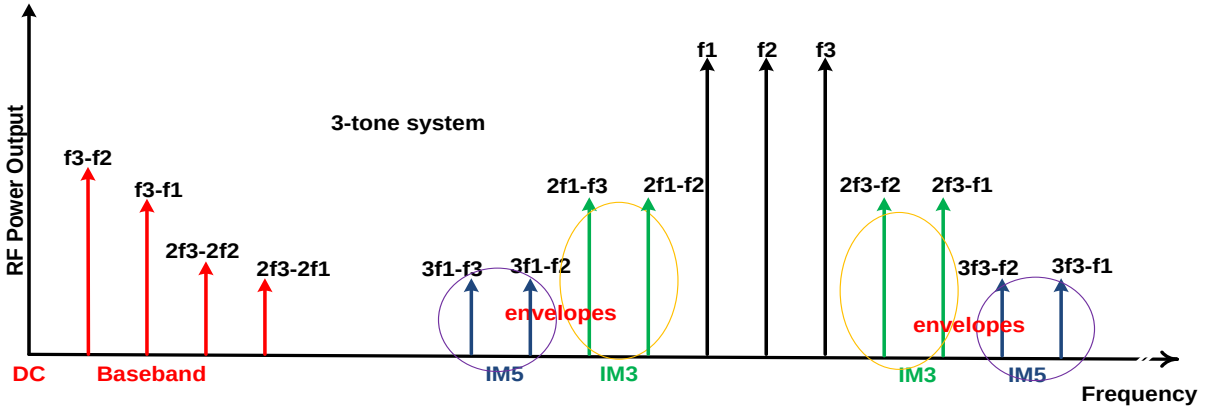

Figure 3.1 (b) showing the number of IM3 and IM5 distortion envelopes in a basic 3-tone system

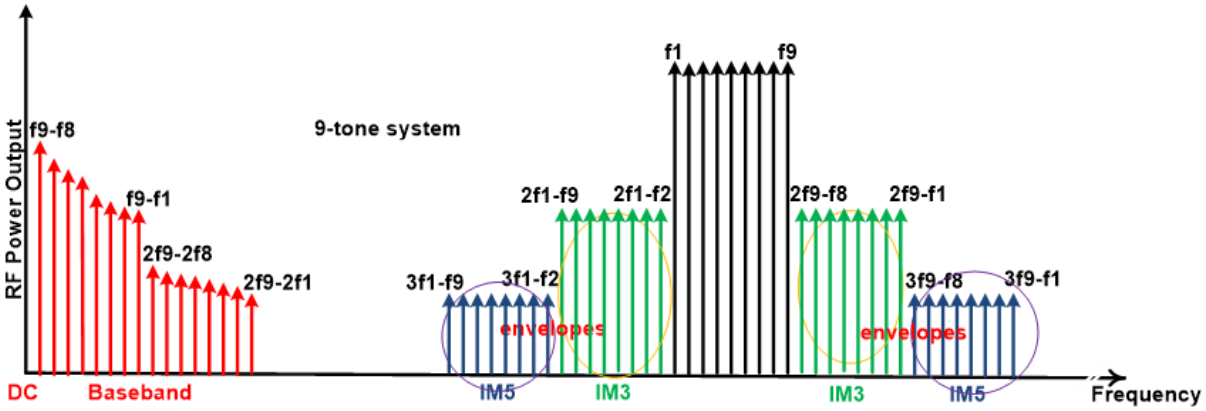

Figure 3.1 (c) showing the number of IM3 and IM5 distortion envelopes in a basic 9-tone system

These coefficients are the keys used to simply optimise the time varying baseband voltage signal. In this formulation, 'engineering' the optimized time-varying baseband voltage signal requires the determination of only a small numbers of constant coefficients. This eases the optimization process because it reduces the number of variables to be determined to a limited set of coefficients. In addition, the baseband specification is formulated not in terms of impedance, but in terms of the desired envelope voltage signal. The key part of this approach is the baseband envelope formulation and control.

3.1.1 Baseband signal and envelope signal mathematical formulation

In this chapter, we will consider a mathematical description for the baseband signal, formulated in the envelope domain. This is the formulation required to achieve the proposed baseband envelope linearization (BEL). It also defines what signals are required to be measured and used to validate the approach. It then addresses the measurement system requirements to undertake this characterization task. Results using the classical 2-tone signals are presented. The global objective of the formulation is then further investigated in subsequent chapter 3, 4 and 5 respectively.

3.1.2 An envelope domain formulation of the required baseband signal

The envelope domain with respect to RF and microwave engineering practically refers to the analysis and representation of mathematical functions and signals with respect to both time and frequency simultaneously. In this chapter the envelope domain is used to mathematically model the behaviour of the RFPA device when subjected to complex modulated input signals and a baseband linearization signal.

3.2 Distortion Modelling

3.2.1 Distortion without baseband signal

Consider a non-linear system shown by the block diagram of figure 3.2.1.

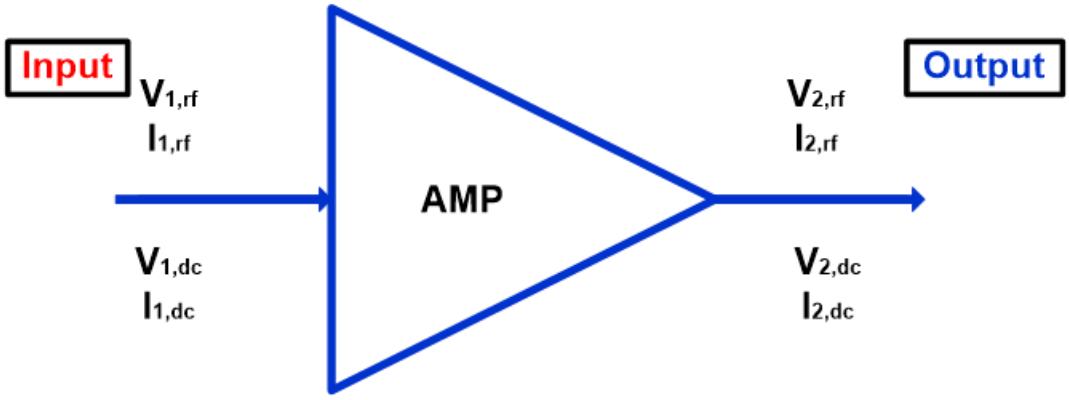

Figure 3.2.1 showing a representation of a non-linear system without baseband signal

Where $V_{1,dc}$ and $V_{2,dc}$ are the DC bias voltages, defined in the envelope domain, at the input bias port represented by the suffix 1, and the output bias port represented by the suffix 2. $V_{1,rf}$ and $V_{2,rf}$ are the time varying carrier RF voltages at the input and output ports. Similarly, $I_{1,dc}$ and $I_{2,dc}$ are the resulting DC currents components at the input and the output ports. $I_{1,rf}$ and $I_{2,rf}$ represents the time varying carrier RF currents components developed at both the input and the output ports. $V_{1,rf}$ can also be represented as

$$V_{1,rf}(t) = M_{1,rf}(t)\cos\left(\omega_c t + \phi_{1,rf}(t)\right) \quad (3.2.1.1)$$

Which is the same as $V_{1,rf}(t) = \frac{M_{1,rf}(t)\, e^{j\omega_c t+\phi_{1,\mathrm{rf}}(t)} + M_{1,rf}(t)\, e^{-j\omega_c t+\phi_{1,\mathrm{rf}}(t)}}{2}$ (3.2.1.2)

where $M_{1,\mathrm{rf}}(t)$ and $\phi_{1,\mathrm{rf}}(t)$ are the magnitude and phase of the modulated input signal respectively, and ω_c is the RF carrier frequency.

This signal can also be presented mathematically in the complex envelope (I-Q) domain as:

$$\hat{V}_{1,rf}(t) = M_{1,rf}(t)\cos\left(\phi_{1,rf}(t)\right) - jM_{1,rf}(t)\sin\left(\phi_{1,rf}(t)\right) \quad (3.2.1.3)$$

Similarly, the RF output current response of the device can be represented as

$$I_{2,rf}(t) = M_{2,rf}(t)\cos\left(\omega_c t + \phi_{2,rf}(t)\right) \quad (3.2.1.4)$$

Which is the same as $I_{2,rf}(t) = \frac{M_{2,rf}(t)\, e^{j\omega_c t+\phi_{2,\mathrm{rf}}(\mathrm{t})} + M_{2,rf}(t)\, e^{-j\omega_c t+\phi_{2,\mathrm{rf}}(\mathrm{t})}}{2}$ (3.2.1.5)

where $M_{2,rf}(t)$ and $\phi_{2,rf}(t)$ are the magnitude and phase of the complex modulated output current respectively, and ω_c is the carrier frequency.

Again, this signal can also be presented mathematically in the complex envelope (I-Q) domain:

$$\hat{I}_{2,rf}(t) = M_{2,rf}(t)\cos\left(\phi_{2,rf}(t)\right) - jM_{2,rf}(t)\sin\left(\phi_{2,rf}(t)\right) \quad (3.2.1.6)$$

In the envelope domain, this carrier output current resulting from the mixing interaction of the voltage stimuli could be given conceptually as follows:-

$$\hat{I}_{2,rf}(t) =$$

$$f\left(\hat{V}_{1,rf}(t), V_{1,dc}\hat{V}_{1,rf}(t), V_{2,dc}\hat{V}_{1,rf}(t), |\hat{V}_{1,rf}(t)|^2\hat{V}_{1,rf}(t), V_{1,dc}|\hat{V}_{1,rf}(t)|^2\hat{V}_{1,rf}(t), V_{2,dc}|\hat{V}_{1,rf}(t)|^2\hat{V}_{1,rf}(t), \ldots\right) \quad (3.2.1.7)$$

These are all the mixing components that produce an envelope signal around the carrier. In summary, this all-complex-alpha-terms representation can be written as

$$\hat{I}_{2,rf}(t) = \sum_{n=0}^{m} \alpha_{2n+1}|\hat{V}_{1,rf}(t)|^{2n}\hat{V}_{1,rf}(t) \quad (3.2.1.8)$$

Coefficient α_{2n+1} is a function of $V_{1,dc}$ and $V_{2,dc}$. Note that

$$|\hat{V}_{1,rf}(t)|^2 = \hat{V}_{1,rf}(t) * \hat{V}_{1,rf}{}^{\#}(t) \quad (3.2.1.9)$$

$$\left|\hat{I}_{2,rf}(t)\right| = \sum_{n=0}^{m} \alpha_{2n+1}|\hat{V}_{1,rf}(t)|^{2n}\left|\hat{V}_{1,rf}(t)\right| \quad (3.2.1.10)$$

Where the alpha-terms are real-numbers and $\hat{V}_{1,rf}{}^{\#}(t)$ is the conjugate of $\hat{V}_{1,rf}(t)$.

The key here is to identify the independent variables, as these are the terms that are required to control the system. The independent variables in this case are:-

$V_{1,dc}$, $V_{2,dc}$ and only $V_{1,rf}(t)$ – the fundamental RF input signal which is a time varying signal. Hence, for a defined DC bias, the equation (3.2.1.8) is a function of the input RF voltage only.

It can be seen from equation (3.2.1.8) that only odd order terms are present in this equation.

The equation (3.2.1.8) represent the distortion model for the RFPA output current model.

3.2.2 Coefficient Extraction

If it is possible to measure the input and output voltage and current envelopes then the coefficients of this model can be extracted. This can be done using a least square technique, which was considered adequate for this formulation.

Consider now equation (3.2.1.8), this equation can be written in matrix form as shown in the equation (3.2.2.3) below.

$$\hat{I}_{p,rf}(t) = \sum_{n=0}^{m} \alpha_{2n+1} |\hat{V}_{1,rf}(t)|^{2n} \hat{V}_{1,rf}(t) \quad (3.2.2.1)$$

in matrix form as

$$y(t) = N u_n(t) \quad (3.2.2.2)$$

Such that

$$y(t) = \hat{I}_{p,rf}(t) \quad (3.2.2.3)$$

The measured RF output current envelopes

Where

$$u_n(t) = \left[\hat{V}_{1,rf}(t) \ldots \left|\hat{V}_{1,rf}(t)\right|^{2n} \hat{V}_{1,rf}(t) \ldots . \left|\hat{V}_{1,rf}(t)\right|^{2n} \hat{V}_{1,rf}(t)\right] \quad (3.2.2.4)$$

The measured RF input voltage envelopes

N is the model coefficient matrix represented as

$$N = \begin{bmatrix} \alpha_1 \\ \cdots \\ \alpha_{2n+1} \\ \cdots \\ \alpha_{2m+1} \end{bmatrix} \quad (3.2.2.5)$$

Such that

$$N = \left(u_n^H(t)u_n(t)\right)^{-1} u_n^H(t)y(t) \quad (3.2.2.6)$$

Hence, the normalised mean squared error (NMSE) is given by equation (3.2.2.7)

$$NMSE(dBc) = 10log_{10}\left\{\frac{\sum_t |y(t)-u_n(t)M|^2}{\sum_t |y(t)|^2}\right\} \quad (3.2.2.7)$$

Hence the extracted current envelope from the model in our own case is given by

$$\hat{I}_{p,rf}(t) = |y(t)|\left(\frac{\hat{V}_{1,rf}(t)}{|\hat{V}_{1,rf}(t)|}\right) \quad (3.2.2.8)$$

And hence

$$\hat{I}_{p,rf}(t) = |u_n(t)|M\left(\frac{\hat{V}_{1,rf}(t)}{|\hat{V}_{1,rf}(t)|}\right) \quad (3.2.2.9)$$

This model can be used to extract RF envelopes magnitude and the envelope phases.

3.2.3 Distortion modelling with baseband signal

Consider again a non-linear system as shown below with baseband $V_{2,bb}$

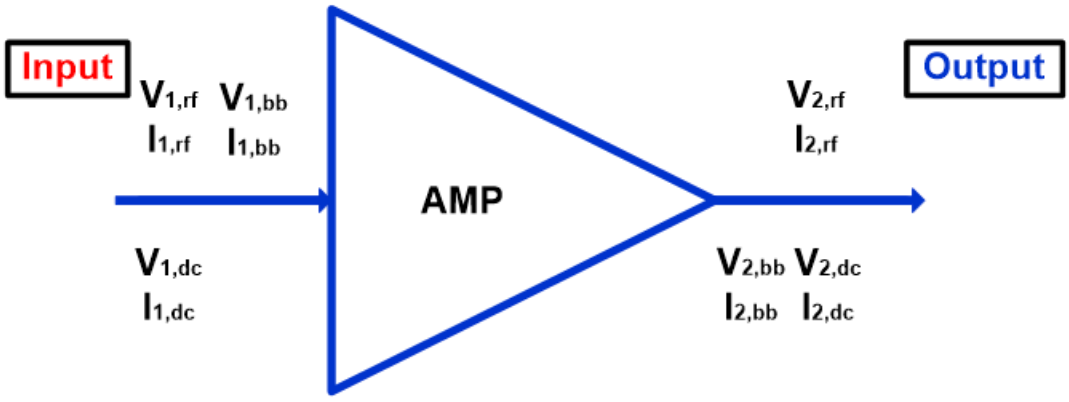

Figure 3.2.3 showing a representation of a non-linear system with baseband signal

Similarly, $V_{2,bb}(t)$, is a time varying component, that can also be represented in the complex envelope (I-Q) domain as

$$\hat{V}_{2,bb}(t) = I(t) + jQ(t) \tag{3.2.3.1}$$

But in this case, $Q(t) = 0$ This is because baseband cannot be used to suppress phase distortion components.

Again, an output current will result at the output port of the device as a result of the mixing interaction of the voltage stimuli.

The key is to identify the number of independent variables just as in the previous model.

The resulting output current can be represented by

$$\hat{I}_{2,rf}(t) = f\left(\begin{matrix}\hat{V}_{1,rf}(t), V_{1,dc}\hat{V}_{1,rf}(t), V_{2,dc}\hat{V}_{1,rf}(t), \hat{V}_{2,bb}(t)\hat{V}_{1,rf}(t), \hat{V}^{\#}_{2,bb}(t)\hat{V}_{1,rf}(t), \left|\hat{V}_{1,rf}(t)\right|^2\hat{V}_{1,rf}(t), . \\ V_{1,dc}\left|\hat{V}_{1,rf}(t)\right|^2\hat{V}_{1,rf}(t), V_{2,dc}\left|\hat{V}_{1,rf}(t)\right|^2\hat{V}_{1,rf}(t), \hat{V}_{2,bb}(t)\left|\hat{V}_{1,rf}(t)\right|^2\hat{V}_{1,rf}(t), \hat{V}^{\#}_{2,bb}(t)\left|\hat{V}_{1,rf}(t)\right|^2\hat{V}_{1,rf}(t).\end{matrix}\right) \tag{3.2.3.2}$$

This represents all the possible mixing process that can produce a signal around the carrier.

Again, this can be written in short form as:-

$$\hat{I}_{2,rf}(t) = \sum_{\substack{i=0\\j=0\\n=0}}^{\substack{m\\l\\k}} \left(\hat{V}_{2,bb}(t)\right)^i \left(\hat{V}^{\#}_{2,bb}(t)\right)^j |\hat{V}_{1,rf}(t)|^{2n}\hat{V}_{1,rf}(t)\alpha_{i,j,2n+1} \tag{3.2.3.3}$$

Where $\alpha_{i,j,2n+1} = f\left(V_{1,dc}V_{2,dc}\right)$ (3.2.3.4)

and $V_{p,bb}$ is the baseband injected at port p.

Also, from equation (3.2.3.3), the independent variables are $V_{1,dc}$, $V_{2,dc}$,$V_{1,rf}$ and $\hat{V}_{2,bb}(t)$.

Only $V_{1,rf}(t)$ and $V_{2,bb}(t)$ are time varying components.

Consider now a specific case (our case) where the baseband voltage is defined as a function of the input signal envelope, as follows:-

$$\hat{V}_{2,bb}(t) = \sum_{i=0}^{k} |\hat{V}_{1,rf}(t)|^{2i}\, \beta_{2l} \tag{3.2.3.5}$$

Where *l* represents higher order distortion cancellation index.

The output current resulting from the mixing interaction of all the voltage stimuli is given as:-

$$\hat{I}_{2,rf}(t) = \sum_{\substack{l=0 \\ j=0 \\ n=0}}^{\substack{m \\ l \\ o}} \left(\sum_{i=0}^{k} |\hat{V}_{1,rf}(t)|^{2i}\, \beta_{2i}\right)^{l} \left(\sum_{i=1}^{k} |\hat{V}_{1,rf}(t)|^{2i}\, \beta_{2i}\right)^{j} |\hat{V}_{1,rf}(t)|^{2n} \hat{V}_{1,rf}(t) \alpha_{i,j,2n+1} \tag{3.2.3.6}$$

$$\hat{I}_{2,rf}(t) = \sum_{\substack{l=0 \\ j=0 \\ n=0}}^{\substack{m \\ l \\ o}} \left(\sum_{i=0}^{k} \beta_{2i}\right)^{l} \left(\sum_{i=0}^{k} \beta_{2i}\right)^{j} |\hat{V}_{1,rf}(t)|^{2(il+ij+n)} \hat{V}_{1,rf}(t) \alpha_{i,j,2n+1} \tag{3.2.3.7}$$

$$\hat{I}_{2,rf}(t) = \sum_{n=0}^{m} |\hat{V}_{1,rf}(t)|^{2n} \hat{V}_{1,rf}(t)\, \chi_{2n+1} \tag{3.2.3.8}$$

Where $\chi_{2n+1} = f(\beta_2, \beta_4, .. \beta_{2k})$ (3.2.3.9)

Similar result to previous observation without baseband injection is observed, but in this case, the coefficients are function of beta terms. From equation (3.2.3.9), 'n' can only assume values starting from 1.

These beta terms are the peculiar coefficients associated with the resulting current as a result of the baseband injection into the system.

Equations (3.2.3.9) and (3.2.1.8), suggests that we could determine a baseband signal to be injected into the device to linearize it.

3.2.4 Baseband voltage engineering

From equation (3.2.3.9), if we consider a case where n=2, hence defining distortion up to the 5th order meaning that we are modelling the current up to the 5th order, our baseband voltage can then be represented as:-

$$\hat{V}_{2,bb}(t) = \beta_0 + |\hat{V}_{1,rf}(t)|^2\beta_2 + |\hat{V}_{1,rf}(t)|^4\beta_4 \quad (3.2.4.1)$$

And hence for analysing the current for the fifth order, we have

$$\hat{I}_{p,rf}(t) = \sum_{n=0}^{3} |\hat{V}_{1,rf}(t)|^{2n}\hat{V}_{1,rf}(t)\,\chi_{2n+1} \quad (3.2.4.2)$$

Where $\chi_{2n+1} = f(\beta_0, \beta_2, \beta_4, .. \beta_{2k})$ (3.2.4.3)

$$\chi_1 = \alpha_{0,0,1} + \beta_0(\alpha_{0,1,1} + \alpha_{1,0,1}) + \beta_0^2\alpha_{1,1,1} \quad (3.2.4.4)$$

$$\chi_3 = \alpha_{0,0,3} + \beta_0(\alpha_{0,1,3} + \alpha_{1,0,3}) + \beta_2(\alpha_{0,1,1} + \alpha_{1,0,1}) + \beta_0\beta_2\alpha_{1,1,1} \quad (3.2.4.5)$$

$$\chi_5 = \alpha_{0,0,5} + \beta_0(\alpha_{0,1,5} + \alpha_{1,0,5}) + \beta_2(\alpha_{0,1,3} + \alpha_{1,0,3}) + \beta_4(\alpha_{0,1,1} + \alpha_{1,0,1})\beta_0\beta_4\alpha_{1,1,1} + 2\beta_0^2\alpha_{1,1,1} \quad (3.2.4.6)$$

From equation (3.2.4.6), it shows that a specifically formulated baseband signal quantified by the appropriate beta coefficients will cause the device to be linearized.

Hence, in this work, the following general envelope formulation for the output baseband voltage envelope signal $\hat{V}_{2,bb}(t)$ is considered as:

$$\hat{V}_{2,bb}(t) = \sum_{p=1}^{q} \beta_{2p}\left|\hat{V}_{1,rf}(t)\right|^{2p} \quad (3.2.4.7)$$

where β_{2p} is the even order voltage component scaling coefficient and q specifies the desired maximum range. A resulting baseband current will be generated which can be represented as:-

$$\hat{I}_{2,bb}(t) = \sum_{n=1}^{m} \alpha_{2n}\left|\hat{V}_{1,rf}(t)\right|^{2n} \quad (3.2.4.8)$$

The motivation for using this formulation lies in the fact that only cancelling odd-order intermodulation terms will be added to the RF output current envelope response. Hence, only the coefficients in equation (3.2.1.8) will be modified such that

$$\alpha_{2n+1}|_{n=1}^{m} = f(\beta_2, \beta_4, \ldots \beta_{2p}, \ldots \beta_{2q}) \quad (3.2.4.9)$$

Consider now a system with intermodulation distortion up to fifth order (m=2). The baseband linearization problem can now be restricted to forth order (q=2), hence equating to

determine the values of β_2 (beta-2) and β_4 (beta-4) that can simultaneously satisfy the two following conditions:

$$\alpha_3 = f(\beta_2, \beta_4) = 0 \quad (3.2.4.10)$$

$$\alpha_5 = g(\beta_2, \beta_4) = 0 \quad (3.2.4.11)$$

and where f and g are unknown generic functions, to be determined empirically.

This equation (3.2.4.7) requires a measurement system that is able to:-

(i). To determine the values of β

(i). Carry out baseband voltage engineering and measurements

(ii). Be able to quantify the values of beta required to cause any device to go linear

(iii). Be able to investigate the behaviour of IM3 and IM5 before and after linearisation

(iv). Be able to investigate the behaviour of the 3rd order and the 5th order coefficients.

(v). Be able to do this in an iterative manner.

This will require a measurement sequence working in a particular flow. In view of this, a flow chart was developed to guide the working of the system as shown in the figure 3.2.4 (a) and 3.2.4 (b).

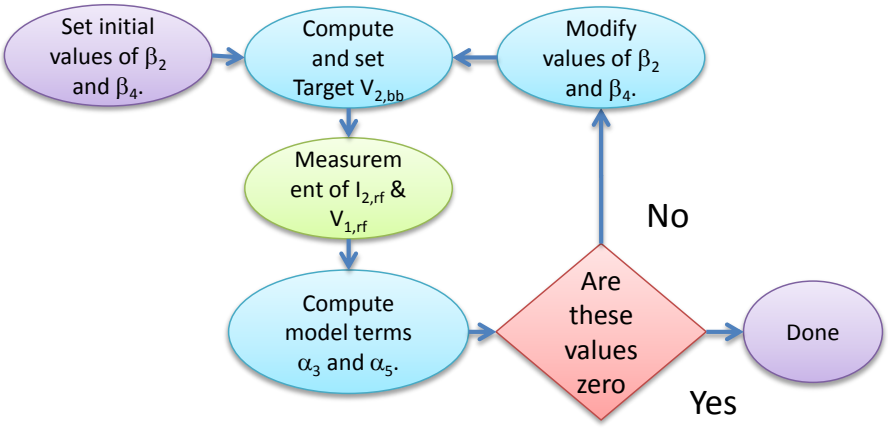

Figure 3.2.4(a) showing inner-loop flow chart for determination of beta linearizing coefficients

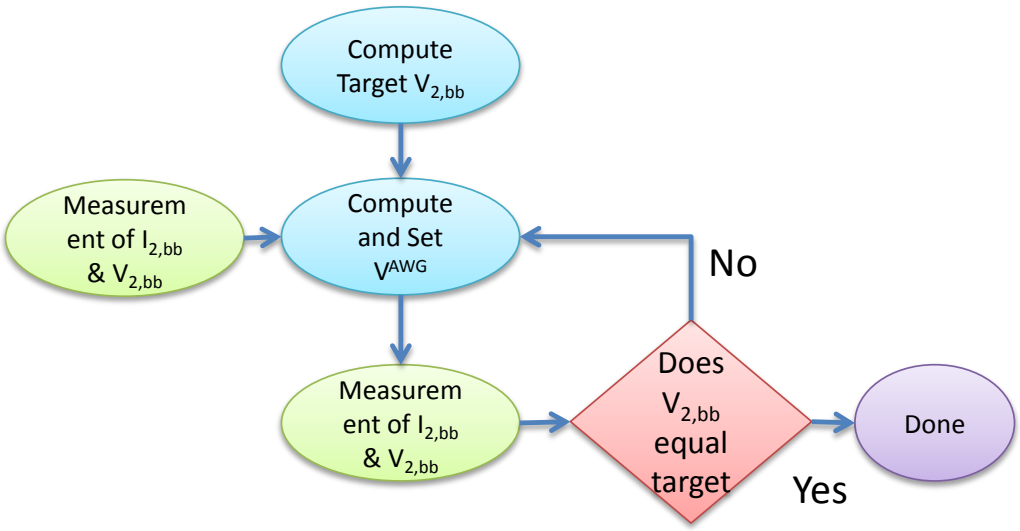

Figure 3.2.4(b) showing outer-loop flow chart for determination linearity

3.2.5 Flow chart real Implementation

Initially, the system is calibrated to determine the values of natural system impedance $Z_s(\omega)$ and load-pull loop gain $G_s(\omega)$, over the desired modulation bandwidth. An iterative process using equation (3.2.5.1) is used to determine the arbitrary waveform generator signal $V_{i+1}^{awg}(\omega)$, that is required to synthesize exactly the desired baseband voltage waveform $V_{2,bb}^{target}(t)$. The measured values of baseband voltage $V_{2,bb}^{meas,i}(t)$ and current $I_{2,bb}^{meas,i}(t)$ at iteration i, are transformed into frequency domain baseband voltage $\tilde{V}_{2,bb}^{meas,i}(\omega)$ and current $\tilde{I}_{2,bb}^{meas,i}(\omega)$, and are then used to compute a new baseband voltage requirement for the arbitrary waveform generator at iteration i+1, also formulated in the frequency domain, using the following equation;

$$V_{i+1}^{awg}(\omega) = (1-w)V_i^{awg}(\omega) + w\left(\frac{V_{2,bb}^{target}(\omega) - Z_s(\omega)I_{2,bb}^{meas,i}(\omega)}{G_s(\omega)}\right) \qquad (3.2.5.1)$$

where w is the static weighting factor. This process is repeated until the desired output baseband target voltage waveform is achieved, within a specified error limit. Typically, when

the desired error limit is set to 1mV, the system converges to the desired targeted baseband voltage within 5-6 iterations.

After this point is engineered, the present values of the distortion coefficients, α_n are determined. If these values are zero, the device is linearized, then the iteration is stopped. If not, the device is not linearized, then new values of the linearization coefficients are determined and the iteration repeated until the device linearizes.

3.3 Measurement system

In recent work, a measurement system was developed to perform baseband load pull using a large signal network analyser (LSNA). This is shown in figure 3.3(a) and a schematic version of it in figure 3.3 (b & c). With this measurement system, it is possible to do open-loop active load-pull. To be able to work with BEL and measure all the components and do the required iteration as highlighted previously, a couple of changes were made to upgrade the measurements system. A few of the key upgrades and why they were included are summarized as follows:-

(i). The baseband amplifier bandwidth was upgraded from 10MHz to 250MHz bandwidth

This was required to be able to utilize the full measurement capability bandwidth of the baseband test bench and hence be able to measure all required components for BEL investigation. Measurement results using the above upgrade is discussed in chapter 5.

(ii). The addition of intelligent control and baseband signal engineering capability Figure 3.3(c) and 3.3(d).

This made it possible to engineer the special baseband injection signals required to linearize the device and hence investigate the linearization coefficients. The result of this is shown in the BEL validation investigation experiment described in chapter 4.

(iii). BEL investigation requires the system to be able to do voltage-pull in addition to its loadpull capability. This was achieved by equation(3.2.5.1). This capability is key to all the measurements required for BEL in this thesis.

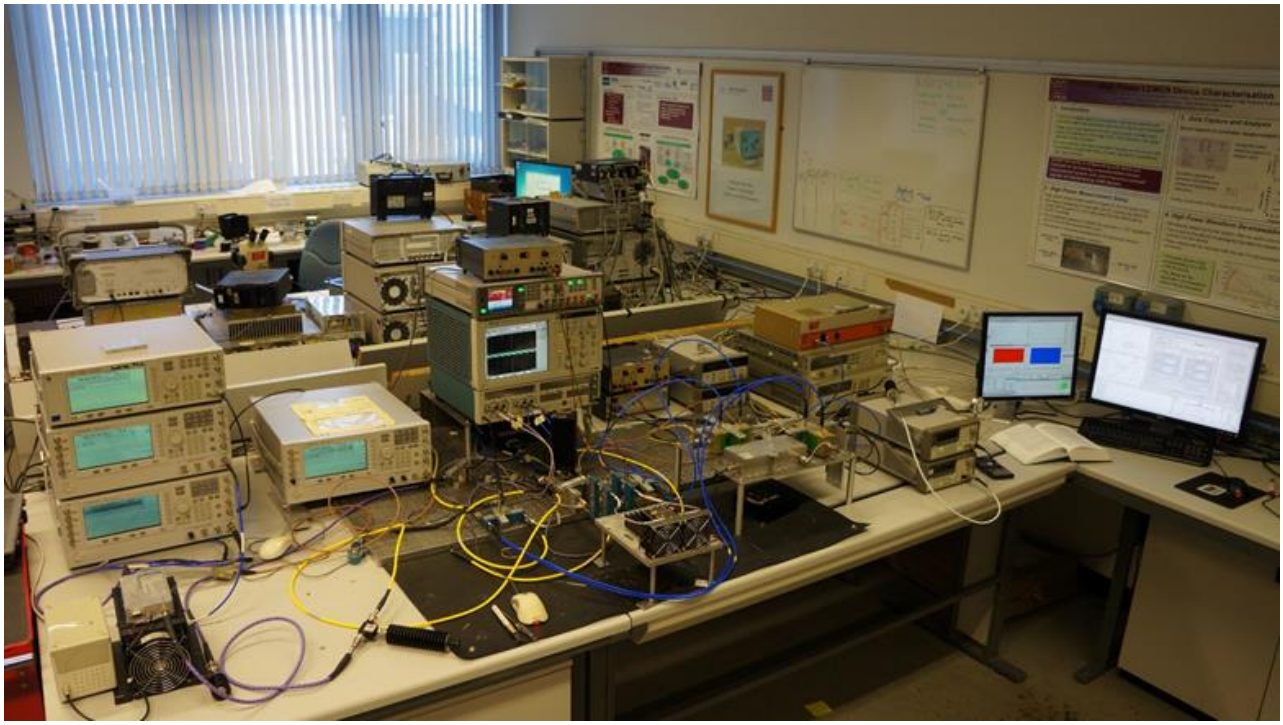

Figure 3.3(a) showing the large signal network analyser measurement system (LSNA).

(iv). BEL required that any arbitrary modulation bandwidth and hence tone-space be measured. Such signals include those with both even numbered and odd numbered tone spacing. With the inherited system, only even numbered tone spacing and a few specific odd numbered tone [11] spacing could be measured until upgraded. The implication of this is that it would have reduced the flexibility of the investigation. This was a result of a stitching problem. This problem was later solved. The solution is shown in appendix B (pg. 188).

(v). Upgrade to allow complete time alignment between the RF waveforms and the baseband waveforms. This is a key requirement to be able to keep the whole system coherent while a measurement is in progress. The implication of this is noise and additional unnecessary distortion in the system. Without this capability, all the experiments performed in this thesis would not have been possible.

A few other ones are included in appendix A (pg. 185) under ‘upgrade’.

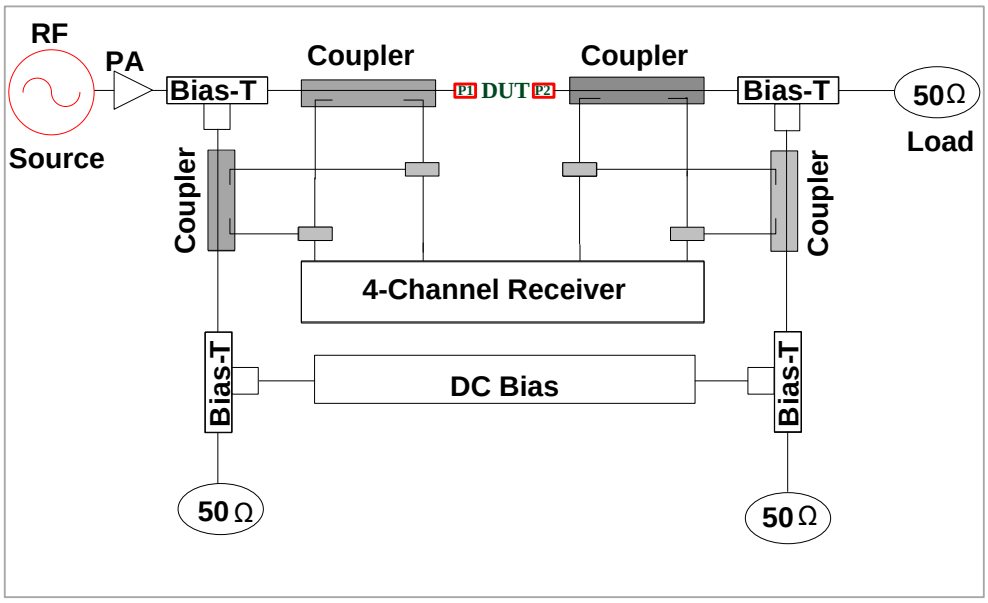

Figure 3.3(b) LSNA before upgrade

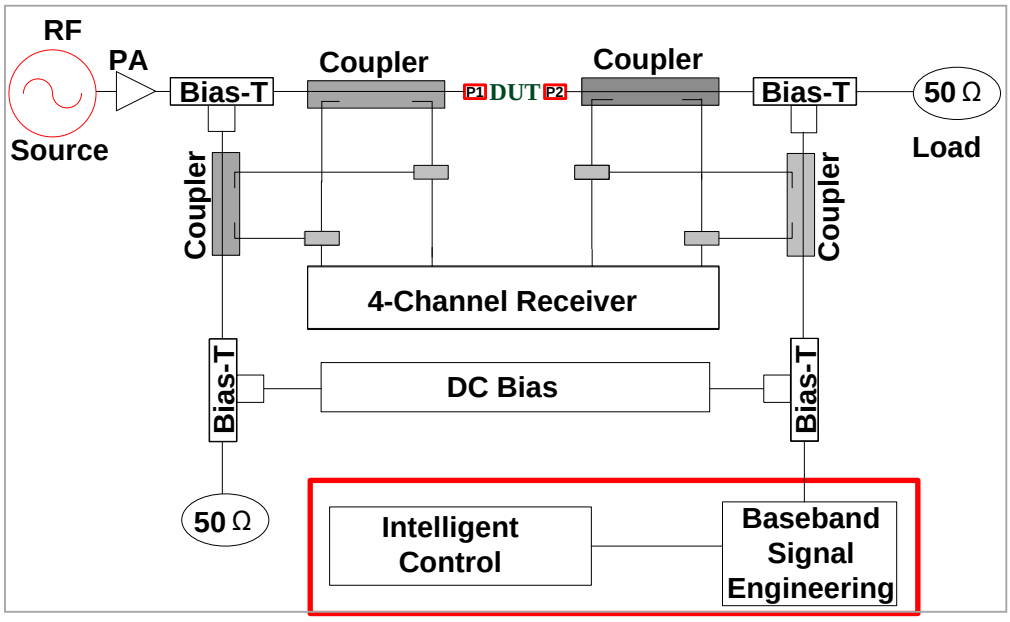

Figure 3.3(c) LSNA after upgrade

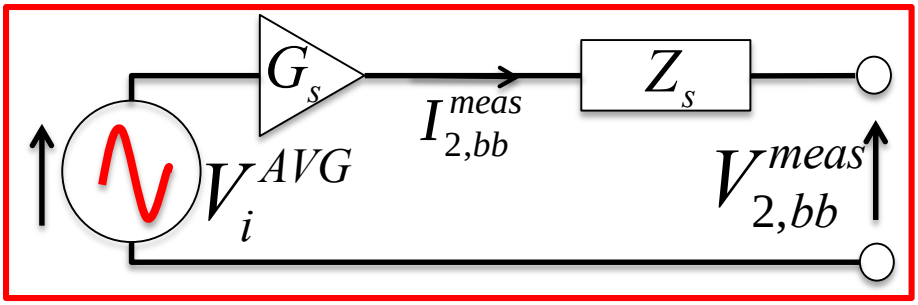

Figure 3.3(d) Baseband Signal Engineering module

$$V_{i+1}^{awg}(\omega) = (1-w)V_i^{awg}(\omega) + w\left(\frac{V_{2,bb}^{target}(\omega) - z_s(\omega)I_{2.bb}^{meas}(\omega)}{G_s(\omega)}\right) \qquad (3.2.5.1)$$

The importance of this upgrade allowed the BEL formulation to be possible. With it, it was possible to iteratively calculate, build the required linearization waveform and compare it to a working equation model until the device linear state is reached. The baseband signal engineering module shown in figure 3.3(d) iteratively engineer the required linearising baseband signal voltage using equation (3.2.5.1)(shown here) with the iterations controlled by the flow charts shown in figure 3.2.4 (a&b). With all these modifications, this measurement system is now able to measure and capture all the various signal components required for this work. Some of these components are shown in the figures 3.3(e) (i-vi).

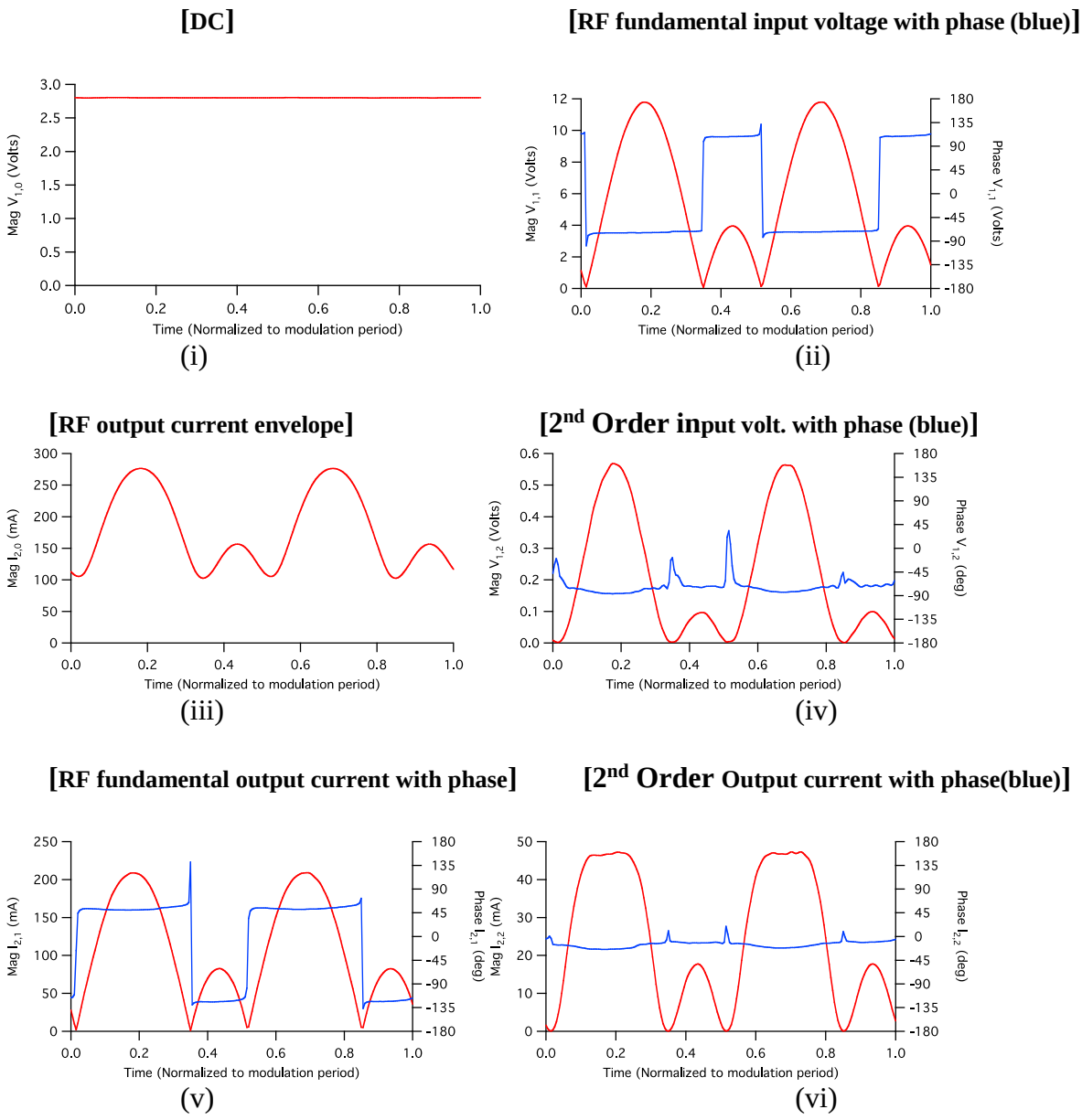

Figure 3.3(e) measured samples of baseband, RF carrier, second order with their phases by the LSNA.

They include measured baseband (DC) (i), RF fundamental input voltage (ii), RF output current envelope magnitude (iii) second order RF input voltage (iv), RF fundamental output current (v), RF second order output current (vi) with their phase plots in blue.

The red and blue curves indicate amplitude and phase respectively. Hence, it was possible to measure particular envelope and phase of particular complex envelope baseband, fundamental and harmonic.

3.3.1 Structure of BEL

BEL is an output port injection technique. The structure is show in the figure below. The engineered baseband signal is injected at the output port of the device (PA) while the device response is captured by the waveform measurement system already described.

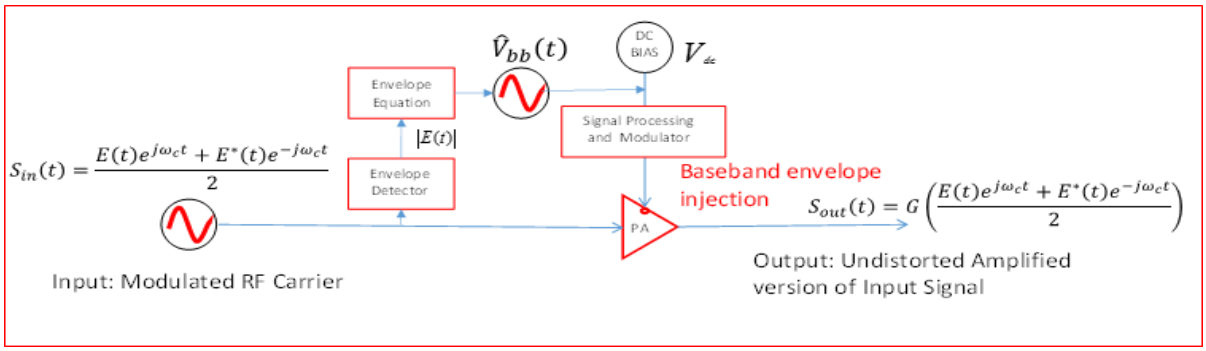

Figure 3.3.1 Structure of the proposed baseband envelope linearizer (BEL)

The advantages of output port injection are:-

(i). The device input signal bandwidth is not changed (not increased).

(ii). The input signal bandwidth is not changed (not increased)

(iii). There is no input-port input signal re-modulation

3.4 Waveform measurements and envelope engineering procedure

To start a measurement, the system is first fully calibrated and vector error corrected.

This calibration is then verified as detailed in appendix C (for calibration, pg.190) for both RF and baseband. The calibration is carried out using a through-reflect and line (TRL) calibration kit over the required RF frequency range to cover the number of harmonics

required. The baseband is also calibrated and fully error corrected to cover the baseband bandwidth and its harmonics.

3.4.1 Engineering a signal waveform

Important points to keep in mind when using this approach.

Concept of waveform engineering with respect to electronics and RFPA design applications,

i. Waveforms can be engineered to emulate electrical component or circuit and their behaviour.
ii. Waveforms can be engineered to emulate electrical quantities like impedance, power, voltage and current.
iii. Waveforms can be engineered to enhance or suppress electrical phenomenon exhibited by circuits or devices in their response to applied stimulus such as distortion.

3.4.2 Initial Step: RF only stimulus

In this step, the definition of the RF requirement, level of compression, and suitable peak envelope power were undertaken. This is called the RF only step. If for instance a measurement is required at a drive level of 1.5dB compression, the RF only step is established at 2.5dB of compression for reasons that will become obvious in in the following discussion. An example of this process is shown below.

3.4.3 Reference baseband short circuit state measurements (initial condition)

For clarity, it is important to show and explain the reference baseband short circuit state.

Using the “BEL” technique, the reference baseband short circuit state is the start or beginning of every measurement and against which we benchmark the various measurements results.

To quantify the level of observed distortion at this state, the measured fundamental envelope transfer function (fundamental RF output current envelope $\hat{I}_{2,rf}(t)$ plotted against the

fundamental RF input voltage envelope $\hat{V}_{1,rf}(t)$) was time aligned to remove the effect of linear delay, and then analysed. A least-squares curve fitting approach already described was used to fit the model, given by equation (3.2.1.8), to the measured envelope transfer characteristic, and hence determine the coefficients α_1, α_3 and α_5 for each case. A typical comparison of the measured and modelled envelope transfer function; $|\hat{I}_{2,rf}(t)|$ versus $|\hat{V}_{1,rf}(t)|$ is shown in Fig. 3.4.3(a)

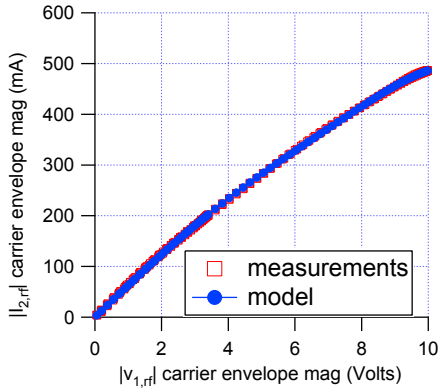

Figure 3.4.3(a)

Hence, for every measurement, it is started off from this point. This is also shown on the Smith Chart in figure 3.4.3(b).

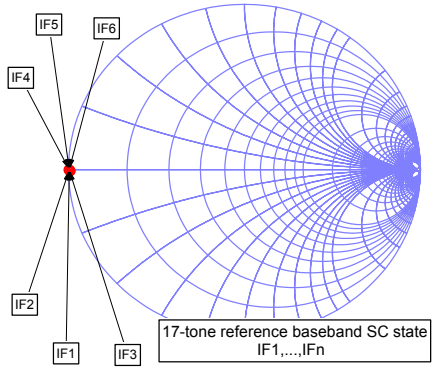

Figure 3.4.3(b) Measured baseband short circuit reference state.

The red dot in the figure 3.4.3(b) represent all the baseband components in the system. In the 17-tone signal for instance, the number of baseband components required for simultaneous

suppression to be used to form linearizing envelopes which is controlled by the linearizing coefficients is 32. This is what is represented in the figure 3 by the red dot. The dot is the convergence of these baseband components which is referred to as intermediate frequencies (IF). IF1 to IF32, only 6 are shown in this case for clarity. For instance, in this 17-tone system, when considering distortion up to the 5^{th} order, the square and the fourth order components of input signal envelope is required to be engineered and controlled by the linearizing coefficients. To suppress IM3, the input signal envelope squared is required, and to suppress IM5, the input signal envelope to the fourth is required. However, since we are applying simultaneous suppression which means suppressing both the IM3 and the IM5 at the same time, we will require the envelope squared plus the envelope fourth which in this case, will give a total of 32 baseband components.

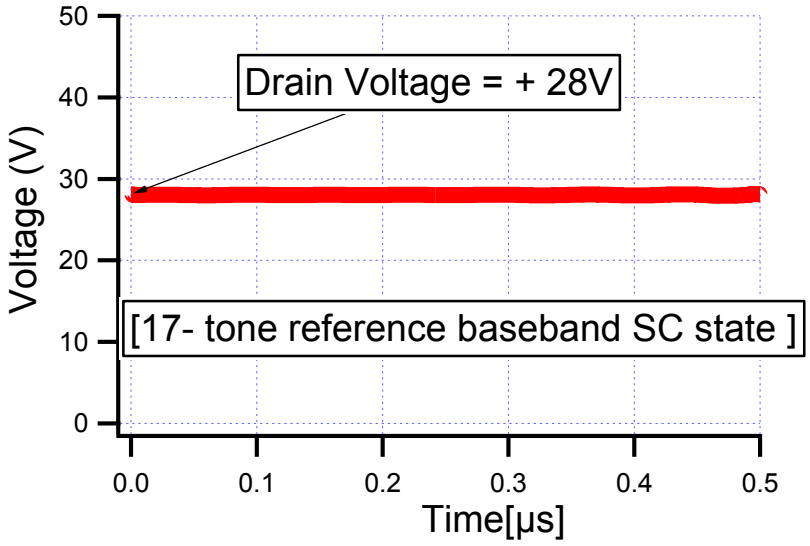

Figure 3.4.3(c) engineered measured reference baseband short circuit state

Also figure 3.4.3(c) shows the engineered reference baseband short circuit state of the device before measurements begin. This is represented by the engineered and measured flat straight red line showing a perfect baseband short circuit in agreement with the one on the position shown on the Smith Chart of figure 3.4.3(b). Every baseband reference state is established as

shown. Note this is the result obtained when $\beta_2 = 0$ and $\beta_4 = 0$, the reference baseband short circuit case.

3.4.4 Device linear state measurements (final state)

This state is established when the device has been linearized. It is the state achieved when the linearity behaviour of the device is considered to be satisfactory as regards the goal of the investigation. This is done using equation (3.2.4.7) which defines $\hat{V}_{2,bb}(t)$. It involves the process of using the linearizing coefficients when β_2 and β_4 are not equal to zero. An initial guess of the values is made and the iterative process is run. The result given by the measurement system of this iterative measurement determines what the next values will be. The revised coefficients are used and measurement repeated until the required linearity is achieved. At the linear state, when the measured fundamental envelope transfer function is plotted, it should give a straight line through the origin as shown in the figure 3.4.4. Additional plots can then be generated depending on the requirements and goals of the experiment. The linearizing baseband signal can also be plotted depending on the signal complexity.

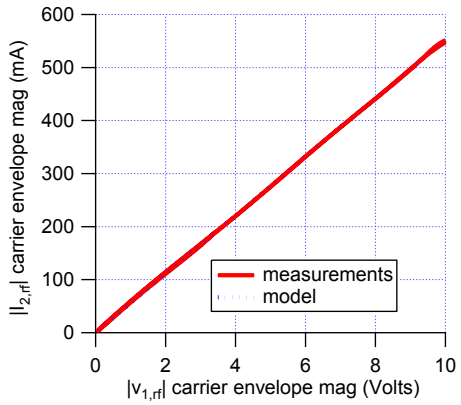

Fig. 3.4.4 showing a linear state envelope dynamic transfer characteristics.

As a measurement worked example and formulation validation, the results of a measured 2-tone excitation signal is shown in the following section.

3.5 Measurement example (2-tone modulation)

Consider now an example where a classical two-tone modulated signal is utilized. In this measured example, a commercially available 10W, GaN-on-Si device was used. It was perturbed with a 2-tone 8MHz bandwidth modulated excitation. The device was biased in class AB delivered a peak envelope power of approximately 38dBm.

3.5.1 RF Only State Plots: - Before engineering the reference baseband short circuit state

The task here was to determine the device pre-initial conditions with the baseband components 'un-engineered'. The results are shown in figures 3.5.1(i-v).

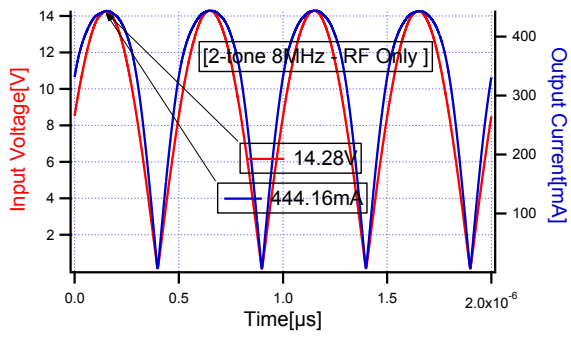

Figure 3.5.1: (i) measured RF input voltage/output current envelopes

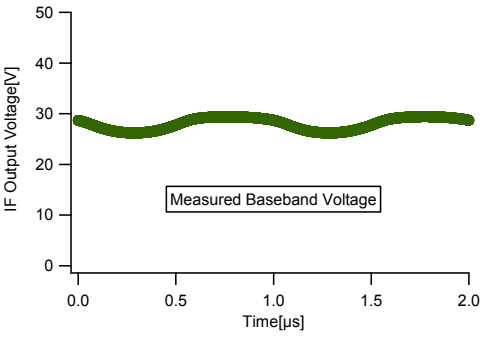

(ii) Measured baseband Voltage

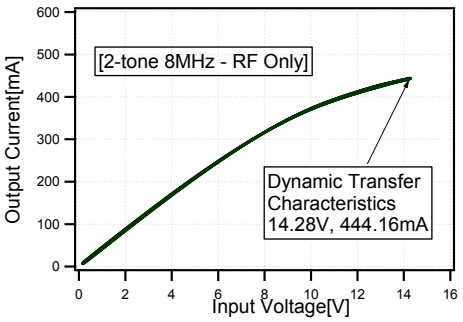

(iii) Measured compressed RF envelope dynamic transfer characteristics

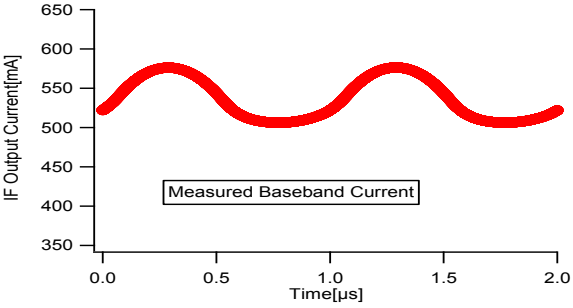

(iv) Measured baseband current

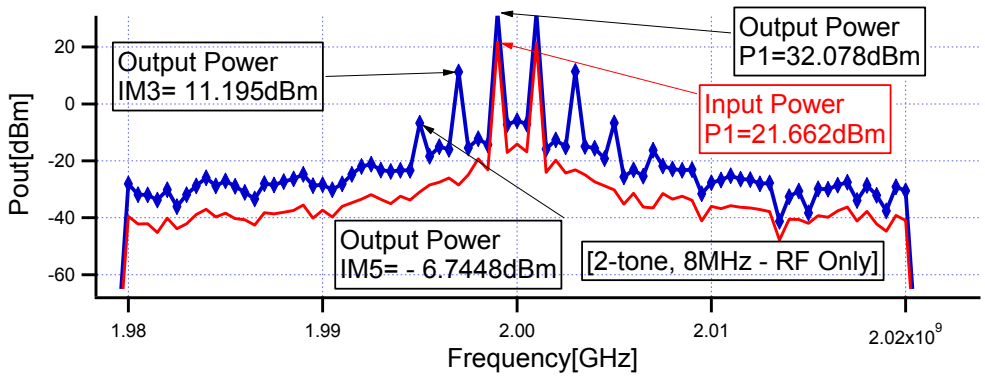

(v) Measured traditional RF input power – output power spectral distribution

The figures in 3.5.1(i-v), show the device pre-initial conditions. The pre-initial condition is the step before the reference baseband short circuits step. Graph-plots (i) & (iii) show the input voltage/output current envelopes and the envelope dynamic transfer characteristics. These are used as visual linearity condition tracer as will be seen in other plots of its kind. While graph-plots (ii) & (iv) show the simple visual of the baseband voltage and current at this state. Graph-plot (v) show the input/output power spectrum. This is a visual plot that also helps to indicate the level of distortion, linearity achieved and visual spectral conditions. With these plots, a decision can be made if the device has been successfully compressed to a level considered satisfactory for the required measurements to commence.

3.5.2 Engineered Reference Baseband Short Circuit State measurements result

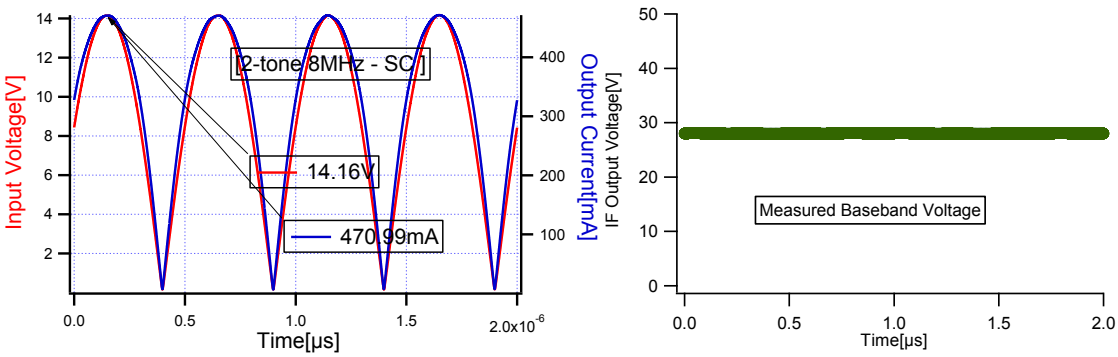

Figure 3.5.2: (i) Measured RF input voltage - output current envelopes

(ii) Measured Baseband Voltage

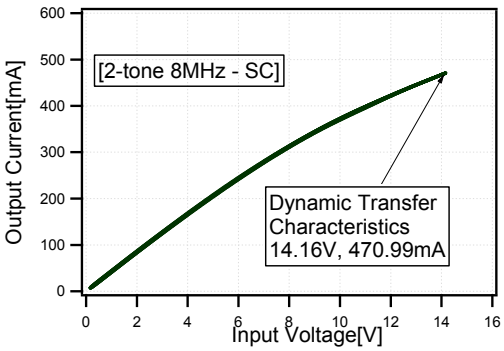

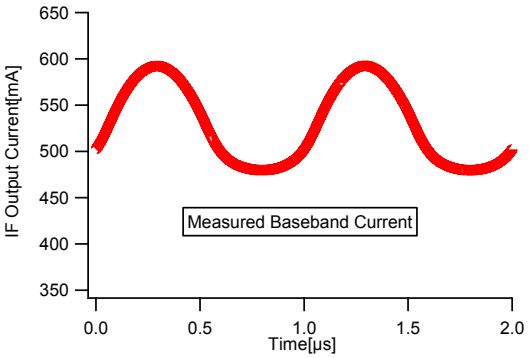

(iii),-Measured Compressed RF Envelope dynamic transfer characteristics

(iv) Measured Baseband current

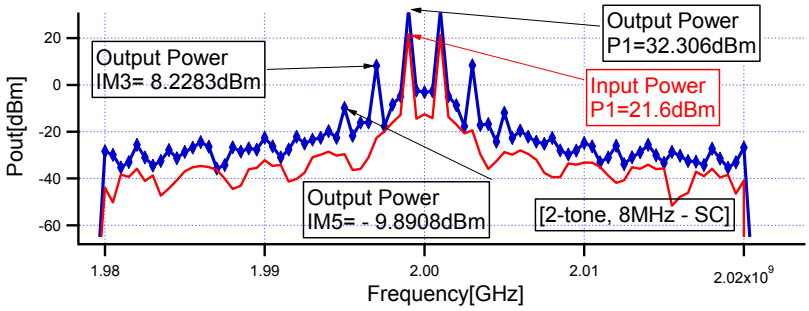

(v) Traditional Measured RF input power – output power spectra

The figures in 3.5.2(i-v), show the device baseband reference short circuit conditions. This is beginning of the measurements. This state is established so that when the device has become linearized, a comparison can be made between the linear state and this present state. The importance is that it helps to determine how much linearity has been achieved. The graph-plots (i) & (iii) show the input voltage/output current envelopes and the envelope dynamic transfer characteristics. While graph-plots (ii) & (iv) show the simple visual of the baseband voltage and current at this state. Graph-plot (v) show the input/output power spectrum. This is a visual plot that also helps to determine the level of distortion, linearity achieved and visual spectral conditions.

3.5.3 Linear State measurements result

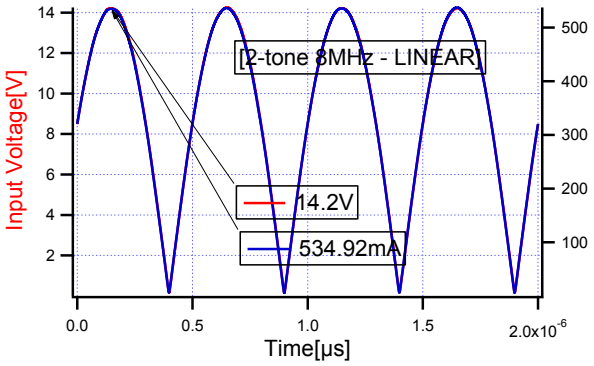

Figure 3.5.3: (i) Measured linear RF input voltage - output current envelopes

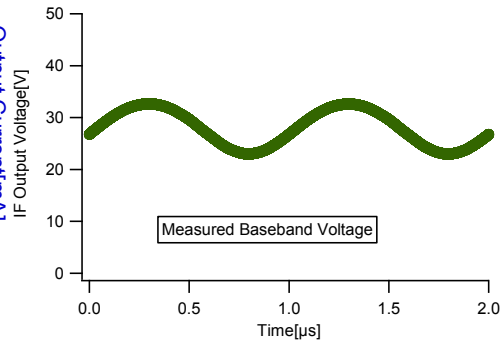

(ii) Measured linearizing Baseband Voltage

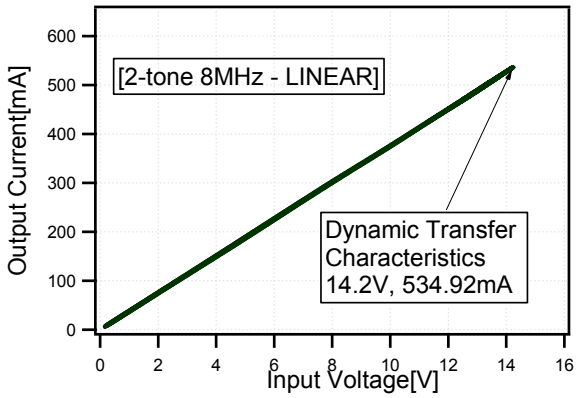

(iii) Measured linear RF Envelope dynamic transfer characteristics

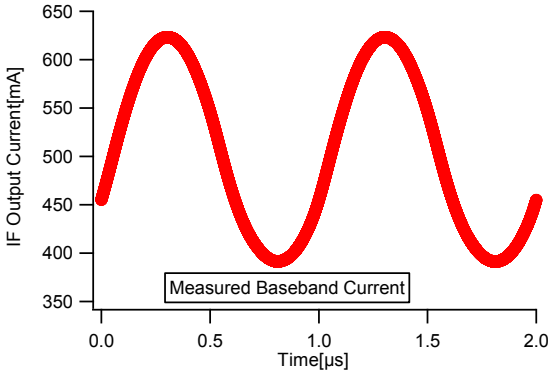

(iv) Measured Baseband current

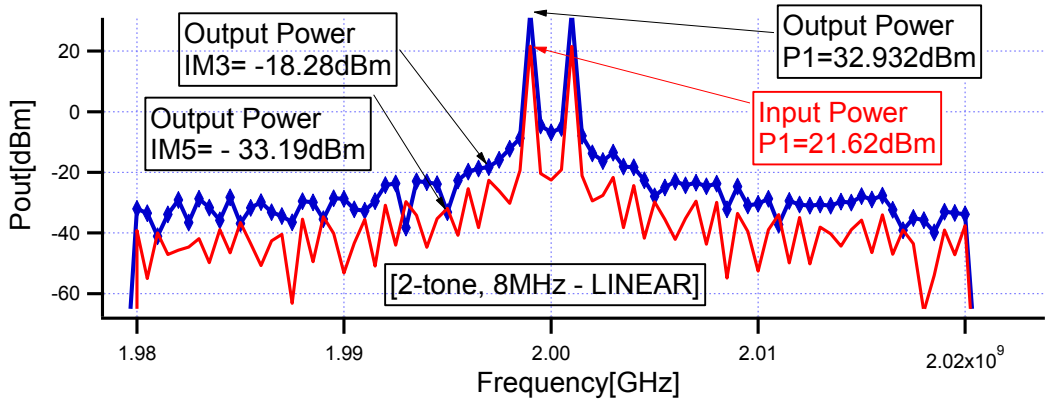

(v) Measured Traditional RF input power – output power distribution spectrum

Figures 3.5.1, 3.5.2 and 3.5.3 show in summary the results obtained for the measured, 2-tone modulated RF, 8MHz bandwidth signal, when applied to a 10W GaN-on-Si device. These figures describe the process from the pre-initial condition (RF only), initial condition (reference baseband short circuit state) to the final condition called the linear state. The linear state is reached after the required baseband signal has been engineered and injected into the device to linearize it. All these conditions are shown in figures 3.5.1, 3.5.2 and 3.5.3 respectively. Once the device is in its linear state, this is the end of the measurements.

The importance of these 3 stages is that after the device is linearised, it is possible to determine how much linearity has been achieved by simple comparison. For instance, the graph-plots (i) & (iii) in all the figures, show the input voltage/output current envelopes and the envelope dynamic transfer characteristics which convey a progressive linear state message. The visual linearity condition shown here is that the input voltage/output current envelopes have lined-up on each other perfectly while the envelope dynamic transfer characteristics has now become a straight line through the origin. This indicates that the device has been linearised successfully. The graph-plots (ii) & (iv) in all figures show the simple visual of the baseband voltage and current up until when the device was linearised. Graph-plot (v) in all the figures show the input/output power spectrum. Graph-plot (v) indicate the levels of distortion, linearity achieved and visual spectral regrowth conditions if there are any.

For instance, in this case for a two tone envelope, a simultaneous harmonic suppression of approximately 50dBc suppression has been achieved, a figure very close to the dynamic range of the measurement system.

3.6 Baseband impedance to voltage engineering

3.6.1 Automation control

In this section, we discuss the difference and need to move from baseband impedance waveform engineering - recent work to baseband envelope voltage waveform engineering present (new) work and hence BEL. With baseband impedance waveform engineering, a few things are worthy of note when compared to envelope baseband voltage waveform engineering. In an experimental measurement some of these things include;

(i). The required level of intermodulation distortion defined for the system and experiment.

This is the level of distortion required to investigate by the experiment. This could be up to the 3^{rd}, order (IMD3), 5^{th} order (IMD5), 7^{th} order (IMD7) or any order required for investigation

(ii). The number of variables needed to be used to control the defined level of distortion.

This is usually related to the level of distortion investigated as defined in (i). With BEL, the number of variables required to suppress any level of IMD is finite and does not scale with the number of tones in the modulation. This is not so with impedance engineering,

(iii). Sequence of control for the variables defined.

With BEL, this could be semi-automatic, automatic or manual because of the reduced number of variables required to be controlled during the experiment. Only manual exercise is possible with impedance control.

(iv). Expected or anticipated level of distortion suppression.

This cannot be exactly pre-determined, but can be assumed and hoped for based on previously achieved results and the technique used. Partially, can also depend on experience.

(v). The baseband impedance to be targeted and the order of distortion.

With BEL, because it is defined in the envelope domain, it is possible to simultaneously suppress or eliminate all the planned order of distortion all at the same time. This is not possible with impedance engineering, and summarised in the table 3.6.1.

# of tones	IM3	IM5	# of variables to control		# of variables to control	
			Impedance control	Simultaneous suppression	envelope control	Simultaneous suppression
2	1	1	1	No	1	Yes
3	2	2	4	No	2	Yes
5	4	4	8	No	2	Yes
7	6	6	12	No	2	Yes
9	8	8	16	No	2	Yes
11	10	10	20	No	2	Yes
13	12	12	24	No	2	Yes
17	16	16	32	No	2	Yes

Table 3.6.1 compares impedance and envelope approaches.

(vi). The level of compression to produce the required distortion level.

This is usually defined as either 1dB, 2dB into compression, It is actually user and measurement specific.

(vii). Possible limitations to the experiment and measurements.

Limitation could arise from either considering the number of tones defined for the modulation, the scaling-up of the number of tones, modulation bandwidth, or the type of device and so on. As discussed in previous chapters, BEL is completely immune to all of these.

(viii). Mathematical model.

As the design or measurement environment requirements changes such as tone complexity, device or bandwidth complexity, the equation models do not need to be modified each time there is a change of any parameter, as already shown chapters 4 and 5 respectively. . This is of great importance and a requirement for robustness.

(ix). Iterative method.

BEL is an iterative technique that definitely converges after 5 or a maximum of 6 very fast iterations, independent of stimulus or environment changes.

In proper perspective for instance, once the inter-modulation distortion order has been defined for any experiment, no matter what happens next, the number of variables required to control the resulting distortion remains unchanged. This is a very powerful reason for using BEL. This is because, BEL does not seek to suppress inter-modulation distortion (IMD) on individual spectral distortion component basis. This would have been particularly difficult to do as the number of modulation tones increase. Take for instance, (impedance engineering) in a 2-tone system, the basic IMD3 is a single spectral line on either side of the carrier each having a single and separate impedance. Similarly, the basic IMD5 is a single spectral line on either side of the carrier and with each having its own separate impedance. When the number of tones increases for example to a 17-tone signal, the basic IMD3 increases to 16 spectral lines on either side of the main carrier channel with each of these spectral lines having their separate individual impedances. So for the 2-tone signal, it will be easier to suppress the IMD3 than for the 17-tone signal which will now have 16 IMD3 spectral lines and 16 IMD5 spectral lines.

In addition, this means that the baseband impedances required to suppress IMD3 will be different from the baseband impedances required to suppress IMD5. In the impedance engineering regime, these two linearizing baseband impedance can only be applied at

separate times and not simultaneously. This means, in a system with 17-tone signal, to suppress IMD3 will require a minimum of 16 baseband impedances to be synthesised and applied at a time different from another 16 required for IMD5. Hence different impedances for within IMD3 suppression and completely different from those required for IMD5 suppression. The implication of this is the need to choose which IMD to suppress (either IMD3 or IMD5) while forgoing the other until another measurement exercise. This is one of the limitations of impedance engineering suppression. However, with BEL, all these problems are solved completely. With any number of tones ‘n’, only 2 variables are required to suppress up to IMD5. In addition to this, the application allows the suppression exercise to be applied simultaneously and at the same time within the same single measurement exercise.

From the information in the table 3.6.1, and from the experiments and measurements carried out and documented in this thesis, it is confirmed that if for example, a fifth order system is considered, no matter the number of tones in the modulation, using BEL, the number of variables to control is a maximum of 2 and a minimum of 1 variable in order to suppress/eliminate the inter-modulation distortion.

So because of this, it is now possible to automate this process since the number of variables are considerably reduced, compared with baseband impedance suppression techniques.

3.7 Chapter summary

In this chapter it was shown that when considering the operation of a non-linear system in the envelope domain it is possible to derive a mathematical equation that can be used to describe the form of the signal necessary to eliminate AM/AM distortion. A key feature of this envelope formulation is that it requires the determination of only a small number of coefficients since the complexity of the signal is accounted for directly.

In order to investigate the validity of this approach a large signal measurement system capable of performing RF voltage and current waveforms measurements while also engineering the RF voltage stimuli was required. To achieve this, a previously developed RF system was upgraded. The capability of this upgraded system was highlighted by showing the sequence of measurements and associated data analysis and presentation that needs to be undertaken to establish and demonstrate the functionality of the BEL concept.

In the subsequent chapters this system will be used to perform a more detailed and systematic investigation of the BEL concept.

3.8 References

[1] Wood, J.; Lefevre, M.; Runton, D.; Nanan, J.-C.; Noori, B.H.; Aaen, P.H., "Envelope-domain time series (ET) behavioral model of a Doherty RF power amplifier for system design," Microwave Theory and Techniques, IEEE Transactions on , vol.54, no.8, pp.3163,3172, Aug. 2006, doi: 10.1109/TMTT.2006.879134.

[2] Huadang, Wang; Jngfu, Bao; Zhengde, Wu, "Multislice behavioral modeling based on envelope domain for power amplifiers," Systems Engineering and Electronics, Journal of , vol.20, no.2, pp.274,277, April 2009.

[3] Maoliu Lin; Zhe Zhang; Xiaojian Ding; Zhiwei Yang, "Envelope domain method characterizing RF nonlinear system excited with a two-tone," Communications and Information Technology, 2005. ISCIT 2005. IEEE International Symposium on , vol.2, no., pp.797,800, 12-14 Oct. 2005, doi: 10.1109/ISCIT.2005.1566987.

[4] Williams, D.J.; Leckey, J.; Tasker, P.J., "Envelope domain analysis of measured time domain voltage and current waveforms provide for improved understanding of factors effecting linearity," Microwave Symposium Digest, 2003 IEEE MTT-S International , vol.2, no., pp.1411,1414 vol.2, 8-13 June 2003.
doi: 10.1109/MWSYM.2003.1212636.

[5] Wood, J.; Lefevre, M.; Runton, D., "Application of an Envelope-Domain Time-Series Model of an RF Power Amplifier to the Development of a Digital Pre-Distorter System," Microwave Symposium Digest, 2006. IEEE MTT-S International , vol., no., pp.856,859, 11-16 June 2006, doi: 10.1109/MWSYM.2006.249809.

[6] Yichi Zhang; Maoliu Lin, "Evaluation of envelope-domain dynamic X-parameter model based on variable-carrier-frequency analysis," Millimeter Waves (GSMM), 2012 5th Global Symposium on , vol., no., pp.236,240, 27-30 May 2012
doi: 10.1109/GSMM.2012.6314044.

[7] Zenteno, E.; Isaksson, M.; Wisell, D.; Keskitalo, N.; Andersen, O., "An envelope domain measurement test setup to acquire linear scattering parameters," ARFTG Microwave Measurement Symposium, 2008 72nd , vol., no., pp.54,57, 9-12 Dec. 2008, doi: 10.1109/ARFTG.2008.4804287.

[8] Ogboi, F.L.; Tasker, P.J.; Akmal, M.; Lees, J.; Benedikt, J.; Bensmida, S.; Morris, K.; Beach, M.; McGeehan, J., "A LSNA configured to perform baseband engineering for device linearity investigations under modulated excitations," Microwave Conference (EuMC), 2013 European , vol., no., pp.684,687, 6-10 Oct. 2013.

[9] Youjiang Liu; Yinong Liu; Banghua Zhou, "Miss-Tuned Envelope Injection for 2.1GHz HPA Based on Polynomial Model," Wireless Communications Networking and Mobile Computing (WiCOM), 2010 6th International Conference on , vol., no., pp.1,5, 23-25 Sept. 2010, doi: 10.1109/WICOM.2010.5600782.

[10] Hong-guang Xu; Qin-yu Zhang; Mao-liu Lin; Huan Wang; Xiao-Lei Li, "An application of envelope analysis for UWB signal acquisition," Communications and Information Technology, 2005. ISCIT 2005. IEEE International Symposium on , vol.2, no., pp.855,858, 12-14 Oct. 2005, doi: 10.1109/ISCIT.2005.1567001.

[11] Muhammad Akmal; “An enhanced modulated waveform measurement system”. A thesis submitted to Cardiff University in candidature for the degree of doctor of philosophy at the centre for high frequency engineering. School of engineering. November 2011.

CHAPTER FOUR

BEL - COMPLEX MODULATION

4.1 3-tone modulated RF signal

In order to use BEL for complex modulation such as 'real' life signals, a deeper understanding is required. A 3-tone modulated signal was preferred (as a starting point) because the knowledge gathered from its investigation can be transferred to more complex signals. One of these complexities include research on signals with various peak-to-average-power ratio (PAPR). Examples of this are 3-tone, 5-tone, 9-tone and n-tone, modulated signals. Another complexity variation include research on varying the modulation bandwidth. The idea was to start with a relatively simple signal and then increase the signal complexity.

4.2 3-tone investigation - envelope measurements analysis and results

In this section, a 3-tone input RF envelope represented by $V_{1,rf}(t)$ at the device input port was measured. This measured 3-tone modulated input RF voltage signal shown in figure 4.2.1. is described by equation (3.2.1.1) shown here.

$$V_{1,rf}(t) = M_{1,rf}(t)\cos\left(\omega_c t + \phi_{1,rf}(t)\right) \qquad (3.2.1.1)$$

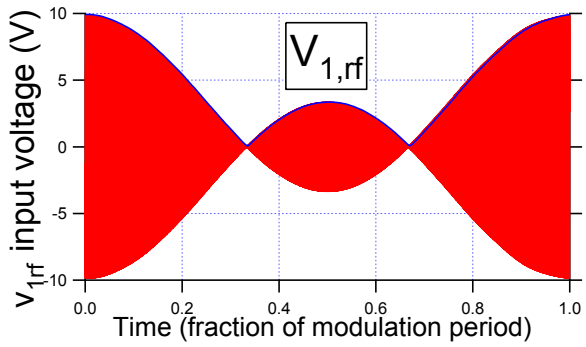

Fig 4.2.1 Measured 3-tone modulated RF input voltage

where $M_{1,rf}(t)$ and $\phi_{1,rf}(t)$ are the magnitude and phase of the modulated input signal respectively, and ω_c is the RF carrier frequency.

The measured 3-tone RF output current is shown in figure 4.2.2. is described by equation (3.2.1.4).

$$I_{2,rf}(t) = M_{2,rf}(t)\cos\left(\omega_c t + \phi_{2,rf}(t)\right) \qquad (3.2.1.4)$$

where $M_{2,rf}(t)$ and $\phi_{2,rf}(t)$ are the magnitude and phase of the complex modulated output current respectively, and ω_c is the carrier frequency.

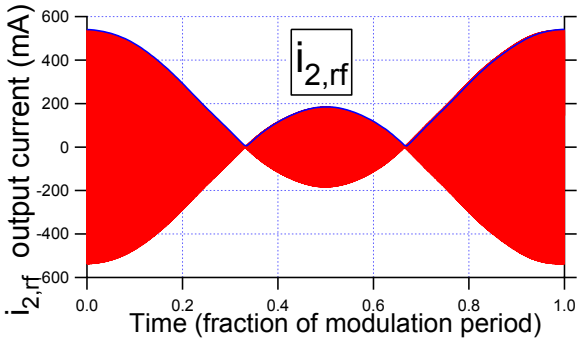

Fig.4.2.2 Measured 3-tone modulated RF output current signal plotted against time.

Mixing analysis tells us that if the baseband voltage, $V_{2,bb}(t)=0$, the memory-less non-linear envelope transfer characteristic between the input voltage envelope $\hat{V}_{1,rf}(t)$ and the output current envelope $\hat{I}_{2,rf}(t)$ is described by equation (3.2.1.8).

$$\hat{I}_{2,rf}(t) = \sum_{n=0}^{m} \alpha_{2n+1} \left|\hat{V}_{1,rf}(t)\right|^{2n} \hat{V}_{1,rf}(t) \qquad (3.2.1.8)$$

where α_1 represents the linear gain of the system, α_3 quantifies the level of third order intermodulation distortion, α_5 quantifies the level of fifth order intermodulation distortion, and so on, up to the desired maximum order m.

Also the output baseband voltage envelope signal $\hat{V}_{2,\mathrm{bb}}(\mathrm{t})$ required to linearize the device is represented in the same manner by equation (3.1.0.14).

$$\hat{V}_{2,bb}(t) = \sum_{p=1}^{q} \beta_{2p} \left|\hat{V}_{1,rf}(t)\right|^{2p} \qquad (3.1.0.14)$$

where β_{2p} is the even order voltage component scaling coefficient and q specifies the desired maximum range.

4.3 Experimental Setup

For this experiment, intermodulation distortion up to fifth order (m=2) was considered. Therefore, the baseband linearization signal included maximum 4th order (q=2) components.

The measurement system described earlier in chapter 3 was calibrated to the device package plane using a custom built 50 Ω TRL test fixture, - over a 50MHz baseband bandwidth and over a 100 MHz bandwidth around each of the RF components (fundamental and spectral components). Using a 3-tone signal with a uniform 1 MHz tone spacing, modulated excitation signal with peak-to-average power ratio (PAPR) of 4.77dB and 2GHz center frequency, the GaN device was biased in class AB, with RF fundamental and all harmonic frequencies terminated into a passive 50Ω. The device used was a 10W - Cree GaN HEMT GaN-on-SiC device. Drain and gate bias voltages were 28V and -2.8V respectively, giving a quiescent drain current of approximately 20% I_{DSS}. The device was compressed to 1.5dB of compression. The load condition at 1.5dB of compression (exhibited 5th order distortion), although not quite optimal (for 7th order distortion which was exhibited at approximately 2dB

of compression), was considered sufficiently close (to 7th order system) for this (5th order linearization) demonstration.

4.4 Reference baseband short circuit state and analysis

The measured fundamental RF input voltage envelope $\hat{V}_{1,rf}(t)$ and fundamental RF output current envelope $\hat{I}_{2,rf}(t)$ (which is the direct response of the fundamental input voltage) magnitudes are shown in the figure 4.4(a). Also shown in figure 4.4(b) is the fundamental RF input voltage envelope $\hat{V}_{1,rf}(t)$ phase and the fundamental RF output current envelope $\hat{I}_{2,rf}(t)$ phase, respectively.

Complex envelope magnitude **Complex envelope phsae**

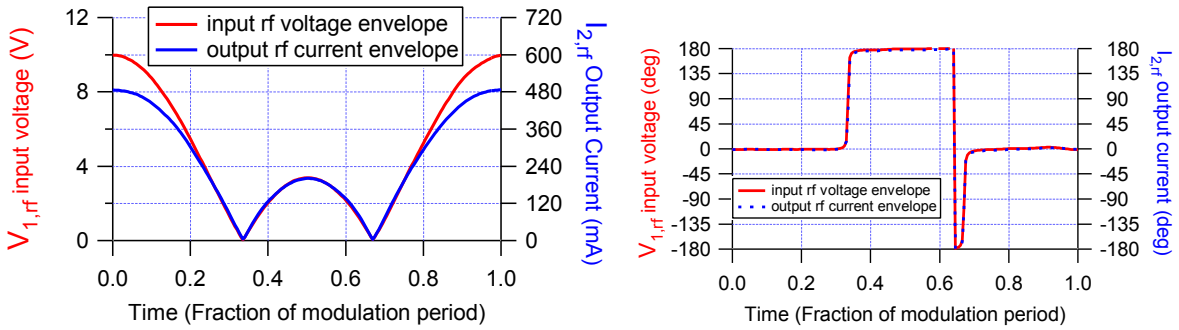

(a). (b)

Fig. 4.4. Complex (a) magnitude and (b) phase of the time aligned, measured fundamental input signal voltage and current.

To quantify the level of observed distortion, the measured fundamental envelope transfer function (fundamental RF output current envelope $\hat{I}_{2,rf}(t)$ plotted against the fundamental RF input voltage envelope $\hat{V}_{1,rf}(t)$) was time aligned to remove the effect of linear delay, and then analyzed. A least-squares curve fitting approach was used to fit the equation (3.2.1.8), to the measured envelope transfer characteristic, and hence determine the coefficients α_1, α_3 and α_5 for each case.

The measured and modeled envelope transfer function; $\left|\hat{I}_{2,rf}(t)\right|$ versus $\left|\hat{V}_{1,rf}(t)\right|$ is shown in Fig. 4.4(c). The results in this case also confirms that the DUT has very little observable memory. This was as a result of the limitation imposed on the experiment by the 10MHz bandwidth baseband amplifier. Hence higher order baseband components that could not controlled experienced different impedances that constituted in the small observable memory.

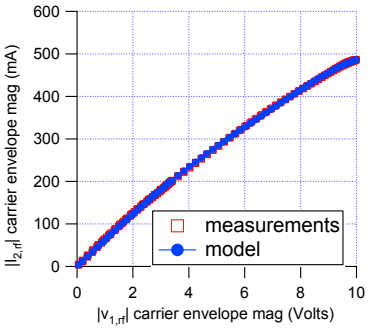

(c)

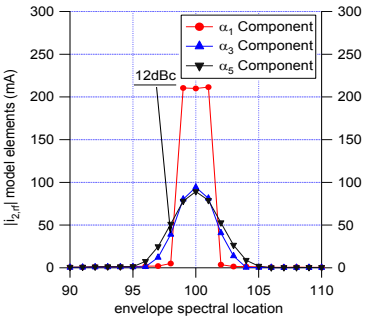

(d)

Fig 4.4. Measured and modeled (c) envelope transfer and (d) distortion level when $V_{2,bb}(t) = 0$ at the reference baseband short circuit state.

Fig. 4.4(d) shows the resulting spectral contributions of each component generated by the current model. The labels shown on the spectral graph are the corresponding computed output power levels. The maximum power level of the out-of-band distortion, in this un-linearized 1.5 dB compressed case, can be seen to be -12 dBc as shown on figure 4.4(d). Note this is the result obtained when $\beta_2 = 0$ and $\beta_4 = 0$, the reference baseband short circuit case.

Also shown is the spectral contribution Figure 4.4(d) of the individual model components. For this state, the values of the 3rd order and the 5th order distortion coefficients are $\alpha_3 = -0.2, \alpha_5 = 0.0008$ as shown in table 4.4 below.

α_1	α_3	α_5
61.68	-0.21	0.000082

Table 4.4 showing values of the linear gain and the distortion coefficients of the system

Fig. 4.4(e&f), shows the measured transfer magnitude and phase of the fundamental input voltage $\widehat{V}_{1,rf}(t)$ at the baseband short circuit reference state. The plots confirm the presence of AM/AM distortion and minimal AM/PM distortion.

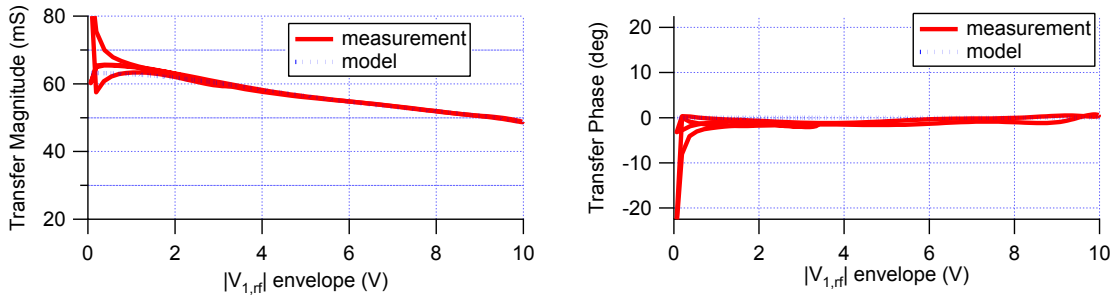

(e) (f)

Fig. 4.4. (e) Measured transfer magnitude and (f) phase of the fundamental input voltage $\widetilde{V}_{1,rf}(t)$ envelope at the reference baseband short circuit state.

4.5 Investigating the Linearization Design Space

To investigate how effective precisely engineered baseband voltages can be in linearizing the device, a sequence of measurements were performed; sweeping the baseband voltage waveform describing coefficients β_2 and β_4 over a selected range, thus systematically varying the injected voltage waveform. The variation of the level of observed distortion in the measured fundamental transfer characteristic was then determined. This was done by sweeping the values of the linearization coefficients shown in figure 4.5(a&b).

The observed variations of the distortion observed, quantified in terms of IM3 and IM5 dBc values, can be summarized in the form of power contour plots shown in figure 4.5(a&b).

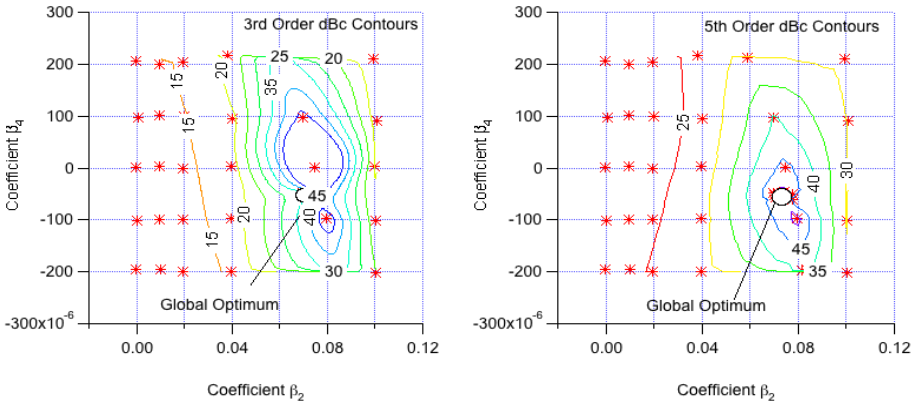

(a) (b)

Fig 4.5. Power contour plots of measured (a) IM3and (b) IM5 distortion observed in dBc while sweeping the values of the linearizing coefficients β_2 and β_4.

These plots figure 4.5 (a&b) clearly highlight that there are values of the linearizing coefficients β_2 and β_4 that can simultaneously minimize the level of distortion.

To quantify this more directly, it is better to use the extracted values of the third order distortion term α_3 and fifth order distortion term α_5, which are determined by fitting the model given by equation (3.2.1.8) to the measured envelope transfer characteristic.

Again this information is best summarized in the form of contour plots, shown in figure 4.5(c, d &e).

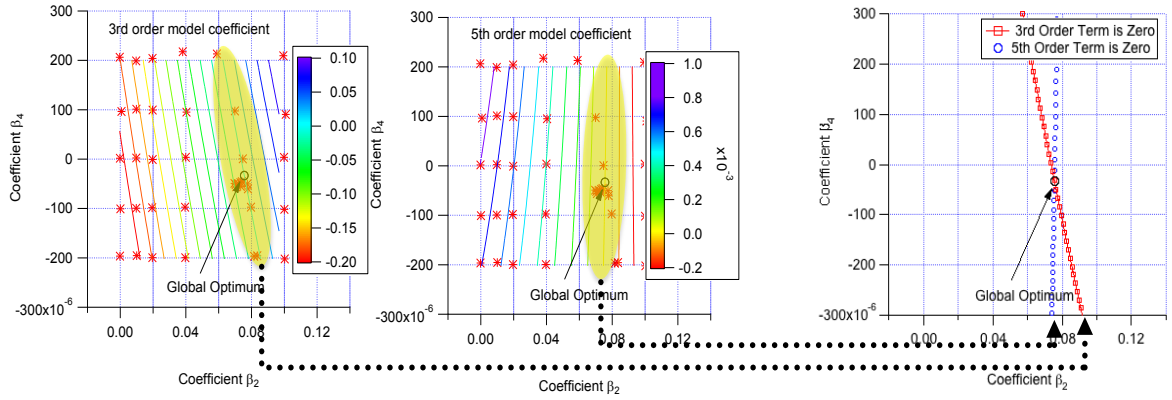

(c) (d) (e)

Fig 4.5. Contour plots of measured third (c) order term α_3 and fifth (d) order term α_5 values as a function of swept β_2 and β_4 and (e) the global (crossing) optimum point.

3rd order model coefficients		5th order model coefficients	
β_2	β_4	β_2	β_4
4.97339e-05	0.0708907	-9.02121e-06	0.0757411
4.43314e-05	0.0711933	-3.85116e-06	0.0757669
3.29482e-05	0.0718386	-6.28512e-07	0.0757847
2.13488e-05	0.0724957	4.70959e-06	0.0758072
1.61611e-05	0.0727902	7.76649e-06	0.0758235
3.56296e-06	0.0735065	1.32858e-05	0.075851
-6.278e-07	0.0737474	1.61612e-05	0.075867
-1.00101e-05	0.0742814	1.89087e-05	0.0758818
-1.74137e-05	0.0747084	2.45544e-05	0.0759053
-2.35694e-05	0.0750599	2.71448e-05	0.0759198
-3.42025e-05	0.0756747	3.29474e-05	0.0759485
-4.92665e-05	0.0765442	3.53648e-05	0.0759616
-5.09914e-05	0.076644	4.13404e-05	0.0759863
-5.15381e-05	0.076676	4.36056e-05	0.0759985
-6.77772e-05	0.0776193	4.97337e-05	0.0760285
-7.36638e-05	0.0779642	5.6095e-05	0.0760544
-8.45638e-05	0.0785982	5.81281e-05	0.076065
-9.1228e-05	0.078986	6.46655e-05	0.0760965
-0.000101353	0.0795823	6.65226e-05	0.0761066
-0.000104727	0.0797792	7.32144e-05	0.076134
-0.00011814	0.0805713	7.49161e-05	0.0761428

Table 4.5 showing values of the linearization coefficients around the global (yellow) optimum point and the region on the contour plot for which α_3=0 and α_5=0 (region of no-distortion)

The figure 4.5(c&d) again highlights that there are values of coefficients β_2 and β_4 that can simultaneously minimize the value of third order and fifth order distortion. The shaded portion of the plot of coefficients β_2 - β_4 loci show the regions for the case when α_3=0 and α_5=0. This means that a region exists on these contour plots (c) and (d), (shaded-region) where α_3=0 and α_5=0 respectively. This is referred to as the region of minimal-distortion. A close examination of these loci confirms that the regions of minimal-distortion actually cross at a point shown in (e). This crossing-point was recognised as the global optimum where both α_3 and α_5 are simultaneously zero. It is these values of β_2 and β_4 that define the baseband injection signal necessary to eliminate the non-linearity in device's AM/AM response. This technique suppresses the AM/AM distortion and not the AM/PM (Chapter six) experienced by the device. Table 4.5 show the values of the linearising coefficients for the 3rd and 5th order around the global optimum point.

4.6 Baseband linearization and linear state

The measurement system was now configured to demonstrate the successful implementation of baseband linearization. Using the optimum values determined above, the required 'linearizing" output baseband voltage was computed using equation (3.2.4.7). This computed target waveform along with the measured output baseband voltage waveform achieved are shown in Fig 4.6(a&b), indicating the ability of the system to correctly identify and engineer the required baseband voltage signal. The corresponding measured value of the baseband current $I_{2,bb}(t)$ defined by equation (3.2.4.8) is also shown in figure 4.6(c&d). Note, the current and voltage variations are in phase, indicating that this condition would in practice require an active envelope tracking (ET) type of drain bias. This is interesting as it raises the possibility of improving efficiency and linearity simultaneously [9]. The 'zoomed-in' plot also

shows, that the measured and the target time varying baseband voltage $V_{2,bb}(t)$ have considerable agreement. Secondly, that the measured baseband current $I_{2,bb}(t)$ has the same functional behavior as the linearizing baseband voltages as shown on graph-plots (c) and (d).

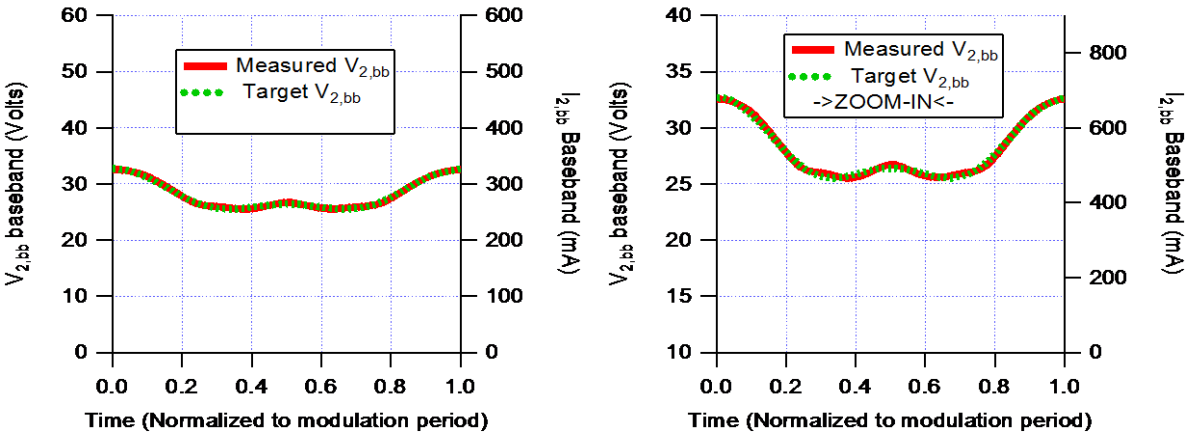

(a)

(b)

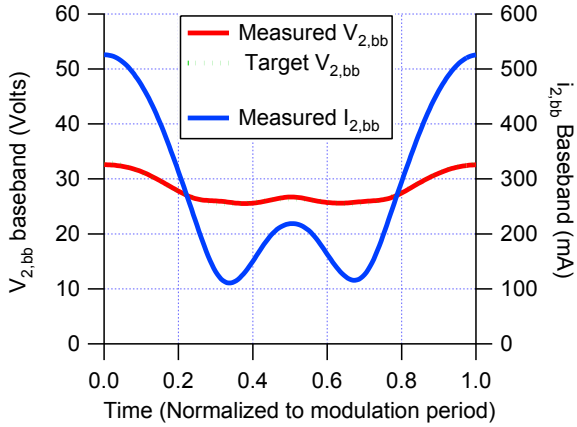

(c)

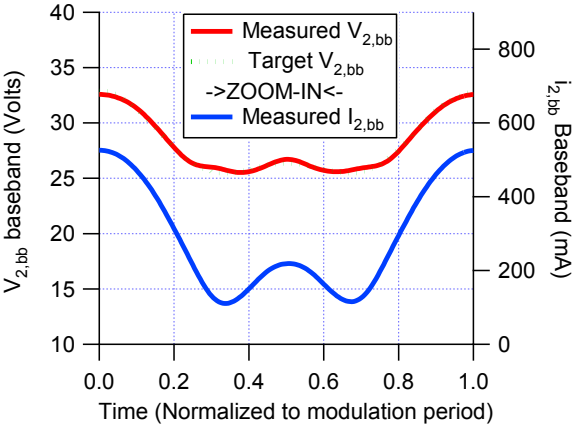

(d)

Fig. 4.6. The optimum output baseband linearising voltage waveform (target green), measured (red), both depicting ET-type pattern and the linearising baseband current (blue) described by equation (3.2.4.8) shown here.

$$I_{2,bb}(t) = \sum_{n=1}^{m} \alpha_{2n} \left|\hat{V}_{1,rf}(t)\right|^{2n} \qquad (3.2.4.8)$$

With the linearizing baseband voltage signal now applied the resulting, linear transfer characteristic is shown in Figure 4.6(e&f) is achieved. The spectral contribution of each component generated by the current model obtained in this state is also shown.

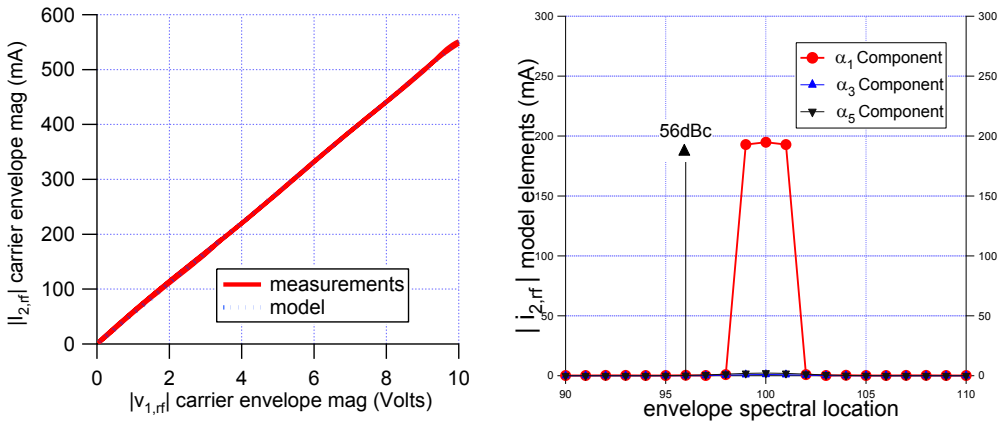

(e) (f)

Fig. 4.6. (e) Comparison of the measured and modeled envelope transfer function, for the optimum $V_{2,bb}(t)$ case. (f) The spectral contribution, of the individual modelled components. $\alpha_3 = \alpha_5 = 0, \beta_2 = 0.076, \beta_4 = -0.000033$. α_1= 55.41.

In this case both the third order and fifth order IMD contributions were reduced to below -56dBc, which is an improvement of 42dBc over the reference, baseband short circuit solution. The actual measured input and output power spectra around the carrier are shown in Figure 4.6 (g & h).

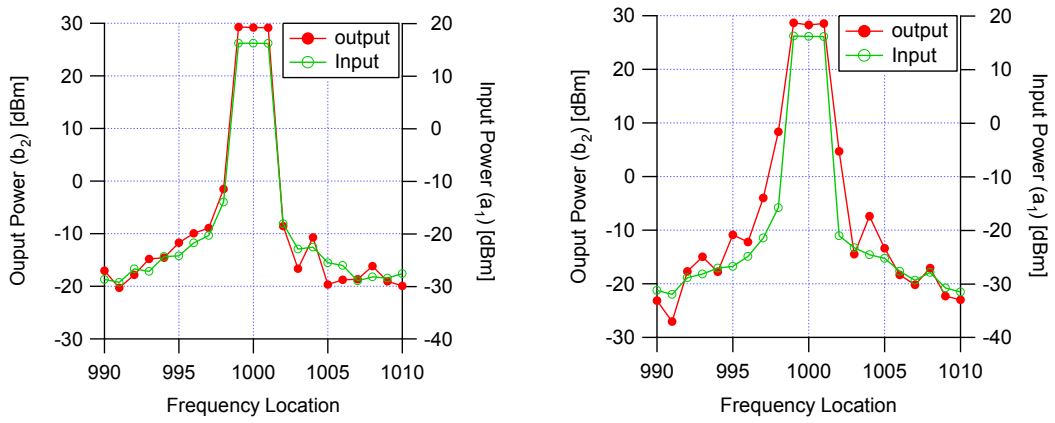

(g) (h)

Fig. 4.6. Measured (g) input and output power spectra around the carrier at linear and (h) baseband short circuit states.

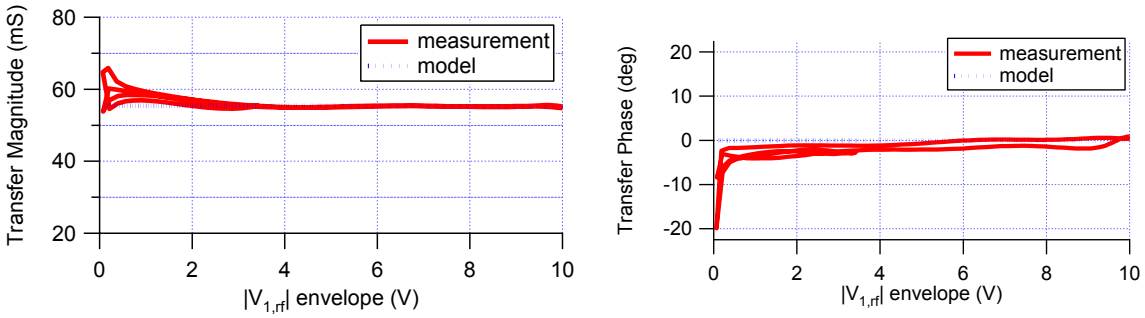

(i) (j)

Fig. 4.6. Measured (i) transfer magnitude and (j) phase of the fundamental input voltage $\tilde{V}_{1,rf}(t)$ envelope at the linear state.

It is important to realize that the plot in Figure 4.6(g&h) shows that the modulated excitation being used to excite the device is certainly not perfect, and contains significant distortion, mostly due to the driver amplifier being used. As both axis cover 60dB dynamic range, it is still effective in showing however that no detectable, additional distortion is being introduced by the baseband signal being used to linearize the device. Shown in Fig. 4.6 (i&j) are the plots of the measured transfer (i) magnitude and (j) phase of $\hat{V}_{1,rf}(t)$ envelope at the linear state

showing considerable linearity. It is important to note however that this technique is an AM/AM only linearizer.

4.7 Chapter summary

A formulation for defining baseband injection signals to minimize AM/AM distortions RFPA devices under arbitrary modulation was experimentally validated. The ability of the approach to simultaneously minimize both third and fifth order distortion terms was demonstrated using a 3-tone modulated signal, where the optimum baseband signal voltage for third and fifth order IMD suppression was successfully determined and then used to linearize the device.

4.8 References

[1] Andrei Grebennikov, “RF and Microwave Power Amplifier Design”. McGraw-Hill ISBN 0-07-144493-9

[2] Joel Vuolevi and Timo Rahkonen,” Distortion in RF Power Amplifiers”, Norwood, MA: Artech House, 2003.

[3] John Wood, David E. Root, “Fundamentals of nonlinear behavioral modeling for RF and microwave design”. Artech House, 2005.

[4] J. C. Pedro, N. B. Carvalho, “Intermodulation Distortion in Microwave and Wireless Circuits” Artech House, 2003.

[5] Chi-Shuen Leung, Kwok-Keung, M. Cheng, “A new approach to amplifier linearization by the generalized baseband signal injection method,” IEEE microwave and wireless components letters, vol. 12, no.9, September, 2002.

[6] Lei Ding, G. Tong Zhou. “Effects of Even-Order Nonlinear Terms on Power Amplifier Modelling and Predistortion Linearization”. IEEE Transactions On Vehicular Technology, Vol. 53, No. 1, January 2004.

[7] Vincent W. Leung, Junxiong Deng, Prasad S. Gudem, and Lawrence E. Larson. “Analysis of Envelope Signal Injection for Improvement of RF Amplifier Intermodulation Distortion”, IEEE Journal of solid-state circuits, vol. 40, no. 9, September 2005

[8] Akmal, M.; Lees, J.; Jiangtao, S.; Carrubba, V.; Yusoff, Z.; Woodington, S.; Benedikt, J.; Tasker, P.J.; Bensmida, S.; Morris, K.; Beach, M.; McGeehan, J., "An enhanced modulated waveform measurement system for the robust characterization of microwave devices under modulated excitation," *Microwave Integrated Circuits Conference (EuMIC), 2011 European* , vol., no., pp.180,183, 10-11 Oct. 2011

[9] Akmal, M.; Carrubba, V.; Lees, J.; Bensmida, S.; Benedikt, J.; Morris, K.; Beach, M.; McGeehan, J.; Tasker, P.J., "Linearity enhancement of GaN HEMTs under complex modulated excitation by optimizing the baseband impedance environment," *Microwave Symposium Digest (MTT), 2011 IEEE MTT-S International* , vol., no., pp.1,4, 5-10 June 2011. doi: 10.1109/MWSYM.2011.5972833

[10] Akmal, M.; Ogboi, F.L.; Yusoff, Z.; Lees, J.; Carrubba, V.; Choi, H.; Bensmida, S.; Morris, K.; Beach, M.; McGeehan, J.; Benedikt, J.; Tasker, P.J., "Characterization of electrical memory effects for complex multi-tone excitations using broadband active baseband load-pull," *Microwave Conference (EuMC), 2012 42nd European* , vol., no., pp.1265,1268, Oct. 29 2012-Nov. 1 2012

[11] Akmal, M.; Lees, J.; Bensmida, S.; Woodington, S.; Carrubba, V.; Cripps, S.; Benedikt, J.; Morris, K.; Beach, M.; McGeehan, J.; Tasker, P.J., "The effect of baseband impedance termination on the linearity of GaN HEMTs," *Microwave Conference (EuMC), 2010 European* , vol., no., pp.1046,1049, 28-30 Sept. 2010

[12] Akmal, M.; Lees, J.; Bensmida, S.; Woodington, S.; Benedikt, J.; Morris, K.; Beach, M.; McGeehan, J.; Tasker, P.J., "The impact of baseband electrical memory effects on the dynamic transfer characteristics of microwave power transistors," *Integrated Nonlinear Microwave and Millimeter-Wave Circuits (INMMIC), 2010 Workshop on* , vol., no., pp.148,151,26-27April2010 doi: 10.1109/INMMIC.2010.5480111

[13] Akmal, M.; Lees, J.; Carrubba, V.; Bensmida, S.; Woodington, S.; Benedikt, J.; Morris, K.; Beach, M.; McGeehan, J.; Tasker, P.J., "Minimization of baseband electrical memory effects in GaN HEMTs using active IF load-pull," *Microwave Conference Proceedings (APMC), 2010 Asia-Pacific* , vol., no., pp.5,8, 7-10 Dec. 2010

[14] Benedikt, J.; Tasker, P.J., "High-power time-domain measurement bench for power amplifier,development,"*ARFTG,Conference, Digest,Fall2002.60th*,vol.,no.,pp.107,110,5-6Dec.2002, doi: 10.1109/ARFTGF.2002.1218692

[15] Lees, J.; Akmal, M.; Bensmida, S.; Woodington, S.; Cripps, S.; Benedikt, J.; Morris, K.; Beach, M.; McGeehan, J.; Tasker, P., "Waveform engineering applied to linear-efficient PA design," *Wireless and Microwave Technology Conference (WAMICON), 2010,IEEE11thAnnual*,vol.,no.,pp.1,5,12-13April2010 doi: 10.1109/WAMICON.2010.5461847

[16] Lees, J.; Williams, T.; Woodington, S.; McGovern, P.; Cripps, S.; Benedikt, J.; Tasker, P., "Demystifying Device related Memory Effects using Waveform Engineering and Envelope Domain Analysis," *Microwave Conference, 2008. EuMC 2008.38th,European*,vol.,no.,pp.753,756,27-31Oct.2008doi: 10.1109/EUMC.2008.4751562

[17] Ogboi, F.L.; Tasker, P.J.; Akmal, M.; Lees, J.; Benedikt, J.; Bensmida, S.; Morris, K.; Beach, M.; McGeehan, J., "A LSNA configured to perform baseband engineering for device linearity investigations under modulated excitations," *Microwave Conference (EuMC), 2013 European* , vol., no., pp.684,687, 6-10 Oct. 2013

[18] Tasker, P.J., "RF Waveform Measurement and Engineering," *Compound Semiconductor Integrated Circuit Symposium, 2009. CISC 2009.AnnualIEEE*vol.,no.,pp.1,4,11-14Oct.2009doi: 10.1109/csics.2009.5315818

[19] Tasker,P.J.,"Practicalwaveformengineering,"*Microwave Magazine,IEEE*,vol.10,no.7,pp.65,76,Dec.2009 doi: 10.1109/MMM.2009.934518

[20] Tasker, P.J., "Non-linear characterisation of microwave devices," *High Performance Electron,Devices,for,Microwave,and,OptoelectronicApplications,1999.EDMO.1999Symposiumon*,vol.,no.,pp.147,152,1999 doi: 10.1109/EDMO.1999.821476

[21] Tasker, P.J.; Reinert, W.; Braunstein, J.; Schlechtweg, M., "Direct Extraction of All Four Transistor Noise Parameters from a Single Noise Figure Measurement," *Microwave Conference, 1992. 22nd European* , vol.1, no., pp.157,162, 5-9 Sept. 1992 doi: 10.1109/EUMA.1992.335733

[22] Williams, D.J.; Leckey, J.; Tasker, P.J., "Envelope domain analysis of measured time domain voltage and current waveforms provide for improved understanding of factors effecting linearity," *Microwave Symposium Digest, 2003 IEEE MTT-S International* , vol.2, no., pp.1411,1414vol.2,8-13June2003doi: 10.1109/MWSYM.2003.1212636

[23] Williams, D.J.; Leckey, J.; Tasker, P.J., "A study of the effect of envelope impedance on intermodulation asymmetry using a two-tone time domain measurement system," *Microwave Symposium Digest, 2002 IEEE MTT-S International* , vol.3, no., pp.1841,1844 vol.3, 2-7June2002doi: 10.1109/MWSYM.2002.1012221

[24] Williams, D.; Tasker, P.J., "Thermal parameter extraction technique using DC I-V data,forHBTtransistors,"*HighFrequencyPostgraduateStudentColloquium,2000*,vol.,no.,pp.71,75,2000doi: 10.1109/HFPSC.2000.874085

[25] Williams, D.J.; Tasker, P.J., "An automated active source and load pull measurement system,"*HighFrequencyPostgraduateStudent Colloquium,2001.6thIEEE*,vol.,no.,pp.7,12,2001doi: 10.1109/HFPSC.2001.962150

[26] Z. Yusoff, J. Lees, J. Benedikt, P.J. Tasker, S.C. Cripps, “Linearity improvement in RF power amplifier system using integrated Auxiliary Envelope Tracking system,” *IEEE MTT-S Int. Microw. Symp. Dig.*, 2011, vol., no., pp.1-4, 5-10 June 2011.

[27] Wood, J.; Lefevre, M.; Runton, D.; Nanan, J.-C.; Noori, B.H.; Aaen, P.H., "Envelope-domain time series (ET) behavioral model of a Doherty RF power amplifier for system design," Microwave Theory and Techniques, IEEE Transactions on , vol.54, no.8, pp.3163,3172, Aug. 2006 doi: 10.1109/TMTT.2006.879134.

[28] Maoliu Lin; Zhe Zhang; Xiaojian Ding; Zhiwei Yang, "Envelope domain method characterizing RF nonlinear system excited with a two-tone," Communications and Information Technology, 2005. ISCIT 2005. IEEE International Symposium on , vol.2, no., pp.797,800, 12-14 Oct. 2005 doi: 10.1109/ISCIT.2005.1566987.

[29] Huadang, Wang; Jngfu, Bao; Zhengde, Wu, "Multislice behavioral modeling based on envelope domain for power amplifiers," Systems Engineering and Electronics, Journal of , vol.20, no.2, pp.274,277, April 2009.

[30] Wood, J.; Lefevre, M.; Runton, D., "Application of an Envelope-Domain Time-Series Model of an RF Power Amplifier to the Development of a Digital Pre-Distorter System," Microwave Symposium Digest, 2006. IEEE MTT-S International , vol., no., pp.856,859, 11-16 June 2006 doi: 10.1109/MWSYM.2006.249809.

[31] Yichi Zhang; Maoliu Lin, "Evaluation of envelope-domain dynamic X-parameter model based on variable-carrier-frequency analysis," Millimeter Waves (GSMM), 2012 5th Global Symposium on , vol., no., pp.236,240, 27-30 May 2012
doi: 10.1109/GSMM.2012.6314044,.

[32] Zenteno, E.; Isaksson, M.; Wisell, D.; Keskitalo, N.; Andersen, O., "An envelope domain measurement test setup to acquire linear scattering parameters," ARFTG Microwave Measurement Symposium, 2008 72nd , vol., no., pp.54,57, 9-12 Dec. 2008, doi: 10.1109/ARFTG.2008.4804287.

[33] Shoucair, F. S., "Joseph Fourier's Analytical Theory of Heat: A Legacy to Science and Engineering," Education, IEEE Transactions on , vol.32, no.3, pp.359,366, 1989 doi: 10.1109/TE.1989.386497.

[34] Tasker, P.J., "Practical waveform engineering," Microwave Magazine, IEEE , vol.10, no.7, pp.65,76, Dec. 2009, doi: 10.1109/MMM.2009.934518.

[35] Tasker, P.J., "RF Waveform Measurement and Engineering," Compound Semiconductor Integrated Circuit Symposium, 2009. CISC 2009. Annual IEEE , vol., no., pp.1,4, 11-14 Oct. 2009, doi: 10.1109/csics.2009.5315818.

[36] Iwata, M.; Kamiyama, T.; Uno, T.; Yahata, K.; Ikeda, H., "First pass design of a high power 145W, high efficiency class-J GaN power amplifier using waveform engineering," Power Amplifiers for Wireless and Radio Applications (PAWR), 2013 IEEE Topical Conference on , vol., no., pp.7,9, 20-20 Jan. 2013, doi: 10.1109/PAWR.2013.6490171.

[37] Sheikh, Aamir; Roff, C.; Benedikt, J.; Tasker, P.J.; Noori, B.; Aaen, P.; Wood, J., "Systematic waveform engineering enabling high efficiency modes of operation in Si LDMOS at both L-band and S-band frequencies," Microwave Symposium Digest, 2008 IEEE MTT-S International , vol., no., pp.1143,1146, 15-20 June 2008 doi: 10.1109/MWSYM.2008.4633259.

[38] Casbon, M. A; Tasker, P.J.; Benedikt, J., "Waveform Engineering beyond the Safe Operating Region: Fully Active Harmonic Load Pull Measurements under Pulsed Conditions," Compound Semiconductor Integrated Circuit Symposium (CSICS), 2011 IEEE , vol., no., pp.1,4, 16-19 Oct. 2011, doi: 10.1109/CSICS.2011.6062435.

[39] Di Falco, S.; Raffo, A; Vannini, G.; Vadala, V., "Low-frequency waveform engineering technique for class-F microwave power amplifier design," Microwave

Integrated Circuits Conference (EuMIC), 2011 European , vol., no., pp.288,291, 10-11 Oct. 2011.

[40] Casbon, M.A; Tasker, P.J.; Wei-Chou Wang; Che-Kai Lin; Wen-kai Wang; Wohlmuth, W., "Advanced RF IV Waveform Engineering Tool for Use in Device Technology Optimization: RF Pulsed Fully Active Harmonic Load Pull with Synchronized 3eV Laser," Compound Semiconductor Integrated Circuit Symposium (CSICS), 2013 IEEE , vol., no., pp.1,4, 13-16 Oct. 2013,

doi: 10.1109/CSICS.2013.6659212.

[41] FitzPatrick, D.; Saini, R.; Lees, J.; Benedikt, J.; Cripps, S.C.; Tasker, P.J., "A waveform engineering approach to the design of improved efficiency wideband MMIC amplifiers," Wireless and Microwave Technology Conference (WAMICON), 2011 IEEE 12th Annual , vol., no., pp.1,6, 18-19 April 2011,

doi: 10.1109/WAMICON.2011.5872859.

[42] Zhancang Wang; Pengelly, R.S., "A waveform engineered power amplifier design for envelope tracking," Wireless and Microwave Technology Conference (WAMICON), 2014 IEEE 15th Annual , vol., no., pp.1,5, 6-6 June 2014

doi: 10.1109/WAMICON.2014.6857735.

[43] Roff, C.; Benedikt, J.; Tasker, P.J.; Wallis, D.J.; Hilton, K.P.; Maclean, J.O.; Hayes, D.G.; Uren, M.J.; Martin, Trevor, "Analysis of DC–RF Dispersion in AlGaN/GaN HFETs Using RF Waveform Engineering," Electron Devices, IEEE Transactions on , vol.56, no.1, pp.13,19, Jan. 2009, doi: 10.1109/TED.2008.2008674

[44] Le Gallou, N.; Sturesson, F., "RF waveform engineering applied to GaAs MESFET radiation safe operating area," Microwave Symposium Digest, 2009. MTT '09. IEEE MTT-S International , vol., no., pp.889,892, 7-12 June 2009

doi: 10.1109/MWSYM.2009.5165840.

[45] Carrubba, V.; Clarke, AL.; Woodington, S.P.; McGenn, W.; Akmal, M.; AlMuhaisen, A; Lees, J.; Cripps, S.C.; Tasker, P.J.; Benedikt, J., "High-speed device characterization using an active load-pull system and waveform engineering postulator," Microwave Measurement Conference (ARFTG), 2011 77th ARFTG , vol., no., pp.1,4, 10-10 June 2011, doi: 10.1109/ARFTG77.2011.6034553.

[46] Wright, P.; Lees, J.; Tasker, P.J.; Benedikt, J.; Cripps, S.C., "An efficient, linear, broadband class-J-mode PA realised using RF waveform engineering," Microwave Symposium Digest, 2009. MTT '09. IEEE MTT-S International , vol., no., pp.653,656, 7-12 June 2009, doi: 10.1109/MWSYM.2009.5165781

[47] Lees, J.; Williams, T.; Woodington, S.; McGovern, P.; Cripps, S.; Benedikt, J.; Tasker, P., "Demystifying Device related Memory Effects using Waveform Engineering and Envelope Domain Analysis," Microwave Conference, 2008. EuMC 2008. 38th European , vol., no., pp.753,756, 27-31 Oct. 2008.

doi: 10.1109/EUMC.2008.4751562.

[48] Lees, J.; Akmal, M.; Bensmida, S.; Woodington, S.; Cripps, S.; Benedikt, J.; Morris, K.; Beach, M.; McGeehan, J.; Tasker, P., "Waveform engineering applied to linear-efficient PA design," Wireless and Microwave Technology Conference (WAMICON), 2010 IEEE 11th Annual , vol., no., pp.1,5, 12-13 April 2010

doi: 10.1109/WAMICON.2010.5461847.

[49] Benedikt, J.; Gaddi, R.; Tasker, P.J.; Goss, M., "High-power time-domain measurement system with active harmonic load-pull for high-efficiency base-station amplifier design," Microwave Theory and Techniques, IEEE Transactions on , vol.48, no.12, pp.2617,2624, Dec 2000, doi: 10.1109/22.899021.

[50] McGenn, W.; Benedikt, J.; Tasker, P.J.; Powell, J.; Uren, M., "RF waveform investigation of VSWR sweeps on GaN HFETs," Microwave Integrated Circuits Conference (EuMIC), 2011 European , vol., no., pp.17,20, 10-11 Oct. 2011.

[51] Tasker, P.J.; Carrubba, V.; Wright, P.; Lees, J.; Benedikt, J.; Cripps, S., "Wideband PA Design: The "Continuous" Mode of Operation," *Compound Semiconductor Integrated Circuit Symposium (CSICS), 2012 IEEE* , vol., no., pp.1,4, 14-17 Oct. 2012 doi: 10.1109/CSICS.2012.6340118.

[52] Bonser, W., "Engineering design steps for fast, simple and economical waveform development," Military Communications Conference, 2001. MILCOM 2001. Communications for Network-Centric Operations: Creating the Information Force. IEEE , vol.1, no., pp.195,201 vol.1, 2001, doi: 10.1109/MILCOM.2001.985789.

CHAPTER FIVE

SIGNAL COMPLEXITY INVESTIGATION

Since the BEL formulation, introduced and experimentally validated in the previous chapters, is generalized in the envelope domain it should be able to describe the required "linearizing" baseband injection signal, for an arbitrary amplitude modulated signal, using a set of linearizing coefficients that are signal complexity invariant. Signal complexity can be considered in two parts, signal envelope bandwidth and signal envelope shape.

This chapter will therefore be split into two sections. Section one, called modulation envelope bandwidth complexity and section two called modulation envelope shape complexity.

5.1 Section one: Modulation bandwidth complexity

5.1.1 Wide Bandwidth up to 20MHz

Previously in chapter four, 2 parts to signal complexity were identified. One of these includes complexity with respect to modulated signals, each having different peak-to-average-power ratio (PAPR). The second part with respect to multiple signals, each having different modulation speed. Examples of those can be seen in varying modulation bandwidth. This section of the chapter investigates using BEL on signals with different modulation bandwidths. It proposes to linearize a 3-tone modulated signal with a modulation bandwidth varying from 2MHz to 20MHz in steps of 2MHz. The purpose of this investigation is to verify that the linearizing coefficients β_2 and β_4 are truly invariant of varying modulation

bandwidth. Only β_2 and β_4 are considered in this case because distortion only up to the 5th order is considered.

5.2 Experimental setup

To investigate the scaling up of baseband linearization to higher modulation bandwidths, the waveform measurement system described in chapter 3 is calibrated and vector error corrected using the 50 Ohm custom made TRL calibration kit. This system has a 100MHz RF modulation bandwidth, but since the baseband bandwidth is limited to 100MHz, linearization investigations are limited to RF modulated signal with bandwidths less than 25MHz.

In this investigation the modulation bandwidth of a 3-tone signal was varied from 2MHz to 20MHz in 2MHz steps. In all cases the PAPR of the 3-tone excitation was 4.77dB, the RF excitation was centered at 2GHz, while maintaining a constant peak envelope power of approximately 38dBm. This ensured that the device under test, a10W, CREE HFET, was driven to a compression level of approximately 1.5dB. The GaN device was biased in class AB, with RF fundamental and all harmonic frequencies terminated using a passive 50Ω load. The drain and gate bias voltages of 28V and -2.08V respectively were used, giving a quiescent drain current of approximately 12% I_{DSS}, for each modulation bandwidth.

5.3 Bandwidth Considerations

Consider, a RF modulated system with a modulated envelope $\widehat{V}_{1,rf}(t)$given by $E(t)$ having a bandwidth $\Delta\omega$. In this investigation we will consider a 3-tone modulated stimulus with δ tone spacing, hence $\Delta\omega = 2\delta$. Signals produced by odd order intermodulation distortion (IMD) not only distort the in-band signal but also generate out of band components. The m^{th} odd order IMD term will increase the bandwidth to $m\Delta\omega$. If these terms are to be removed,

cancelled, using pre-distortion, analogue or digital, the modulation bandwidth of the signal must now increase significantly and also become $m\Delta\omega$. So for a modulation signal of 20MHz bandwidth and considering distortion only up to 5th order, this would require the pre-distorter and the power amplifier to have a modulation bandwidth of at least 100MHz.

In the case of baseband linearization the bandwidth of the RF modulated signal remains unchanged, however a modulated baseband signal is required. In chapter 3, it was shown that this baseband signal can be computed using equation (3.2.4.7) shown here.

$$\hat{V}_{2,bb}(t) = \sum_{p=1}^{q} \beta_{2p} |E(t)|^{2p} \qquad (3.2.4.7)$$

The bandwidth of this signal is given by $2q\Delta\omega$. So for a modulation signal of 20MHz bandwidth and considering distortion only up to 5th order, hence linearization can be achieved with q=2, a baseband signal with only an 80MHz is required. This reduced bandwidth requirement for baseband linearization compared to pre-distortion could become very significant in future communication systems requiring high modulation bandwidths >20MHz.

5.4 Linearity Investigations

5.4.1 Reference baseband short circuit state measurements result

Initially the non-linear behavior of the transistor was characterized into a reference baseband output voltage envelope. The reference state is the classical, ideal, baseband short circuit condition. A typical result is achieved as shown in Fig. 5.4.1(a&b), for 8MHz 3-tone stimuli. All the other are very similar (see appendix D, pg.202).

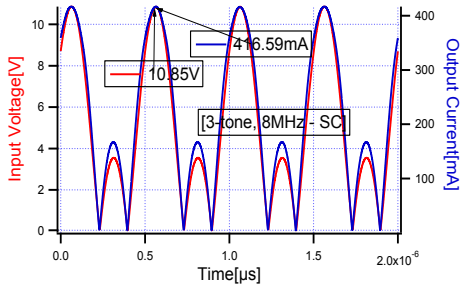

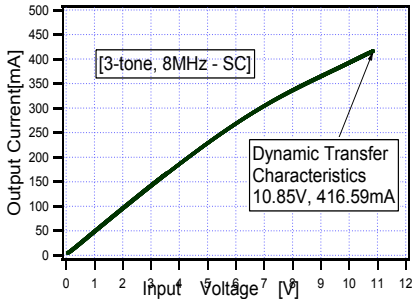

Figure 5.4.1 (a). Measured RF Input voltage/output current envelopes

Figure 5.4.1(b). Measured RF envelope dynamic transfer characteristics

In each case, the dynamic envelope transfer characteristic was modeled by equation (3.2.1.8) shown here.

$$\hat{I}_{2,rf}(t) = \sum_{n=0}^{m} \alpha_{2n+1} |E(t)|^{2n} E(t). \quad (3.2.1.8)$$

where α_1 represents the linear gain of the system, α_3 quantifies the level of third order intermodulation distortion, α_5 quantifies the level of fifth order intermodulation distortion, and so on, up to the desired maximum order m. In this case m=3 is sufficient, distortion up to fifth order, to fit the measured behavior and the extracted coefficient values, α_{2n+1}, obtained are summarized in table 5.4.1.

Bandwidth	α_1	α_3	α_5
2MHz	48.31	-0.110	0.0002
4MHz	44.47	-0.104	0.0002
6MHz	48.64	-0.12	0.0003
8MHz	48.55	-0.122	0.0003
10MHz	48.82	-0.12	0.0002
12MHz	48.74	-0.121	0.0003
14MHz	49.01	-0.093	0.000075
16MHz	48.67	-0.128	0.0003
18MHz	54.98	-0.18	0.0006
20MHz	54.06	-0.18	0.0006

TABLE 5.4.1. Coefficients describing the non-linearity of the observed dynamic envelope transfer characteristic measured as a function of increasing modulation bandwidth; baseband short circuit reference state.

These results clearly highlight, certainly over this bandwidth that the non-linear behavior of the transistor is modulation bandwidth invariant, this is consistent with the previous assumption in chapter 3. This confirms the advantage of the envelope domain based formulation for determining the required baseband linearization signal. If the envelope transfer characteristic is stimulus invariant so should the linearizing baseband voltage envelope (1) coefficients be stimulus invariant.

5.4.2 Linear state measurements result – after baseband Linearization

The two, β_2 and β_4, optimized linearization coefficients, required to compute the necessary output baseband stimulus using the established equation set in chapter 3, to linearize the transistor were now determined as shown in chapter 4.

A resulting linearized characteristic, again selecting for the 8MHz is shown in the following figures 5.4.2 (a&b). In all cases the device was successfully linearized. The dynamic envelope transfer characteristics becoming a straight line through the origin.

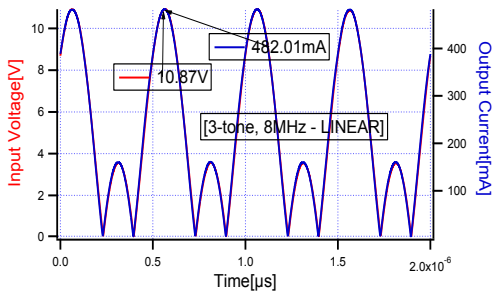

Figure 5.4.2 (a). Measured RF input voltage/output current envelopes

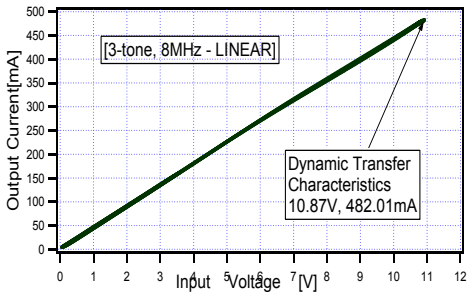

Figure 5.4.2 (b). Measured RF envelope dynamic transfer characteristics

The beta values determined are summarised in table 5.4.2.

Bandwidth	β_2	β_4
2MHz	0.0012	-8.8e-5
4MHz	0.0178	-8.7e-5
6MHz	0.02	-8.6e-5
8MHz	0.018	-9e-5
10MHz	0.018	-9e-5
12MHz	0.016	-9e-5
14MHz	0.003	-9e-5
16MHz	0.018	-9e-5
18MHz	0.0178	-8.4e-5
20MHz	0.0013	-8.9e-5

TABLE 5.4.2. Optimized β linearization coefficients determined as a function of increasing modulation bandwidth.

The computed β optimisation coefficients as shown in table 5.4.2 are almost constant over the 20MHz bandwidth. The small variation experienced at 2MHz, 14MHz and 20MHz may be attributed to experimental variations.

This linearized performance achieved for the entire 20MHz bandwidth is shown in the figure 5.4.2(c).

Fig. 5.4.2(c) shows that the two, β_2 and β_4, optimized linearization, determined coefficient (plotted on a very-fine-grid) to achieve this level of linearization were basically almost constant over the entire 20MHz bandwidth.

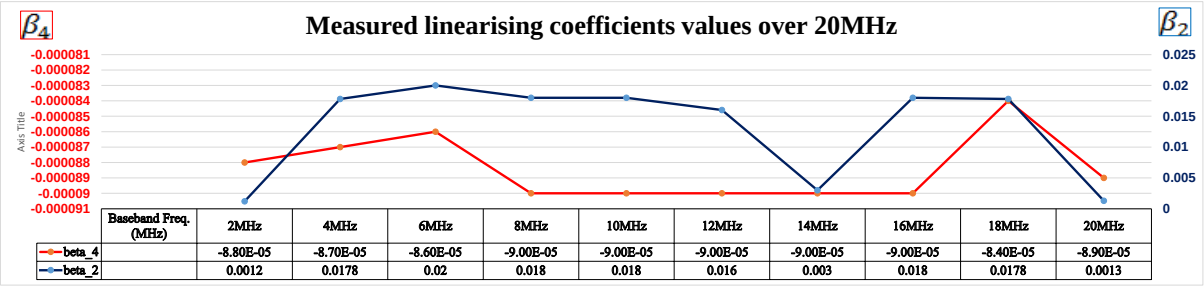

Baseband Freq. (MHz)	2MHz	4MHz	6MHz	8MHz	10MHz	12MHz	14MHz	16MHz	18MHz	20MHz
beta_4	-8.80E-05	-8.70E-05	-8.60E-05	-9.00E-05	-9.00E-05	-9.00E-05	-9.00E-05	-9.00E-05	-8.40E-05	-8.90E-05
beta_2	0.0012	0.0178	0.02	0.018	0.018	0.016	0.003	0.018	0.0178	0.0013

Fig. 5.4.2 (c) .Measured linearizing coefficients values over 20MHz

Since the β values are almost invariant then so is the required baseband linearization signal, this is plotted versus period, as shown in figure 5.4.2(d). This follows a self-repeating pattern.

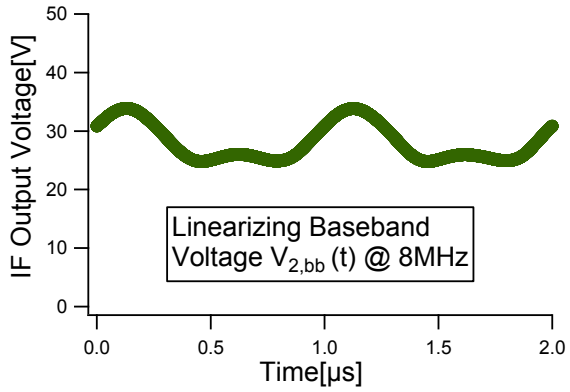

Fig. 5.4.2(d), The measured linearizing baseband signal

5.5 Spectral Analysis and Plots

More traditional this performance improvement is presented in terms of the minimizing the spectral regrowth. Fig. 5.5(a&b), shows the spectral performance improvements achieved in the case of 8MHz 3-tone stimulus.

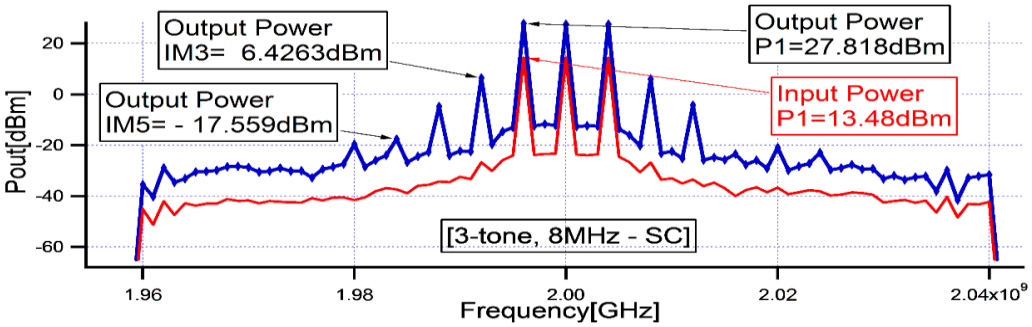

Figure 5.5 (a). Measured – baseband short circuit reference state

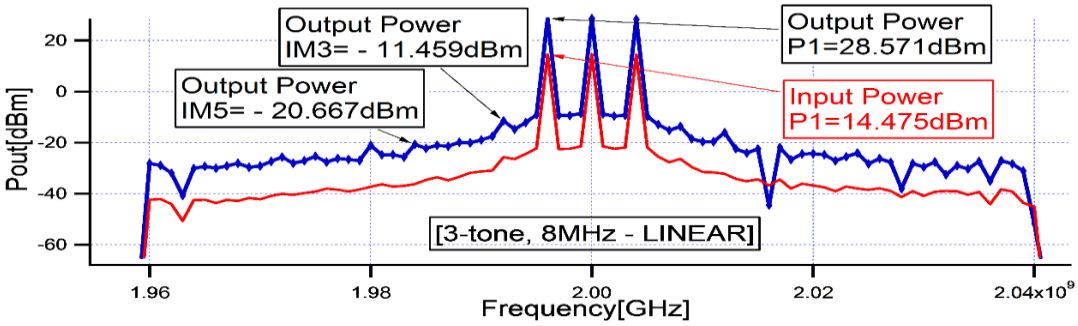

Figure 5.5 (b). Measured - linear state

Fig. 5.5, Measured 8MHz 3-tone power spectrum (a) before and after (b) applying baseband linearization.

Distortion in all cases was reduced to a level around -40dB, a value limited more by the dynamic range of the measurement system than the ability of the optimized baseband enveloped derived signal to linearize. A summary of the linearization and suppression achieved over the entire 20MHz bandwidth is shown in Fig. 5.5(c). In all cases the IM3 suppression was approximately 20dBc across-board. IM5 was successfully suppressed to the noise-floor of the measurement system.

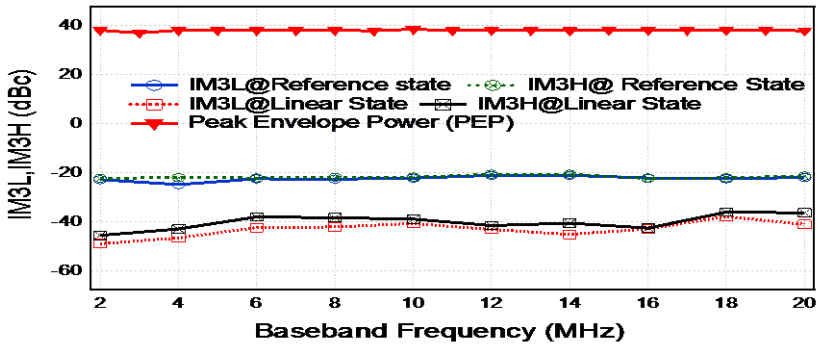

Fig. 5.5(c). Measured 20dBc suppression in IM3 over 20MHz tone spacing referenced to the baseband short circuit state.

5.6 Baseband Linearization at High Bandwidth

Fig. 5.6(a&b) shows that even in the case where the modulation bandwidth is 20MHz, hence the linearization bandwidth is now 80MHz, approaching the bandwidth limitations of the measurement system harmonic suppression of down to -30dBc was still achieved.

This is evident from the figures shown below.

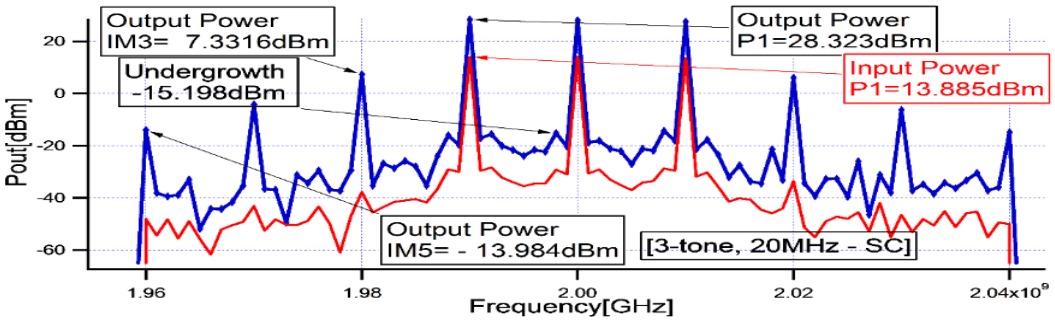

Figure 5.6 (a). Measured RF input power – output power spectrum

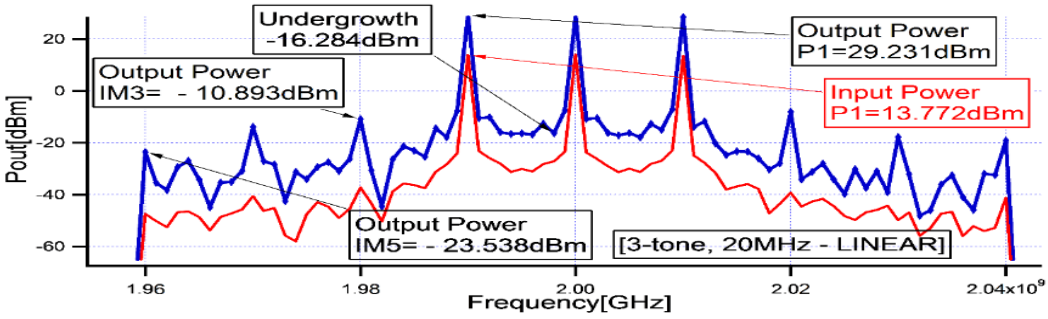

Figure 5.6 (b). Measured RF input power – output power spectrum

The more traditional power spectrum shows the input power spectrum and the output power spectrum. The main purpose for showing the more traditional power spectrum plot such as that shown in figure 5.6 (a & b), is to show the following.

(i). Show the level of suppression achieved

(ii). To compare the input power to the output power

(iii). To show how clean the signal going into the device is

(iv). To show that no noise is added to the device response after linearization

(v). To show that the output power can actually track the input power and the input power changes as a result of the linearization exercise.

(vi). To show simultaneous suppression is possible.

(vii). To identify the distortion

(viii). To show that the main signal is not distorted by the linearization exercise

(ix). To show and identify the presence of the targeted distortion

(x). To show and identify the removed/suppressed distortion after the linearization exercise.

This (new) work shows that the technique can function with input signals comparable with wide-bandwidth applications like WCDMA, and LTE in minimizing the impact of AM/AM distortion. The BEL concept when coupled with a pre-distortion solution could then also address the AM/PM distortion component.

5.7 Summary - section one

It has been shown that the BEL formulation introduced to determine the baseband linearization signal does provide for a solution that appears to be bandwidth invariant. Supporting the argument that this formulation generalized in the envelope domain should be able to describe the required "linearizing" baseband injection signal, for an arbitrary amplitude modulated envelope, using a limited set of coefficients that are independent of the bandwidth of the modulated signal. It is important to note that the technique in minimizing the impact of AM/AM distortion has been shown to function at frequencies comparable with wide-bandwidth applications like WCDMA and LTE. Thus supporting the argument that this concept when coupled with a pre-distortion solution could then also address both the AM/AM and the AM/PM distortion components.

Note that this solution should also apply if the "shape" of the signal is varied. This is the focus of next section 2.

5.8 Section Two: Modulation envelope complexity

Similar to section one of this chapter, this generalised formulation, in the envelope domain is proposed to be able to describe the required "linearizing" baseband injection signal, for an arbitrary amplitude modulated signal, using a set of linearizing coefficients that are signal complexity invariant. The signal complexity with respect to bandwidth was considered in section one of this chapter.

In this section two, we will now investigate the ability of the formulation linearizing coefficient invariance, with respect to varying envelope complexity with respect to shape.

5.9 Envelope complexity

The focus of this section two is to investigate the invariance of the linearizing coefficients with respect to envelope complexity. Varying envelope complexity refers to modulated signals, each having different peak-to-average-power ratio (PAPR). Examples of this is in 3-tone, 5-tone, 9-tone and n-tone, modulated signals set. The purpose of this investigation is to further verify that the linearizing coefficients β_2 and β_4 are invariant to signals with varying PAPR. Also, only β_2 and β_4 are considered in this case because distortion up to the 5^{th} order is only considered.

5.10 Experimental setup

To investigate this concept, the baseband measurement system described in chapter 3, capable of measuring multiple-complex modulated voltage and current waveforms while 'engineering' and injecting intelligent baseband voltage signals into the device, was utilized. For this investigation, a 75W, 10KHz-250MHz wideband baseband amplifier from "Amplifier Research" Model 75A250, was used to amplify the engineered injected baseband voltage. The advantage of this is that we are able to precisely engineer and absolutely control the baseband

components associated with this system. The modulated RF time domain terminal voltage and current waveforms were also captured by the measurement system. Hence, it was possible to compute all the necessary measured envelope components at baseband, RF and harmonic frequencies.

The measurement system was vector calibrated at the device package plane using a custom built 50 Ω thru-reflect-line (TRL), calibration kit, over, precisely 50MHz baseband bandwidth and 100MHz RF bandwidth, for each of the first three harmonics. Stimuli with increasing complexities were measured, using equally spaced tones on a 9-tone grid. Using a tone spacing of 0.5MHz, peak to average power ratio (PAPR) for the 3-tone, 5-tone and 9-tone are 4.77dB, 6.99dB and 9.54dB respectively. The fundamental excitation was centered at 2GHz, while delivering a peak envelope power (PEP) of approximately 38dBm for each of applied modulation. The input signal was adjusted in each case to maintain approximately 1.5dB compression and an approximately constant envelope dynamic swing. The transistor, a 10W Cree GaN HEMT, was biased in class AB, with the RF fundamental and all harmonic frequencies terminated into a passive 50Ω load. The drain and gate bias voltages of +28V and -2.08V were used, giving a quiescent drain current of approximately 12% I_{DSS}, for each modulation type. The load condition, although not quite optimal, was considered sufficiently close for this investigation.

5.11 Linearization Investigation of various envelope complexities

As in the previous investigations, the transistor inherent non-linearity is initially observed and measured using the baseband short circuit condition. The RF fundamental dynamic envelope transfer characteristic and the input voltage output current envelopes measured are shown below for the various envelope complexities.

5.11.1 Reference baseband short circuit state measurements result

An example of the results achieved are shown in Fig. 5.11.1(a&b), for the 9-tone stimuli. It shows that an operating condition has been appropriately selected with considerable distortion produced, as evident in the observed compressed dynamic envelope transfer characteristics.

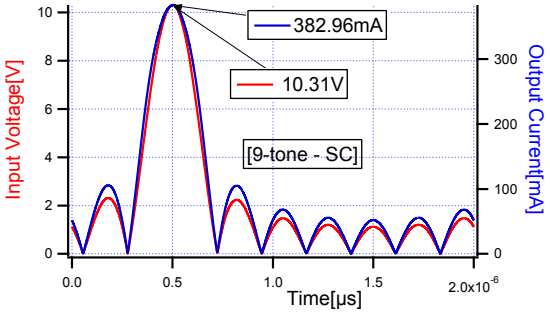

Figure 5.11.1 (a)

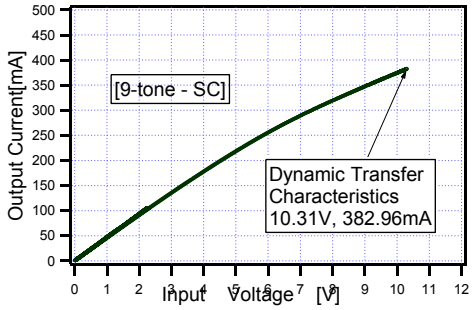

Figure 5.11.1 (b)

Fig. 5.11.1 Measured 9-tone fundamental (a) RF input voltage/output current envelopes and the, measured, 9-tone (b) RF fundamental dynamic envelope transfer characteristic for the baseband short circuit condition.

The plots for 3-tone, 5-tone respectively, are shown in appendix E (pg.205) and not here since their compressive characteristics are similar.

Note that the observed dynamic envelope transfer characteristic modeled by equation (3.2.1.8) shown here.

$$\hat{I}_{2,rf}(t) = \sum_{n=0}^{m} \alpha_{2n+1} \left|\hat{V}_{1,rf}(t)\right|^{2n} \hat{V}_{1,rf}(t). \qquad (3.2.1.8)$$

where α_1 represents the linear gain of the system, α_3 quantifies the level of third order intermodulation distortion (IMD), α_5 quantifies the level of fifth order intermodulation distortion (IMD), and so on, up to the desired maximum order m. In this case m=3 is sufficient, distortion up to fifth order, to fit the measured behaviour and the coefficient

values, α_{2n+1}, extracted are given in table 5.11.1 Hence only three terms in equation (3.2.1.8) are required. Note the insensitivity of these envelope coefficients $(\alpha_1, \alpha_3, \alpha_5)$ to the varying stimulus modulation complexity.

Modulation	α_1	α_3	α_5
3-tone	47.59	-0.134	0.00038
5-tone	47.57	-0.137	0.00042
9-tone	46.75	-0.131	0.00038

TABLE 5.11.1 Coefficients describing the non-linearity of the observed dynamic envelope transfer characteristic measured as a function of increasing modulation bandwidth; baseband short circuit reference state.

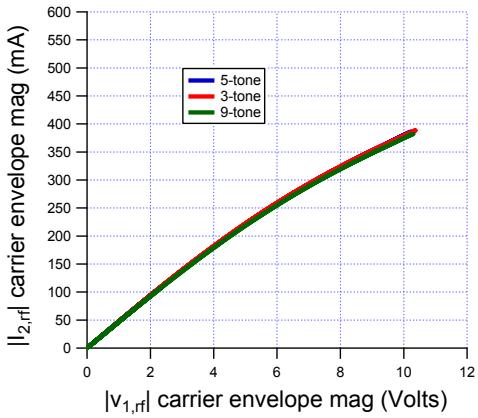

Figure 5.11.1(c), shows the overlays of all the measured transfer characteristics 3,5,9 tones.

These results Figure 5.11.1(c), clearly highlight, certainly over this stimulus shape modification that the non-linear behavior of the transistor is envelope type invariant, this is consistent with the previous investigations in chapter 5 section one. This confirms the advantage of the formulation. If the envelope transfer characteristic is stimulus invariant so should the linearizing baseband voltage envelope coefficients be stimulus invariant.

5.11.2 Linear state measurements result (after applying baseband linearization)

The baseband linearization formulation, was now used to 'engineer' the required output baseband stimulus to linearize the transistors dynamic RF transfer characteristic. In this case just two coefficients, β_2 and β_4, need to be optimized to compute the necessary output baseband linearizing stimulus using BEL. Fig. 5.11.2(a&b), show the linearized performance achieved. The results for the other modulation schemes are shown in Appendix E (pg.205). The dynamic envelope transfer characteristics now becoming a straight line through the origin.

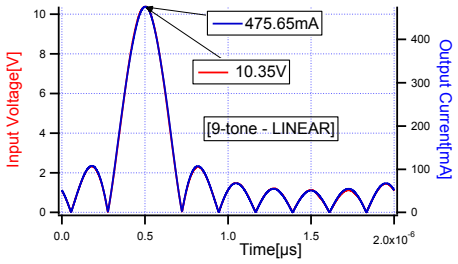

Figure 5.11.2 (a)

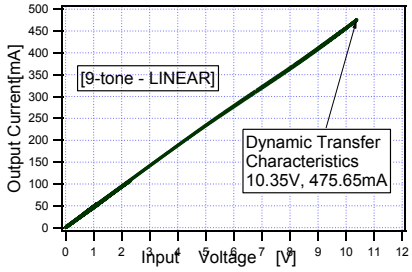

Figure 5.11.2 (b)

Fig. 5.11.2.(a) Measured 9-tone fundamental linear RF input voltage/output current envelopes, (b), measured, 9-tone linear RF dynamic transfer characteristic achieved using an optimized output baseband injection signal.

The two, β_2 and β_4, optimized linearization coefficients were required to compute the necessary output baseband stimulus using BEL, to linearize the transistor and were found to be almost invariant.

The values determined are summarised in table 5.11.2

modulation	β_2	β_4
3-tone	0.0785	-8.06e-5
5-tone	0.0819	-2.34e-5
9-tone	0.0678	-1.186e-5

TABLE 5.11.2 Optimized linearization coefficients determined as a function of increasing modulation envelope complexity.

It is believed that the values in the table suggest invariance since the little changes observed are due to the real measurement system in-ability to forcefully energise the exact spot on the device input-voltage-output-current (I-V) plane due to physical parameters such as temperature as the envelope complexity were changed in the same continuous instance of measurement. This can be due changing peak-to-average power ratio, level of drive adjustment to maintain the same drive level while changing envelope complexity was changed form 9-tone to 5-tone and 3-tone on a 9-tone grid.

In all cases the device has been very successfully linearized. The dynamic envelope transfer characteristics becoming a straight line through the origin and the input voltage and output current envelopes overlap perfectly well.

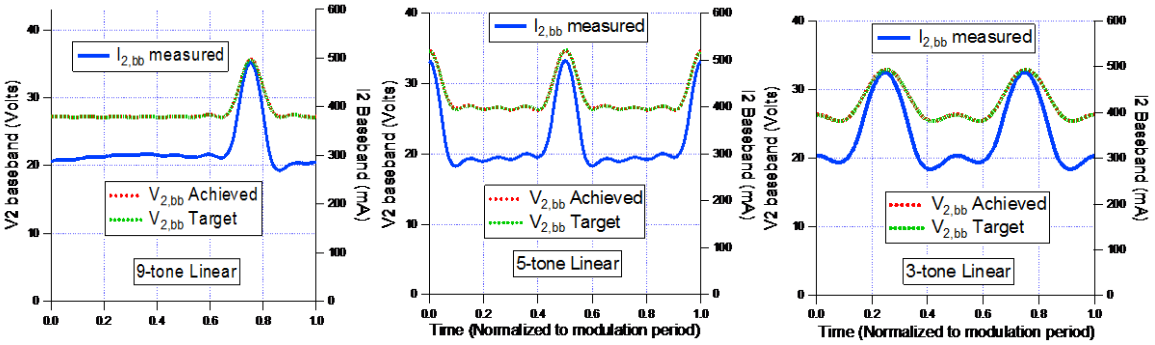

(i) (ii) (iii)

Figure 5.11.2 (c) Measured linearizing baseband voltage waveforms for the (i) 9-tone, (ii) 5-tone and (iii) 3-tone stimulus respectively.

The linearizing waveforms shown in figure 5.11.2(c), show that while the linearization coefficients are invariant the actually time varying baseband signal changes as the stimulus changes.

It is important to note, that in all cases, independent of signal complexity, the determination of the optimized output baseband signal necessary to achieve this linear performance required the determination of just two linearization coefficients, $\beta_2$andβ_4. In fact the values of these coefficients were also insensitive to varying stimulus modulation complexity. Note, this does not mean that the baseband linearizing voltage is actually stimulus invariant. The envelope formulation does ensure that the actual time varying baseband signal does change as the stimulus changes.

5.12 Spectral analysis and plots

More traditionally the presented performance improvement is observed in terms of the elimination of spectral regrowth as shown in the figures 5.12(a,b&c).

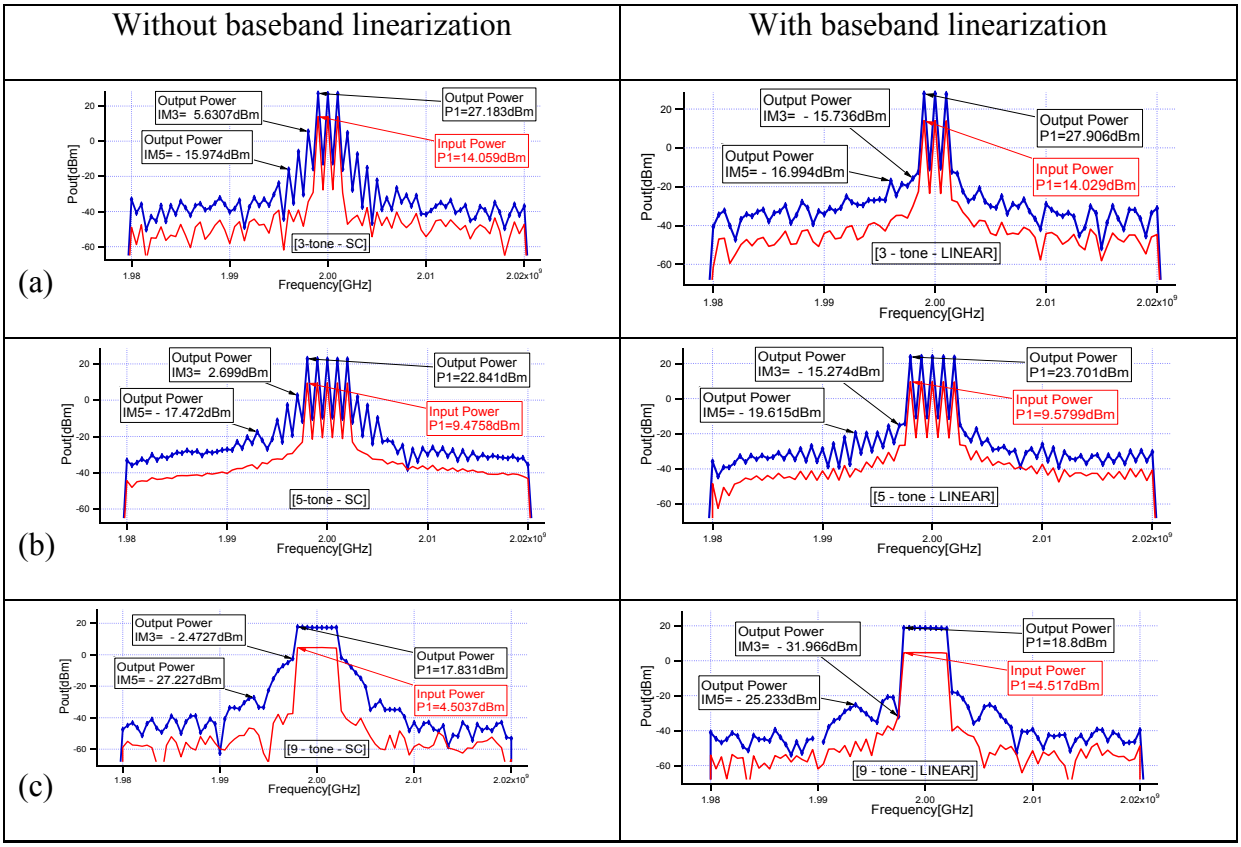

Fig. 5.12 shows (a) 3-tone, (b) 5-tone and (c) 9-tone stimulus respectively as a result of linearizing the envelope transfer characteristic.

In all cases a very similar level of improvement was observed. Spectral regrowth, distortion, in all cases was simultaneously reduced to a level around -50dBc, a value believed to be limited more by the dynamic range of the measurement system than the ability of the optimized baseband enveloped derived signal to linearize, and eliminated the AM/AM distortion.

5.13 Chapter summary

In this chapter the ability of the envelope linearization formulation to successfully compute the baseband signal necessary to eliminate AM/AM distortion with increasingly complex signals has been demonstrated. This property was validated with modulated signals of increasing complexity from 3-tones to 17-tones. In each case a 10W Cree GaN HEMT device was driven 1.5dB into compression generating non-linear behaviour up to 5th order. Irrespective of the signal complexity the device was successfully linearized using just two-linearization coefficients. Distortion was reduced to around similar levels, which are values very close to the dynamic range of the measurement system. As in the case of varying the modulation envelope bandwidth the value of linearization coefficients was also independent of the modulation envelope shape, hence in general the envelope complexity of the modulated signal.

5.14 References

[1] Ogboi, F.L.; Tasker, P.J.; Akmal, M.; Lees, J.; Benedikt, J.; Bensmida, S.; Morris, K.; Beach, M.; McGeehan, J., "A LSNA configured to perform baseband engineering for device linearity investigations under modulated excitations," *Microwave Conference (EuMC), 2013 European* , vol., no., pp.684,687, 6-10 Oct. 2013

[2] Andrei Grebennikov, "RF and Microwave Power Amplifier Design". McGraw-Hill ISBN 0-07-144493-9

[3] Joel Vuolevi and Timo Rahkonen," Distortion in RF Power Amplifiers", Norwood, MA: Artech House, 2003.

[4] Chi-Shuen Leung, Kwok-Keung, M. Cheng, "A new approach to amplifier linearization by the generalized baseband signal injection method," IEEE microwave and wireless components letters, vol. 12, no.9, September, 2002.

[5] Akmal, M.; ,et al "Linearity enhancement of GaN HEMTs under complex modulated excitations by optimizing the baseband impedance environment," *Microwave Symposium Digest (MTT), 2011 IEEE MTT-S International* , vol., no., pp.1,1, 5-10 June 2011, doi: 10.1109/MWSYM.2011.5973183.

[6] Akmal, M.; Ogboi, F.L.; Yusoff, Z.; Lees, J.; Carrubba, V.; Choi, H.; Bensmida, S.; Morris, K.; Beach, M.; McGeehan, J.; Benedikt, J.; Tasker, P.J., "Characterization of electrical memory effects for complex multi-tone excitations using broadband active baseband load-pull," *Microwave Conference (EuMC), 2012 42nd European* , vol., no., pp.1265,1268, Oct. 29 2012-Nov. 1 2012

[7] Yusoff, Z.; Lees, J.; Benedikt, J.; Tasker, P.J.; Cripps, S.C., "Linearity improvement in RF power amplifier system using integrated Auxiliary Envelope Tracking system,"

Microwave Symposium Digest (MTT), 2011 IEEE MTT-S International , vol., no.,pp.1,4,5-10June2011doi: 10.1109/MWSYM.2011.5972769

[8] Reynolds, J., "Nonlinear distortions and their cancellation in transistors," Electron Devices, IEEE Transactions on , vol.12, no.11, pp.595,599, Nov 1965, doi: 10.1109/T-ED.1965.15615

[9] Francois, B.; Kaymaksut, E.; Reynaert, P., "Burst mode operation as an efficiency enhancement technique for RF power amplifiers," General Assembly and Scientific Symposium, 2011 XXXth URSI , vol., no., pp.1,4, 13-20 Aug. 2011 doi:10.1109/URSIGASS.2011.6050496.

[10] Lynn, C.F.; Parson, J.; Kelly, P.; Taylor, M.; Mankowski, J.; Dickens, J.; Neuber, A; Kristiansen, M., "Burst mode operation of >100 MW reflex triode vircator," Plasma Science (ICOPS), 2013 Abstracts IEEE International Conference on , vol., no., pp.1,1, 16-21 June 2013 doi: 10.1109/PLASMA.2013.6635085.

[11] Leeson, M.S., "Spectrally sliced transmission with burst mode operation," Optoelectronics, IEE Proceedings - , vol.151, no.4, pp.211,218, 26 Aug. 2004 doi: 10.1049/ip-opt:20040672.

[12] Parveg, D.R.; Singerl, P.; Wiesbauer, A; Nemati, H.M.; Fager, C., "A broadband, efficient, overdriven class-J RF power amplifier for burst mode operation," Microwave Conference (EuMC), 2010 European , vol., no., pp.1666,1669, 28-30 Sept. 2010.

[13] Jin-ho choi; Dong-Young Huh; Young-seok Kim, "The improved burst mode in the stand-by operation of power supply," Applied Power Electronics Conference and Exposition, 2004. APEC '04. Nineteenth Annual IEEE , vol.1, no., pp.426,432 Vol.1, 2004, doi: 10.1109/APEC.2004.1295844.

[14] Cvijetic, N.; Tanaka, A; Yue-Kai Huang; Cvijetic, M.; Ip, E.; Yin Shao; Ting Wang, "4+G mobile backhaul over OFDMA/TDMA-PON to 200 cell sites per fiber with 10Gb/s upstream burst-mode operation enabling < 1ms transmission latency," Optical Fiber Communication Conference and Exposition (OFC/NFOEC), 2012 and the National Fiber Optic Engineers Conference , vol., no., pp.1,3, 4-8 March 2012.

[15] Shuli Chi; Singerl, P.; Vogel, C., "Efficiency Optimization for Burst-Mode Multilevel Radio Frequency Transmitters," Circuits and Systems I: Regular Papers, IEEE Transactions,on,vol.60,no.7,pp.1901,1914,July2013,doi:10.1109/TCSI.2012.222648U

[16] Pato, S.V.; Meleiro, R.; Fonseca, D.; Andre, P.; Monteiro, P.; Silva, H., "All-Optical Burst-Mode Power Equalizer Based on Cascaded SOAs for 10-Gb/s EPONs," Photonics Technology Letters, IEEE , vol.20, no.24, pp.2078,2080, Dec.15, 2008 doi: 10.1109/LPT.2008.2006629.

[17] Ossieur, P.; Xing-Zhi Qiu; Bauwelinck, J.; Vandewege, J., "Sensitivity penalty calculation for burst-mode receivers using avalanche photodiodes,", Journal of Lightwave Technology, vol.21, no.11, pp.2565, 2575, Nov. 2003 doi: 10.1109/JLT.2003.819141.

[18] Boyogueno, A; Slamani, M., "Power penalty improvement for burst-mode fibre optic receivers," Electrical and Computer Engineering, 2000 Canadian Conference on , vol.2, no., pp.976,980 vol.2, 2000, doi: 10.1109/CCECE.2000.849611.

[19] Jri Lee; Mingchung Liu, "A 20-Gb/s Burst-Mode Clock and Data Recovery Circuit Using Injection-Locking Technique," Solid-State Circuits, IEEE Journal of , vol.43, no.3, pp.619,630, March 2008, doi: 10.1109/JSSC.2007.916598.

[20] Brigati, S.; Colombara, P.; D'Ascoli, L.; Gatti, U.; Kerekes, T.; Malcovati, P., "A SiGe BiCMOS burst-mode 155-Mb/s receiver for PON," Solid-State Circuits, IEEE Journal of , vol.37, no.7, pp.887,894, Jul 2002, doi: 10.1109/JSSC.2002.1015687.

[21] Reviriego, P.; Maestro, J.A; Larrabeiti, D.; Larrabeiti, D., "Burst Transmission for Energy-Efficient Ethernet," Internet Computing, IEEE , vol.14, no.4, pp.50,57, July-Aug. 2010, doi: 10.1109/MIC.2010.52.

[22] Cao, B.; Mitchell, J.E., "Modelling optical burst equalisation in next generation access network," Transparent Optical Networks (ICTON), 2010 12th International Conference on , vol., no., pp.1,4, June 27 2010-July 1 2010, doi: 10.1109/ICTON.2010.5549289.

[23] Ishihara, N.; Nakamura, M.; Akazawa, Y.; Uchida, N.; Akahori, Y., "3.3 V, 5O Mb/s CMOS transceiver for optical burst-mode communication," Solid-State Circuits Conference, 1997. Digest of Technical Papers. 43rd ISSCC., 1997 IEEE International , vol., no., pp.244,245, 8-8 Feb. 1997, doi: 10.1109/ISSCC.1997.585372.

[24] Seebacher, D.; Bosch, W.; Singerl, P.; Schuberth, C., "Efficiency enhancement of burst mode transmitters by RF energy recovery," Ph.D. Research in Microelectronics and Electronics (PRIME), 2013 9th Conference on , vol., no., pp.221,224, 24-27 June 2013, doi: 10.1109/PRIME.2013.6603147.

[25] Nguyen, C.; Nguyen, N.X.; Grider, D.E., "Drain current compression in GaN MODFETs under large-signal modulation at microwave frequencies," Electronics Letters , vol.35, no.16, pp.1380,1382, 5 Aug 1999, doi: 10.1049/el:19990957.

[26] Wei, C.J.; Klimashov, A; Zhu, Y.; Lawrence, E.; Tkachenko, G., "Large-signal PHEMT switch model, which accurately predicts harmonics and two-tone inter-modulation distortion," Microwave Symposium Digest, 2005 IEEE MTT-S International , vol., no., pp.4 pp.,, 12-17 June 2005, doi: 10.1109/MWSYM.2005.1516880.

[27] Hausmair, K.; Shuli Chi; Vogel, C., "How to reach 100% coding efficiency in

multilevel burst-mode RF transmitters," Circuits and Systems (ISCAS), 2013 IEEE International Symposium on , vol., no., pp.2255,2258, 19-23 May 2013
doi: 10.1109/ISCAS.2013.6572326.

[28] Shuli Chi; Singerl, P.; Vogel, C., "Efficiency Optimization for Burst-Mode Multilevel Radio Frequency Transmitters," Circuits and Systems I: Regular Papers, IEEE Transactions on , vol.60, no.7, pp.1901,1914, July 2013, doi: 10.1109/TCSI.2012.2226487.

[29] Yong-Hun Oh; Ho-Yong Kang; Kyoohyun Lim; Jongsik Kim; Sang-Gug Lee, "A fully integrated CMOS burst-mode upstream transmitter for gigabit-class passive optical network applications," Solid State Circuits Conference, 2007. ESSCIRC 2007. 33rd European , vol., no., pp.516,519, 11-13 Sept. 2007, doi: 10.1109/ESSCIRC.2007.4430355.

[30] Yong-Hun Oh; Quan Le; Yen, N.D.B.; Sang-Gug Lee; Ho-Yong Kang; Tae-Whan Yoo, "A CMOS burst-mode up-stream transmitter for fiber-optic gigabit ethernet applications," Advanced Communication Technology, 2005, ICACT 2005. The 7th International Conference on , vol.2, no., pp.1283,1286, 0-0 0
doi: 10.1109/ICACT.2005.246200.

[31] Bende, Andre Boyogueno, "Design and implementation of optoelectronic interfaces for high-speed burst-mode transmissions," Journal of Vacuum Science & Technology B: Microelectronics and Nanometer Structures , vol.18, no.4, pp.1962,1966, Jul 2000
doi: 10.1116/1.1303811.

[32] Nakamura, M.; Ishihara, N.; Akazawa, Yukio, "A 156-Mb/s CMOS optical receiver for burst-mode transmission," Solid-State Circuits, IEEE Journal of , vol.33, no.8, pp.1179,1187, Aug 1998, doi: 10.1109/4.705356.

[33] Tavares, G.N.; Tavares, L.; Piedade, M.S., "A new ML-based data-aided feedforward

symbol synchronizer for burst-mode transmission," Circuits and Systems, 2000. Proceedings. ISCAS 2000 Geneva. The 2000 IEEE International Symposium on , vol.2, no., pp.357,360 vol.2, 2000, doi: 10.1109/ISCAS.2000.856335.

[34] Bauwelinck, J.; Wei Chen; Verhulst, D.; Martens, Y.; Ossieur, P.; Xing-Zhi Qiu; Vandewege, J., "A high-resolution burst-mode laser transmitter with fast and accurate level monitoring for 1.25 Gb/s upstream GPONs," Solid-State Circuits, IEEE Journal of , vol.40, no.6, pp.1322,1330, June 2005, doi: 10.1109/JSSC.2005.848024.

[35] Shastri, B.J.; M'Sallem, Y.B.; Zicha, N.; Rusch, L.A; LaRochelle, S.; Plant, D.V., "Experimental Study of Burst-Mode Reception in a 1300 km Deployed Fiber Link," Optical Communications and Networking, IEEE/OSA Journal of , vol.2, no.1, pp.1,9, January 2010, doi: 10.1364/JOCN.2.000001.

[36] Mitsuyama, Y.; Andales, Z.; Onoye, T.; Shirakawa, I, "Burst mode: a new acceleration mode for 128-bit block ciphers," Custom Integrated Circuits Conference, 2002. Proceedings of the IEEE 2002 , vol., no., pp.151,154, 2002 doi: 10.1109/CICC.2002.1012786.

[37] Vacondio, F.; Simonneau, C.; Voicila, A; Tanguy, J.-M.; de Valicourt, G.; Dutisseuil, E.; Lorcy, L.; Antona, J.-C.; Charlet, G.; Bigo, S., "Experimental demonstration of a PDM QPSK real-time burst mode coherent receiver in a packet switched network," Optical Communications (ECOC), 2012 38th European Conference and Exhibition on , vol., no., pp.1,3, 16-20 Sept. 2012.

[38] Qiu, X.Z.; Yi, Y.C.; Ossieur, P.; Verschuere, S.; Verhulst, D.; De Mulder, B.; Chen, W.; Bauwelinck, J.; De Ridder, T.; Baekelandt, B.; Melange, C.; Vandewege, J., "High Performance Burst-Mode Upstream Transmission for Next Generation PONs," Optical Fiber Communication & Optoelectronic Exposition & Conference, 2006.

AOE 2006. Asian , vol., no., pp.1,3, 24-27 Oct. 2006, doi: 10.1109/AOE.2006.307318.

[39] Gi-Hong Im; Cheol-Jin Park, "All digital 1.62 Mb/s QPSK burst-mode system for FTTC/VDSL transmission," Consumer Electronics, IEEE Transactions on , vol.46, no.4, pp.1088,1097, Nov 2000, doi: 10.1109/30.920466.

[40] Ishihara, N.; Nakamura, M.; Akazawa, Y.; Uchida, N.; Akahori, Y., "3.3 V, 5O Mb/s CMOS transceiver for optical burst-mode communication," Solid-State Circuits Conference, 1997. Digest of Technical Papers. 43rd ISSCC., 1997 IEEE International , vol., no., pp.244,245, 8-8 Feb. 1997, doi: 10.1109/ISSCC.1997.585372.

[41] Hausmair, K.; Shuli Chi; Singerl, P.; Vogel, C., "Aliasing-Free Digital Pulse-Width Modulation for Burst-Mode RF Transmitters," Circuits and Systems I: Regular Papers, IEEE Transactions on , vol.60, no.2, pp.415,427, Feb. 2013, doi: 10.1109/TCSI.2012.2215776.

[42] Shuli Chi; Hausmair, K.; Vogel, C., "Coding efficiency of bandlimited PWM based burst-mode RF transmitters," Circuits and Systems (ISCAS), 2013 IEEE International Symposium on , vol., no., pp.2263,2266, 19-23 May 2013
doi: 10.1109/ISCAS.2013.6572328.

[43] Francois, B.; Reynaert, P.; Wiesbauer, A; Singerl, P., "Analysis of burst-mode RF PA with direct filter connection," Microwave Conference (EuMC), 2010 European , vol., no., pp.974,977, 28-30 Sept. 2010.

[44] Shrimpton, D.H.; Dobbyn, C.; Casey, T., "Towards the convergence of interactive television and WWW," Multimedia Services and Digital Television by Satellite (Ref. No. 1999/111), IEE Colloquium on , vol., no., pp.6/1,6/6, 1999
doi: 10.1049/ic:19990629.

[45] Carlucci, J.B., "Social Media Television in Today's Cable Systems," Consumer Communications and Networking Conference (CCNC), 2010 7th IEEE , vol., no., pp.1,5, 9-12 Jan. 2010, doi: 10.1109/CCNC.2010.5421636.

[46] JESTY, L.C., "Television as a communication problem," Proceedings of the IEE - Part IIIA: Television , vol.99, no.20, pp.761,770, 1952
doi: 10.1049/pi-3a.1952.0093.

[47] Arai, J., "Three-dimensional television system based on spatial imaging method using integral photography," Acoustics, Speech and Signal Processing (ICASSP), 2012 IEEE International Conference on , vol., no., pp.5449,5452, 25-30 March 2012
doi: 10.1109/ICASSP.2012.6289154.

[48] Chandaria, J.; Hunter, J.; Williams, A, "The carbon footprint of watching television, comparing digital terrestrial television with video-on-demand," Sustainable Systems and Technology (ISSST), 2011 IEEE International Symposium on , vol., no., pp.1,6, 16-18 May 2011, doi: 10.1109/ISSST.2011.5936908.

[49] Sheng, S., "Mobile television receivers: A free-to-air overview," Communications Magazine, IEEE , vol.47, no.9, pp.142,149, September 2009
doi: 10.1109/MCOM.2009.5277468.

[50] Redondo-Garcia, J.L.; Boton-Fernandez, V.; Lozano-Tello, A, "Linked Data methodologies for managing information about television content: Applying Linked Data principles in the OntoTV system, in order to improve the collection processes and the way television information is accessed," Information Systems and Technologies (CISTI), 2012 7th Iberian Conference on , vol., no., pp.1,6, 20-23 June 2012.

[51] Kunic, S.; Sego, Z., "3D television," ELMAR, 2011 Proceedings , vol., no., pp.127,131, 14-16 Sept. 2011.

[52] Bove, V.M.; Barabas, J.; Jolly, S.; Smalley, D., "How to build a holographic television system," 3DTV-Conference: The True Vision-Capture, Transmission and Dispaly of 3D Video (3DTV-CON), 2013 , vol., no., pp.1,4, 7-8 Oct. 2013 doi: 10.1109/3DTV.2013.6676637.

[53] Woon Hau Chin; Zhong Fan; Haines, R., "Emerging technologies and research challenges for 5G wireless networks," Wireless Communications, IEEE , vol.21, no.2, pp.106,112, April 2014, doi: 10.1109/MWC.2014.6812298.

[54] Yanikomeroglu, H., "Towards 5G wireless cellular networks: Views on emerging concepts and technologies," Signal Processing and Communications Applications Conference (SIU), 2012 20th , vol., no., pp.1,2, 18-20 April 2012, doi: 10.1109/SIU.2012.6204422.

[55] Zakrzewska, A; Ruepp, S.; Berger, M.S., "Towards converged 5G mobile networks-challenges and current trends," ITU Kaleidoscope Academic Conference: Living in a converged world - Impossible without standards?, Proceedings of the 2014 , vol., no., pp.39,45, 3-5 June 2014, doi: 10.1109/Kaleidoscope.2014.6858478.

[56] Al-Manthari, B.; Hassanein, H.; Nasser, N., "Packet scheduling in 3.5G high-speed downlink packet access networks: breadth and depth," Network, IEEE , vol.21, no.1, pp.41,46, Jan.-Feb. 2007, doi: 10.1109/MNET.2007.314537.

[57] Monserrat, J.F.; Droste, H.; Bulakci, O.; Eichinger, J.; Queseth, O.; Stamatelatos, M.; Tullberg, H.; Venkatkumar, V.; Zimmermann, G.; Dotsch, U.; Osseiran, A, "Rethinking the mobile and wireless network architecture: The METIS research into 5G," Networks and Communications (EuCNC), 2014 European Conference on , vol., no., pp.1,5, 23-26 June 2014, doi: 10.1109/EuCNC.2014.6882682.

[58] Demestichas, P.; Georgakopoulos, A; Karvounas, D.; Tsagkaris, K.; Stavroulaki, V.; Jianmin Lu; Chunshan Xiong; Jing Yao, "5G on the Horizon: Key Challenges for the Radio-Access Network," Vehicular Technology Magazine, IEEE , vol.8, no.3, pp.47,53, Sept. 2013, doi: 10.1109/MVT.2013.2269187.

CHAPTER SIX

BEL – LIMITATIONS OF FORMULATION

6.1 BEL and AM/PM Distortion

6.1.1 AM/AM AND AM/PM DISTORTION ARE DE-COUPLED

In the previous chapters we have shown that baseband injection can be used to eliminate AM/AM distortion. This is achieved by determining the beta values that set the alpha values in equation (3.2.1.8) shown here to zero. In this case it is assumed that the system being linearized, has little or no AM/PM distortion, hence the alpha terms are real numbers.

$$\hat{I}_{2,rf}(t) = \sum_{n=0}^{m} \alpha_{2n+1} |\hat{V}_{1,rf}(t)|^{2n} \hat{V}_{1,rf}(t) \qquad (3.2.1.8)$$

In practice this is not the case and so the alpha terms are complex numbers. Since baseband linearization can only modify the AM/AM behaviour, BEL have, in practice being linearizing the following equation (3.2.1.10) shown here.

$$\left|\hat{I}_{2,rf}(t)\right| = \sum_{n=0}^{m} \alpha_{2n+1} |\hat{V}_{1,rf}(t)|^{2n} \left|\hat{V}_{1,rf}(t)\right| \qquad (3.2.1.10)$$

In this case the alpha terms are real numbers.

This situation is shown in figure 6.1.1(a and b). This is also similar to most of the measurement investigated so far. With the level of AM/PM being small hence extracting "real" alpha terms was appropriate. In figure 6.1.1, the green curve show the model extracted by BEL, while the red squares show actual measurement.

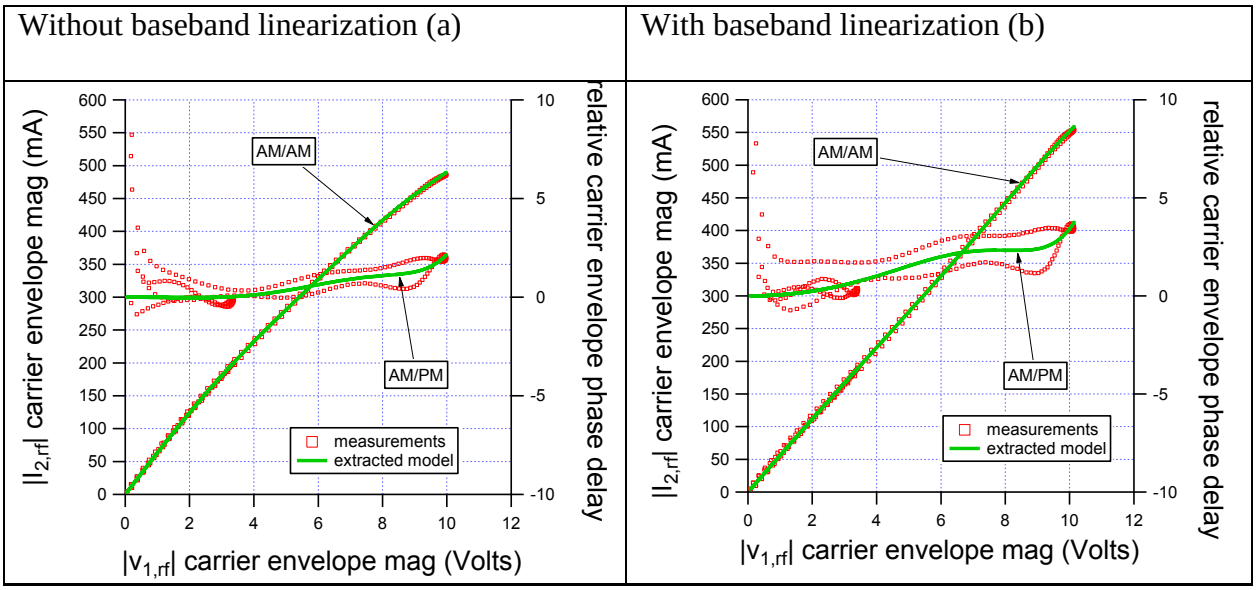

Figures 6.1.1 shows the states of the measured AM/AM and AM/PM distortion at (a) the reference baseband short circuit state and (b) for linear correction of 10W GaN-on-SiC RFPA device.

The plot on the right (b) show the state (linear) of the device after the linearizing baseband signal was injected into the device. The AM/AM plot is running from the origin to the top right-hand part of the plot. The AM/PM plot is running almost horizontal across the plot page.

As shown in Figure 6.1.1, by injecting a baseband using the introduced formulation, it is possible to eliminate the AM/AM distortion. It is also observed that the level of the AM/AM distortion (plot on the right) has been completely removed, leaving only the AM/PM distortion almost unchanged. However, it can be seen that the AM/PM distortion suggest a de-coupled behaviour from the AM/AM as it was un-affected by the linearization exercise.

A similar measurements is shown below in figure 6.1.1(c and d), on a 25W GaN-on Si device. These show the same AM/AM and AM/PM distortion behaviour before and after the devices had been linearized, and a behaviour similar to the GaN-on-SiC shown in Figure 6.1.1 (a and b).

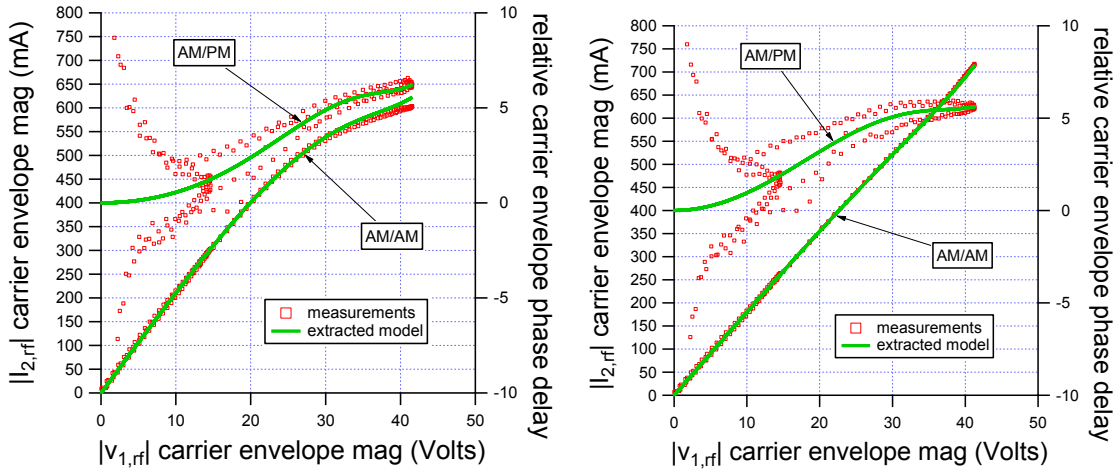

(c) (d)

Figure 6.1.1 (c) before linearization and (d) showing measured complex envelope dynamic transfer characteristics of the AM/AM and AM/PM after linearisation.

The results of similar experiment on a 10W Silicon LDMOS device are shown in

Figure 6.1.1(e and f)

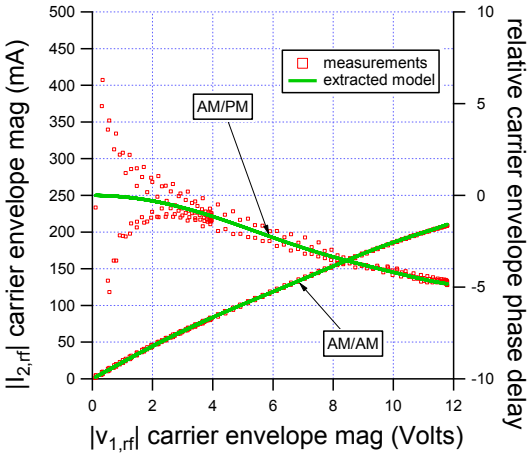

Figure 6.1.1 (e)

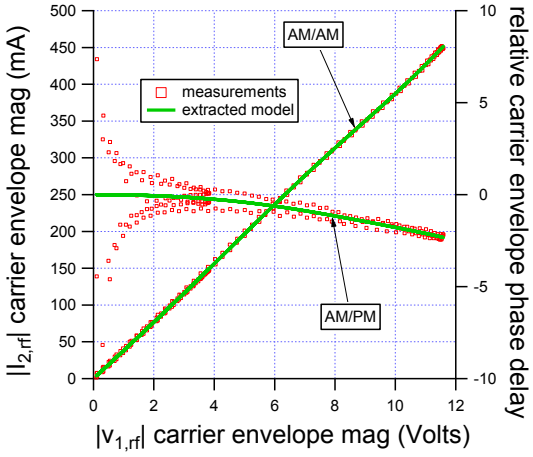

Figure 6.1.1(f)

Figure 6.1.1 (e) before linearization and (f) showing measured complex envelope dynamic transfer characteristics of the AM/AM and AM/PM after linearization.

In these figures 6.1.1 (a, b, c, d, e and f), show similar behavior with the pattern of AM/AM and AM/PM distortion. When the device is in its compressed state, the AM/AM plot shows a compression (curved line), but in its linearised state it becomes a straight line through the origin. Similarly, in both plots, we see a repeated behavior as shown earlier regarding the AM/PM distortion plot seemingly un-affected by the linearization exercise.

These measurement results on different devices depict a behavior between AM/AM and AM/PM distortion, which is not device related. In addition, the spreading shown by the red squares of figures 6.1.1 c, d, e and f, at lower power, is attributed to the simple propagation delay experienced by the signal envelope between the input and the output ports of the device [66].

Since these distortion appear de-coupled, it is possible to suppress either without affecting the other. This knowledge is very useful in small cell [62] – [64] design, where digital signal processing power (DPD) does not always scale with decreasing maximum RF power, it is possible to use an AM/AM linearizer to suppress AM/AM distortion effectively and cheaply, while reduced complexity DPD can be used to suppress AM/PM distortion. This observation was explored in the following technology application investigation of BEL.

6.2 BEL and other device Technologies

In previous chapters, it has been shown that BEL was used extensively to carry out investigation of gallium-nitride-on-silicon-carbide (GaN-on-SiC) devices. BEL was also used to linearise devices of other technologies, including a gallium-nitride-on-silicon (GaN-on-Si) and silicon (Si) type devices using a 3-tone modulation.

Two specific device technologies were further investigated namely; a 25W GaN-on-Si HFET depletion-mode device, and a 10W, Silicon (Si) LDMOS type, enhancement-mode device. The GaN-on-Si device was biased at a drain voltage of +28V and a gate voltage of -1.3V, and the silicon LDMOS type device was biased at +32V drain voltage and +2.8V gate voltage targeting class AB operation and in both cases giving a quiescent current of 12% I_{DSS}. Both devices were driven into 2.4dB compression, with the output terminated using passive 50 Ohm loads. The silicon device gave a peak envelope power (PEP) of approximately 33dBm while the 25W GaN-on-Si HFET device delivered, a peak envelope power (PEP) of 40dBm.

6.2.1 Reference baseband short-circuit state measurement result

Reference conditions were established with the baseband output voltage set to zero (reference baseband short circuit state) and are shown in Fig. 6.2.1 (a&b) GaN-on-Si, (c&d)LDMOS.

Results indicate a well behaved AM/PM (green curve) distortion in the (a) 25W GaN-on-Si HFET with only (b) 5th order distortion present. Results also indicate different behaved AM/PM (green curve) distortion in the (c) 10W LDMOS device and (d) 7th order distortion present. It is important to note that the excitation driver amplifier is a 30W power amplifier while the GaN-on-Si is a 25W device and the LDMOS device a 10W device.

The responses are shown in figure 6.2.1(a, b, c and d) respectively for the two devices, referenced in both measurements baseband short circuit state.

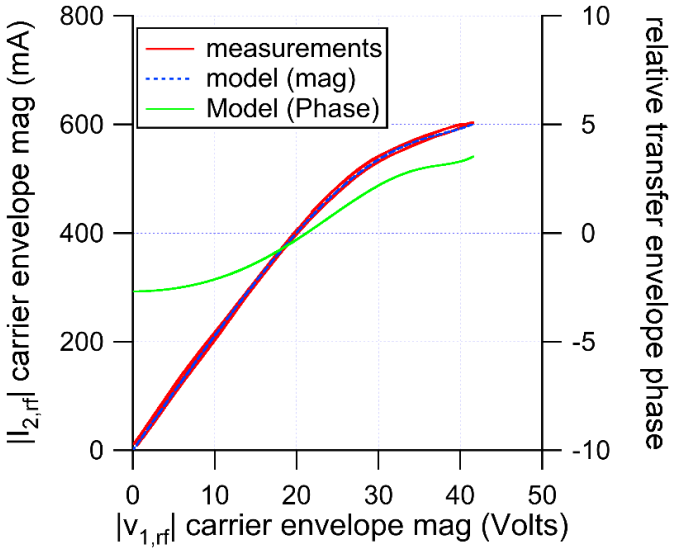

Figure 6.2.1 (a). Shows the measured complex RF envelope dynamic transfer characteristics depicting the AM/AM (red) and the AM/PM (green) distortion curves (GaN-on-Si).

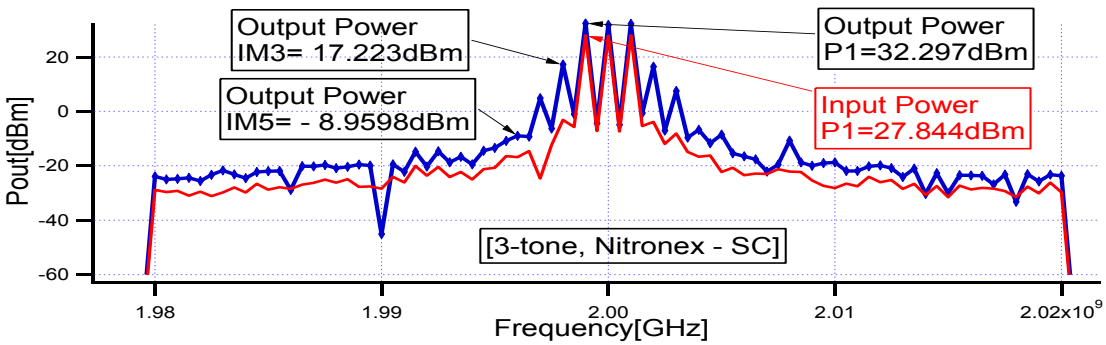

Figure 6.2.1 (b). Show the measured RF input power – output power spectrum at the reference

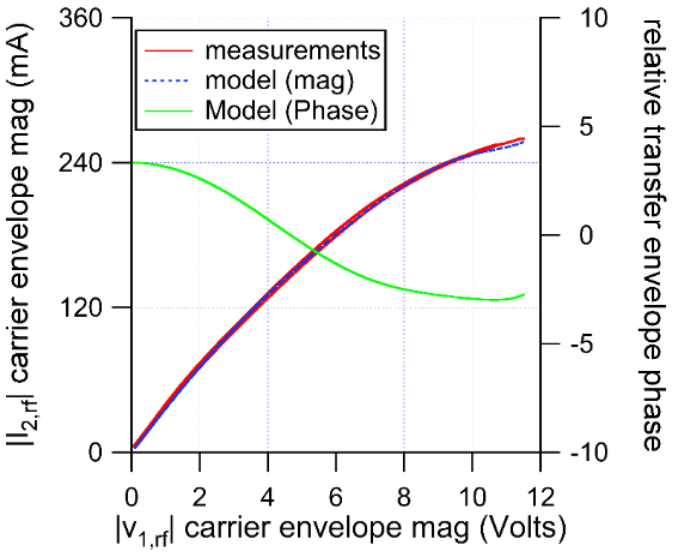

baseband short circuit state (GaN-on-Si).

Figure 6.2.1 (c) Silicon LDMOS

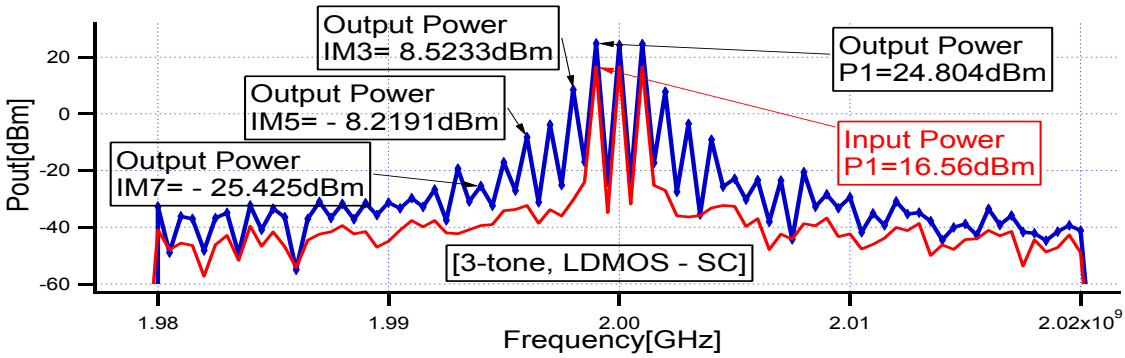

Figure 6.2.1 (d) Silicon LDMOS

Fig. 6.2.1 LDMOS device: Measured reference baseband short circuit state. (c) Dynamic transfer characteristic and (d) Power Spectra.

6.2.2 Linear state measurements result

The optimized baseband injection voltage signal was determined by adjusting the values of β_2 and β_4 in order to simultaneously minimize α_3 and α_5. The results achieved are shown in Fig. 6.2.2(a and b) (25W GaN-on-Si HFET) to 6.2.2(c and d) (10W Si LDMOS). In the case of the (a)25W GaN-on-Si HFET the results clearly show that this device was successfully linearized with respect to AM/AM. This is shown by the red (AM/AM) and blue (model defined by β_2 and β_4) curve on the dynamic transfer characteristic of Fig. 6.2.2(a). The green curve on the same figure, show the strong presence but a very well behaved AP/PM distortion. A result similar to that previously reported on the 10W GaN-on SiC HFET device in chapter 4. However, in this case only modest overall linearity improvement of 13.62dBc and 2.56dBc in IM3 and IM5 respectively were achieved. It is believed that this level of AM/PM distortion, insensitive to baseband injection, observed in this device explains this limited overall improvement in linearity.

In the case of the 10W LDMOS, elimination of the AM/AM distortion was not completely possible. Hence, only an improvement of 10dBc was achieved in IM3 and none in terms of IM5 for this device. This was thought to be due to the device exhibiting a different AM/PM distortion, shown by the green curve on the dynamic transfer characteristics of Fig. 6.2.2(c). Also a strong presence of the 7th, order term, shown in Fig. 6.2.2(d) and 6.2.1(d) respectively. These cannot be addressed using only two β_{2p} even order voltage component scaling coefficients (effective for 3rd and 5th order terms) nor AM/AM distortion cancellation. However, the model

defined by the coefficients and the AM/AM curve in these figures all agree, confirming AM/AM distortion mitigation effectiveness.

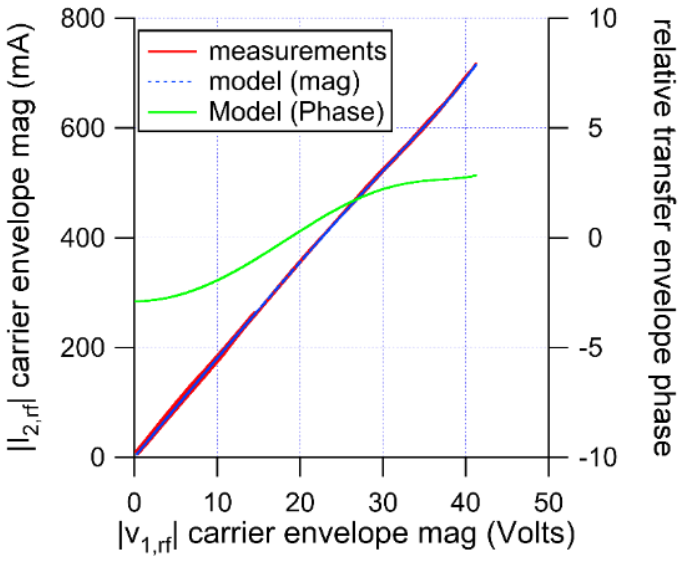

Figure 6.2.2 (a). (GaN-on-Si)

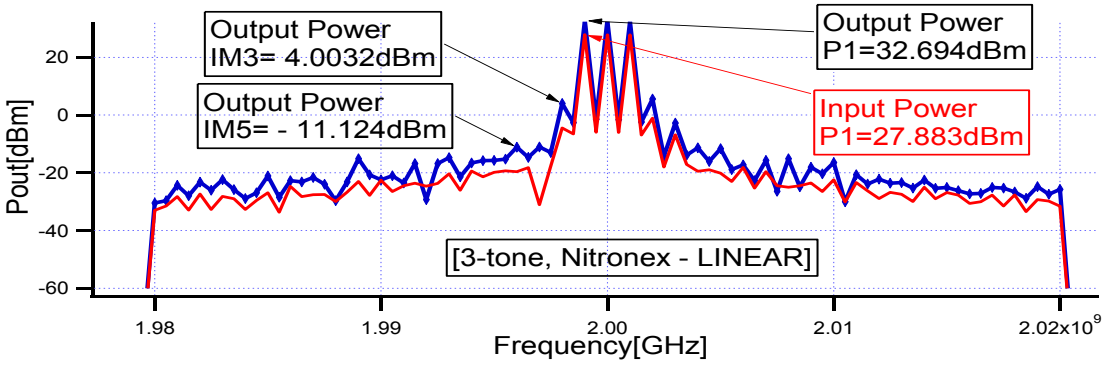

Figure 6.2.2 (b). (GaN-on-Si)

Fig. 6.2.2, 25W GaN-on-Si HFET Device: Measured linear state. (a) RF Envelope Dynamic transfer characteristic and (b) RF Input power – output power Spectra.

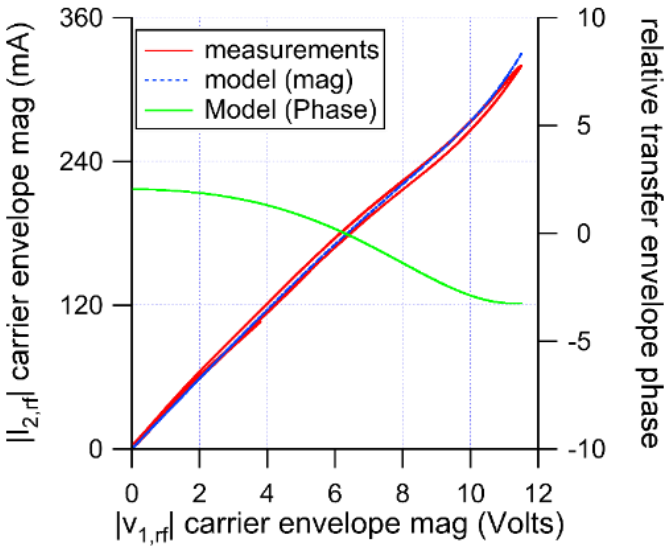

Figure 6.2.2(c). Silicon LDMOS

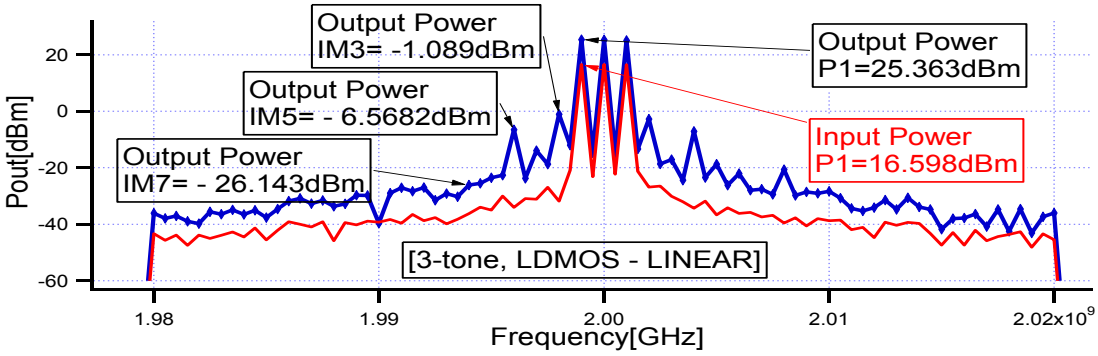

(d). Silicon LDMOS

Fig. 6.2.2. LDMOS device: Measured linear state. (c) RF Envelope Dynamic transfer characteristic and (d) RF Input power – output power Spectra.

6.3 Device technology performance pre-summary

All the devices tested, were driven at different drive (compression) levels. The way the devices were made to show AM/AM and severe AM/PM distortion was to drive the devices into a deep level of compression. By so doing, any device can literarily be driven into any state required in order for it to exhibit the type of distortion considered satisfactory for the goal of the investigation during the experiment. The level of compression used was from 1.5dB to approximately 2.5dB compression at the reference baseband short circuit state. More importantly, it has been shown that it is possible to suppress AM/AM distortion independent of AM/PM distortion.

6.4 BEL Performance Repeatability

6.4.1 Similarity, repeatability and reliability

A set of selected measurements were carried out to show performance repeatability and reliability of the BEL method. They were called repeatability measurements. To do this, a number of repeated measurements were made. A few measurement parameters that will have no effect on performance but show that these were new and different from previous measurements were made. Some of these parameters were change in envelope size, and change in modulation bandwidth. These repeatability measurements showed similar levels of suppression and repeatability. These are shown in the following figures 6.6, and 6.7 respectively. They were 2 devices of the same technology (GaN-on-SiC) and was never used in earlier measurements. A 3-tone signal was used on both devices.

6.5 Suppression repeatability measured with two new different devices “A” and “B”

A new measurement was performed (Figure 6.6 and 6.7), similar to the one performed in chapter three. The idea was to see if similar level of suppression could be achieved with this new measurement. Similar devices (denoted as “A” and “B”), were used for this experiment. Only the envelope size and modulation bandwidth were slightly modified to show that these measurement are different from the earlier measurements. Although, it was carried out on several similar devices, all other measurement parameters was kept approximately similar to the measurement which result was shown earlier in chapter three. The results in these new measurements showed a similar level of suppression. More importantly, this recent measurements confirms the repeatability of performance achieved by BEL in chapter three.

6.6 Device “A” measurements large envelope size (13.46V)

6.6.1 Reference baseband short circuits state measurements result

Figure 6.6.1 show the measured reference baseband short circuit state response of device A and figure 6.6.2 show the measured linear state response of device A.

Before Linearisation:-

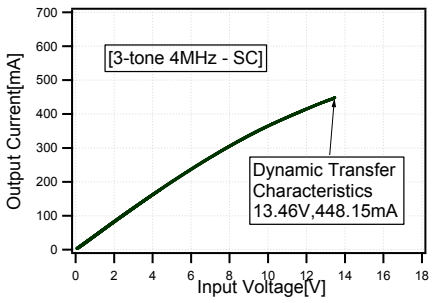

Figure 6.6.1(a). Measured RF envelope dynamic Transfer characteristics

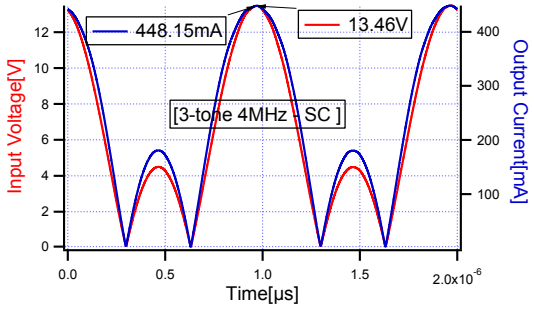

Figure 6.6.1 (b) RF input voltage –output current envelopes

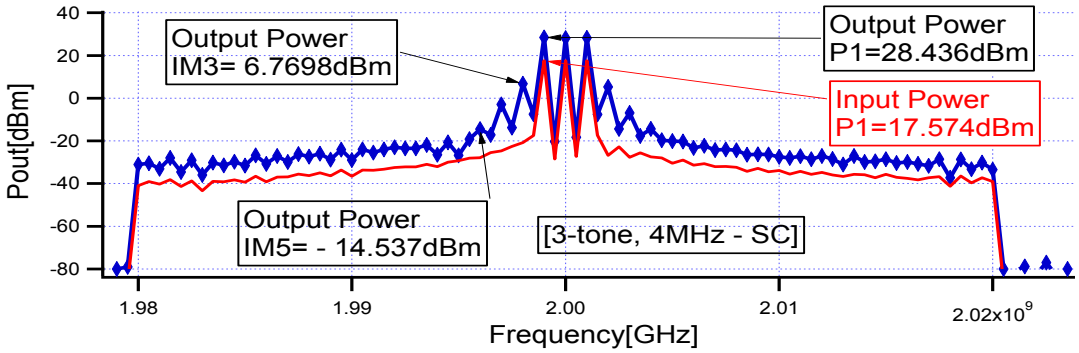

Figure 6.6.1 (c). Measured RF input power – output power spectra, measured at the reference baseband short circuit state of the device A

6.6.2 Linear State measurements result

After Linearisation:-

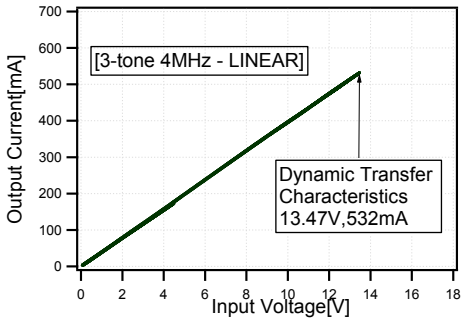

Figure 6.6.2 (a). Measured RF envelope dynamic transfer characteristics

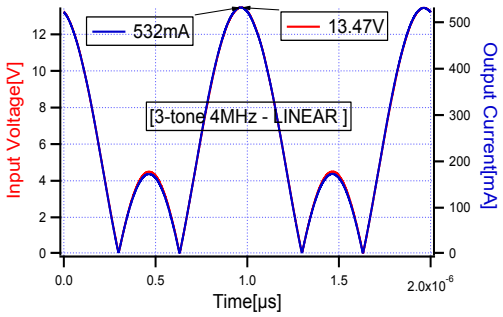

Figure 6.6.2 (b) RF input voltage – output current envelopes

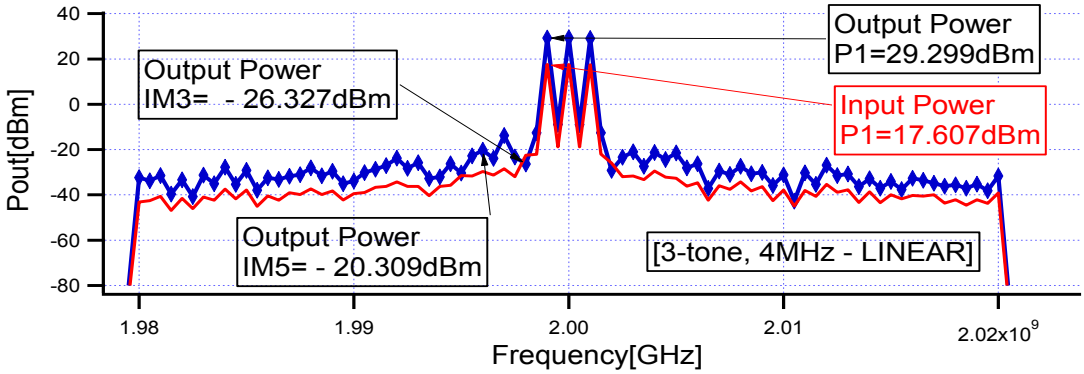

Figure 6.6.2 (c). Measured RF input power – output power spectra of the linearized device

In this new measurement with device A, distortion is reduced to approximately 50dBc, a level similar to that shown earlier in chapter three and also a level very close to the noise-floor of the measurement system.

6.7 Device "B" measurements – 8MHz bandwidth

6.7.1 Reference baseband short circuits state measurements result

Using the same modulation scheme, device B was tested as device A

Before linearization:-

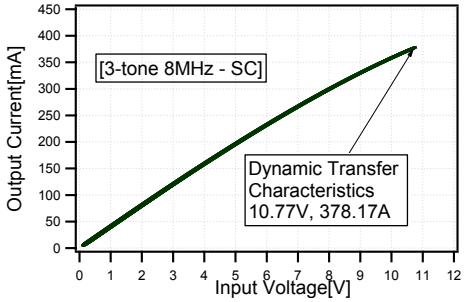

Figure 6.7.1(a). Measured RF envelope dynamic transfer characteristics

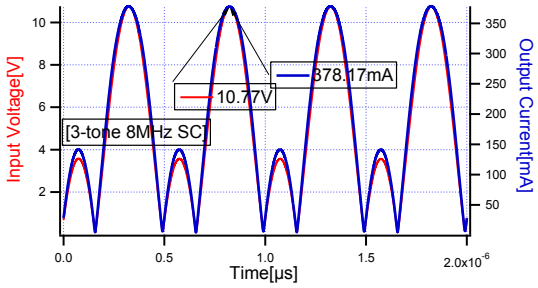

Figure 6.7.1 (b) RF input voltage – output current envelopes

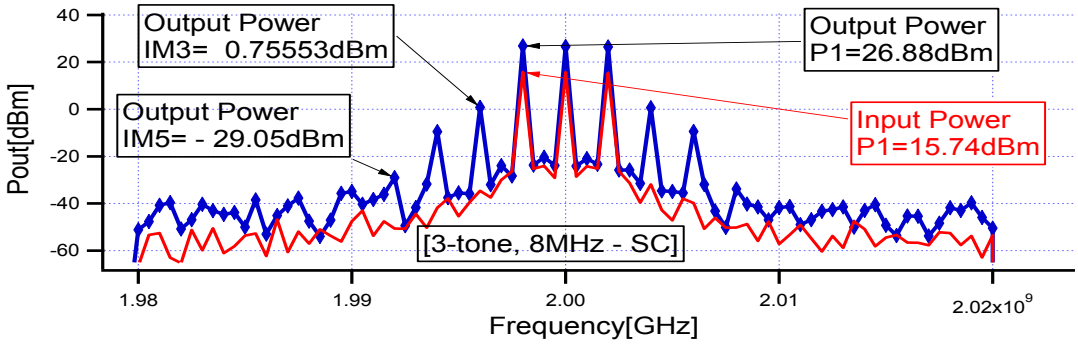

Figure 6.7.1 (c). Measured RF input power – output power spectra, measured at the reference short circuit state of the device B

6.7.2 Linear state measurements result

After Linearisation:-

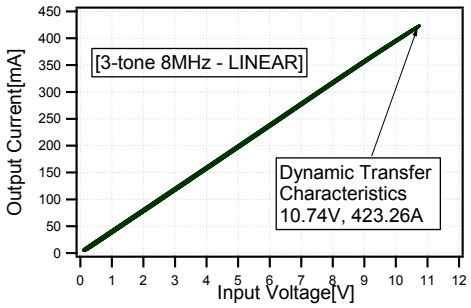

Figure 6.7.2 (a). Measured RF envelope dynamic transfer characteristics

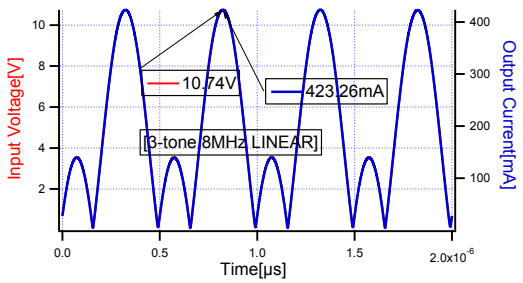

Figure 6.7.2 (b) RF input voltage – output output current envelopes

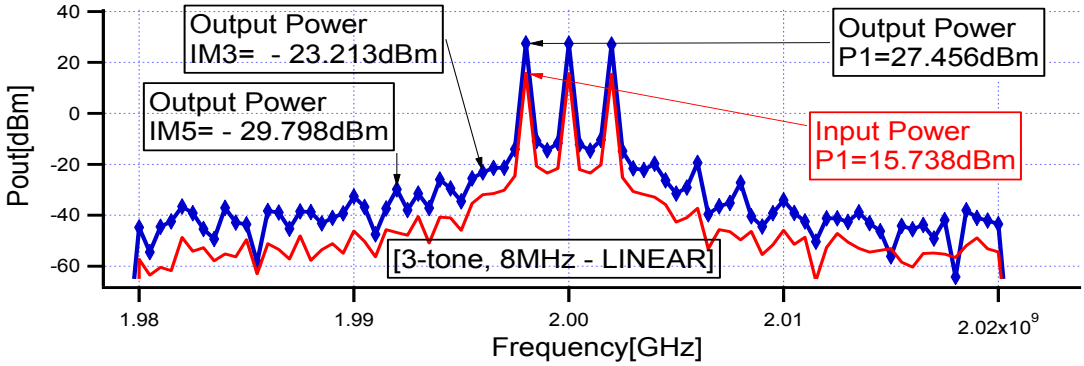

Figure 6.7.2 (c). Measured RF input power – output power spectra, measured at the linear state of the device B

For device B in figure 6.7.1 and 6.7.2 distortion is reduced to approximately 50dBc, a level similar to that for device A.

More importantly, this measurement results show that BEL distortion suppression ability is repeatable when compared with previous measurements in chapters 3, 4 and 5.

6.8 BEL – separating wanted signal from distortion

6.8.1 Advantage – how BEL recognizes distortion

The feature to recognize distortion is an advantage of the envelope domain. Its results has been shown in previous chapters 3, 4, 5 and 6 respectively. In the envelope domain, the distortion envelope and the main signal envelope are two very different envelopes. This distinction is shown in equations (3.2.1.8) below together with its expansion equation. First of all, from the expansion form of equation (3.2.1.8), it can be seen that the 3rd order distortion and the fifth order distortions have unique distortion coefficients (α_3 and α_5) which are different to the coefficients of the main signal (α_1) – termed the linear gain of the system.

Secondly, the distortion envelope – formation is also different. The distortion envelope formation, is a mixed-combination of an even-power-envelope-modulus multiplied by a particular-IMD-order-distorted envelope. This is shown and represented by the output current envelope equation, its linear component and its distortion components as written below (6.8.1.1).

$$\hat{I}_{2,rf}(t) = \sum_{n=0}^{m} \alpha_{2n+1} \left|\hat{V}_{1,rf}(t)\right|^{2n} \hat{V}_{1,rf}(t). \qquad (3.2.1.8)$$

The expanded form shows the linear term components and the distortion term components.

$$\hat{I}_{2,rf}(t) = \alpha_1 \hat{V}_{1,rf}(t) + \alpha_3 \left|\hat{V}_{1,rf}(t)\right|^2 \hat{V}_{1,rf}(t) +$$

$$\alpha_5 \left|\hat{V}_{1,rf}(t)\right|^4 \hat{V}_{1,rf}(t) + \ldots + \alpha_{2n+1} \left|\hat{V}_{1,rf}(t)\right|^{2n} \hat{V}_{1,rf}(t) \qquad (6.8.1.1)$$

The distortion envelopes components are shown in red colour in the expanded form of equation (3.2.1.8) as shown by equation (6.8.1.1), while the linear term is shown in black in the same equation representation.

On the other hand, due to these differences, the baseband signal to be injected is very carefully formulated with this understanding. In equation (3.2.4.7), this represents the general notion of the injected baseband signal. In its expanded form, equation (6.8.1.2) however, the similarities to the distortion envelopes formation is shown in blue. These comprise even-power-envelope-modulus multiplied by a control coefficient each. The control coefficients are used to simply quantify the required baseband signal and hence the level of linearization required.

These are shown in blue are used to then targeted to the distortion envelopes components already shown in red in equation (6.8.1.1).

BEL is hence able to recognize and depict the distortion envelopes as completely different from the required signal envelope. Due to this, amplification is essentially unaffected and noise is drastically reduced by this process. This phenomenon is propagated thought this thesis and papers and is also shown in the equations analysis below and their expanded forms. Equation (3.2.1.8) and its expanded form equation (6.8.1.1) and equation (3.2.4.7) and its expanded form equation (6.8.1.2) are used entirely for all the experimental measurements carried out and shown in this thesis respectively.

Therefore, shown below is the engineered and injected baseband signal in equation (3.2.4.7) and its expanded form equation (6.8.1.2).

$$\hat{V}_{2,bb}(t) = \sum_{p=1}^{q} \beta_{2p} \left|\hat{V}_{1,rf}(t)\right|^{2p} \tag{3.2.4.7}$$

$$\hat{V}_{2,bb}(t) = \beta_2 \left|\hat{V}_{1,rf}(t)\right|^{2} + \beta_4 \left|\hat{V}_{1,rf}(t)\right|^{4} + \ldots + \beta_{2p} \left|\hat{V}_{1,rf}(t)\right|^{2p} \tag{6.8.1.2}$$

By appropriately engineering the beta terms and injecting the resulting ‘engineered’ signal into the device output port, it was always possible to cause a set of mixing terms that we can use to

simultaneously target and suppress/eliminate the distortion envelope component terms and their contribution to the entire system and engineer a linearized version of the required signal from the device response. At the end of the day, the output current signal is left with an un-distorted and un-compressed but amplified version of the linear term.

6.9 Chapter summary

The robustness with respect to device technology of an envelope domain formulation which describes the baseband injection signal required to minimize the AM/AM distortion has been investigated. Different device technologies were investigated and the formulation was able to minimize AM/AM distortion, hence confirming it would be a useful tool to use in conjunction with DSP. However, the need to use a more complex signal to cater for higher than 5^{th} order distortion was shown. Also, as expected, baseband injection has no impact on AM/PM distortion.

Importantly, this experiment confirmed that BEL is able to effectively suppress AM/AM distortion even in the presence of severe AM/PM distortion.

6.10 References

[1] Andrei Grebennikov, “RF and Microwave Power Amplifier Design”. McGraw-Hill ISBN 0-07-144493-9

[2] John Wood, David E. Root, “Fundamentals of nonlinear behavioral modeling for RF and microwave design”. Artech House, 2005.S Int. Microwave Symp. Dig., vol. 3, pp. 1721-1724, June 2003.

[3] Boumaiza, S.; Mkadem, F.; Ben Ayed, M., "Digital predistortion challenges in the context of software defined transmitters," General Assembly and Scientific Symposium,2011XXXthURSI,vol.,no.,pp.1,4,13-20Aug.2011doi: 10.1109/URSIGASS.2011.6050519

[4] Abd-Elrady, E., "A Recursive Prediction Error algorithm for digital predistortion of FIR Wiener systems," Communication Systems, Networks and Digital Signal Processing, 2008. CNSDSP 2008. 6th International Symposium on , vol., no., pp.698,701, 25-25 July 2008 doi: 10.1109/CSNDSP.2008.4610732

[5] Salkintzis, A.K.; Hong Nie; Mathiopoulos, P.T., "ADC and DSP challenges in the development of software radio base stations," Personal Communications, IEEE , vol.6, no.4, pp.47,55, Aug 1999, doi: 10.1109/98.788215

[6] Mehendale, M., "Challenges in the design of embedded real-time DSP SoCs," VLSI Design, 2004. Proceedings. 17th International Conference on , vol., no., pp.507,511, 2004, doi: 10.1109/ICVD.2004.1260971

[7] Mitra, B., "Consumer digitization: accelerating DSP applications, growing VLSI design challenges," Design Automation Conference, 2002. Proceedings of ASP-DAC 2002. 7th

Asia and South Pacific and the 15th International Conference on VLSI Design. Proceedings. , vol., no., pp.3,4, 2002, doi: 10.1109/ASPDAC.2002.994869

[8] Ogboi, F.L.; Tasker, P.J.; Akmal, M.; Lees, J.; Benedikt, J.; Bensmida, S.; Morris, K.; Beach, M.; McGeehan, J., "A LSNA configured to perform baseband engineering for device linearity investigations under modulated excitations," Microwave Conference (EuMC), 2013 European , vol., no., pp.684,687, 6-10 Oct. 2013

[9] Gharaibeh, K.M.; Gard, K.G.; Steer, M.B., "In-band distortion of multisines," Microwave Theory and Techniques, IEEE Transactions on , vol.54, no.8, pp.3227,3236,Aug.2006,doi:,10.1109/TMTT.2006.879170. Available online and accessed on the 17/08/2014 http://ieeexplore.ieee.org/stamp/stamp.jsp?tp=&arnumber=1668339&isnumber=34931

[10] Gharaibeh, K.M.; Steer, M.B., "Modeling distortion in multichannel communication systems," Microwave Theory and Techniques, IEEE Transactions on , vol.53, no.5, pp.1682,1692, May 2005, doi: 10.1109/TMTT.2005.847064.

[11] Gharaibeh, K.M.; Yaqot, A, "Target classification in Wireless Sensor Network using Particle Swarm Optimization (PSO)," Sensors Applications Symposium (SAS), 2012 IEEE , vol., no., pp.1,5, 7-9 Feb. 2012, doi: 10.1109/SAS.2012.6166290.

[12] Gharaibeh, K.M.; Gard, K.G.; Steer, M.B., "Accurate estimation of digital communication system metrics - SNR, EVM and ρ in a nonlinear amplifier environment," ARFTG Microwave Measurements Conference, Fall 2004. 64th , vol., no., pp.41,44, 2-3 Dec. 2004, doi: 10.1109/ARFTGF.2004.1427570.

[13] Gharaibeh, K.M.; Gard, K.; Steer, M.B., "Statistical modeling of the interaction of

multiple signals in nonlinear RF systems," Microwave Symposium Digest, 2002 IEEE MTT-S International , vol.1, no., pp.143,147 vol.1, 2-7 June 2002
doi: 10.1109/MWSYM.2002.1011579.

[14] Gharaibeh, K.M.; Gard, K.; Gutierrez, H.; Steer, M.B., "The importance of nonlinear order in modeling intermodulation distortion and spectral regrowth," Radio and Wireless Conference, 2002. RAWCON 2002. IEEE , vol., no., pp.161,164, 2002
doi: 10.1109/RAWCON.2002.1030142.

[15] Gharaibeh, K.M.; Steer, M.B., "Characterization of cross modulation in multichannel amplifiers using a statistically based behavioral modeling technique," Microwave Theory and Techniques, IEEE Transactions on , vol.51, no.12, pp.2434,2444, Dec. 2003,doi:,10.1109/TMTT.2003.819195.

[16] Gharaibeh, K.M.; Gard, K.G.; Steer, M.B., "Estimation of in-band distortion in digital communication system," Microwave Symposium Digest, 2005 IEEE MTT-S International , vol., no., pp.4 pp.,, 12-17 June 2005, doi: 10.1109/MWSYM.2005.1517127.

[17] Gharaibeh, K.M.; Gard, K.G.; Steer, M.B., "The applicability of Noise Power Ratio (NPR) in real communication signals," ARFTG Conference, 2006 67th , vol., no., pp.251,253, 16-16 June 2006, doi: 10.1109/ARFTG.2006.4734397.

[18] Gharaibeh, K.M.; Gard, K.; Steer, M.B., "The impact of nonlinear amplification on the performance of CDMA systems," Radio and Wireless Conference, 2004 IEEE , vol., no., pp.83,86, 19-22 Sept. 2004, doi: 10.1109/RAWCON.2004.1389077.

[19] Gharaibeh, K.; Steer, M., "Statistical modeling of cross modulation in multichannel

power amplifiers using a new behavioral modeling technique," Microwave Symposium Digest, 2003 IEEE MTT-S International , vol.1, no., pp.343,346 vol.1, 8-13 June 2003, doi: 10.1109/MWSYM.2003.1210948. Available online and accessed on the 17/08/2014.

[20] Gharaibeh, K.M., "Behavioral modeling of nonlinear power amplifiers using threshold decomposition-based piece wise linear approximation," Radio and Wireless Symposium, 2008 IEEE , vol., no., pp.755,758, 22-24 Jan. 2008 doi: 10.1109/RWS.2008.4463602.

[21] Gharaibeh, K.M.; Gard, K.; Steer, M.B., "Characterization of in-band distortion in RF front-ends using multi-sine excitation," Radio and Wireless Symposium, 2006 IEEE , vol., no., pp.487,490, 17-19 Jan. 2006, doi: 10.1109/RWS.2006.1615200.

[22] Gharaibeh, K.M.; Gard, K.G.; Steer, M.B., "Estimation of co-channel nonlinear distortion and SNDR in wireless systems," Microwaves, Antennas & Propagation, IET , vol.1, no.5, pp.1078,1085, October 2007, doi: 10.1049/iet-map:20070034.

[23] Chunming Liu; Heng Xiao; Qiang Wu; Fu Li; Tam, K.W., "Nonlinear distortion analysis of RF power amplifiers for wireless signals," Signal Processing, 2002 6th International Conference on , vol.2, no., pp.1282,1285 vol.2, 26-30 Aug. 2002 doi: 10.1109/ICOSP.2002.1180026.

[24] Kuran, S.; Huang, C.-W.P.; Xu, S., "A novel integrated design simulation method for linear cellular and WLAN power amplifiers," *Electronics, Circuits and Systems, 2003. ICECS 2003. Proceedings of the 2003 10th IEEE International Conference on* , vol.3, no., pp.1256,1259Vol.3,14-17Dec.2003doi: 10.1109/ICECS.2003.1301742.

[25] Cabral, P.M.; Pedro, J.C.; Garcia, Jose A; Cabria, L., "A linearized polar transmitter for wireless applications," Microwave Symposium Digest, 2008 IEEE MTT-S International , vol., no., pp.935,938, 15-20 June 2008, doi: 10.1109/MWSYM.2008.4632987.

[26] Cabria, L.; Cabral, P.M.; Pedro, J.C.; Garcia, J.A, "A class E power amplifier design for drain modulation under a high PAPR WiMAX signal," RF Front-ends for Software Defined and Cognitive Radio Solutions (IMWS), 2010 IEEE International Microwave Workshop Series on , vol., no., pp.1,4, 22-23 Feb. 2010, doi: 10.1109/IMWS.2010.5440968.

[27] Marante, R.; Cabria, L.; Cabral, P.; Pedro, J.C.; Garcia, J.A, "Temperature dependent memory effects on a drain modulated GaN HEMT power amplifier," Integrated Nonlinear Microwave and Millimeter-Wave Circuits (INMMIC), 2010 Workshop on , vol., no., pp.75,78, 26-27 April 2010, doi: 10.1109/INMMIC.2010.5480133.

[28] Cotimos Nunes, L.; Cabral, P.M.; Pedro, J.C., "AM/AM and AM/PM Distortion Generation Mechanisms in Si LDMOS and GaN HEMT Based RF Power Amplifiers," Microwave Theory and Techniques, IEEE Transactions on , vol.62, no.4, pp.799,809, April 2014, doi: 10.1109/TMTT.2014.2305806.

[29] Cabral, P.M.; Pedro, J.C.; Carvalho, N.B., "Dynamic AM-AM and AM-PM behavior in microwave PA circuits," Microwave Conference Proceedings, 2005. APMC 2005. Asia-Pacific Conference Proceedings , vol.4, no., pp.4 pp.,, 4-7 Dec. 2005
doi: 10.1109/APMC.2005.1606809.

[30] Pedro, J.C.; Cabral, P.M.; Cunha, T.R.; Lavrador, P.M., "A Multiple Time-Scale

Power Amplifier Behavioral Model for Linearity and Efficiency Calculations," Microwave Theory and Techniques, IEEE Transactions on , vol.61, no.1, pp.606,615, Jan. 2013, doi: 10.1109/TMTT.2012.2227779.

[31] Cabria, L.; Garcia, J.A; Cabral, P.M.; Pedro, J.C., "Linearization of a polar transmitter for EDGE applications," Integrated Nonlinear Microwave and Millimetre-Wave Circuits, 2008. INMMIC 2008. Workshop on , vol., no., pp.115,118, 24-25 Nov. 2008 doi: 10.1109/INMMIC.2008.4745730.

[32] Nunes, L.C.; Cabral, P.M.; Pedro, J.C., "AM/PM distortion in GaN Doherty power amplifiers," Microwave Symposium (IMS), 2014 IEEE MTT-S International , vol., no., pp.1,4, 1-6 June 2014, doi: 10.1109/MWSYM.2014.6848333.

[33] Lavrador, P.; Cunha, T.R.; Cabral, P.; Pedro, J.C., "The Linearity-Efficiency Compromise," Microwave Magazine, IEEE , vol.11, no.5, pp.44,58, Aug. 2010 doi: 10.1109/MMM.2010.937100.

[34] Cabral, P.M.; Pedro, J.C.; Carvalho, N.B., "Bias Networks Impact on the Dynamic AM/AM Contours in Microwave Power Amplifiers," *Integrated Nonlinear Microwave and Millimeter-Wave Circuits, 2006 International Workshop on* , vol., no., pp.38,41, 30-31 Jan. 2006, doi: 10.1109/INMMIC.2006.283503.

[35] Marante, R.; Garciá, J.A; Cabria, L.; Aballo, T.; Cabral, P.M.; Pedro, J.C., "Nonlinear characterization techniques for improving accuracy of GaN HEMT model predictions in RF power amplifiers," Microwave Symposium Digest (MTT), 2010 IEEE MTT-S International , vol., no., pp.1680,1683, 23-28 May 2010, doi: 10.1109/MWSYM.2010.5517652.

[36] Pedro, J.C.; Martins, J.P.; Cabral, P.M., "New method for phase characterization of nonlinear distortion products," Microwave Symposium Digest, 2005 IEEE MTT-S International , vol., no., pp.4 pp.,, 12-17 June 2005, doi: 10.1109/MWSYM.2005.1516789.

[37] Marante, R.; Garcia, J.A; Cabral, P.M.; Pedro, J.C., "Impact of Ron(VDD) dependence on polar transmitter residual distortion," Integrated Nonlinear Microwave and Millimetre-Wave Circuits, 2008. INMMIC 2008. Workshop on , vol., no., pp.123,126, 24-25 Nov. 2008, doi: 10.1109/INMMIC.2008.4745732.

[38] Nunes, L.C.; Cabral, P.M.; Pedro, J.C., "A physical model of power amplifiers AM/AM and AM/PM distortions and their internal relationship," Microwave Symposium Digest (IMS), 2013 IEEE MTT-S International , vol., no., pp.1,4, 2-7 June 2013, doi: 10.1109/MWSYM.2013.6697497.

[39] Cabral, P.M.; Cabria, L.; Garcia, J.A; Pedro, J.C., "Polar transmitter architecture used in a Software Defined Radio context," RF Front-ends for Software Defined and Cognitive Radio Solutions (IMWS), 2010 IEEE International Microwave Workshop Series on , vol., no., pp.1,4, 22-23 Feb. 2010, doi: 10.1109/IMWS.2010.5440965.

[40] Pedro, J.C.; Garcia, J.A; Cabral, P.M., "Nonlinear Distortion Analysis of Polar Transmitters," Microwave Theory and Techniques, IEEE Transactions on , vol.55, no.12, pp.2757,2765, Dec. 2007,doi: 10.1109/TMTT.2007.909145.

[41] Pires, S.C.; Cabral, P.M.; Pedro, J.C., "A carrier-burst transmitter implementation: Design of bandpass filter and amplifier-BPF connection," Integrated Nonlinear

Microwave and Millimetre-Wave Circuits (INMMIC), 2012 Workshop on , vol., no., pp.1,3, 3-4 Sept. 2012, doi: 10.1109/INMMIC.2012.6331929.

[42] Pedro, Jose Carlos; Cabral, P.M.; Cunha, Telmo Reis; Lavrador, Pedro Miguel, "A new power amplifier behavioral model for simultaneous linearity and efficiency calculations," Microwave Symposium Digest (MTT), 2012 IEEE MTT-S International , vol., no., pp.1,3, 17-22 June 2012, doi: 10.1109/MWSYM.2012.6259393.

[43] Pires, S.C.; Cabral, P.M.; Pedro, J.C., "RF carrier phase-burst transmitter," *Microwave Symposium Digest (IMS), 2013 IEEE MTT-S International* , vol., no., pp.1,4, 2-7 June 2013, doi: 10.1109/MWSYM.2013.6697471.

[44] Pedro, J.C.; Garcia, J.A; Cabral, P.M., "Nonlinear Distortion Analysis of Polar Transmitters," Microwave Symposium, 2007. IEEE/MTT-S International , vol., no., pp.957,960, 3-8 June 2007, doi: 10.1109/MWSYM.2007.380177.

[45] Penalver, C.M.; Peire, J.; Martinez, Pedro M., "Microprocessor Control of DC/AC Static Converters," Industrial Electronics, IEEE Transactions on , vol.IE-32, no.3, pp.186,191, Aug. 1985, doi: 10.1109/TIE.1985.350156.

[46] Ortiz, AM.; Olivares, T.; Castillo, J.C.; Orozco-Barbosa, L.; Marron, P.J.; Royo, F., "Intelligent role-based routing for dense wireless sensor networks," Wireless and Mobile Networking Conference (WMNC), 2010 Third Joint IFIP , vol., no., pp.1,6, 13-15 Oct. 2010, doi: 10.1109/WMNC.2010.5678768.

[47] Ciccognani, W.; Colantonio, P.; Giannini, F.; Limiti, E.; Rossi, M., "AM/AM and AM/PM power amplifier characterisation technique," *Microwaves, Radar and Wireless*

Communications, 2004. MIKON-2004. 15th International Conference on , vol.2, no., pp.678,681 Vol.2, 17-19 May 2004, doi: 10.1109/MIKON.2004.1357126.

[48] Zhiwen Zhu; Xinping Huang; Caron, M.; Leung, H., "A Blind AM/PM Estimation Method for Power Amplifier Linearization," *Signal Processing Letters, IEEE* , vol.20, no.11, pp.1042,1045, Nov. 2013, doi: 10.1109/LSP.2013.2280394. Available online and accessed on the 20/08/2014

http://ieeexplore.ieee.org/stamp/stamp.jsp?tp=&arnumber=6594895&isnumber=6584011

[49] Cunha, T.R.; Cabral, P.M.; Nunes, L.C., "Characterizing power amplifier static AM/PM with spectrum analyzer measurements," *Multi-Conference on Systems, Signals & Devices (SSD), 2014 11th International* , vol., no., pp.1,4, 11-14 Feb. 2014 doi: 10.1109/SSD.2014.6808883.

[50] Butel, Y.; Adam, T.; Cogo, B.; Soulard, M., "High efficiency LOW AM/PM 6W C-band MMIC power amplifier for a space radar program," *Microwave Conference, 2000. 30th European* , vol., no., pp.1,4, Oct. 2000, doi: 10.1109/EUMA.2000.338704.

[51] Sorace, R.; Reines, R.; Carlson, N.; Glasgow, M.; Novak, T.; Conte, K., "AM/PM distortion in nonlinear circuits [power amplifier applications]," *Vehicular Technology Conference, 2004. VTC2004-Fall. 2004 IEEE 60th* , vol.6, no., pp.3994,3996 Vol. 6, 26-29 Sept. 2004, doi: 10.1109/VETECF.2004.1404827.

[52] Piazzon, L.; Giofre, R.; Colantonio, P.; Giannini, F., "Investigation of the AM/pm distortion in Doherty Power Amplifiers," *Power Amplifiers for Wireless and Radio*

Applications (PAWR), 2014 IEEE Topical Conference on , vol., no., pp.7,9, 19-23 Jan. 2014, doi: 10.1109/PAWR.2014.6825729.

[53] Nunes, L.C.; Cabral, P.M.; Pedro, J.C., "AM/PM distortion in GaN Doherty power amplifiers," *Microwave Symposium (IMS), 2014 IEEE MTT-S International* , vol., no., pp.1,4, 1-6 June 2014, doi: 10.1109/MWSYM.2014.6848333.

[54] Sang-Min Han; Popov, O.; Sun-Ju Park; Dal Ahn; Jongsik Lim; Won-Sang Yoon; Seongmin Pyo; Young-Sik Kim, "Adaptive calibration method for AM/PM distortion in nonlinear devices," *Radio-Frequency Integration Technology, 2009. RFIT 2009. IEEE International Symposium on* , vol., no., pp.76,79, Jan. 9 2009-Dec. 11 2009 doi: 10.1109/RFIT.2009.5383748.

[55] Gagliardi, R.M., "Coupled AGC-Costas Loops with AM/PM Conversion," *Communications, IEEE Transactions on* , vol.28, no.1, pp.122,127, Jan 1980 doi: 10.1109/TCOM.1980.1094578.

[56] Horst, S.; Cressler, J.D., "AM/PM Nonlinearities in SiGe HBTs," *Silicon Monolithic Integrated Circuits in RF Systems, 2009. SiRF '09. IEEE Topical Meeting on* , vol., no., pp.1,4, 19-21 Jan. 2009, doi: 10.1109/SMIC.2009.4770544.

[57] Dudak, C.; Kahyaoglu, N.D., "A descriptive study on AM-AM and AM-PM conversion phenomena through EVM-SNR relation," *Power Amplifiers for Wireless and Radio Applications (PAWR), 2012 IEEE Topical Conference on* , vol., no., pp.69,72, 15-18 Jan. 2012, doi: 10.1109/PAWR.2012.6174945.

[58] Ooi, B.Z.M.; Lee, S.W.; Chung, B.K., "EVM measurements using orthogonal separation at the output of a non-linear amplifier," Microwaves, Antennas & Propagation, IET , vol.6, no.7, pp.813,821, May 16 2012, doi: 10.1049/iet-map.2011.0390.

[59] Kim, J.H.; Jeong, J.H.; Kim, S.M.; Park, C.S.; Lee, K.C., "Prediction of error vector magnitude using AM/AM, AM/PM distortion of RF power amplifier for high order modulation OFDM system," *Microwave Symposium Digest, 2005 IEEE MTT-S International* , vol., no., pp.4 pp.,, 12-17 June 2005, doi: 10.1109/MWSYM.2005.1517143.

[60] Wang, A K.; Ligmanowski, R.; Castro, J.; Mazzara, A, "EVM Simulation and Analysis Techniques," *Military Communications Conference, 2006. MILCOM 2006. IEEE* , vol., no., pp.1,7, 23-25 Oct. 2006, doi: 10.1109/MILCOM.2006.302043.

[61] Wang, A K.; McAllister, AM., "EVM measurement techniques for MUOS," *Military Communications Conference, 2009. MILCOM 2009. IEEE* , vol., no., pp.1,7, 18-21 Oct. 2009, doi: 10.1109/MILCOM.2009.5379776.

[62] Bastug, E.; Guenego, J.-L.; Debbah, M., "Proactive small cell networks," *Telecommunications (ICT), 2013 20th International Conference on* , vol., no., pp.1,5, 6-8 May 2013, doi: 10.1109/ICTEL.2013.6632164.

[63] Andrews, J.G.; Claussen, H.; Dohler, M.; Rangan, S.; Reed, M.C., "Femtocells: Past, Present, and Future," *Selected Areas in Communications, IEEE Journal on* , vol.30, no.3, pp.497,508, April 2012, doi: 10.1109/JSAC.2012.120401.

[64] Claussen, Holger; Ho, Lester T.W.; Samuel, Louis G., "An overview of the femtocell concept," *Bell Labs Technical Journal* , vol.13, no.1, pp.221,245, Spring 2008 doi: 10.1002/bltj.20292.

[65] Haberland, Bernd; Derakhshan, Fariborz; Grob-Lipski, Heidrun; Klotsche, Ralf; Rehm, Werner; Schefczik, Peter; Soellner, Michael, "Radio base stations in the cloud," *Bell Labs Technical Journal* , vol.18, no.1, pp.129,152, June 2013 doi: 10.1002/bltj.21596.

[66] Lees, J.; Williams, T.; Woodington, S.; McGovern, P.; Cripps, S.; Benedikt, J.; Tasker, P., "Demystifying Device related Memory Effects using Waveform Engineering and Envelope Domain Analysis," *Microwave Conference, 2008. EuMC 2008. 38th European* , vol., no., pp.753,756, 27-31 Oct. 2008, doi: 10.1109/EUMC.2008.4751562

CHAPTER SEVEN

CONCLUSION AND FUTURE WORK

7.1 Conclusion

This research has been predominantly concerned with the formulation of a novel technique which can be used in linearising RFPA devices. It also migrated from baseband impedance engineering to baseband envelope engineering and demonstrated new knowledge learnt. This was done by considering baseband signals in the envelope domain. In this domain, baseband IMD's are viewed not in terms of impedances but in terms of voltage envelopes. A time varying baseband signal was then developed based on mathematical equation to suppress the IMD's. This is what was called baseband envelope linearisation (BEL). Baseband envelope engineering is a very useful technique. In doing this, it also showed that the technique has the ability of simultaneous suppression. Simultaneous suppression means that in a system having IM3 and IM5, it is possible to suppress both distortions at the same time. Also it showed that the linearization coefficients are signal complexity invariant.

Baseband linearization technique is not a new technique, but the formulation used in this thesis to create the linearising baseband signal and applied to linearise RFPA devices is new. This formulation and its application termed BEL technique is new.

This has two important implications. In a PA for instance, if IMD is considered up to the 5^{th} order, one implication is that only two coefficients will be required to completely suppress both

IMD3 and IMD5 no matter the complexity of the signal or device technology. The second implication is that for the same 5^{th} order system, the linearizing coefficients are invariant to complexity. They will be the same if it is possible to energise exactly the same spot on the IV plane and if the temperature of the device can be kept constant. The work also considered modulated signal complexity in two forms. Complexity with respect to multiple signals having different PAPR. The second is complexity with respect to how fast the signal modulation is changing. In this technique, the highest distortion suppression achieved was 56dBc. The work considered devices of different technologies (GaN-on-Si, GaN-on-SiC and Si-LDMOS devices). In each case, BEL was able to suppress the associated distortion around the carrier. Looking into the future, if linearity up to 56dBc suppression might be considered a good achievement, then consider this technique. Another important highlight of this technique is that it is cost effective and is compatible with emerging architectures such as envelope tracking ET. BEL can be used with DPD to reduce the DSP power complexity so using BEL does not mean discarding presently used architectures. In addition, it has been shown that BEL is invariant to phase distortion, so BEL can be used to correct amplitude distortion and a separate DPD be used to correct phase distortion.

7.2 Future work

The potential of baseband envelope engineering is a far reaching one. To fully realise its potential, and strategy, some further development needs to be done. Some of these include the following:-

7.2. (a). Addition of AM/PM capability to BEL.

In this case, by second harmonic injection instead of baseband, and modifying the present equations, BEL could be upgraded to an AM/AM – AM/PM linearizer. This option will be extremely attractive to industry because it will be a very cost effective and a very performance effective solution.

7.2. (b). The second future work upgrade of BEL is to deploy it on a more modern measurement system than on that used in this thesis. At the moment, it is deployed on a LSNA that is a combination of so many parts that is not easy to assemble together to work as it should. If it is deployed on a more modern, newer and faster system, with higher dynamic range such as the planned national instrument (NI) system at Cardiff University, Centre for High Frequency Engineering facility, then the real advantage could be fully exploited.

7.2.(c). BEL : Proposed practical implementation: The third future work pattern for BEL is its proposed practical implementation in a real base station. The plan for this is seen in the figure below. Its deployment is in two flavours. One is to deploy it as it is, meaning that the equations will be programmed on the transmitter system of the Telco and used. The second deployment is to wait until it has been upgraded to include AM/PM capability.

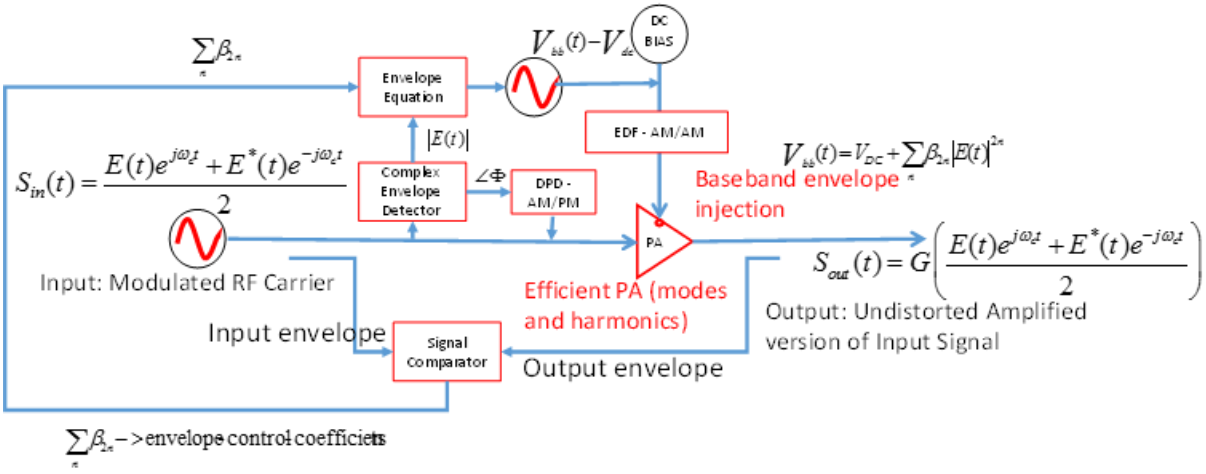

Figure 7.2 Base-station adaptation of BEL

7.2. (d). It is believed that BEL equations can also be used on an envelope tracking (ET) system.

7.2(e). BEL also needs to be tested on real-life communications signal and we believe will retain even better functionality

7.3 Proposed deployment with digital pre-distortion (DPD)

The advantages that BEL can produce if used with other linearizing techniques, in particular DPD are many. Some of them are as listed below in addition to its functionality. The idea here is that, if we use DPD to suppress only AM/PM distortion, certain improvements can be achieved which are:-

(i). Reduced number of operations on the DPD system

(ii). Reduced number of computation on the DPD system

(iii). Reduced channel bandwidth utilization from the DPD system

(iv). Reduced input bandwidth usage leading to bandwidth efficiency

(v). Reduced device bandwidth expansion leading to reduced change in device thermal state

(vi). More environmentally friendly deployment, reduced CO_2 emission

(vii). Reduced DPD complexity

(viii). Possibility of DPD power scale-down with RF power scale-down

(ix). Real realization of "small cell design" due to reduced overall power consumption

(x). Reduced cost to user

(xi). Reduced DPD complexity as a result of reduced DPD computation

(xii). Reduced running cost as a result of reduced heat

(xiii). Reduced manufacturing cost because of non-disposal of existing system

(vix). Extended battery life (power efficiency)

(vx). Link reliability as a result of the realization of small cell

Some of these points are already on the way to fruition. For instance, the NI equipment has been acquired and with students trying to understand its workings so that such works can be carried out on it. Also, a student is already working towards realising the AM/PM implementation of BEL within the Centre for High Frequency facility.

7.4 Concluding remarks

As the communication industry goes into the regime of 5G and beyond, with the growth of small cell, research of new concepts and technologies will be required to drive down power. It is earnestly hoped that this work will provide a possible solution.

7.5 References

[1] Angeliki Alexiou, "Smart Antennas and Related Technologies, White Paper, and briefing" Lucent Technologies, Bell Labs, Wireless research, Swindon, Wiltshire, UK, alexiou@lucent.com, Martin Haardt, Ilmenau University of Technology, Communications Research Laboratory, D-98684, ILmeanau, Germany, haardt@ieee.org. WWRF9, Zurich, July 02nd, 2003, 2007. Available online at http://wg4.ww-rf.org/Smart_antennas_white_presentation.PDF. Accessed on the 03rd, January, 2010.

[2] Webb, W., "The future of wireless communications - is it working out as planned?," Broadband Communications, Networks and Systems, 2008. BROADNETS 2008. 5th International Conference on , vol., no., pp.xi,xi, 8-11 Sept. 2008
doi: 10.1109/BROADNETS.2008.4769025. Available on www.ieeexplore.org at http://ieeexplore.ieee.org/stamp/stamp.jsp?tp=&arnumber=4769025&isnumber=4769015. Available online and accessed on the 26th, August, 2014

[3] Bria, A; Gessler, F.; Queseth, O.; Stridh, R.; Unbehaun, M.; Jiang Wu; Zander, J.; Flament, M., "4th-generation wireless infrastructures: scenarios and research challenges," Personal Communications, IEEE , vol.8, no.6, pp.25,31, Dec 2001
doi: 10.1109/98.972165. Available on www.ieeexplore.org at http://ieeexplore.ieee.org/stamp/stamp.jsp?tp=&arnumber=972165&isnumber=20958. Available online and accessed on the 26th, August, 2014

[4] Jin Cao; Maode Ma; Hui Li; Yueyu Zhang; Zhenxing Luo, "A Survey on Security Aspects for LTE and LTE-A Networks," Communications Surveys & Tutorials, IEEE , vol.16, no.1, pp.283,302, First Quarter 2014
doi: 10.1109/SURV.2013.041513.00174.

[5] Cisco systems incorporated (Adaptive DFE Modeling, using IBISv4.2, (Ehsan Kabir, Susmita Mutsuddy, Abdulrahman Rafiq, Luis Boluna), IBIS Sumit -)1st, February, 2007, San Jose, California, (Wireless network) Available Online at:www.cisco.com 03rd, August, 2010.

[6] Khattri, V.; Tiwari, N.K.; Katiyar, V., "A hypothesis to develop personal network system for future telecommunication in proceed of 4G," Computing for Sustainable Global Development (INDIACom), 2014 International Conference on , vol., no., pp.436,440, 5-7 March 2014, doi: 10.1109/IndiaCom.2014.6828175.

[7] Sanchez, IA, "On the protection of future telecommunication mission operations," Satellite Telecommunications (ESTEL), 2012 IEEE First AESS European Conference on , vol., no., pp.1,6, 2-5 Oct. 2012, doi: 10.1109/ESTEL.2012.6400148.

[8] Aloisio, M.; Angeletti, P.; Coromina, F.; De Gaudenzi, R., "Technological challenges of future broadband telecommunication satellites in Q/V-band," Wireless Information Technology and Systems (ICWITS), 2012 IEEE International Conference on , vol., no., pp.1,4, 11-16 Nov. 2012, doi: 10.1109/ICWITS.2012.6417801.

[9] Aloisio, M.; Angeletti, P.; Coromina, F.; De Gaudenzi, R., "Exploitation of Q/V-band for future broadband telecommunication satellites," Vacuum Electronics Conference (IVEC), 2012 IEEE Thirteenth International , vol., no., pp.351,352, 24-26 April 2012 doi: 10.1109/IVEC.2012.6262191.

[10] Nishimura, H.; Iwasa, E.; Irie, M.; Kondoh, S.; Kaneko, M.; Fukumoto, T.; Iio, M.; Ueda, K., "Applying flexibility in scale-out-based web cloud to future telecommunication session control systems," Intelligence in Next Generation Networks (ICIN), 2012 16th

International Conference on , vol., no., pp.1,7, 8-11 Oct. 2012, doi: 10.1109/ICIN.2012.6376026.

[11] Lucente, M.; Stallo, C.; Rossi, T.; Mukherjee, S.; Cianca, E.; Ruggieri, M.; Dainelli, V., "Analysis and design of a point-to-point radio-link at W band for future satellite telecommunication experiments," Aerospace Conference, 2011 IEEE , vol., no., pp.1,10, 5-12 March 2011, doi: 10.1109/AERO.2011.5747255.

[12] Konsgen, A; Singh, A; Ma Jun; Weerawardane, T.; Goerg, C., "Responsiveness of future telecommunication networks under disaster situations," Ultra Modern Telecommunications and Control Systems and Workshops (ICUMT), 2012 4th International Congress on , vol., no., pp.892,899, 3-5 Oct. 2012
doi: 10.1109/ICUMT.2012.6459787.

[13] De Sanctis, M.; Rossi, T.; Mukherjee, S.; Ruggieri, M., "Future perspectives of the alphasat TDP#5 Telecommunication Experiment," Aerospace Conference, 2013 IEEE , vol., no., pp.1,9, 2-9 March 2013, doi: 10.1109/AERO.2013.6497432.

[14] Lepeltier, P.; Bosshard, P.; Maurel, J.; Labourdette, C.; Navarre, G.; David, J.F., "Recent achievements and future trends for multiple beam telecommunication antennas," Antenna Technology and Applied Electromagnetics (ANTEM), 2012 15th International Symposium on , vol., no., pp.1,6, 25-28 June 2012
doi: 10.1109/ANTEM.2012.6262426.

[15] Abbasi, A; Baroudi, U., "Immersive Environment: An Emerging Future of Telecommunications," MultiMedia, IEEE , vol.19, no.1, pp.80,80, Jan. 2012
doi: 10.1109/MMUL.2012.7.

[16] Kampichler, W.; Lindner, M.; Haindl, B.; Eier, D.; Gronau, B., "LISP: A novel approach towards a future communication infrastructure multilink service," Digital Avionics Systems Conference (DASC), 2013 IEEE/AIAA 32nd , vol., no., pp.4B3-1,4B3-10, 5-10 Oct. 2013, doi: 10.1109/DASC.2013.6712582.

[17] Narita, I; Fishbune, R.; Malik, R.; Mohr, D.; Chandra, H.; Schaffer, M.; Fu, H., "High-voltage DC-DC power module development," Electronics Packaging (ICEP), 2014 International Conference on , vol., no., pp.193,196, 23-25 April 2014
doi: 10.1109/ICEP.2014.6826687.

[18] Kistchinsky, A, "Gan solid-state microwave power amplifiers — State-of-the-art and future trends," Microwave & Telecommunication Technology, 2009. CriMiCo 2009. 19th International Crimean Conference, vol., no., pp.11,16, 14-18 Sept. 2009. Available online and accessed on the 26th, August, 2014
http://ieeexplore.ieee.org/stamp/stamp.jsp?tp=&arnumber=5293252&isnumber=5292809

APPENDIX A

UPGRADE – MEASUREMENT SYSTEM

Upgraded measurement system LSNA

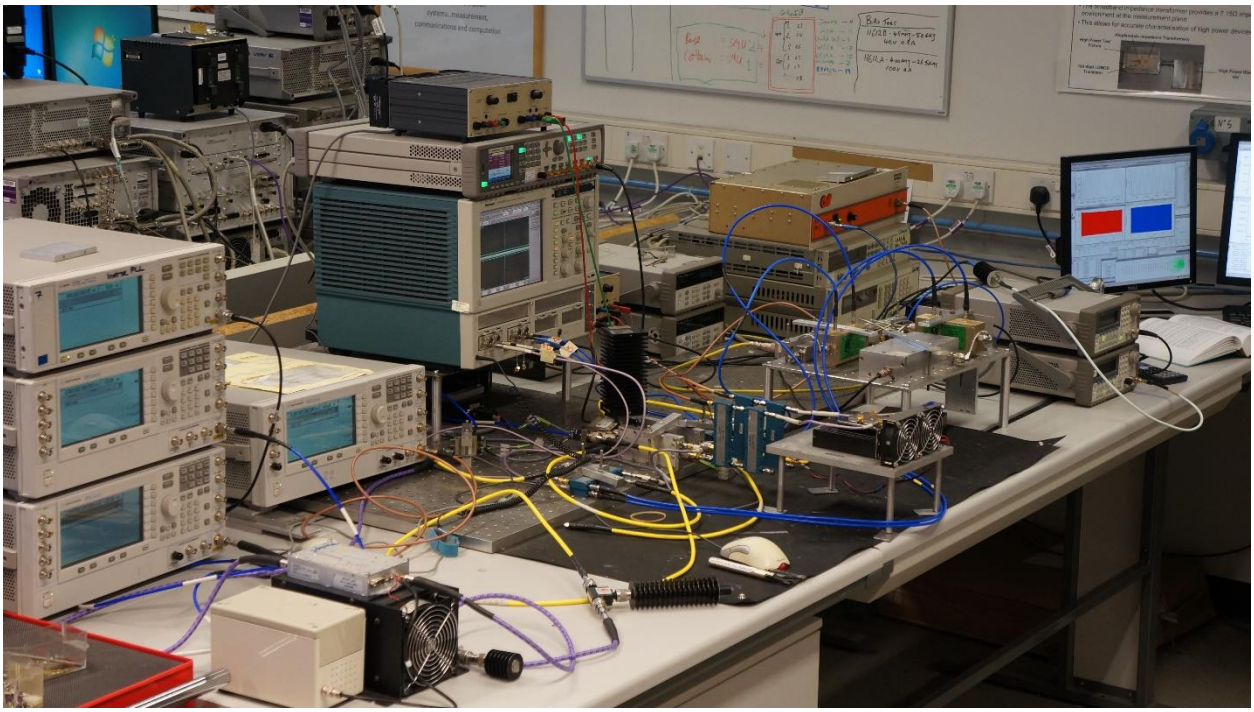

Completely Upgraded Complex LSNA envelope load-pull measurement system

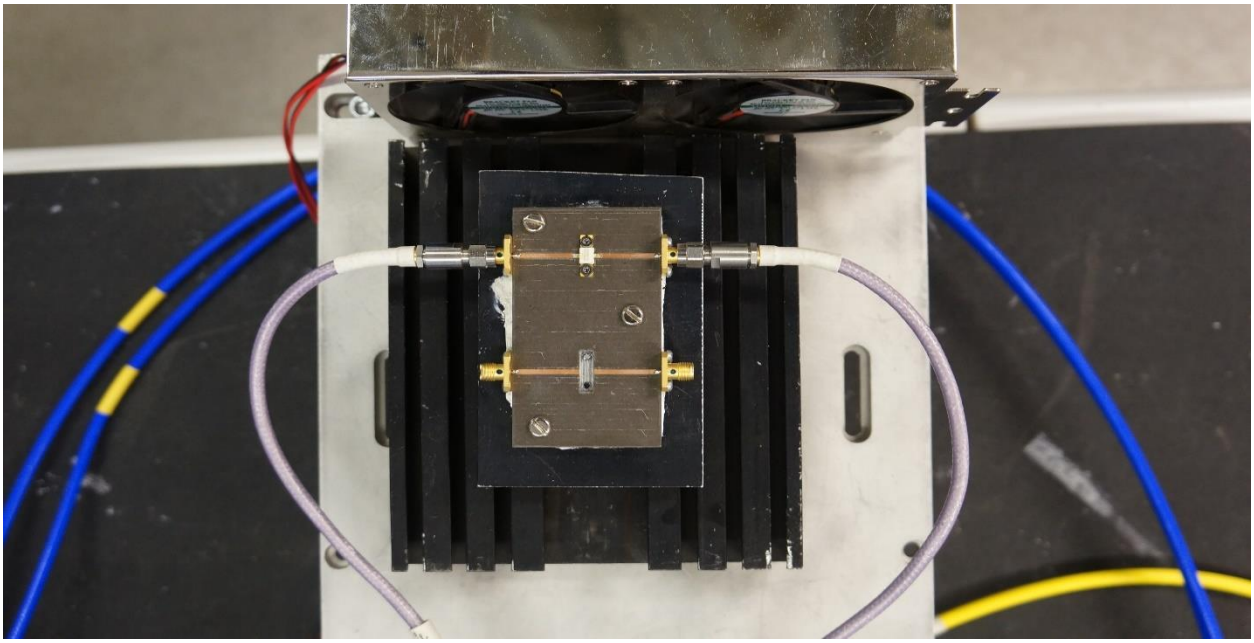

Typical device in measurement (DUT)

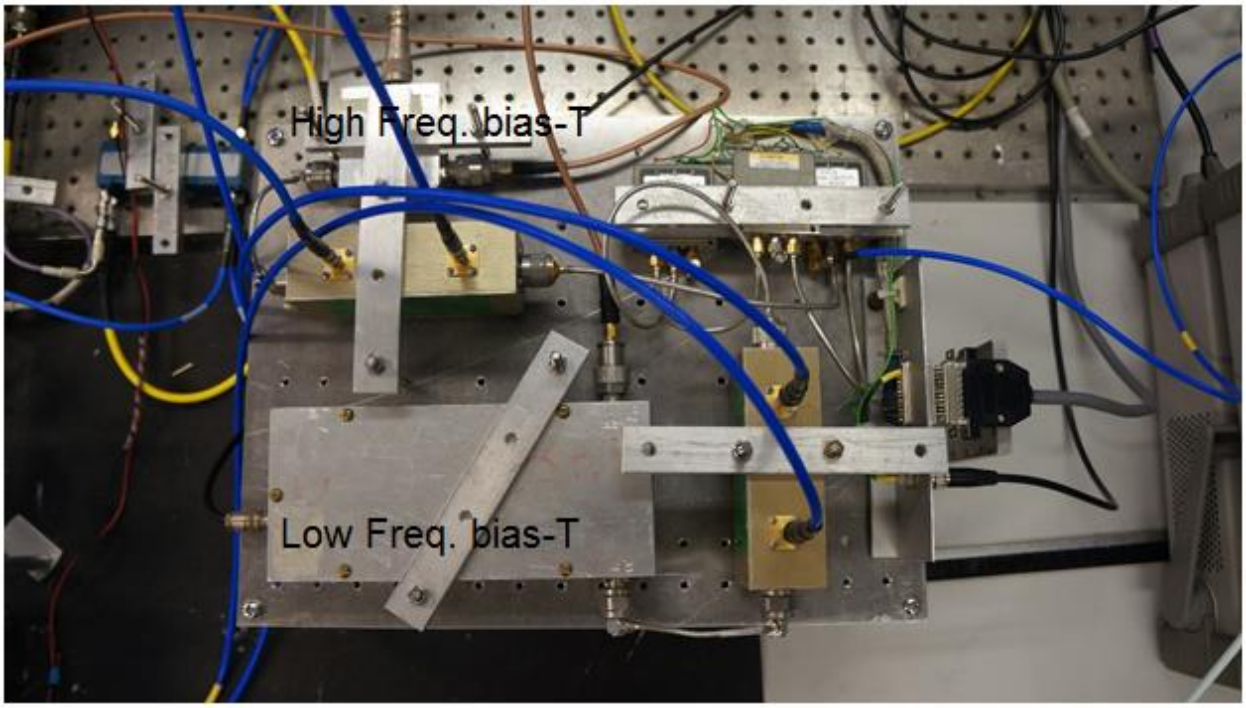

Baseband (IF) measurement bench 200MHz bandwidth

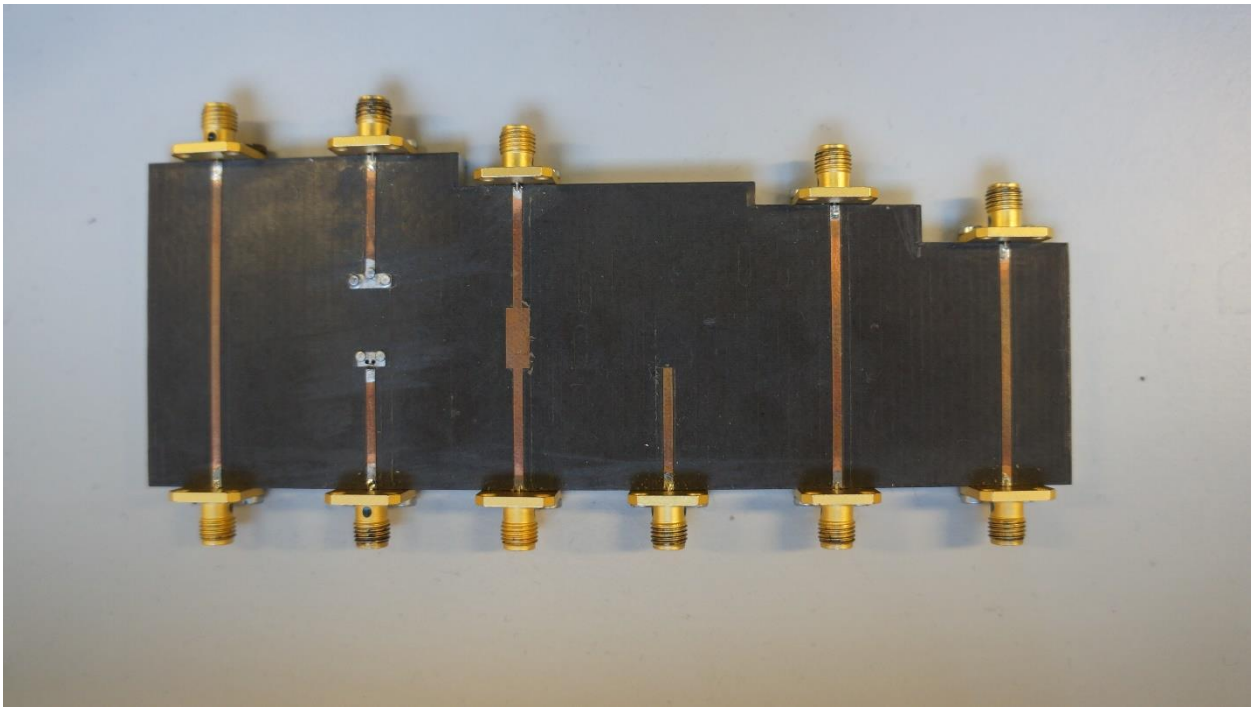

TRL (Thru-Reflect-Line) Calibration Kit

APPENDIX B

SOLUTION TO STITCHING PROBLEM

Measured 5-tone 3MHz modulation (tone spacing) frequency

Reference baseband short circuit state measurements

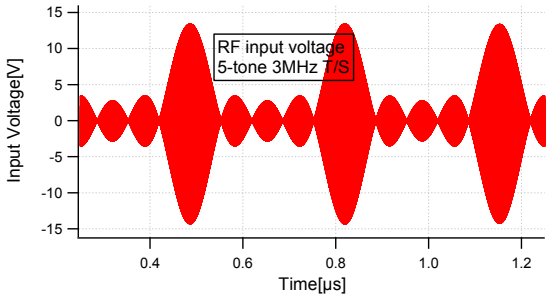

(a). Measured RF input voltage envelopes

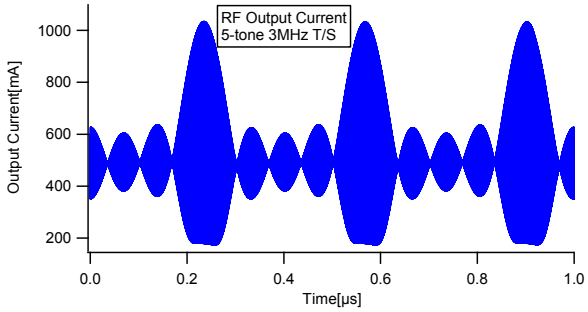

(b). Measured RF output current envelopes

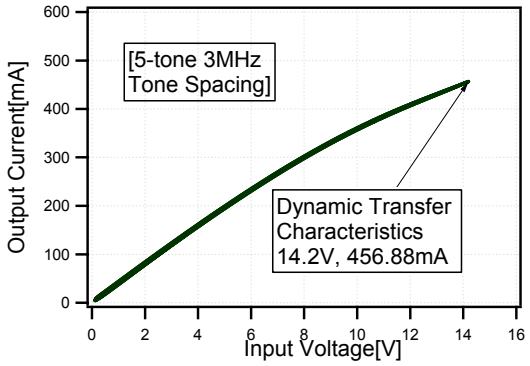

(c). Measured RF envelope dynamic transfer characteristics

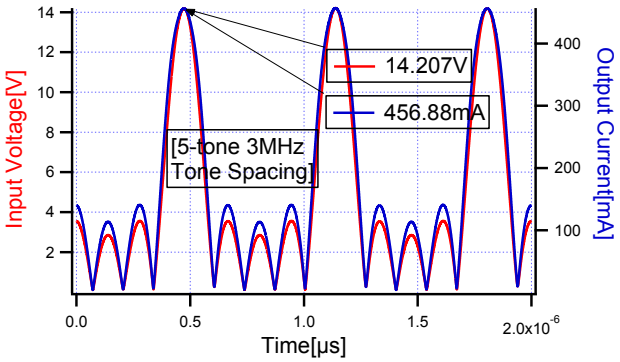

(d). Measured RF input voltage – Output current envelopes

Measured 5-tone 3 MHz modulation frequency (tone spacing) showing no stitching problem.

Measured Reference baseband short circuit state of the device.

Measured 5-tone 3MHz modulation (tone spacing) frequency

Linear state measurements

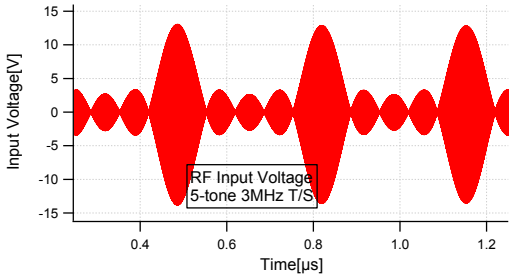

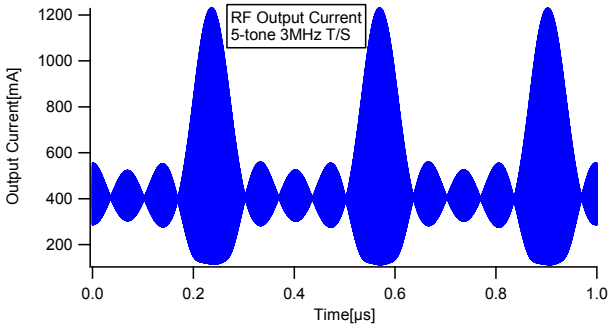

(a). Measured RF input voltage envelopes (b). Measured RF output current envelopes

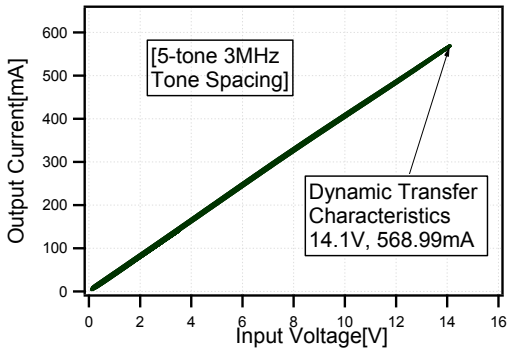

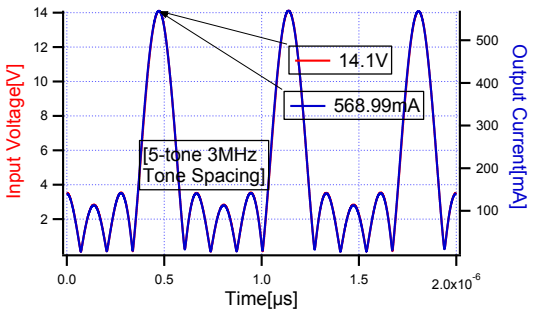

(c). Measured RF envelope dynamic transfer characteristics

(d). Measured RF input voltage – Output current envelopes

Measured 5-tone 3MHz modulation frequency (tone spacing) showing no stitching problem. Measured at the linear state of the device.

This measurement has added an important upgrade to the measurement system such that arbitrary modulations can be measured. In addition, it also shows that BEL can be applied to arbitrary frequency scheme.

APPENDIX C

CALIBRATION

APPENDIX "C" Calibration 05-07-2014

Calibration over the required RF frequency and baseband (IF) frequency are in two stages each.

Under RF calibration, there is Small signal calibration and large signal calibration.

Under Baseband (IF) calibration, there is also small signal calibration and large signal calibration.

The results of the calibration are verified by the graphs and the values of the calibration coefficients shown below.

Small Signal Calibration results

Thru Measurements with Delay -16.584psec

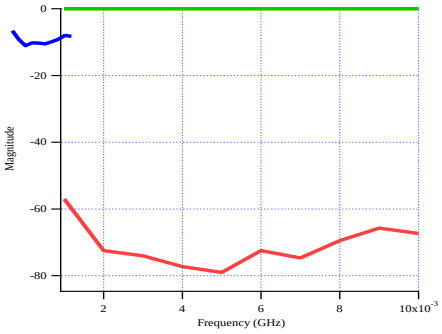

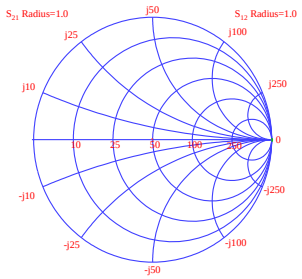

Short Standard Measurements (S11)

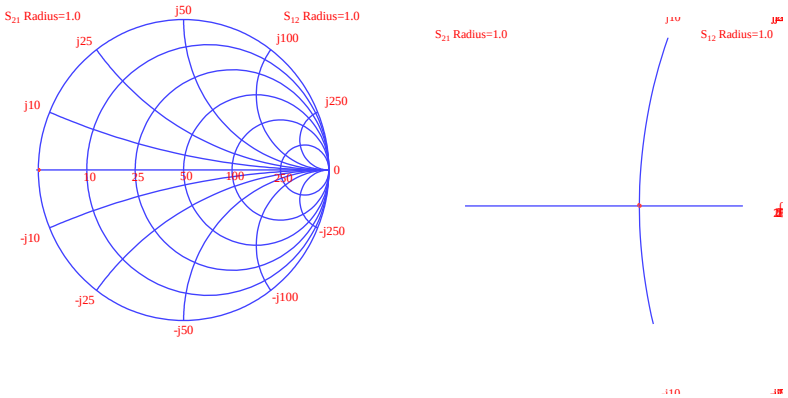

S22

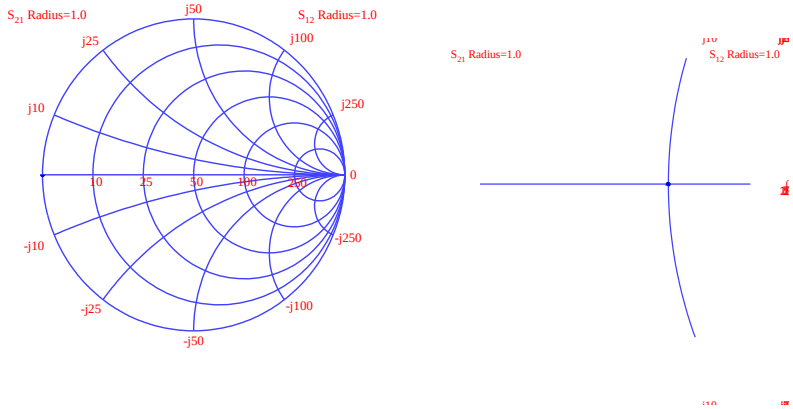

Both S11 and S22

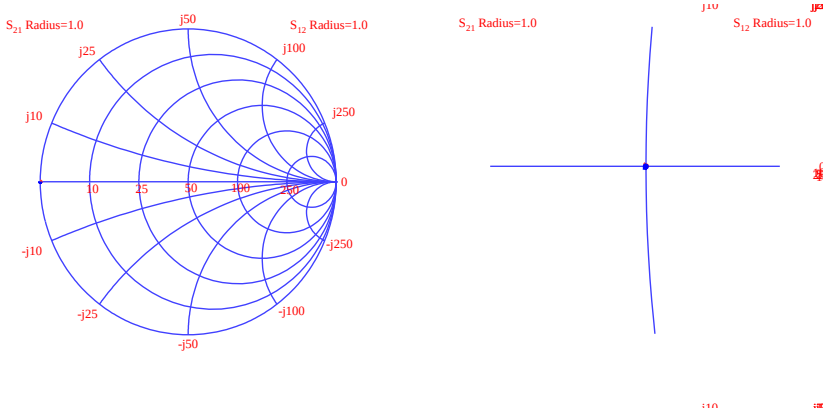

Open Standard Measurements (S11)

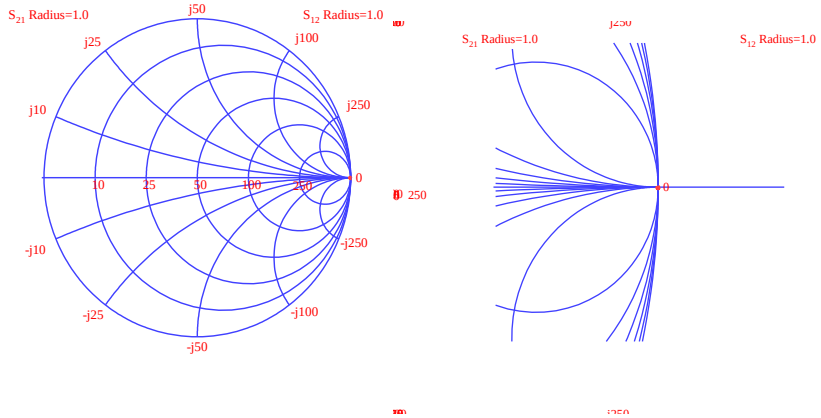

S22

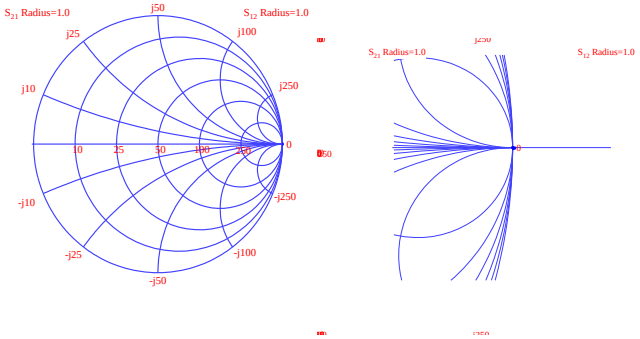

S11 and S22

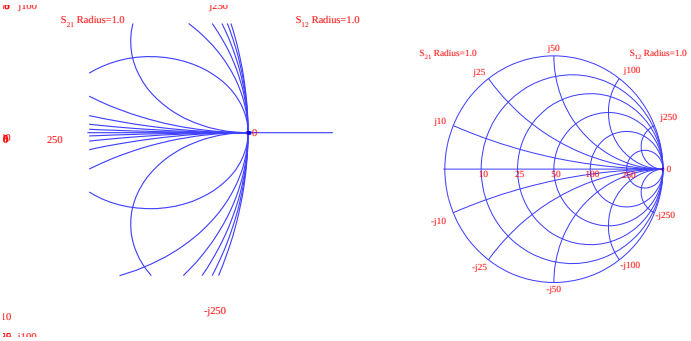

Match Standard Measurements (S11)

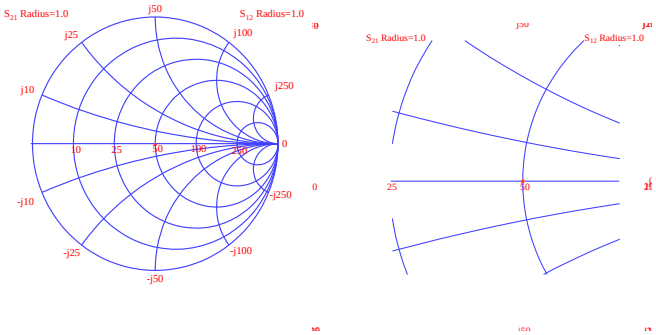

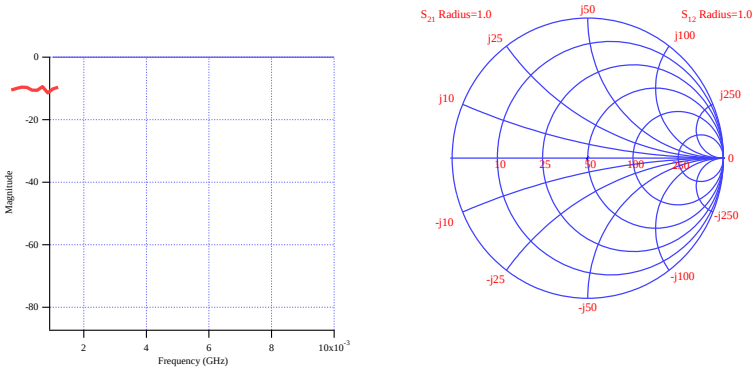

S22

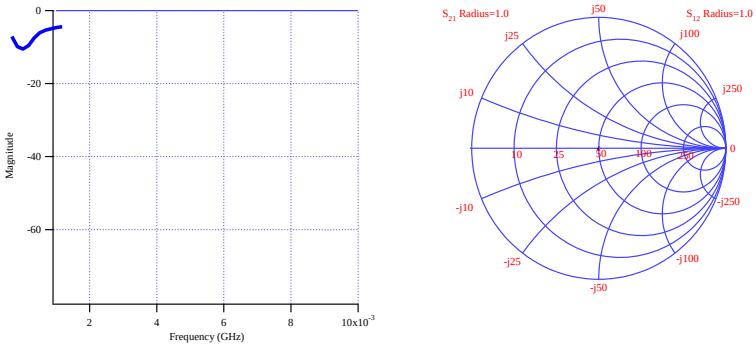

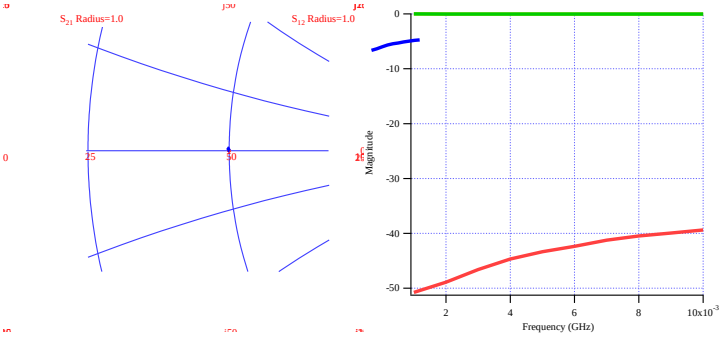

Cable Measurements

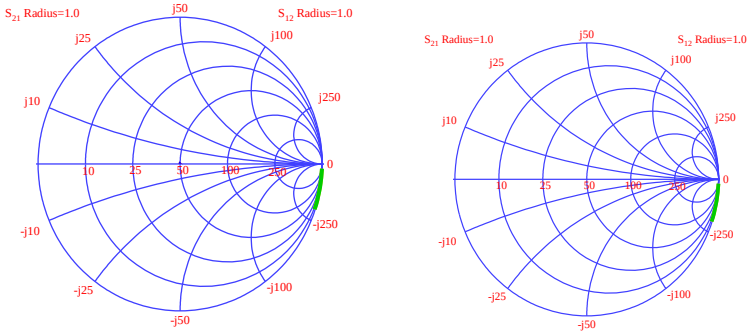

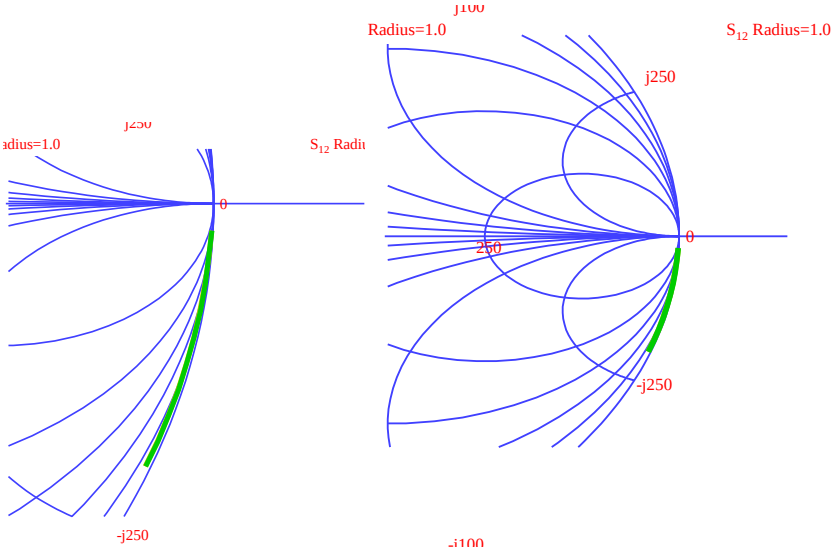

Short at port 1(S11)

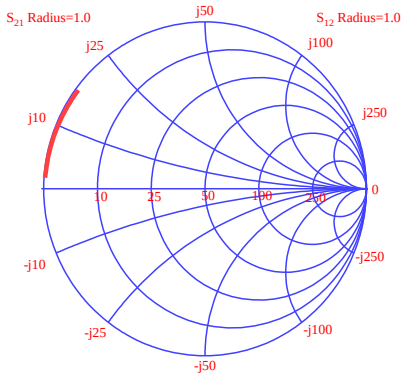

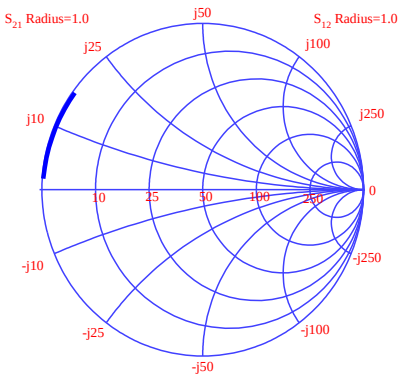

S22

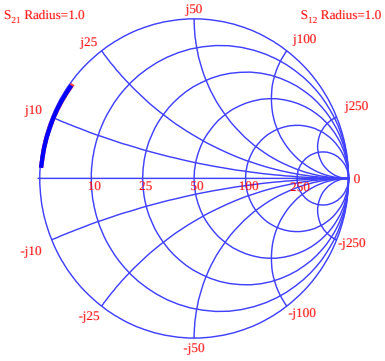

Beta File – calibration coefficients

```
! Filename: C:Documents and
Settings:ogboi:Desktop:Modulated_2009:Cal1:IF_CAL:Beta_1
! Comment: Calibration: Calibration  TMR Beta, harmonic no.1
! Info:  05 July 2014 16:47:30 AVERAGES=  128 PARAMETER=Beta_avg
# GHZ S RI R 50
 0.001      1.03388       -0.0490795
 0.002      1.03066       0.0138316
 0.003      1.02828       0.0525044
 0.004      1.02549       0.0881534
 0.005      1.02122       0.119287
 0.006      1.01724       0.148774
 0.007      1.01239       0.177455
 0.008      1.00705       0.205179
 0.009      1.00145       0.232296
 0.01      0.994948       0.25914
```

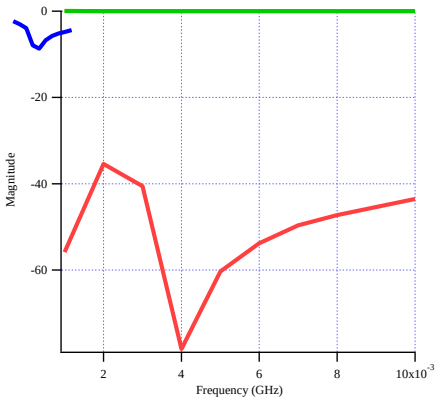

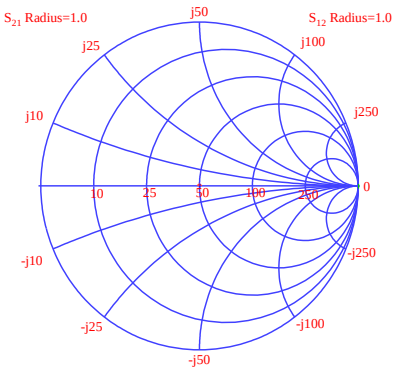

Full Calibration Verification

S21

0.001	0.998191	-1.83399
0.002	0.997898	-3.648972
0.003	0.997830	-5.463380
0.004	0.997533	-7.274512
0.005	0.996854	-9.056885
0.006	0.996548	-10.845689
0.007	0.996733	-12.653447
0.008	0.996186	-14.434394
0.009	0.996205	-16.245557
0.01	0.995927	-18.037598

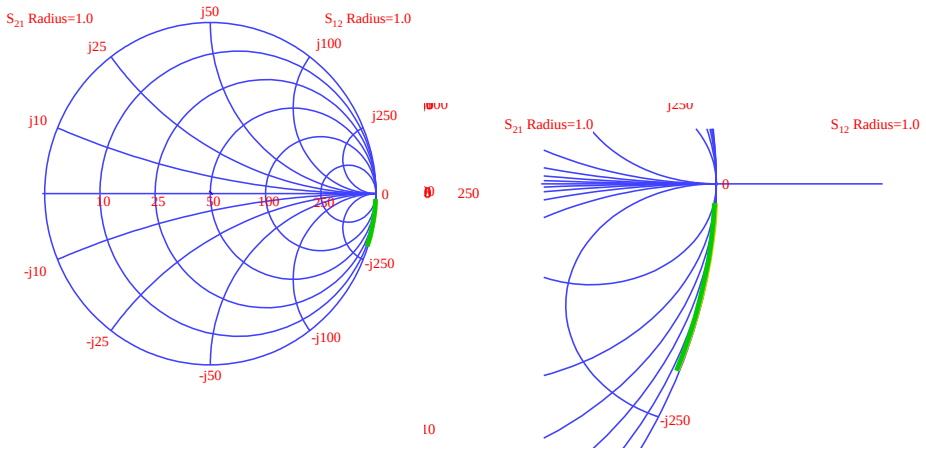

RF Small Signal Calibration

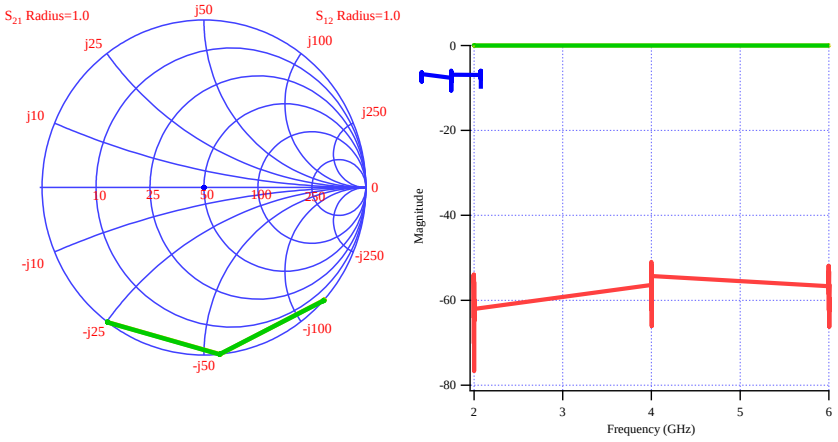

Beta File

```
! Filename: C:Documents and
Settings:ogboi:Desktop:Modulated_2009:Cal1:RF_CAL:Beta_1
! Comment: Calibration: Calibration  TMR Beta, harmonic no.1
! Info:  05 July 2014 16:36:31 AVERAGES=  128 PARAMETER=Beta_avg
# GHZ S RI R 50
 1.996      -0.442178       -0.985407
 1.9964      -0.434549       -0.988887
 1.9968      -0.428835       -0.990924
 1.9972      -0.420185       -0.994621
 1.9976      -0.413339       -0.998427
 1.998      -0.403986       -1.00033
 1.9984      -0.394677       -1.00322
 1.9988      -0.389852       -1.00678
 1.9992      -0.380565       -1.00968
 1.9996      -0.374163       -1.01263
 2     -0.365941       -1.0134
 2.0004      -0.357092       -1.01384
 2.0008      -0.350004       -1.01644
 2.0012      -0.34249       -1.01825
 2.0016      -0.333693       -1.02007
```

```
2.002     -0.324713      -1.02248
2.0024     -0.319214      -1.0248
2.0028     -0.310616      -1.02932
2.0032     -0.302279      -1.02839
2.0036     -0.294619      -1.03083
2.004     -0.284448      -1.0328
3.996     -0.647107      0.776617
3.9964     -0.653435      0.772117
3.9968     -0.660677      0.766984
3.9972     -0.667879      0.762493
3.9976     -0.672879      0.757015
3.998     -0.679497      0.751139
3.9984     -0.687054      0.745715
3.9988     -0.692407      0.740071
3.9992     -0.698823      0.736052
3.9996     -0.705345      0.72906
4     -0.710725      0.726051
4.0004     -0.716532      0.719559
4.0008     -0.722336      0.71269
4.0012     -0.728206      0.70814
4.0016     -0.734061      0.702924
4.002     -0.738914      0.698097
4.0024     -0.745839      0.690968
4.0028     -0.749899      0.684431
4.0032     -0.757734      0.678117
4.0036     -0.761515      0.672567
4.004     -0.768895      0.668122
5.996     1.05081      0.255865
5.9964     1.04698      0.265325
5.9968     1.04679      0.27374
5.9972     1.04561      0.287057
5.9976     1.04058      0.291829
5.998     1.03711      0.302047
5.9984     1.03555      0.310306
5.9988     1.03354      0.32179
5.9992     1.02864      0.331114
5.9996     1.02611      0.338581
6     1.02311      0.350593
6.0004     1.01804      0.357473
6.0008     1.01583      0.3669
6.0012     1.01406      0.378611
6.0016     1.01173      0.387015
6.002     1.0071      0.395253
6.0024     1.00519      0.405766
6.0028     1.00176      0.414948
6.0032     0.996854      0.423395
6.0036     0.993996      0.434077
6.004     0.989598      0.439462
```

Short S11

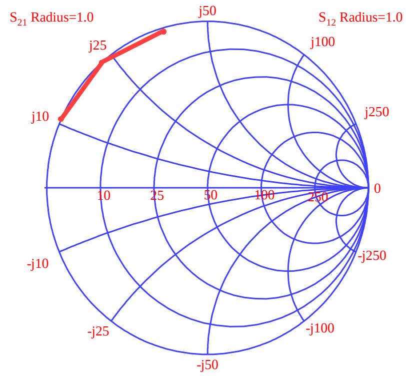

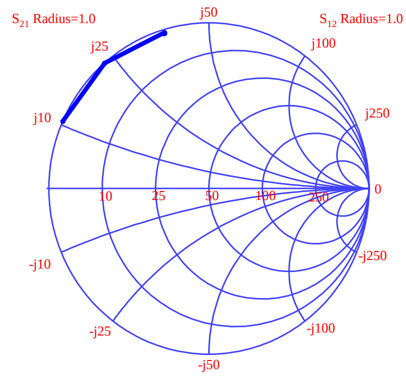

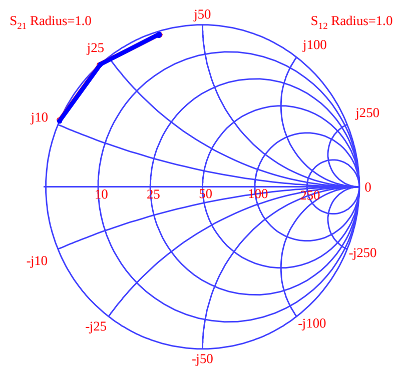

Open S11

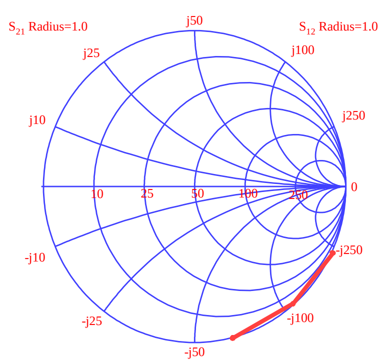

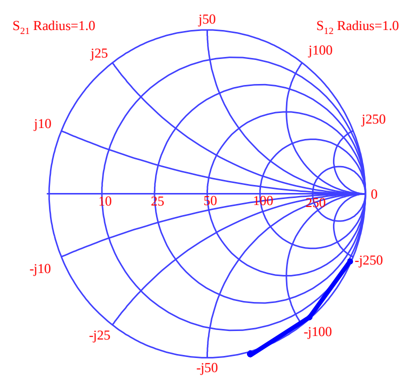

Open S22

Both

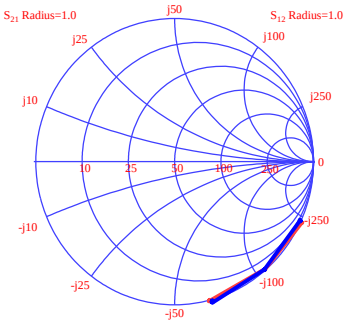

RF Full Cal

Measured Power

```
! Filename: C:Documents and
Settings:ogboi:Desktop:Modulated_2009:Cal1:RF_CAL:Power_1
! Comment: Calibration: 1  Absolute Power Calibration Data, harmonic no.1
! Info:  05 July 2014 18:20:05 AVERAGES=  128 PARAMETER=Absolute_Power2
# GHZ S RI R 50
 1.996     0.990602      0
 1.9964     0.990547      0
 1.9968     0.99051      0
 1.9972     0.990551      0
 1.9976     0.99075      0
 1.998     0.991553      0
 1.9984     0.99166      0
 1.9988     0.991714      0
 1.9992     0.991756      0
 1.9996     0.991752      0
 2     0.991754      0
 2.0004     0.984955      0
 2.0008     0.984756      0
 2.0012     0.984567      0
 2.0016     0.984394      0
 2.002     0.983946      0
 2.0024     0.984252      0
 2.0028     0.983888      0
 2.0032     0.983478      0
 2.0036     0.983297      0
 2.004     0.983271      0
 3.996     1.00668      0
 3.9964     1.00649      0
 3.9968     1.00644      0
 3.9972     1.00644      0
 3.9976     1.00653      0
 3.998     1.00648      0
 3.9984     1.00657      0
 3.9988     1.00639      0
 3.9992     1.00663      0
 3.9996     1.00644      0
 4     1.00654      0
 4.0004     1.00646      0
 4.0008     1.00652      0
 4.0012     1.00645      0
 4.0016     1.00643      0
```

4.002	1.00614	0
4.0024	1.00572	0
4.0028	1.00549	0
4.0032	1.00542	0
4.0036	1.0055	0
4.004	1.00536	0
5.996	1.09107	0
5.9964	1.0914	0
5.9968	1.09117	0
5.9972	1.09113	0
5.9976	1.09122	0
5.998	1.09081	0
5.9984	1.09091	0
5.9988	1.09059	0
5.9992	1.09045	0
5.9996	1.09033	0
6	1.09027	0
6.0004	1.09028	0
6.0008	1.09017	0
6.0012	1.0899	0
6.0016	1.08965	0
6.002	1.08937	0
6.0024	1.08941	0
6.0028	1.08932	0
6.0032	1.08936	0
6.0036	1.08912	0
6.004	1.08913	0

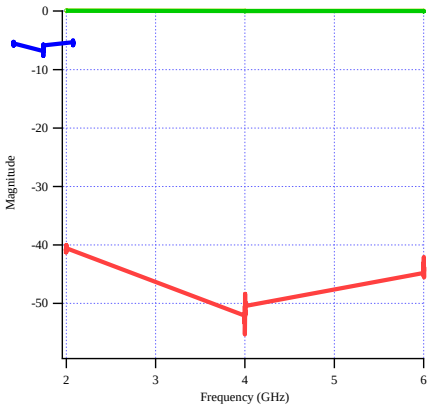

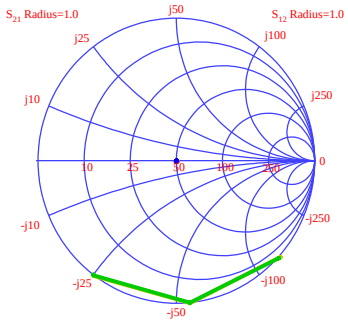

IF Power Verification

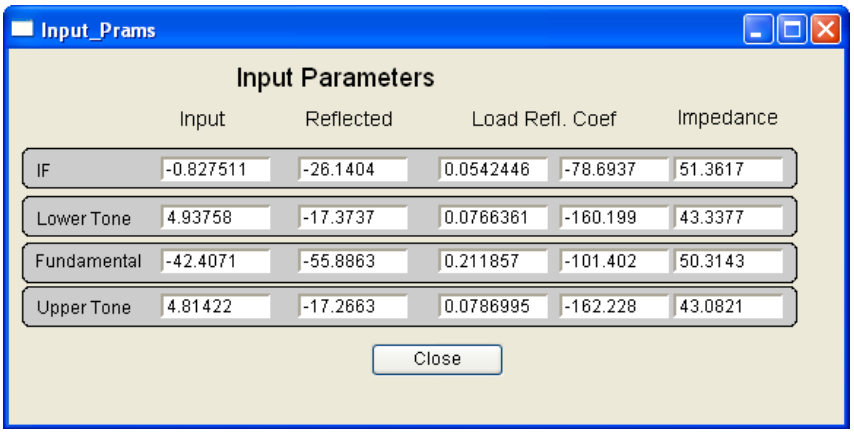
Input_Prams
Input Parameters
Input
Reflected
Load Refl. Coef
Impedance
IF
-0.827511
-26.1404
0.0542446
-78.6937
51.3617
Lower Tone
4.93758
-17.3737
0.0766361
-160.199
43.3377
Fundamental
-42.4071
-55.8863
0.211857
-101.402
50.3143
Upper Tone
4.81422
-17.2663
0.0786995
-162.228
43.0821
Close

APPENDIX D

(chapter 5 section one)

Reference baseband short circuit state measurements 3-tone PAPR = 4.77dB

4MHz bandwidth

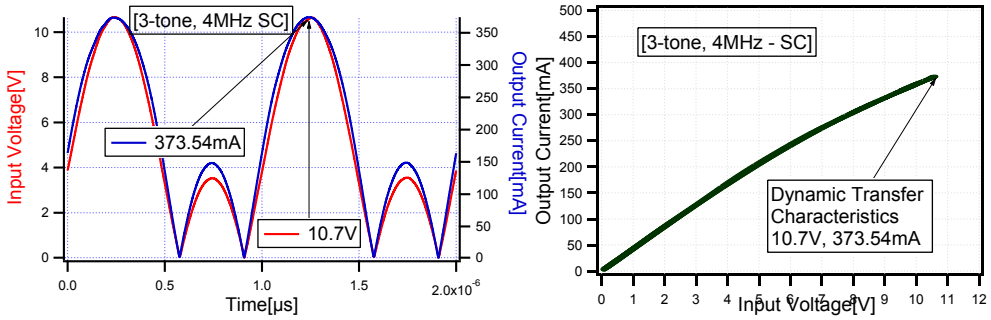

(a). Measured RF Input voltage – output current envelopes

(b). Measured RF envelope dynamic transfer characteristics

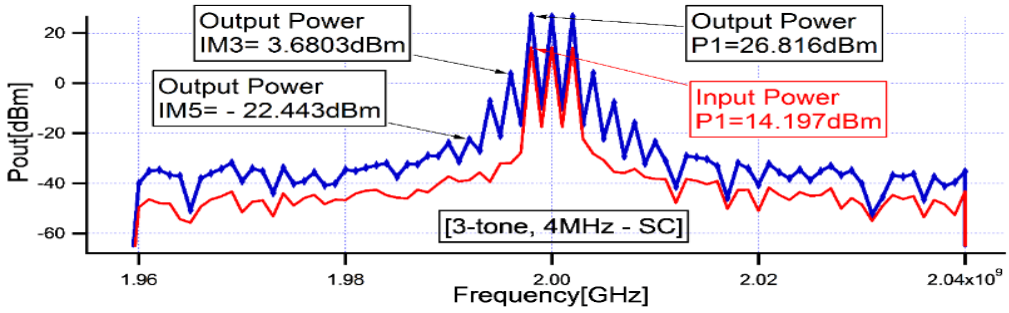

(c). Measured RF input power – output power spectrum

16MHz bandwidth

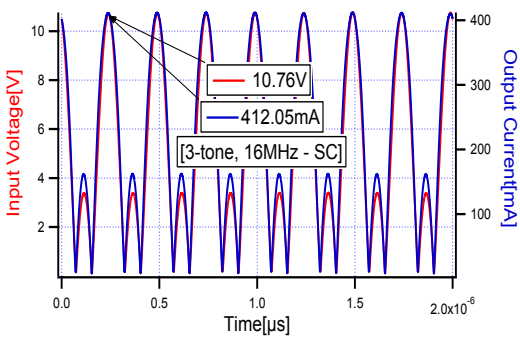

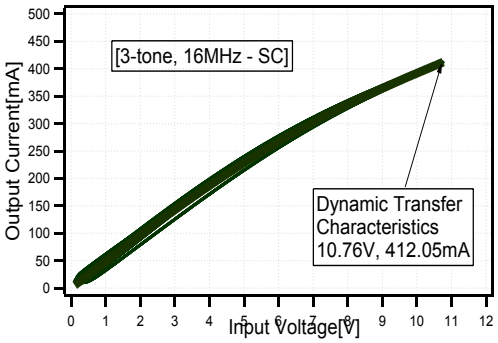

(a). Measured RF Input voltage – output current envelopes

(b). Measured RF envelope dynamic transfer characteristics

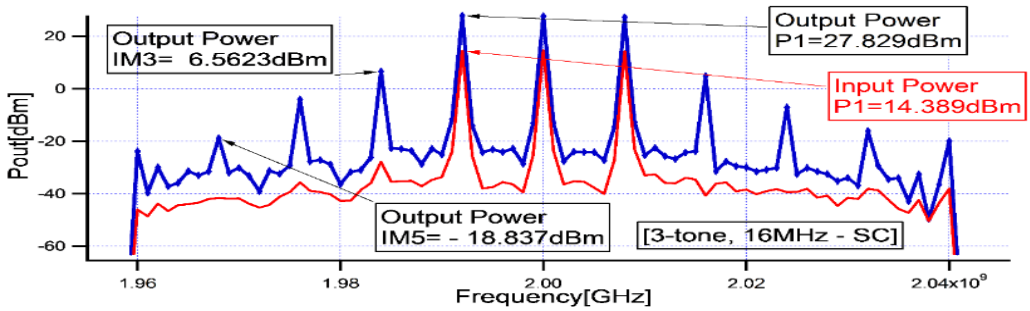

(c). Measured RF input power – output power spectrum

Linear state measurements

4MHz bandwidth

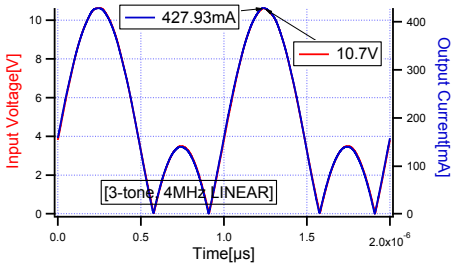

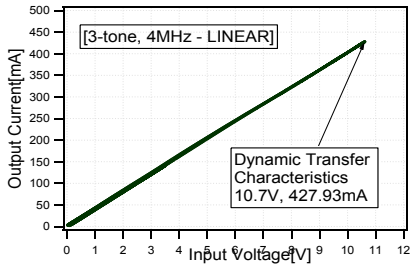

(a). Measured RF Input voltage – output current envelopes

(b). Measured RF envelope dynamic transfer characteristics

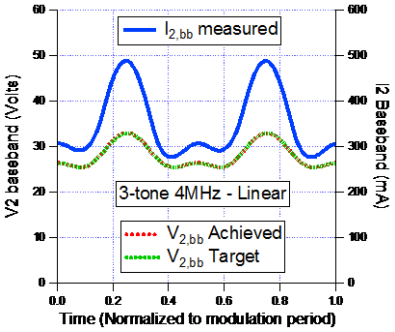

(c). Linearizing baseband signal

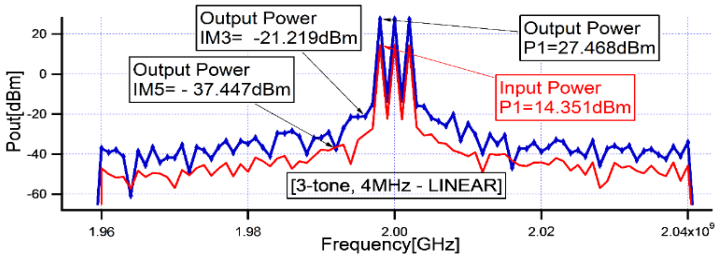

(d). Measured RF input power – output power spectrum

16MHz bandwidth

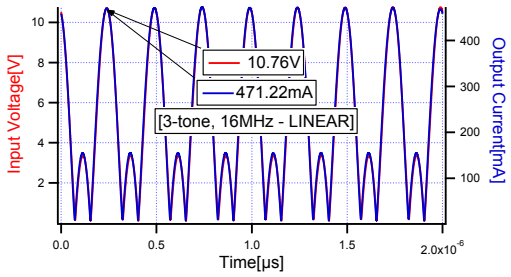

(a). Measured RF Input voltage – output current envelopes

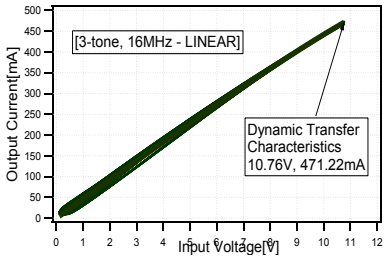

(b). Measured RF envelope dynamic transfer characteristics

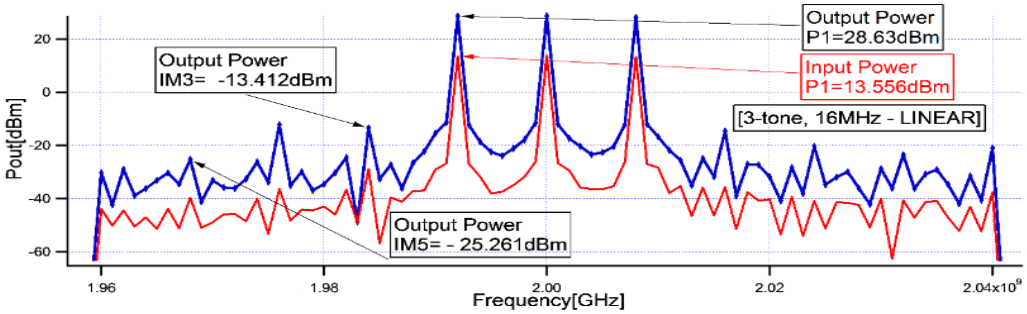

(c). Measured RF input power – output power spectrum

APPENDIX E

(chapter 5 section two)

Reference baseband short circuit state measurements result

3-tone plots (PAPR = 4.77 dB)

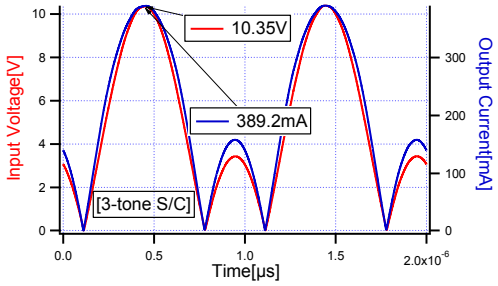

(a). Measured RF Input voltage – output current envelopes

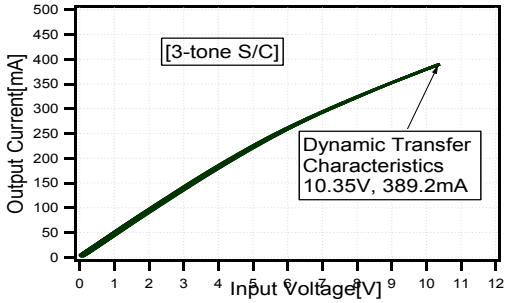

(b). Measured RF envelope dynamic transfer characteristics

5-tone plots (PAPR = 6.99 dB)

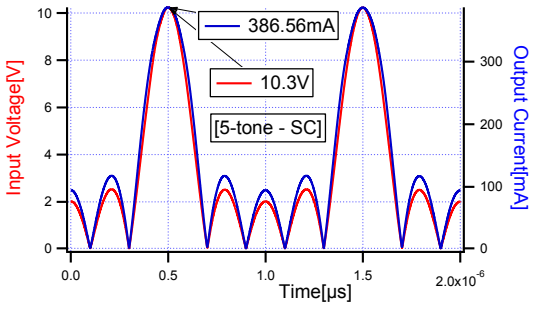

(a). Measured RF Input voltage – output current envelopes

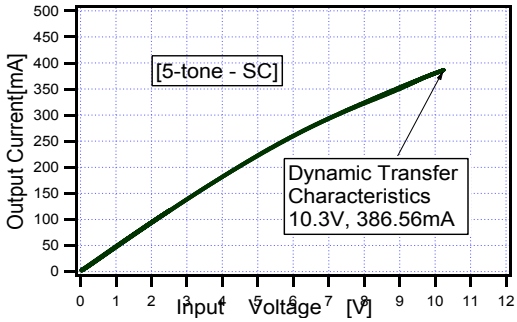

(b). Measured RF envelope dynamic transfer characteristics

Linear state measurements result

3-tone plots (PAPR = 4.77 dB)

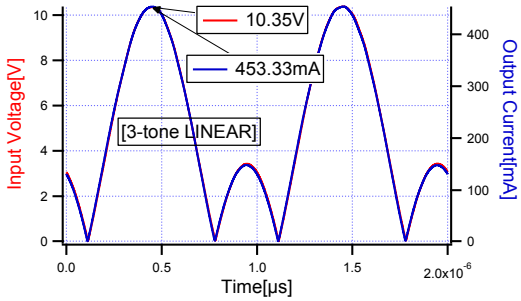

(a). Measured RF Input voltage – output current envelopes

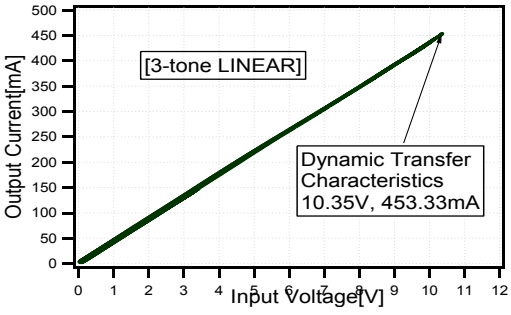

(b). Measured RF envelope dynamic transfer characteristics

5-tone plots (PAPR = 6.99 dB)

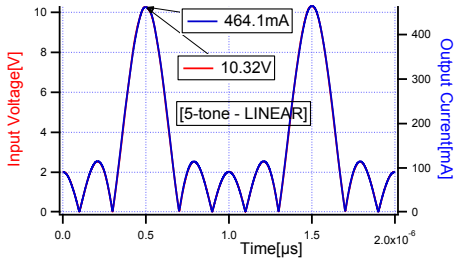

(a). Measured RF Input voltage – output current envelopes

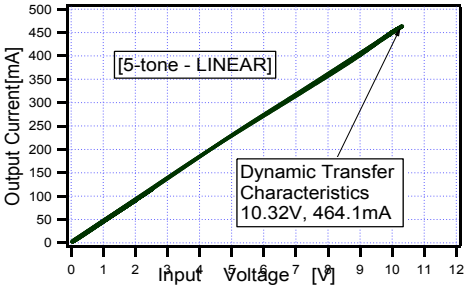

(b). Measured RF envelope dynamic transfer characteristics

Further measurements confirming the concept

This concept was further confirmed for more complex signals. In the communication industry, signals may be defined as complex if it has high peak-to-average-power-ratio (PAPR), such as increase in the number of tones as shown in chapter 5 section two. Another way signal complexity can be defined is its bandwidth just as shown in chapter 5 section one. In addition to these, can also be considered as the size of the envelope that is been transmitted and the speed of the

modulation of the envelope. Complexity can even be seen as the number of services running on a stream of signal like in orthogonal frequency division multiple access (OFDMA) and in multiple-input-multiple-output (MIMO) antennae arrays. To further investigate this technique, more complex signals were considered here. Starting with a 7-tone modulation up to a 17-tone modulation. The results confirms the same concept.

Reference baseband short circuit state measurements result

7-tone plots (PAPR = 8.45 dB)

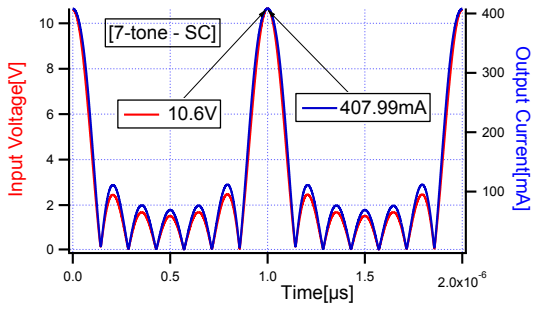

(a). Measured RF Input voltage – output current envelopes

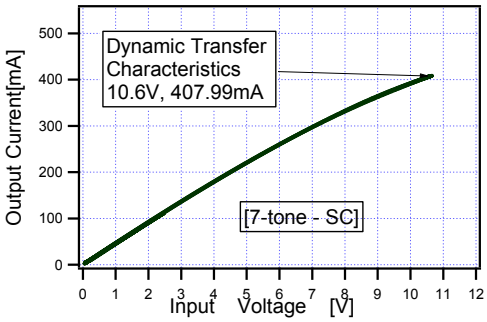

(b). Measured RF envelope dynamic transfer characteristics

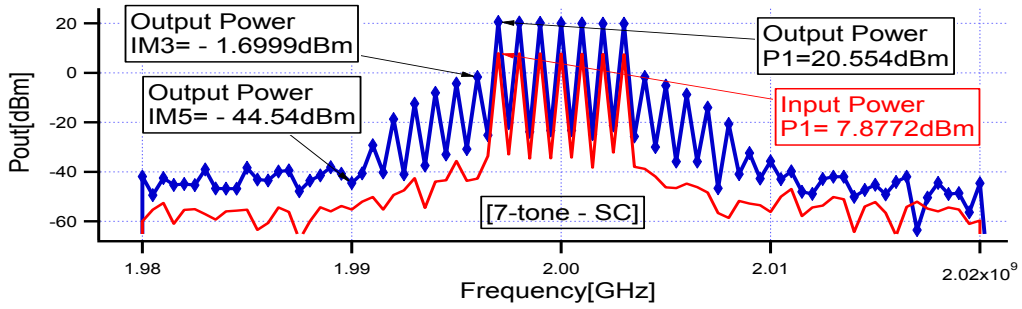

(c). Measured RF input power – output power spectrum

Linear state measurements result

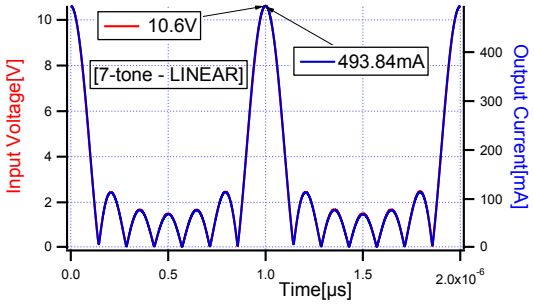

(a). Measured RF Input voltage – output current envelopes

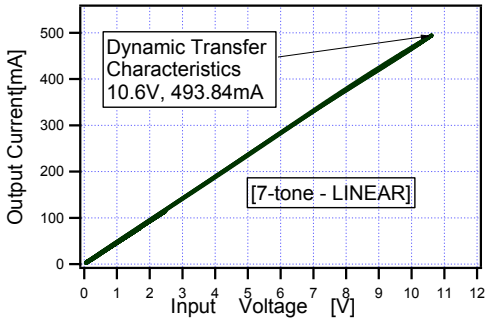

(b). Measured RF envelope dynamic transfer characteristics

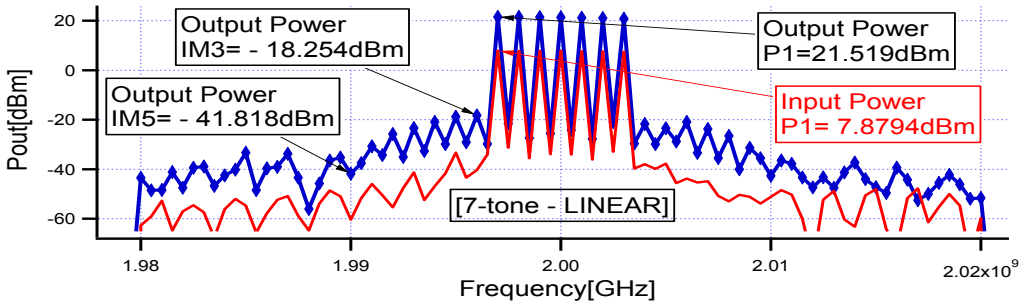

(c). Measured RF input power – output power spectrum

Reference baseband short circuit state measurements result

11-tone plots (PAPR = 10.41 dB)

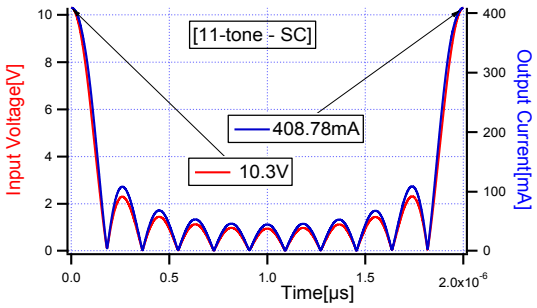

(a). Measured RF Input voltage – output current envelopes

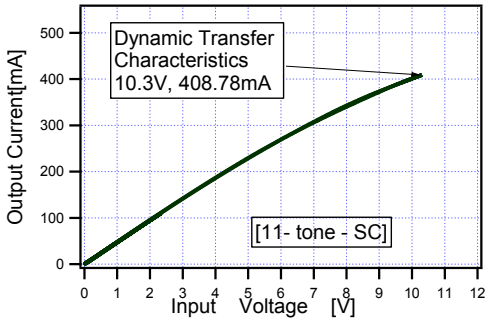

(b). Measured RF envelope dynamic transfer characteristics

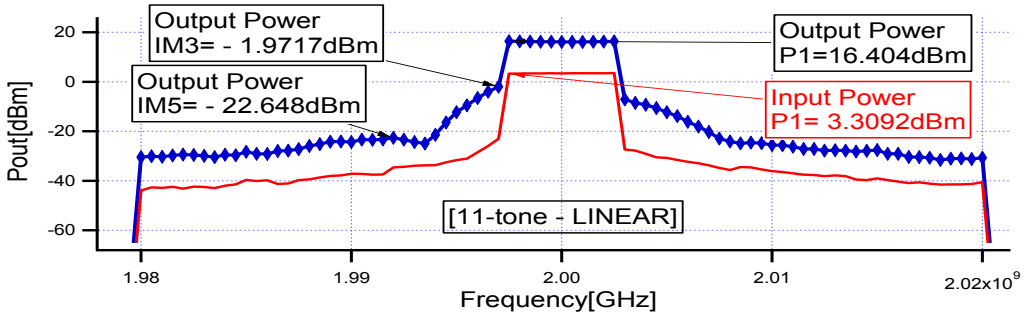

(c). Measured RF input power – output power spectrum

Linear state measurements result

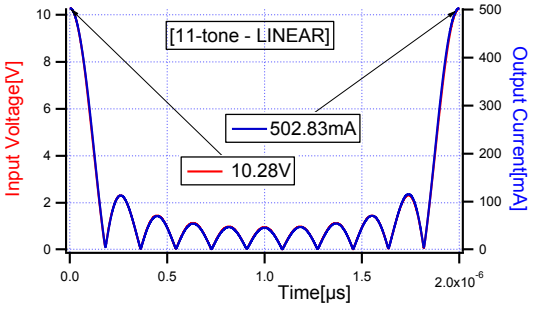

(a). Measured RF Input voltage – output current envelopes

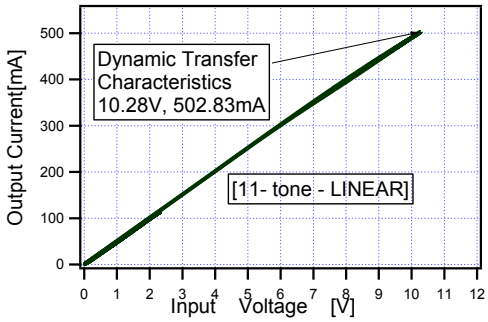

(b). Measured RF envelope dynamic transfer characteristics

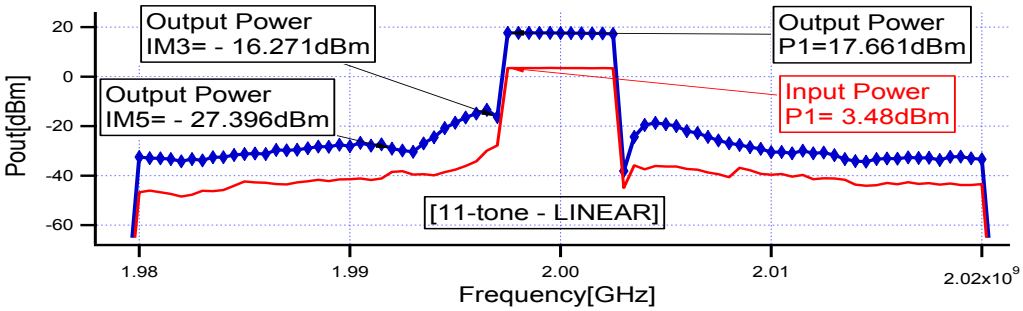

(c). Measured RF input power – output power spectrum

Reference baseband short circuit state measurements result

13-tone plots (PAPR = 11.14 dB)

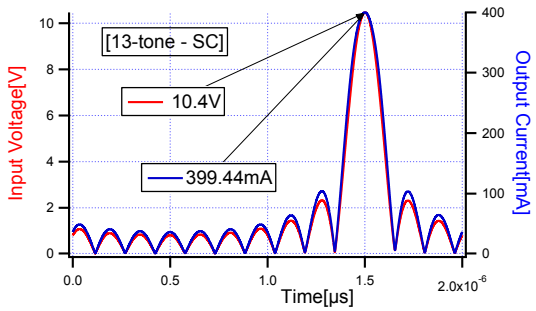

(a). Measured RF Input voltage – output current envelopes

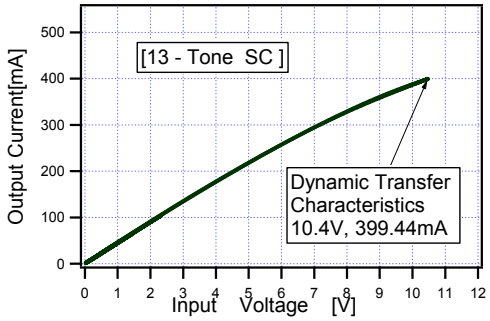

(b). Measured RF envelope dynamic transfer characteristics

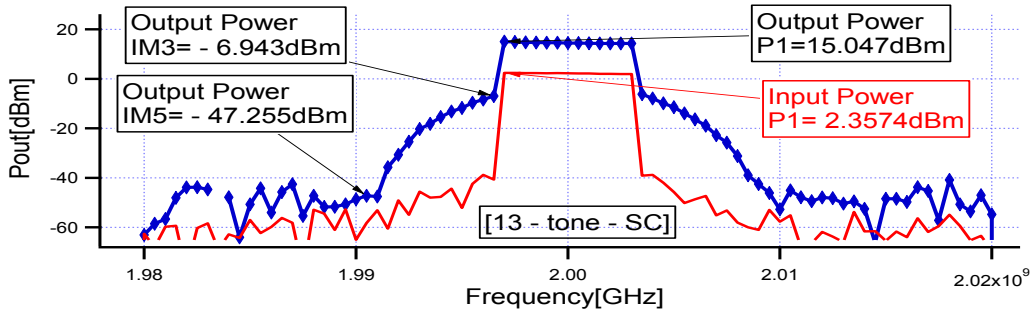

(c). Measured RF input power – output power spectrum

Linear state measurements result

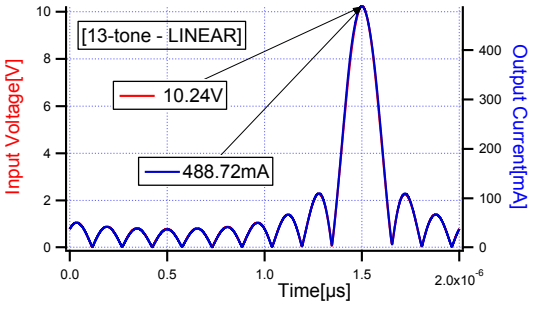

(a). Measured RF Input voltage – output current envelopes

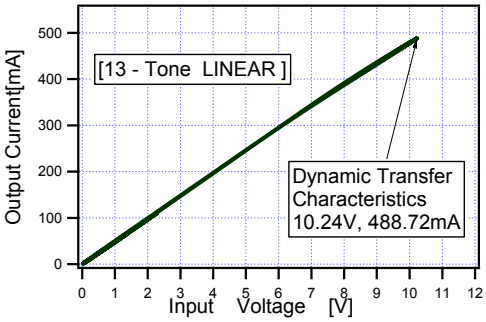

(b). Measured RF envelope dynamic transfer characteristics

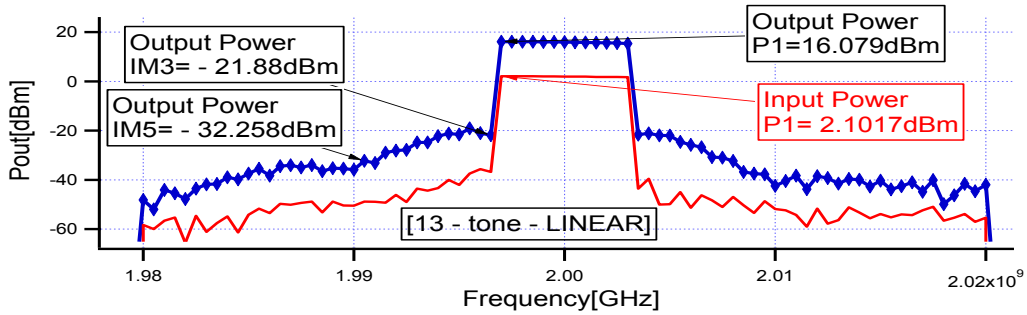

(c). Measured RF input power – output power spectrum

Reference baseband short circuit state measurements result

17-tone plots (PAPR = 12.31dB)

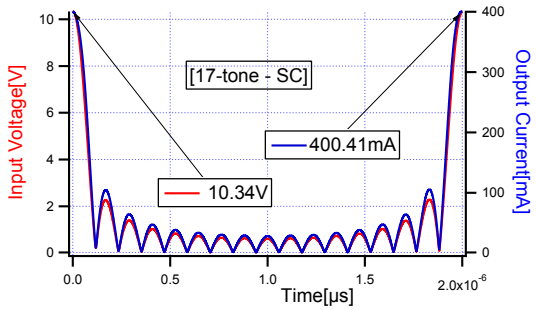

(a). Measured RF Input voltage – output current envelopes

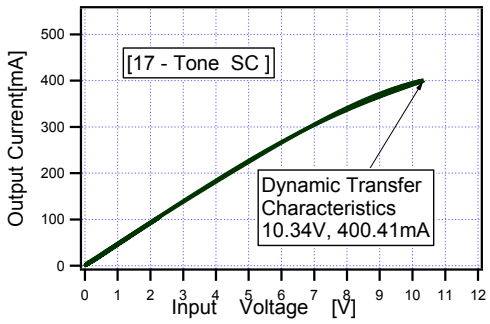

(b). Measured RF envelope dynamic transfer characteristics

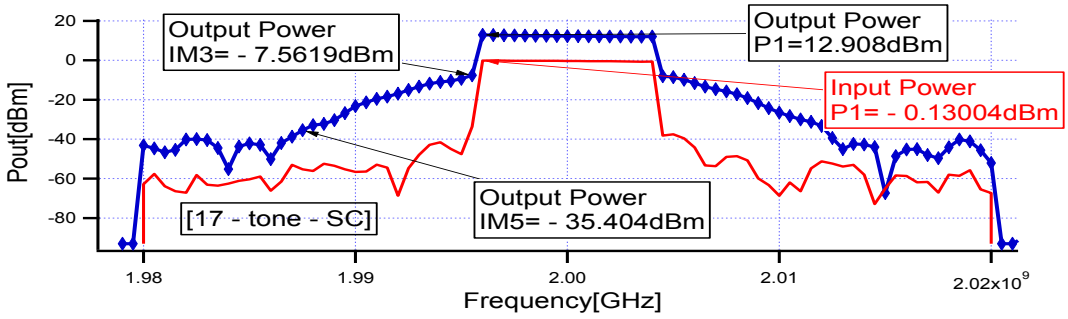

(c). Measured RF input power – output power spectrum

Linear state measurements result

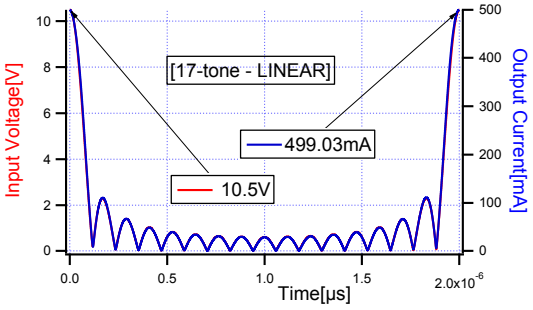

(a). Measured RF Input voltage – output current envelopes

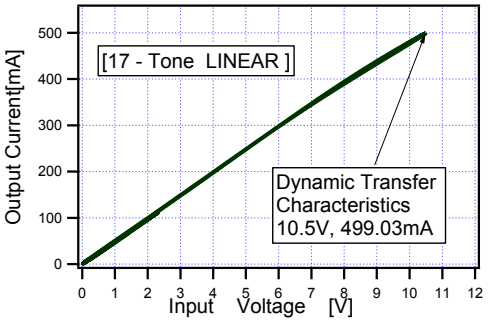

(b). Measured RF envelope dynamic transfer characteristics

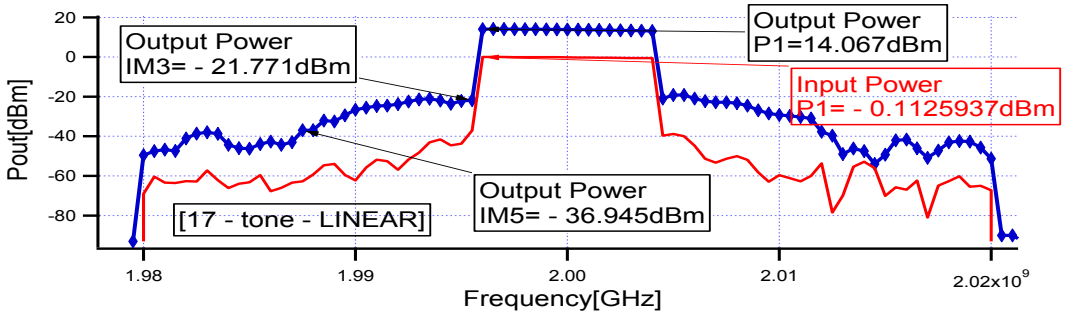

(c). Measured RF input power – output power spectrum

APPENDIX F

Devices used

Device D1

CGH40010

10 W, RF Power GaN HEMT (GaN-on-SiC)

Cree's CGH40010 is an unmatched, gallium nitride (GaN) high electron mobility transistor (HEMT). The CGH40010, operating from a 28 volt rail, offers a general purpose, broadband solution to a variety of RF and microwave applications. GaN HEMTs offer high efficiency, high gain and wide bandwidth capabilities making the CGH40010 ideal for linear and compressed amplifier circuits. The transistor is available in both screw-down, flange and solderdown, pill packages.

Device D2

Gallium Nitride 28V, 25W RF Power Transistor

(GaN-on-Si)

Built using the SIGANTIC® NRF1 process - A proprietary GaN-on-Silicon technology

FEATURES

• Optimized for broadband operation from

DC - 4000MHz

• 25W P3dB CW narrowband power

• 10W P3dB CW broadband power from 500-1000MHz

• Characterized for operation up to 32V

• 100% RF tested

• Thermally enhanced industry standard package

• High reliability gold metallization process

• Lead-free and RoHS compliant

• Subject to EAR99 export control

Device D3

10W, Silicon LDMOS

RESEARCH PUBLICATIONS

Next page.

A LSNA configured to perform Baseband Engineering for Device Linearity Investigations under Modulated Excitations

F.L. Ogboi, P.J. Tasker, M. Akmal, J. Lees, J.Benedikt
Centre for High Frequency Engineering,
Cardiff University,
Cardiff, United Kingdom,
ogboifl2@cardiff.ac.uk

S. Bensmida, K. Morris, M. Beach, J. McGeehan
Centre for Communications Research,
University of Bristol,
Bristol, United Kingdom

***Abstract*—A Large Signal Network Analyzer (LSNA) system has been configured to automatically engineer specific baseband voltage waveforms that, when injected into the output of an active device enable novel device linearization investigations. This is achieved using a formulation, generalized in the envelope domain, to describe the required baseband injection voltage. The advantage of this formulation is that it can be used to compute and then engineer the required baseband injection voltage signals, for arbitrary amplitude modulated envelopes, in terms of a limited set of describing coefficients. Using this approach, it is possible to determine the optimum baseband signal coefficients necessary to linearize a 10W Cree GaN HEMT device using baseband injection techniques. The formulation is validated by experimental investigation, using a 3-tone modulated signal, where the optimum output baseband signal for third and fifth order IMD suppression is successfully identified. For the optimum case, the observed level of IM3 and IM5 distortion was reduced to less than -56dBc whilst driving into 1.5 dB of compression.**

Keywords — Multi-tone modulation; baseband; linearization; non-linear distortion.

I. INTRODUCTION

The raw linearity performance of wireless communications systems is significantly degraded by the power amplifier transistor's odd-order non-linearity, since it is these terms that produce in-band inter-modulation distortions products, with third and fifth-order terms generally dominating [1-4]. Various approaches to minimize and suppress these distortion products have been investigated, ranging from analog pre-distortion, digital pre-distortion, feed-forward techniques and others. In this paper we will focus on output baseband voltage signal injection as it offers a simple technique aligned with the low cost requirement of small-cell transmitters, along with the prospect of combining with envelope tracking (ET) signals. The basic principle of baseband injection is to utilize the transistor's even order non-linearity to generate additional, ideally cancelling, in-band inter-modulation distortion. A number of publications provide specific mathematical analysis and experimental validation [5-7], however, a generic formulation has yet to be presented, making the efficient automation of a baseband driven linearization process difficult to realize. This paper tackles this problem by presenting a generic formulation that allows the required baseband voltage signals to be defined in the envelope domain, and then be utilized in the linearization of a GaN power device. In this approach, the baseband specification is formulated not in terms of impedance, but in terms of the desired envelope voltage signal. Importantly, this allows the linearization solution to reduce to the determination of a limited set of coefficients.

This work is supported by EPSRC (grant EP/F033702/1). We also thank CREE for supplying devices and specially Simon Wood, Ryan Baker and Ray Pengelly

II. BASEBAND SIGNAL FORMULATION

Consider the behavior of a non-linear power transistor subjected to a modulated RF stimulus $V_{1,rf}(t)$ at its input, and a time-varying baseband stimulus $V_{2,bb}(t)$ at its output.

The arbitrary modulated input voltage signal can be represented as:

$$V_{1,rf}(t)= M_{1,rf}(t)\cos(\omega_c t+\phi_{1,rf}(t)) \quad (1)$$

Where $M_{1,rf}(t)$ and $\phi_{1,rf}(t)$ are the magnitude and phase of the modulated input signal respectively, and ω_c is the RF carrier frequency. This signal can also be presented in the complex envelope (I-Q) domain as:

$$\tilde{V}_{1,rf}(t)= M_{1,rf}(t)\cos(\phi_{1,rf}(t)) - jM_{1,rf}(t)\sin(\phi_{1,rf}(t)) \quad (2)$$

Similarly, the RF output current response of the device can be represented as:

$$I_{2,rf}(t)= M_{2,rf}(t)\cos(\omega_c t+\phi_{2,rf}(t)) \quad (3)$$

Where $M_{2,rf}(t)$ and $\phi_{2,rf}(t)$ are the magnitude and phase of the complex modulated output current respectively, and ω_c is the carrier frequency. Again, this signal can be presented in the envelope domain, as:

$$\hat{I}_{2,rf}(t)= M_{2,rf}(t)\cos(\phi_{2,rf}(t)) - jM_{2,rf}(t)\sin(\phi_{2,rf}(t)) \quad (4)$$

Mixing analysis tells us that if $V_{2,bb}(t)=0$, the memory-less non-linear envelope transfer characteristic between the input

voltage envelope $\tilde{V}_{1,rf}(t)$ and the output current envelope $\hat{I}_{2,rf}(t)$ can be modeled as follows:

$$\hat{I}_{2,rf}(t) = \sum^{m}_{n=0} \alpha_{2n+1} | \tilde{V}_{1,rf}(t) |^{2n} \tilde{V}_{1,rf}(t) \quad (5)$$

Where α_1 represents the linear gain of the system, α_3 quantifies the level of third order intermodulation distortion, α_5 quantifies the level of fifth order intermodulation distortion, and so on, up to the desired maximum order m.

In this work, the following general envelope formulation for the output baseband voltage envelope signal $\tilde{V}_{2,bb}(t)$ is considered:

$$\tilde{V}_{2,bb}(t) = \sum^{q}_{p=1} \beta_{2p} | \tilde{V}_{1,rf}(t) |^{2p} \quad (6)$$

where β_{2p} is the even order voltage component scaling coefficient and q specifies the desired maximum range. The motivation for using this formulation lies in the fact that only cancelling odd-order intermodulation terms will be added to the RF output current envelope response. Hence, only the coefficients in (5) will be modified such that

$$\alpha_{2n+1}|^{m}_{n=1} = f(\beta_2, \beta_4, \ldots\ldots \beta_{2p}, \ldots\ldots \beta_{2q}) \quad (7)$$

Consider now a system with intermodulation distortion up to fifth order (m=2). The baseband linearization problem can now be restricted to forth order (q=2), hence equating to determining the values of β_2 (beta-2) and β_4 (beta-4) that can simultaneously satisfy the two following conditions:

$$\alpha_3 = f(\beta_2, \beta_4) = 0$$
$$\alpha_5 = f(\beta_2, \beta_4) = 0 \quad (8)$$

and where f and g are unknown generic functions, to be determined empirically.

III. LSNA System

To investigate this concept, the Large Signal Network Analyzer (LSNA) system described in [8], capable of measuring modulated voltage and current waveforms while also injecting voltage signals into the baseband, is utilized. To ensure that the appropriate output baseband envelope voltage signal can be generated, the system was enhanced by the addition of a 75W, 10KHz-250MHz wideband baseband amplifier from "Amplifier Research" Model 75A250, as shown in Fig. 1. Key to this system is an ability to measure and engineer the modulated time domain terminal voltage and current waveforms. Using this information, it is possible to compute all the necessary measured envelope stimulus components at both baseband and RF (fundamental and harmonics).

The LSNA was calibrated to the device package plane using a custom built 50 Ω TRL test fixture, over a 50MHz baseband bandwidth and over a 100 MHz bandwidth around each of the RF components (fundamental and harmonics). Using a 1 MHz 3-tone, modulated excitation signal with peak-to-average power ratio (PAPR) of 4.77dB and centered at 2GHz, the GaN device was biased in class AB, with RF fundamental and all harmonic frequencies terminated into a passive 50Ω.

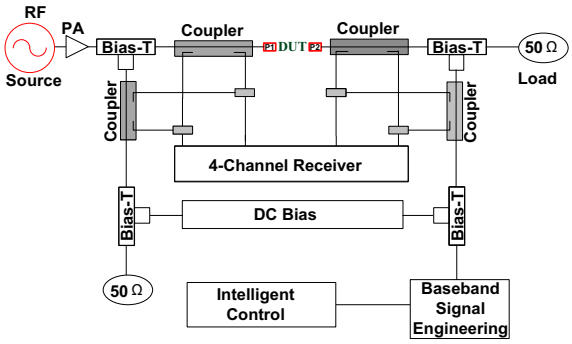

Fig. 1. Large signal RF waveform modulated measurement system

Drain and gate bias voltages were 28V and -2.8V respectively, giving a quiescent drain current of approximately 20% I_{DSS}. The load condition, although not quite optimal, was considered sufficiently close for this demonstration. Typical measured fundamental input voltage $\tilde{V}_{1,rf}(t)$ and output current $\hat{I}_{1,rf}(t)$ complex envelopes are shown in Fig. 2. These use polar form (magnitude and phase), and indicate a clear AM-AM distortion, but only a very weak AM-PM distortion of less than +/- 2 degrees.

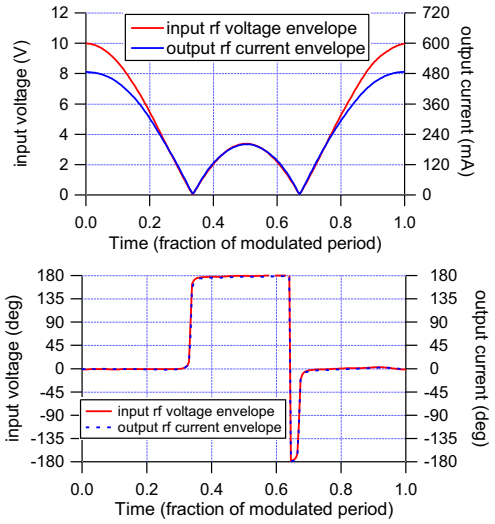

Fig. 2. Magnitude and phase of the time aligned, measured fundamental input voltage $\tilde{V}_{1,rf}(t)$ and output current $\hat{I}_{2,rf}(t)$ envelopes.

IV. Baseband Voltage Engineering

For the measurements shown in Fig. 2, the system was configured to force the baseband output voltage component $V_{2,bb}(t)$ to zero, hence $\beta_2=0$ and $\beta_4=0$. Since the measured baseband output current $I_{2,bb}(t)$ is observed to vary when the baseband output voltage $V_{2,bb}(t)$ is modified, an iterative software control loop was needed to 'engineer' the targeted baseband output voltage. The behavior of the baseband injection system is modeled using the circuit representation shown in Fig. 3.

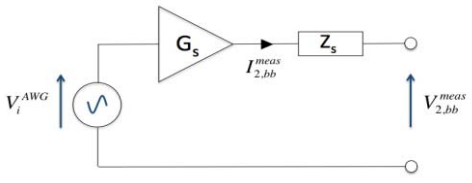

Fig. 3. Circuit Model for baseband voltage engineering

Initially, the system is calibrated to determine the values of natural system impedance $Z_s(\omega)$ and load-pull loop gain $G_s(\omega)$, over the desired modulation bandwidth (in this case 5 MHz). An iterative process using (9) is used to synthesize exactly the desired baseband voltage waveform$V_{2,bb}^{target}(t)$. The measured values of baseband voltage $V_{2bb}^{meas,i}(t)$ and current $I_{2,bb}^{meas,i}(t)$ at iteration i, are transformed into frequency domain baseband voltage $\tilde{V}_{2bb}^{meas,i}(\omega)$ and current $\hat{I}_{2,bb}^{meas,i}(\omega)$, and are then used to compute a new baseband voltage requirement at iteration i+1, also formulated in the frequency domain, using the following equation;

$$V_{i+1}^{awg}(\omega)=$$

$$(1\text{-}w)V_i^{awg}(\omega)+w(V_{2,bb}^{target}(\omega)-Z_s(\omega)I_{2,bb}^{meas,i}(\omega)/\ G_s(\omega)) \quad (9)$$

where w is the static weighting factor. This process is repeated until the desired output baseband target voltage waveform is achieved, within a specified error limit. Typically, when the desired error limit is set to 1mV, the system converges to the desired baseband voltage within 5-6 iterations.

V. Linearization Investigations

To quantify the level of observed distortion, the measured fundamental envelope transfer function (fundamental RF output current envelope $\hat{I}_{2,rf}(t)$ plotted against the fundamental RF input voltage envelope $\tilde{V}_{1,rf}(t)$ was time aligning to remove the effect of linear delay, and then analyzed. A least-squares curve fitting approach was used to fit the model, given by (5), to the measured envelope transfer characteristic, and hence determine the coefficients α_1, α_3 and α_5 for each case. A typical comparison of the measured and modeled envelope transfer function; $|\hat{I}_{2,rf}(t)|$ versus $|\tilde{V}_{1,rf}(t)|$ is shown in Fig. 4. The results in this case also confirm that the DUT has very little observable memory.

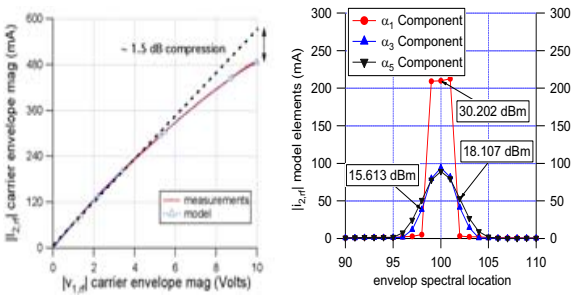

Fig 4. Comparison of the measured and modeled envelope transfer function $V_{2,bb}(t)$=0, and spectral contribution of the modelled components.

Fig. 4 also shows the resulting spectral contributions of each component generated by the current model. The labels shown on the spectral graph are the corresponding computed output power levels. The maximum power level of the out-of-band distortion, in this un-linearised 1.5 dB compressed case, can be seen to be -12 dBc. Note this is the result obtained when β_2=0 and β_4=0, the reference baseband short circuit case.

To investigate how effective precisely engineered baseband voltages can be in linearizing the device, a sequence of measurements was performed; sweeping the baseband voltage waveform describing coefficients β_2 and β_4 over a selected range, thus systematically varying the injected voltage waveform. The variation of the level of observed distortion in the measured fundamental transfer characteristic was then determined. The measured observed variations of the third order distortion term α_3 and fifth order distortion term α_5, plotted as contours is shown in Fig. 5.

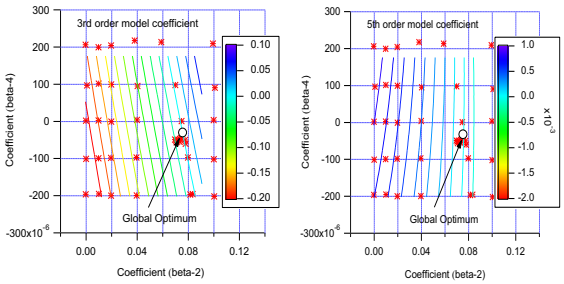

Fig 5. Contour plots of measured third order term α_3 and fifth order term α_5 values as a function of swept β_2 and β_4.

The contour plots in Fig. 5 indicate that there is an optimum set of values for β_2 and β_4 that can simultaneously satisfy the condition α_3=0 and the condition α_5=0. In other words, there is a baseband voltage waveform, that when injected into the device output, will linearize the device.

VI. Baseband Linearization

The measurement system was now configured to demonstrate engineered baseband linearization. Using the optimum values determined above, the required 'linearizing" output baseband voltage was computed using equation (6). This computed target waveform along with the measured output baseband voltage waveform achieved are shown in Fig 6, indicating the ability of the system to correctly identify and engineer the required baseband voltage signal. The corresponding measured value of the baseband current $I_{2,bb}(t)$ is also shown. Note, the current and voltage variations are in phase, indicating that this condition would in practice require an active envelope tracking (ET) type of drain bias. This is interesting as it raises the possibility of improving efficiency and linearity simultaneously [10].

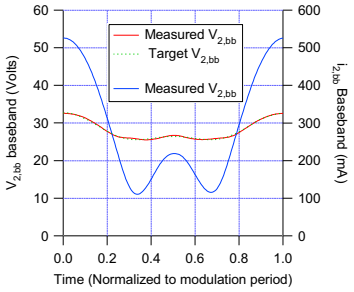

Fig. 6. Measured baseband output current, together with ideal and measured optimum output baseband linearizing voltage waveform

The linearizing baseband voltage signal was applied and the resulting, now linear transfer characteristic is shown in Fig. 7. Again the spectral contributions of each component generated by the current model obtained in this state is also shown, note the x100 scaling increase used for the distortion components.

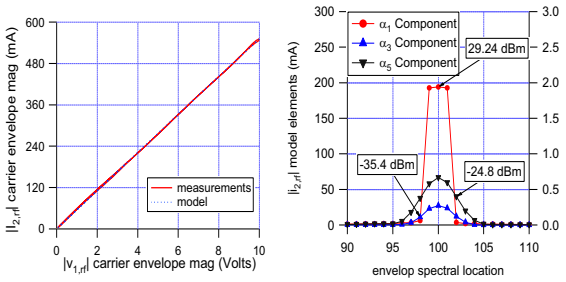

Fig. 7. Comparison of the measured and modeled envelope transfer function for the optimum $V_{2,bb}(t)$ case. Also shown is the spectral contribution of the individual model components.

In this case both the third order and fifth order IMD contributions are now reduced to below -56dBc, which is an improvement of 42dBc over the reference, baseband short circuit solution. The actual measured input and output power spectra around the carrier are shown in Fig. 8.

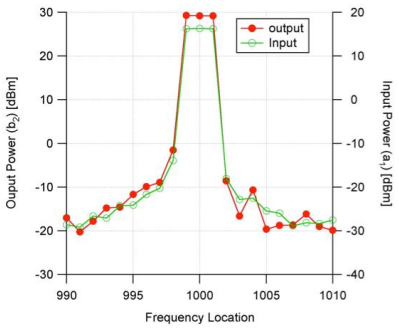

Fig. 8. Measured input and output power spectra around the carrier when the system is baseband "linearized".

It is important to realize that this final plot shows the modulated excitation being used to excite the device is certainly not perfect, and contains significant distortion, mostly due to the driver amplifier being used. As both axis cover 60dB dynamic range, it is still effective in showing however that no detectable, additional distortion is being introduced by the baseband linearized device.

VII. Conclusion

A Large Signal Network Analyzer (LSNA) System has been configured to automatically engineer specific baseband voltages, that when injected into the output of a device enables novel device linearization investigations. This functionality is achieved using a formulation, generalized in the envelope domain, that can be used to describe the required "linearizing" baseband injection signal, for an arbitrary amplitude modulated envelope, using a limited set of coefficients. The ability of the approach to simultaneously minimize both third and fifth order distortion terms has been demonstrated using a 3-tone modulated signal, where the optimum baseband signal voltage for third and fifth order IMD suppression was successfully determined and used to linearize the device. Further work is now planned to use this system to show that this approach can be applied to arbitrary modulated signals and extended to incorporate higher order distortion terms and to include AM/PM.

References

[1] Andrei Grebennikov, "RF and Microwave Power Amplifier Design". McGraw-Hill ISBN 0-07-144493-9.

[2] Joel Vuolevi and Timo Rahkonen," Distortion in RF Power Amplifiers", Norwood, MA: Artech House, 2003.

[3] John Wood, David E. Root, "Fundamentals of nonlinear behavioral modeling for RF and microwave design". Artech House, 2005.

[4] J. C. Pedro, N. B. Carvalho, "Intermodulation Distortion in Microwave and Wireless Circuits" Artech House, 2003.

[5] Chi-Shuen Leung, Kwok-Keung, M. Cheng, "A new approach to amplifier linearization by the generalized baseband signal injection method," IEEE microwave and wireless components letters, vol. 12, no.9, September, 2002.

[6] Lei Ding, G. Tong Zhou. "Effects of Even-Order Nonlinear Terms on Power Amplifier Modelling and Predistortion Linearization". IEEE Transactions On Vehicular Technology, Vol. 53, No. 1, January 2004.

[7] Vincent W. Leung, Junxiong Deng, Prasad S. Gudem, and Lawrence E. Larson. "Analysis of Envelope Signal Injection for Improvement of RF Amplifier Intermodulation Distortion", IEEE Journal of solid-state circuits, vol. 40, no. 9, September 2005.

[8] Akmal, M.; et al.; , "An enhanced modulated waveform measurement system for the robust characterization of microwave devices under modulated excitation," Microwave Integrated Circuits Conference (EuMIC), 2011 European , vol., no., pp.180-183, 10-11 Oct. 2011.

[9] Akmal, M; et al,; , "Characterization of electrical memory effects for complex multi-tone excitations using broadband active baseband load-pull,"Microwave Conference (EuMC), 2012 42nd European,vol,no., pp. 1265,1268, Oct.29 2012-Nov. 1 2012.

[10] Z. Yusoff, J. Lees, J. Benedikt, P.J. Tasker, S.C. Cripps, "Linearity improvement in RF power amplifier system using integrated Auxiliary Envelope Tracking system," IEEE MTT-S Int. Microw. Symp. Dig., 2011, vol., no., pp.1-4, 5-10 June 2011.

†A NOVEL FORMULATION FOR DEFINING LINEARISING BASEBAND INJECTION SIGNALS OF RF POWER AMPLIFIER DEVICES UNDER ARBITRARY MODULATION

†F. L. Ogboi, †P.J. Tasker, †M. Akmal, †J. Lees, †J. Benedikt
†Centre for High Frequency Engineering, Cardiff University, Cardiff, United Kingdom,
*S. Bensmida, *K. Morris, *M. Beach, *J. McGeehan
*Centre for Communications Research, University of Bristol, Woodland Rd, Bristol, BS8 1UB, UK
†Email: ogboifl2@cardiff.ac.uk

***Abstract* — A new formulation, in the envelope domain for linearising RF power amplifier devices is demonstrated. By applying this formulation, it is possible to linearise RF power amplifiers by signal injection using a time varying baseband voltage signal. The formulation defines the baseband inter-modulation distortion (IMD) envelope as a function of the input carrier signal envelope. Irrespective of the modulated RF signal, intermodulation distortion envelopes can always be defined as a finite sum of distortion-envelopes multiplied by their control coefficients.**

These coefficients are the keys used to optimise the time varying baseband voltage signal. In this formulation, 'engineering' the optimized time-varying baseband voltage signal requires the determination of only a finite number of constant coefficients. This eases the optimization process. This formulation was validated in an open-loop active baseband loadpull exercise on a 3-tone amplitude modulated RF signal. The investigation and validation experiment was performed on a Cree 10W GaN HEMT device, biased into class AB at 1.5 dB of compression. When the optimum linearizing baseband voltage was described, computed, engineered and injected into the device, IM3 and IM5 distortions were simultaneously suppressed for the optimum case to less than -56dBc. An improvement of 42dBc over the reference classical short circuit case.

Keywords — Multi-tone modulation, baseband, linearisation, non-linear distortion, envelope, power amplifier

I. INTRODUCTION

The degradation experienced in the linearity performance of wireless communication systems and their core devices is significantly attributable to the power amplifier transistor's non-linear behavior. This is caused by the odd-order non-linearities generated by these devices in their active state. These odd order non-linearities are namely third, fifth, seventh, ninth but with the third and the fifth most disturbing. These in turn produce in-band inter-modulation distortions products, which occur very near the carrier frequencies of interest which makes them very difficult to remove by filtering. Various approaches have been suggested and used to try to suppress and minimize these distortion products ranging from feed-forward techniques, analog pre-distortion, digital pre-distortion and others [5-7].

In this paper we will focus on output baseband envelope voltage signal injection. It offers a simple technique aligned with the low cost requirement of small-cell transmitters, along with the prospect of combining with envelope tracking (ET) signals. We believe that this technique is a possible candidate to enable reduced DSP complexity in making the work of the pre-distorter easier. In addition, bandwidth is reduced when linearizing at baseband. The formulation is based on the basic principle of baseband injection which states that it is possible to utilize the transistor's even order non-linearity to generate additional, ideally cancelling, in-band inter-modulation distortion. In this approach, the baseband specification is formulated not in terms of impedance, but in terms of the desired engineered envelope voltage signal. The importance is that it, allows the linearization solution to reduce to the determination of only a limited set of coefficients.

II. PRINCIPLE OF FORMULATION THEORY

Consider the behavior of a non-linear power transistor subjected to a modulated RF stimulus $V_{1,rf}(t)$ at its input, and a time-varying baseband stimulus $V_{2,bb}(t)$ at its output.

The arbitrary modulated input voltage signal can be represented and shown in Fig.1, as:

$$V_{1,rf}(t) = M_{1,rf}(t)\cos\left(\omega_c t + \phi_{1,rf}(t)\right) \quad (1)$$

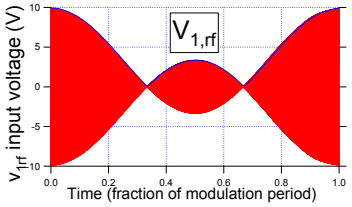

Fig 1. Measured 3-tone modulated RF input voltage signal plotted against time

where $M_{1,rf}(t)$ and $\phi_{1,rf}(t)$ are the magnitude and phase of the modulated input signal respectively, and ω_c is the RF carrier frequency.
This signal can also be presented mathematically in the complex envelope (I-Q) domain as:

$$\hat{V}_{1,rf}(t) = M_{1,rf}(t)\cos\left(\phi_{1,rf}(t)\right) - jM_{1,rf}(t)\sin\left(\phi_{1,rf}(t)\right) \quad (2)$$

Similarly, the RF output current response of the device can be represented and shown in Fig.2, as:

$$I_{2,rf}(t) = M_{2,rf}(t)\cos\left(\omega_c t + \phi_{2,rf}(t)\right) \quad (3)$$

where $M_{2,rf}(t)$ and $\phi_{2,rf}(t)$ are the magnitude and phase of the complex modulated output current respectively, and ω_c is the carrier frequency.

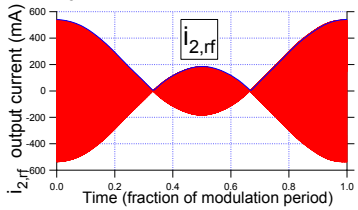

Fig.2. Measured 3-tone modulated RF output current signal plotted against time.

Again, this signal can be presented mathematically in the envelope domain, as:

$$\hat{I}_{2,rf}(t) = M_{2,rf}(t)\cos\left(\phi_{2,rf}(t)\right) - jM_{2,rf}(t)\sin\left(\phi_{2,rf}(t)\right) \quad (4)$$

Mixing analysis tells us that if $V_{2,bb}(t)=0$, the memory-less non-linear envelope transfer characteristic between the input voltage envelope $\hat{V}_{1,rf}(t)$ and the output current envelope $\hat{I}_{2,rf}(t)$ can be modeled as follows:

$$\hat{I}_{2,rf}(t) = \sum_{n=0}^{m} \alpha_{2n+1}\left|\hat{V}_{1,rf}(t)\right|^{2n}\hat{V}_{1,rf}(t) \quad (5)$$

where α_1 represents the linear gain of the system, α_3 quantifies the level of third order intermodulation distortion, α_5 quantifies the level of fifth order intermodulation distortion, and so on, up to the desired maximum order m.

In this work, the following general envelope formulation for the output baseband voltage envelope signal $\hat{V}_{2,bb}(t)$ is considered:

$$\hat{V}_{2,bb}(t) = \sum_{p=1}^{q} \beta_{2p}\left|\hat{V}_{1,rf}(t)\right|^{2p} \quad (6)$$

where β_{2p} is the even order voltage component scaling coefficient and q specifies the desired maximum range. The motivation for using this formulation lies in the fact that only cancelling odd-order intermodulation terms will be added to the RF output current envelope response. Hence, only the coefficients in equation (5) will be modified such that

$$\alpha_{2n+1}|_{n=1}^{m} = f\left(\beta_2, \beta_4, \ldots \beta_{2p}, \ldots \beta_{2q}\right) \quad (7)$$

Consider now a system with intermodulation distortion up to fifth order (m=2). The baseband linearization problem can now be restricted to forth order (q=2), hence equating to determining the values of β_2 (beta-2) and β_4 (beta-4) that can simultaneously satisfy the two following conditions:

$$\alpha_3 = f(\beta_2, \beta_4) = 0$$
$$\alpha_5 = g(\beta_2, \beta_4) = 0 \quad (8)$$

and where f and g are unknown generic functions, to be determined empirically.

III. ENVELOPE MEASUREMENT SYSTEM

To investigate this concept, the Large Signal Waveform Measurement System (LSWMS) described in [8], shown in Fig. 3, capable of measuring modulated voltage and current waveforms while also injecting voltage signals into the baseband, was modified to support the formulation and utilized. The major modification shown in red in Fig. 3 and further described in Fig. 6 was made to ensure that the appropriate output baseband envelope voltage signal can be generated. In addition, the system was further enhanced by the addition of a 75W, 10 KHz-250MHz wideband baseband amplifier from "Amplifier Research" Model 75A250. Key to this system enhancement is an ability to describe, compute, measure, engineer and inject the modulated time domain terminal voltage and current envelope waveforms. Using this information, it is possible to compute all the necessary measured envelope stimulus components at both baseband and RF (fundamental and harmonics).

The LSWMS was calibrated to the device package plane using a custom built 50 Ω TRL test fixture, over a 50MHz baseband bandwidth and over a 100 MHz bandwidth around each of the RF components (fundamental and harmonics). Using a 1 MHz 3-tone, modulated excitation signal with peak-to-average power ratio (PAPR) of 4.77dB and centered at 2GHz, the GaN device was biased in class AB, with RF fundamental and all harmonic frequencies terminated into a passive 50Ω.

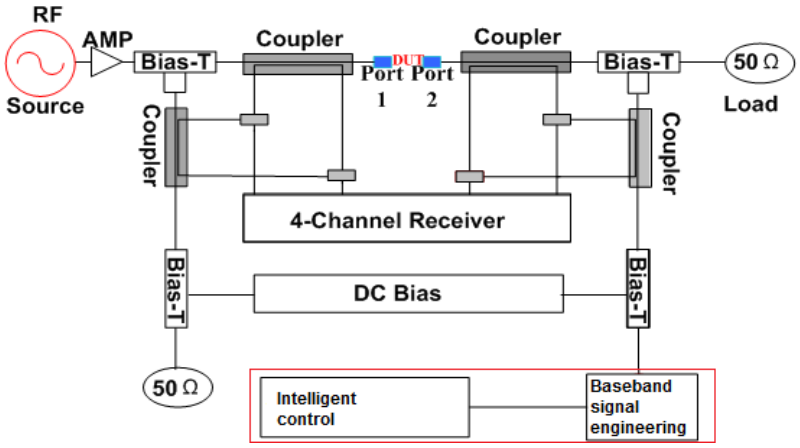

Fig. 3. Large signal modulated RF waveform measurement system.

Drain and gate bias voltages were +28V and -2.8V respectively, giving a quiescent drain current of approximately 20% I_{DSS}. The load condition, although not quite optimal, was considered sufficiently close for this demonstration. Typical measured fundamental input voltage $\hat{V}_{1,rf}(t)$ and output current $\hat{I}_{1,rf}(t)$ complex envelopes are shown in Fig. 4. These use polar form (magnitude and phase), and indicate a clear AM-AM distortion, but only a very weak AM-PM distortion of less than +/- 2 degrees.

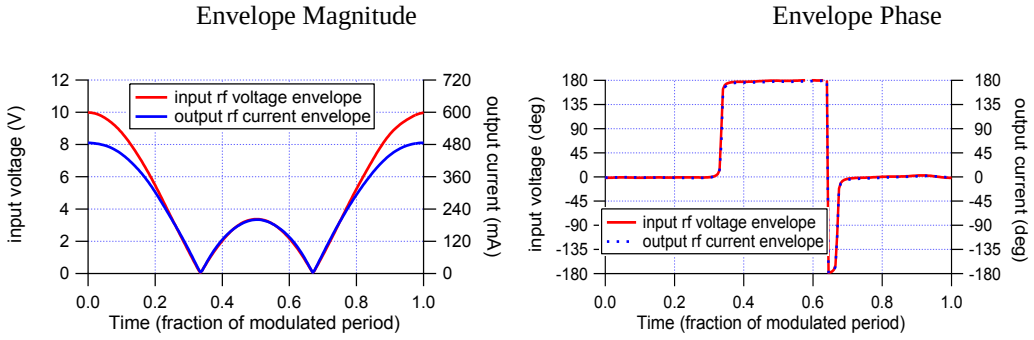

Fig. 4. Measured magnitude and phase of the time aligned fundamental input voltage $\hat{V}_{1,rf}(t)$ and output current $\hat{I}_{2,rf}(t)$ envelopes.

Fig. 5, however shows the measured transfer magnitude and phase of the fundamental input voltage $\widehat{V}_{1,rf}(t)$ at the baseband short circuit reference state. These also confirm the presence of AM/AM distortion and minimal AM/PM distortion.

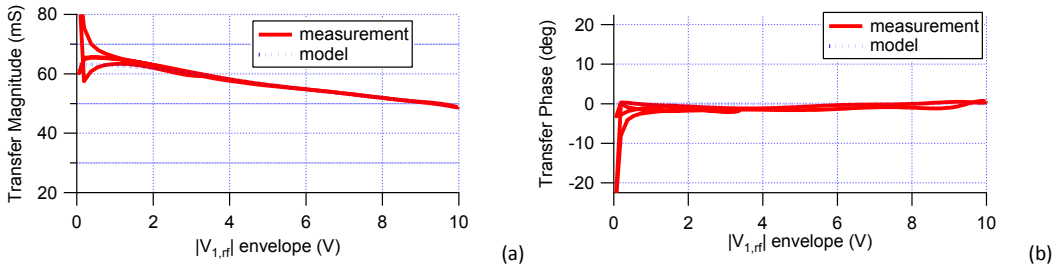

Fig. 5. Measured transfer magnitude (a) and phase (b) of the fundamental input voltage $\widetilde{V}_{1,rf}(t)$ envelope at the reference baseband short circuit state.

IV. ENVELOPE SIGNAL ENGINEERING

For the measurements shown in Fig. 4, the system was configured to force the baseband output voltage component $V_{2,bb}(t)$ to zero, hence $\beta_2 = 0$ and $\beta_4 = 0$. Since the measured baseband output current $I_{2,bb}(t)$ is observed to vary when the baseband output voltage $V_{2,bb}(t)$ is modified, an intelligent, iterative software control loop was needed to 'engineer' the targeted baseband output voltage. This intelligent control loop, is modeled using the circuit representation shown in Fig. 6. It depicts the behavior of the baseband injection system, which is a major modification to the LSWMS. This causes a systematic but scientific iterative waveform-engineering process to occur as the baseband voltage waveform is shaped by the linearising coefficients in each new iteration according to a mathematical model. This process was used to engineer the low frequency signals in the baseband (DC) region to target intermodulation distortion envelopes, as depicted in the spectral map in Fig.7.

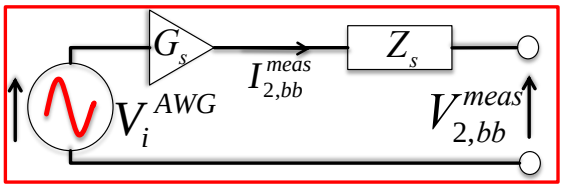

Fig. 6. Circuit Model for baseband voltage engineering.

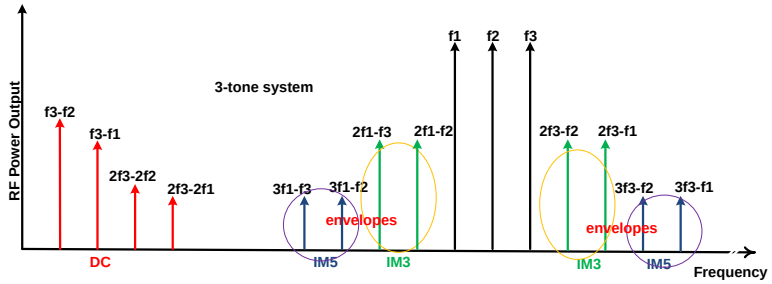

Fig. 7. Spectral map showing intermodulation distortion envelopes.

Initially, the system is calibrated to determine the values of natural system impedance $Z_s(\omega)$ and load-pull loop gain $G_s(\omega)$, over the desired modulation bandwidth (in this case 5 MHz). An iterative process using equation 9 is used to synthesize exactly the desired baseband voltage waveform $V_{2,bb}^{target}(t)$. The measured values of baseband voltage $V_{2,bb}^{meas,i}(t)$ and current $I_{2,bb}^{meas,i}(t)$ at iteration i, are transformed into frequency domain baseband voltage $\widetilde{V}_{2,bb}^{meas,i}(\omega)$ and current $\widetilde{I}_{2,bb}^{meas,i}(\omega)$, and are then used to compute a new baseband voltage requirement at iteration i+1, also formulated in the frequency domain, using the following equation;

$$V_{i+1}^{awg}(\omega) = (1-w)V_i^{awg}(\omega) + w\left(\frac{V_{2,bb}^{target}(\omega) - Z_s(\omega)I_{2,bb}^{meas,i}(\omega)}{G_s(\omega)}\right) \quad (9)$$

where w is the static weighting factor. This process is repeated until the desired output baseband target voltage waveform is achieved, within a specified error limit. Typically, when the desired error limit is set to 1mV, the system converges to the desired baseband voltage within 5-6 iterations.

V. Formulation Application

To quantify the level of observed distortion, the measured fundamental envelope transfer function (fundamental RF output current envelope $\hat{I}_{2,rf}(t)$ plotted against the fundamental RF input voltage envelope $\hat{V}_{1,rf}(t)$) was time aligned to remove the effect of linear delay, and then analyzed. A least-squares curve fitting approach was used to fit the model, given by equation (5), to the measured envelope transfer characteristic, and hence determine the coefficients α_1, α_3 and α_5 for each case. A typical comparison of the measured and modeled envelope transfer function; $|\hat{I}_{2,rf}(t)|$ versus $|\hat{V}_{1,rf}(t)|$ is shown in Fig. 8. The results in this case also confirm that the DUT has very little observable memory.

Fig. 8 shows the resulting spectral contributions of each component generated by the current model. The labels shown on the spectral graph are the corresponding computed output power levels. The maximum power level of the out-of-band distortion, in this un-linearised 1.5 dB compressed case, can be seen to be -12 dBc. Note this is the result obtained when $\beta_2 = 0$ and $\beta_4 = 0$, the reference baseband short circuit case.

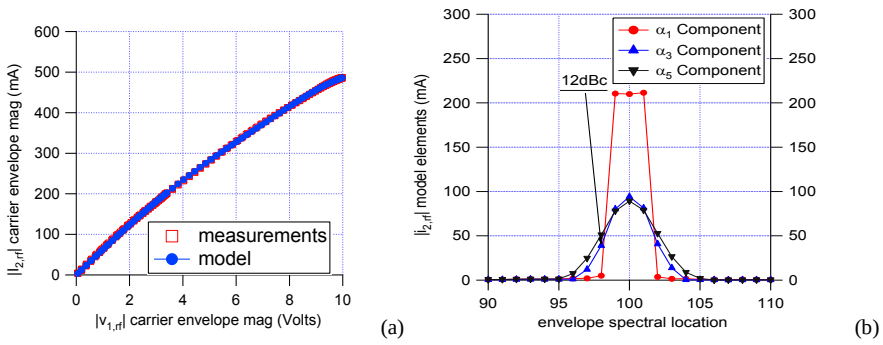

Fig 8. Comparison of the measured and modeled envelope transfer (a) function for the case $V_{2,bb}(t) = 0$. Also shown is the spectral contribution (b) of the individual model components, . $\alpha_3 = -0.2, \alpha_5 = 0.0008$

To investigate how effective precisely engineered baseband voltages can be in linearizing the device, a sequence of measurements was performed; sweeping the baseband voltage waveform describing coefficients β_2 and β_4 over a selected range, thus systematically varying the injected voltage waveform. The variation of the level of observed distortion in the measured fundamental transfer characteristic was then determined. The measured observed variations of the third order distortion term α_3 and fifth order distortion term α_5, were plotted as various contours plots as shown in Fig. 9 – 12.

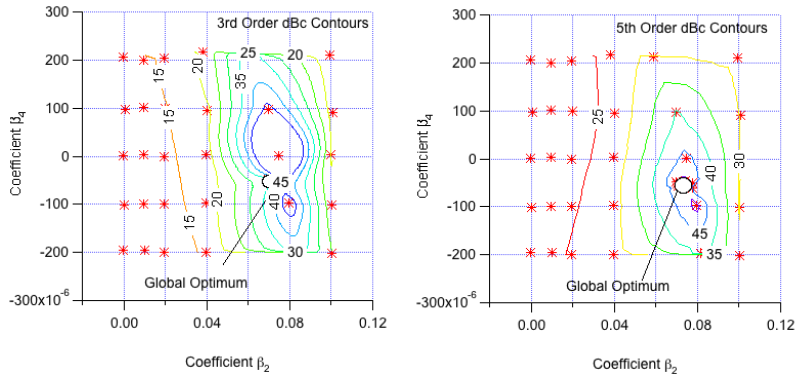

Fig 9. Contour plots of measured third order term α_3 and fifth order term α_5 values as a function of swept β_2 and β_4.

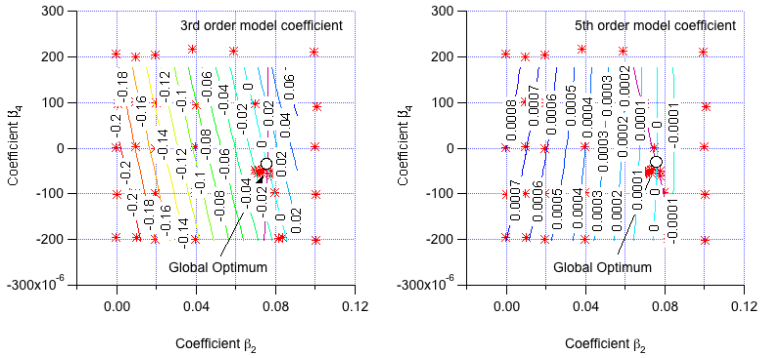

Fig 10. Contour plots of measured third order term α_3 and fifth order term α_5 values as a function of swept β_2 and β_4.

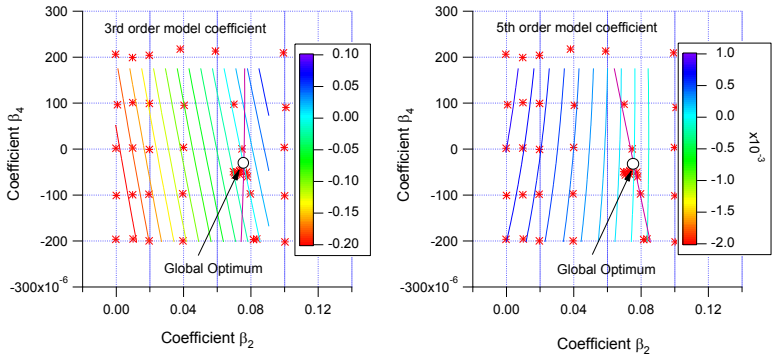

Fig 11. Contour plots of measured third order term α_3 and fifth order term α_5 values as a function of swept β_2 and β_4.

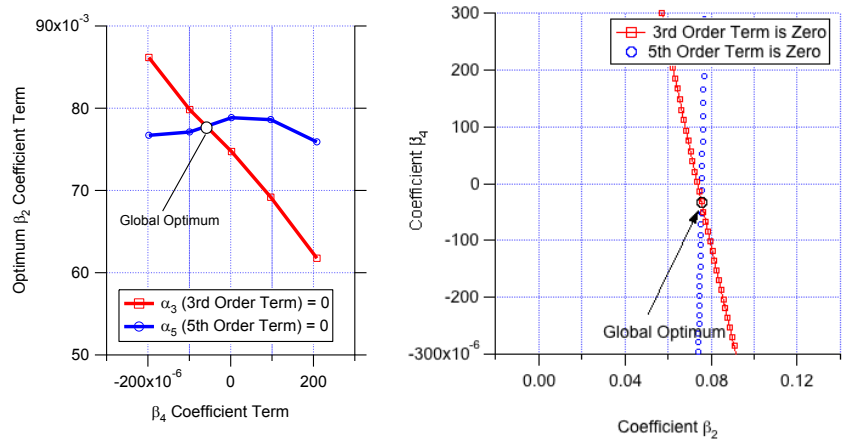

Fig 12. Contour plots of measured third order term α_3 and fifth order term α_5 values as a function of swept β_2 and β_4.

The contour plots in Fig. 9 show the level of suppression, Fig. 10 show the values of the linearizing coefficients around the suppression levels and Fig. 11 show a unified contour-point plot for clarity. All three plots indicate that there is an optimum set of values for β_2 and β_4 that can simultaneously satisfy the condition $\alpha_3 = 0$ and the condition $\alpha_5 = 0$. Fig. 12 however, shows the global optimum-point where simultaneous suppression occurs. In other words, there is a baseband voltage waveform, that when injected into the device output, will linearize the device.

VI. LINEARISED PERFORMANCE

The measurement system was now configured to demonstrate engineered baseband linearization. Using the optimum values determined above, the required 'linearizing" output baseband voltage was computed using equation (6). This computed target waveform along with the measured output baseband voltage waveform achieved are shown in Fig 13, indicating the ability of the system to correctly identify and engineer the required

baseband voltage signal. The corresponding measured value of the baseband current $I_{2,bb}(t)$ defined by equation (10) is also shown. Note, the current and voltage variations are in phase, indicating that this condition would in practice require an active envelope tracking (ET) type of drain bias. This is interesting as it raises the possibility of improving efficiency and linearity simultaneously [9]. The 'zoom-in' plot also show, that the measured and the target time varying baseband voltage $V_{2,bb}(t)$ have considerable agreement. Secondly, that the measured baseband current $I_{2,bb}(t)$ has maintained the same form as the agreeing voltages.

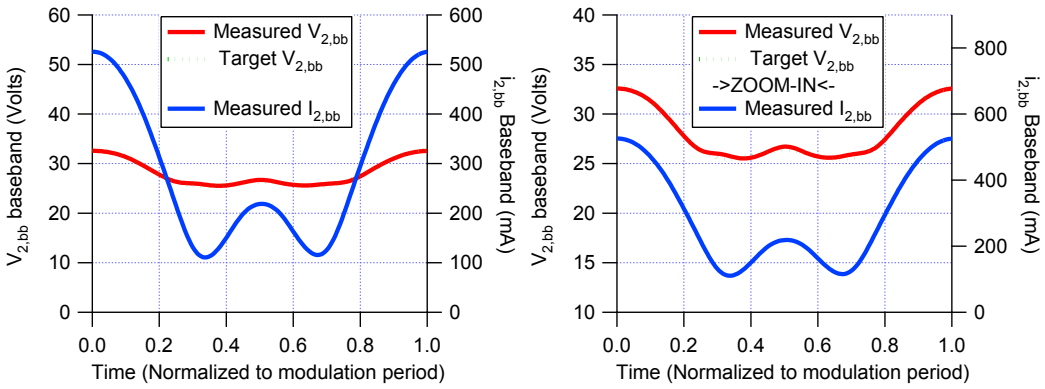

Fig. 13. Measured baseband output current (blue), ideal (green) and measured (red) optimum output baseband linearizing voltage waveform and depicting ET type formation.

$$I_{2,bb}(t) = \sum_{n=1}^{m} \alpha_{2n} \left|\hat{V}_{1,rf}(t)\right|^{2n} \qquad (10)$$

The linearizing baseband voltage signal was applied and the resulting, now linear transfer characteristic is shown in Fig. 14. Again the spectral contribution of each component generated by the current model obtained in this state is also shown.

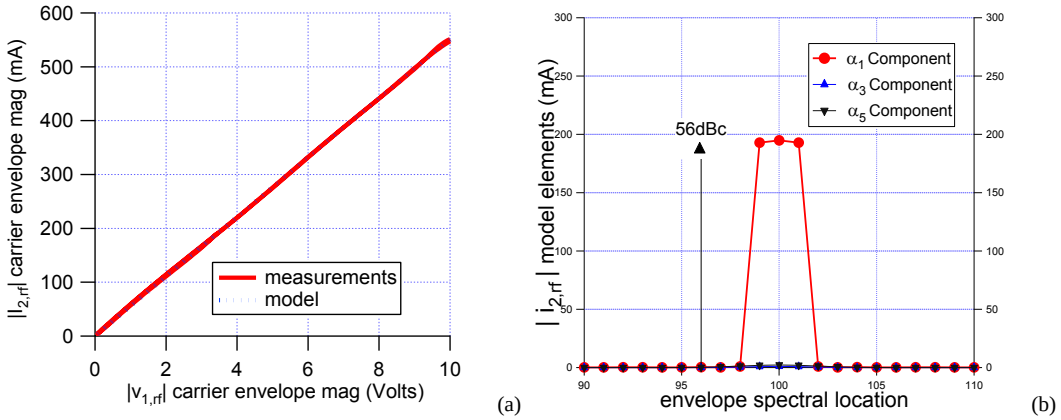

Fig. 14. Comparison of the measured and modeled envelope transfer function (a), for the optimum $V_{2,bb}(t)$ case. Also shown is the spectral contribution (b), of the individual model components. $\alpha_3 = \alpha_5 = 0, \beta_2 = 0.076, \beta_4 = -0.000033$

In this case both the third order and fifth order IMD contributions are now reduced to below -56dBc, which is an improvement of 42dBc over the reference, baseband short circuit solution. The actual measured input and output power spectra around the carrier are shown in Fig. 15.

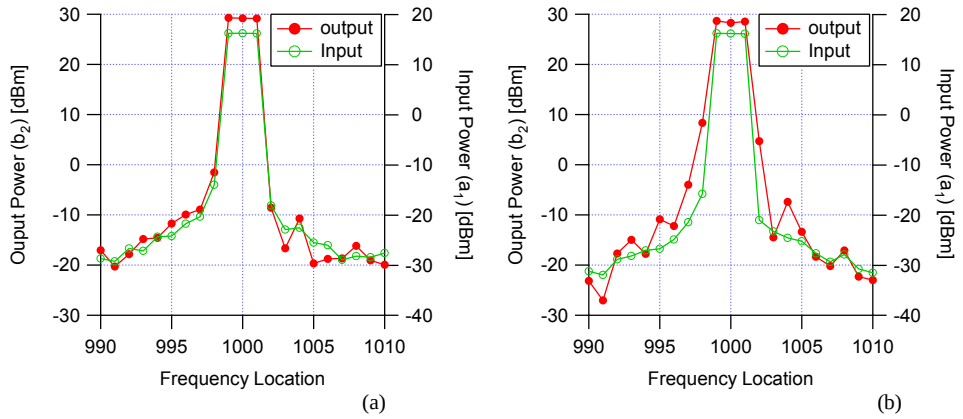

Fig. 15. Measured input and output power spectra around the carrier at linear (a) and baseband short circuit (b) states.

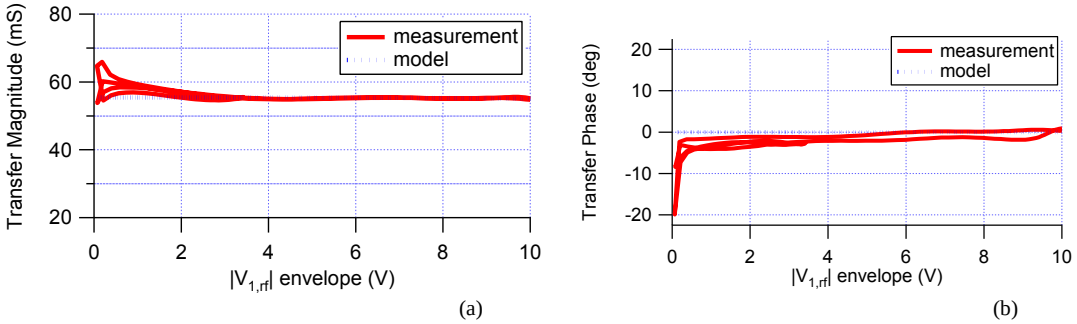

Fig. 16. Measured transfer magnitude (a) and phase (b) of the fundamental input voltage $\breve{V}_{1,rf}(t)$ envelope at the linear state.

It is important to realize that the plot in Fig. 15 shows that the modulated excitation being used to excite the device is certainly not perfect, and contains significant distortion, mostly due to the driver amplifier being used. As both axis cover 60dB dynamic range, it is still effective in showing however that no detectable, additional distortion is being introduced by the baseband signal being used to linearise the device. Shown in Fig. 16 are the plots of the measured transfer magnitude and phase of $\breve{V}_{1,rf}(t)$ envelope at the linear state also showing considerable linearity.

VII. Conclusion

A formulation and technique for defining linearising baseband injection signals of RFPA devices under arbitrary modulation in the AM/AM environment, with the ability to enable automatic engineering of specific baseband voltages, that when injected into the output port of a device causing the device to linearise has been demonstrated.

This functionality is achieved using a formulation, generalized in the envelope domain, which can be used to describe the required "linearizing" baseband injection signal, for an arbitrary amplitude modulated envelope, using a limited set of coefficients. The ability of the approach to simultaneously minimize both third and fifth order distortion terms was demonstrated using a 3-tone modulated signal, where the optimum baseband signal voltage for third and fifth order IMD suppression was successfully determined and then used to linearize the device.

This knowledge can be useful in the design of amplifier bias network at baseband frequency on device performance. As at the time of this submission, this approach has been successfully applied to further linearise, a 3-tone, 5-tone and 9-tone modulation. In addition, it has been used to linearise a modulation bandwidth of 20MHz on a 3-tone system in steps of 2MHz. It has also been used to linearise a HV-LDMOS, GaAs and Nitronex devices. Hence we believe it can be applied to both arbitrary modulation and arbitrary modulation bandwidth and arbitrary RFPA device.

Further work is now planned to use this system to show that this approach can be applied to AM/PM environment and subsequently used in a real base-station network.

ACKNOWLEDGEMENT

This work is supported by EPSRC (grant EP/F033702/1). We also thank CREE for supplying devices and specifically Simon Wood, Ryan Baker and Ray Pengelly.

REFERENCES

[1] Andrei Grebennikov, “RF and Microwave Power Amplifier Design”. McGraw-Hill ISBN 0-07-144493-9

[2] Joel Vuolevi and Timo Rahkonen,” Distortion in RF Power Amplifiers”, Norwood, MA: Artech House, 2003.

[3] John Wood, David E. Root, “Fundamentals of nonlinear behavioral modeling for RF and microwave design”. Artech House, 2005.

[4] J. C. Pedro, N. B. Carvalho, “Intermodulation Distortion in Microwave and Wireless Circuits” Artech House, 2003.

[5] Chi-Shuen Leung, Kwok-Keung, M. Cheng, “A new approach to amplifier linearization by the generalized baseband signal injection method,” IEEE microwave and wireless components letters, vol. 12, no.9, September, 2002.

[6] Lei Ding, G. Tong Zhou. “Effects of Even-Order Nonlinear Terms on Power Amplifier Modelling and Predistortion Linearization”. IEEE Transactions On Vehicular Technology, Vol. 53, No. 1, January 2004.

[7] Vincent W. Leung, Junxiong Deng, Prasad S. Gudem, and Lawrence E. Larson. “Analysis of Envelope Signal Injection for Improvement of RF Amplifier Intermodulation Distortion”, IEEE Journal of solid-state circuits, vol. 40, no. 9, September 2005

[8] Akmal, M.; Lees, J.; Jiangtao, S.; Carrubba, V.; Yusoff, Z.; Woodington, S.; Benedikt, J.; Tasker, P.J.; Bensmida, S.; Morris, K.; Beach, M.; McGeehan, J., "An enhanced modulated waveform measurement system for the robust characterization of microwave devices under modulated excitation," *Microwave Integrated Circuits Conference (EuMIC), 2011 European* , vol., no., pp.180,183, 10-11 Oct. 2011

[9] Akmal, M.; Carrubba, V.; Lees, J.; Bensmida, S.; Benedikt, J.; Morris, K.; Beach, M.; McGeehan, J.; Tasker, P.J., "Linearity enhancement of GaN HEMTs under complex modulated excitation by optimizing the baseband impedance environment," *Microwave Symposium Digest (MTT), 2011 IEEE MTT-S International* , vol., no., pp.1,4, 5-10 June 2011. doi: 10.1109/MWSYM.2011.5972833

[10] Akmal, M.; Ogboi, F.L.; Yusoff, Z.; Lees, J.; Carrubba, V.; Choi, H.; Bensmida, S.; Morris, K.; Beach, M.; McGeehan, J.; Benedikt, J.; Tasker, P.J., "Characterization of electrical memory effects for complex multi-tone excitations using broadband active baseband load-pull," *Microwave Conference (EuMC), 2012 42nd European* , vol., no., pp.1265,1268, Oct. 29 2012-Nov. 1 2012

[11] Akmal, M.; Lees, J.; Bensmida, S.; Woodington, S.; Carrubba, V.; Cripps, S.; Benedikt, J.; Morris, K.; Beach, M.; McGeehan, J.; Tasker, P.J., "The effect of baseband impedance termination on the linearity of GaN HEMTs," *Microwave Conference (EuMC), 2010 European* , vol., no., pp.1046,1049, 28-30 Sept. 2010

[12] Akmal, M.; Lees, J.; Bensmida, S.; Woodington, S.; Benedikt, J.; Morris, K.; Beach, M.; McGeehan, J.; Tasker, P.J., "The impact of baseband electrical memory effects on the dynamic transfer characteristics of microwave power transistors," *Integrated Nonlinear Microwave and Millimeter-Wave Circuits (INMMIC), 2010 Workshop on* , vol., no., pp.148,151, 26-27 April 2010 doi: 10.1109/INMMIC.2010.5480111

[13] Akmal, M.; Lees, J.; Carrubba, V.; Bensmida, S.; Woodington, S.; Benedikt, J.; Morris, K.; Beach, M.; McGeehan, J.; Tasker, P.J., "Minimization of baseband electrical memory effects in GaN HEMTs using active IF load-pull," *Microwave Conference Proceedings (APMC), 2010 Asia-Pacific* , vol., no., pp.5,8, 7-10 Dec. 2010

[14] Benedikt, J.; Tasker, P.J., "High-power time-domain measurement bench for power amplifier development," *ARFTG Conference Digest,Fall2002.60th*,vol.,no.,pp.107,110,5-6Dec.2002, doi: 10.1109/ARFTGF.2002.1218692

[15] Lees, J.; Akmal, M.; Bensmida, S.; Woodington, S.; Cripps, S.; Benedikt, J.; Morris, K.; Beach, M.; McGeehan, J.; Tasker, P., "Waveform engineering applied to linear-efficient PA design," *Wireless and Microwave Technology Conference (WAMICON), 2010 IEEE11thAnnual*,vol.,no.,pp.1,5,12-13April2010 doi: 10.1109/WAMICON.2010.5461847

[16] Lees, J.; Williams, T.; Woodington, S.; McGovern, P.; Cripps, S.; Benedikt, J.; Tasker, P., "Demystifying Device related Memory Effects using Waveform Engineering and Envelope Domain Analysis," *Microwave Conference, 2008. EuMC 2008. 38th European* , vol.,no.,pp.753,756,27-31Oct.2008doi: 10.1109/EUMC.2008.4751562

[17] Ogboi, F.L.; Tasker, P.J.; Akmal, M.; Lees, J.; Benedikt, J.; Bensmida, S.; Morris, K.; Beach, M.; McGeehan, J., "A LSNA configured to perform baseband engineering for device linearity investigations under modulated excitations," *Microwave Conference (EuMC), 2013 European* , vol., no., pp.684,687, 6-10 Oct. 2013

[18] Tasker, P.J., "RF Waveform Measurement and Engineering," *Compound Semiconductor Integrated Circuit Symposium, 2009. CISC 2009.AnnualIEEE*vol.,no.,pp.1,4,11-14Oct.2009doi: 10.1109/csics.2009.5315818

[19]Tasker,P.J.,"Practical waveform engineering," *Microwave Magazine,IEEE*,vol.10,no.7,pp.65,76,Dec.2009 doi: 10.1109/MMM.2009.934518

[20] Tasker, P.J., "Non-linear characterisation of microwave devices," *High Performance Electron Devices for Microwave and OptoelectronicApplications,1999.EDMO.1999Symposiumon*,vol.,no.,pp.147,152,1999 doi: 10.1109/EDMO.1999.821476

[21] Tasker, P.J.; Reinert, W.; Braunstein, J.; Schlechtweg, M., "Direct Extraction of All Four Transistor Noise Parameters from a Single Noise Figure Measurement," *Microwave Conference, 1992. 22nd European* , vol.1, no., pp.157,162, 5-9 Sept. 1992 doi: 10.1109/EUMA.1992.335733

[22] Williams, D.J.; Leckey, J.; Tasker, P.J., "Envelope domain analysis of measured time domain voltage and current waveforms provide for improved understanding of factors effecting linearity," *Microwave Symposium Digest, 2003 IEEE MTT-S International* , vol.2, no., pp.1411,1414vol.2,8-13June2003doi: 10.1109/MWSYM.2003.1212636

[23] Williams, D.J.; Leckey, J.; Tasker, P.J., "A study of the effect of envelope impedance on intermodulation asymmetry using a two-tone time domain measurement system," *Microwave Symposium Digest, 2002 IEEE MTT-S International* , vol.3, no., pp.1841,1844 vol.3, 2-7June2002doi: 10.1109/MWSYM.2002.1012221

[24] Williams, D.; Tasker, P.J., "Thermal parameter extraction technique using DC I-V data for HBT transistors," *High Frequency PostgraduateStudentColloquium,2000*,vol.,no.,pp.71,75,2000doi: 10.1109/HFPSC.2000.874085

[25] Williams, D.J.; Tasker, P.J., "An automated active source and load pull measurement system," *High Frequency Postgraduate Student Colloquium,2001.6thIEEE*,vol.,no.,pp.7,12,2001doi: 10.1109/HFPSC.2001.962150

[26] Z. Yusoff, J. Lees, J. Benedikt, P.J. Tasker, S.C. Cripps, "Linearity improvement in RF power amplifier system using integrated Auxiliary Envelope Tracking system," *IEEE MTT-S Int. Microw. Symp. Dig.*, 2011, vol., no., pp.1-4, 5-10 June 2011.

†Sensitivity of AM/AM linearizer to AM/PM distortion in devices.

F.L. Ogboi†, P. Tasker†, Z. Mohkti†, J. Lees†, J. Benedikt†, S. Bensmida*, K. Morris*, M. Beach*, J. McGeehan*

†Centre for High Frequency Engineering, Cardiff University, The Parade, Cardiff, CF24 3AA, UK

*Centre for Communications Research, University of Bristol, Woodland Road, Bristol, BS8 1UB, UK

†Tel: +44 7531951316, †Email: ogboifl2@Cardiff.ac.uk

Abstract — Baseband injection is a technique that can provide a cost-effective linearizing solution that can be combined with supply modulation techniques such as envelope tracking (ET), to minimize AM/AM distortion and potentially simplify the DSP linearization requirement and associated cost. Recently [8], a new approach for computing the baseband injection stimulus, formulated in the envelope domain, was introduced. The concept was originally demonstrated using a 10W Cree GaN-on-SiC HFET device. In this work its robustness with respect to alternative device technology is investigated using 25W Nitronex NPTB00025 GaN-on-SiC HEMT depletion-mode and a 10W, high-voltage LD-MOS, enhancement-mode devices. Its effectiveness in dealing with AM/AM distortion is confirmed.

Index Terms — Distortion, Modulation, Multi-tone, Power amplifiers, signal.

I. Introduction

Active devices and amplifiers used in the wireless communication industry exhibit non-linear behavior, leading to distortion and reduced linearity [1]-[2]. Typically the power amplifier (PA) is designed targeting the RF power and efficiency specifications while Digital Signal Pre-distortion (DSP) addresses the linearity requirement. However, because of the relatively high power consumption of DSP systems in small-cell architectures, this architecture may be viable in future systems where the trend is increasing modulation bandwidths coupled with the scaling back of RF output power. Baseband injection is a technique that could provide a cost-effective aid by minimizing power amplifier AM/AM distortion, thus simplifying DSP linearization requirement, complexity [3]-[7] and hence power consumption. It can also be combined with supply modulation techniques such as envelope tracking (ET). Recently, a baseband linearization formulation, generalized in the envelope domain, was demonstrated [8]. The beauty of the approach lies in its scalability to different modulated excitations and applicability to different device technologies. It is the latter that is studied in this paper.

II. Baseband Signal Formulation

Consider the behavior of a non-linear power transistor subjected to a modulated RF carrier stimulus at its input.

$$V_{1,rf}(t) = \frac{\hat{V}_{1,rf}(t)e^{j\omega_c t} + \hat{V}_{1,rf}(t)^* e^{-j\omega_c t}}{2}. \quad (1)$$

where $\hat{V}_{1,\mathrm{rf}}(t)$ is the input carrier voltage envelope and ω_c is the RF carrier frequency.

The RF output carrier current response of the device is given as follows:

$$I_{2,rf}(t) = \frac{\hat{I}_{2,rf}(t)e^{j\omega_c t} + \hat{I}_{2,rf}(t)^* e^{-j\omega_c t}}{2}. \quad (2)$$

Assuming that the transistor is a memory-less non-linear system the envelope transfer characteristic can be modeled as follows:

$$\hat{I}_{2,rf}(t) = \sum_{n=0}^{m} \alpha_{2n+1} \left|\hat{V}_{1,rf}(t)\right|^{2n} \hat{V}_{1,rf}(t). \quad (3)$$

where α_1 represents the linear gain of the system, α_3 quantifies the level of third order intermodulation distortion, α_5 quantifies the level of fifth order intermodulation distortion, and so on, up to the desired maximum order m.

In [8], an envelope formulation for the output baseband voltage envelope signal $\hat{V}_{2,\mathrm{bb}}(t)$ was introduced, as follows:

$$\hat{V}_{2,bb}(t) = \sum_{p=1}^{q} \beta_{2p} \left|\hat{V}_{1,rf}(t)\right|^{2p}. \quad (4)$$

where β_{2p} are the even order voltage component scaling coefficients and q specifies the selected maximum range; bandwidth. The motivation for using this formulation lies in the fact that only cancelling odd-order intermodulation terms will be added to the RF output current envelope response. Hence, only the coefficients in (3) will be modified such that

$$\alpha_{2n+1}|_{n=1}^{m} = f\left(\beta_2, \beta_4, \ldots \beta_{2p}, \ldots \beta_{2q}\right). \quad (5)$$

Optimizing baseband linearization requires the determination of the coefficients β_{2p} that set $\alpha_{2n+1}|_{n=1}^{m} = 0$, independent of signal complexity and device technology.

III. Measurement System

In this paper we will confine analysis to addressing systems with intermodulation distortion up to fifth order (m=2). The baseband linearization range will now be restricted to forth order (q=2), hence equating to determining the values of β_2 and β_4 that can simultaneously set $\alpha_3 = 0$ and $\alpha_5 = 0$. This was performed using the measurements system shown in Fig.

978-1-4799-4423-1/14/$31.00 ©2014 IEEE

1, a fully vector-error corrected modulated LSNA-based measurement system integrated with both RF fundamental and harmonic load-pull and baseband signal injection.

All the measurements are calibrated to the device package plane using a custom built 50 Ω TRL test fixture. The calibration extended over a wide bandwidth, precisely 50MHz baseband bandwidth and 100MHz RF bandwidth for each of the first three harmonics. A modulated 3-tone excitation centered at 2 GHz, with 2MHz tone spacing and PAPR of 4.77dB was used with fundamental and all harmonic frequencies terminated into a passive 50Ω load environment.

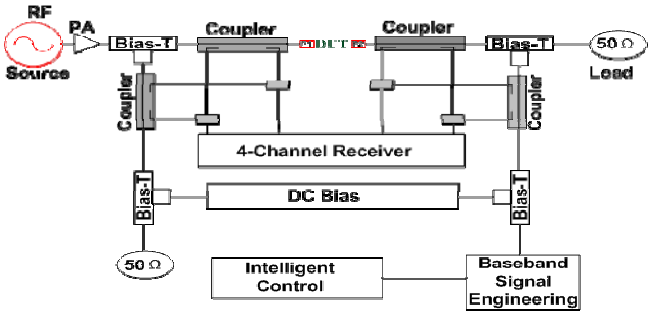

Fig. 1. Baseband waveform engineering and modulated RF measurement system

IV. Technology Nonlinear Behaviour

Two device technologies were investigated; a 25W Nitronex NPTB00025 GaN-on-SiC HFET depletion-mode device, and a 10W, high-voltage LD-MOS, enhancement-mode device. The Nitronex device was biased at a drain voltage of +28V and a gate voltage of -1.3V, and the LDMOS device was biased at +32V drain voltage and +2.8V gate voltage targeting class AB operation on both devices and giving a quiescent current of 12% of I_{DSmax}. They were then both driven into 2.4dB compression, with the output terminated into passive 50 Ohms. The LDMOS device giving a peak envelope power (PEP) of approximately 33dBm and the 25W GaN-on-SiC HFET device, a peak envelope power PEP of 40dBm. Reference conditions were established with baseband output voltage set to zero (reference baseband short circuit state) and are shown in Fig. 2 and 3. Results indicate a non-well behaved AM/PM (green curve) distortion in the 10W LDMOS device and 7th order distortion. A well behaved AM/PM (green curve) distortion in the 25W GaN-on-SiC HFET with only 5th order distortion present.

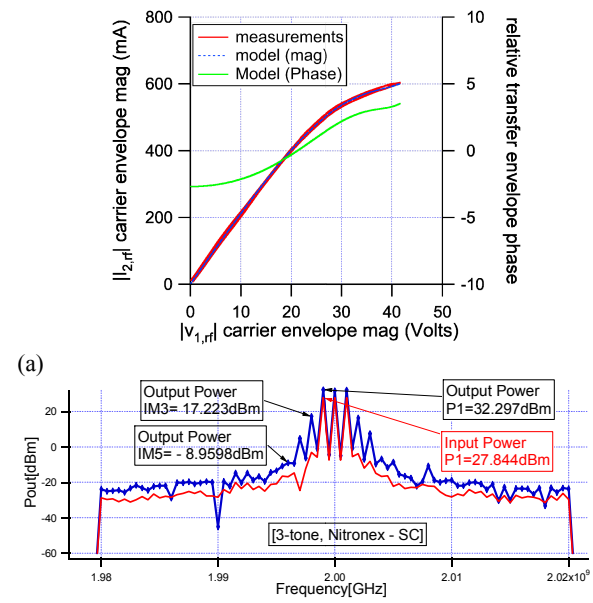

Fig. 2 25W GaN-on-SiC HFET Device: Measured reference baseband short circuit state. (a) Dynamic transfer characteristic and (b) Power Spectra.

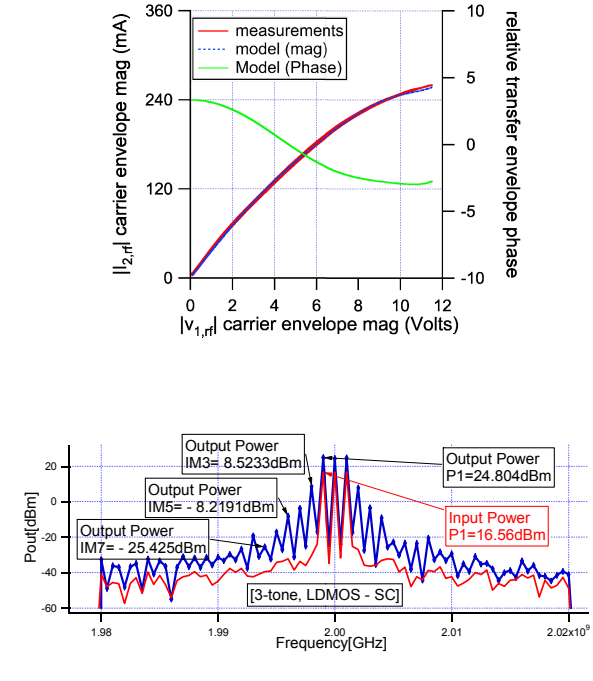

Fig. 3. LDMOS device: Measured reference baseband short circuit state. (a) Dynamic transfer characteristic and (b) Power Spectra.

V. Linearization Results Analysis

The optimized baseband injection signal was determined by adjusting the values of β_2 and β_4 in order to simultaneously

minimize α_3 and α_5. The results achieved are shown in Fig. 2 to 5. In the case of the 25W GaN-on-SiC HFET the results clearly show that this device was successfully linearized with respect to AM/AM. This is shown by the red (AM/AM) and blue (model defined by β_2 and β_4) curve on the dynamic transfer characteristic of Fig.4a, a considerable agreement. The green curve on the same figure, show the strong presence but a very well behaved AP/PM distortion. A result similar to that previously reported on the 10W GaN-on SiC HFET device [8]. However, in this case only modest overall linearity improvement of 13.62dBc in IM3 with the IM5 2.56dBc from the noise-floor were achieved. We believe that this level of AM/PM distortion, insensitive to baseband injection, observed in this device explains this limited overall improvement in linearity.

In the case of the 10W LDMOS, elimination of the AM/AM distortion was not completely possible. Hence, only an improvement of 10dBc was achieved in IM3 and none on IM5 on this device. This is because this device exhibited a non-well behaved AM/PM distortion, shown by the green curve on the dynamic transfer characteristics of Fig. 3a and 5a. Also a strong presence of the 7th, order term, shown in Fig.3b and 5b respectively. These cannot be addressed using only two β_{2p} even order voltage component scaling coefficients (meant for 3rd and 5th order term) nor AM/AM distortion canceller. However, the model defined by the coefficients and the AM/AM curve in these figures all agree, confirming AM/AM distortion mitigation effectiveness.

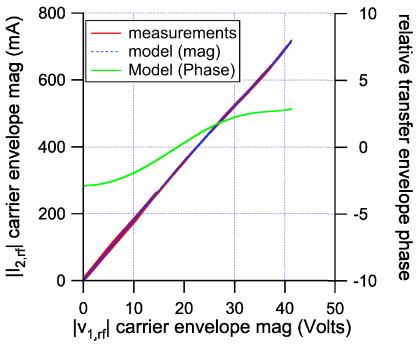

(a)

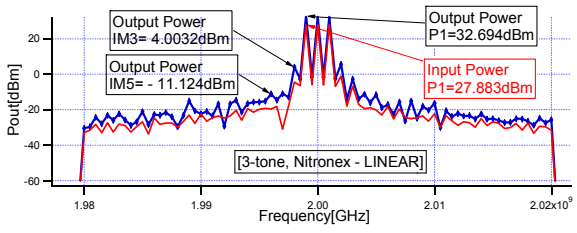

(b)

Fig. 4 25W GaN-on-SiC HFET Device: Measured linear state. (a) Dynamic transfer characteristic and (b) Power Spectra.

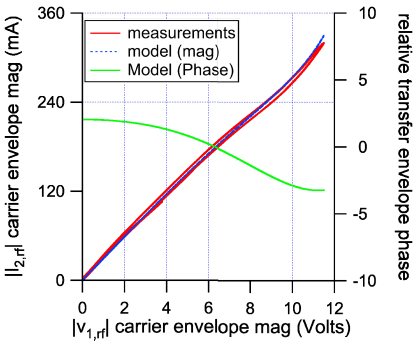

(a)

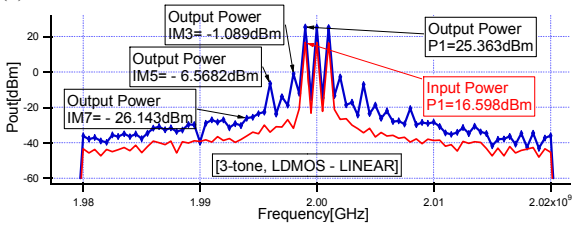

(b)

Fig. 5. LDMOS device: Measured linear state. (a) Dynamic transfer characteristic and (b) Power Spectra.

VI. Conclusion

The robustness with respect to device technology of an envelope domain formulation which describes the baseband injection signal required to minimize the AM/AM distortion has been investigated. In both device technology investigated the formulation was able to minimize AM/AM distortion, hence confirming it would be a useful tool to use in conjunction with DSP. However, the need to use a more complex signal for higher than 5th order distortion was shown. Also, as expected, baseband injection has no impact on AM/PM distortion.

Importantly, this experiment confirmed [8] AM/AM efficacy, in the presence of severe AM/PM distortion.

New work on [8] is now planned to cost effectively suppress AM/AM, AM/PM distortions and also improve device efficiency.

Acknowledgement

This work has been carried out as part of EPSRC grant EP/F033702/1. The authors would also like to thank CREE for supporting this activity and supplying the devices; specifically Ray Pengelly and Mr. Simon Wood.

References

[1] Andrei Grebennikov, “RF and Microwave Power Amplifier Design”. McGraw-Hill ISBN 0-07-144493-9

[2] John Wood, David E. Root, “Fundamentals of nonlinear behavioral modeling for RF and microwave design”. Artech House, 2005.S Int. Microwave Symp. Dig., vol. 3, pp. 1721-1724, June 2003.

[3] Boumaiza, S.; Mkadem, F.; Ben Ayed, M., "Digital predistortion challenges in the context of software defined transmitters," General Assembly and Scientific Symposium, 2011 XXXth URSI , vol., no., pp.1,4, 13-20 Aug. 2011 doi: 10.1109/URSIGASS.2011.6050519

[4] Abd-Elrady, E., "A Recursive Prediction Error algorithm for digital predistortion of FIR Wiener systems," Communication Systems, Networks and Digital Signal Processing, 2008. CNSDSP 2008. 6th International Symposium on , vol., no., pp.698,701, 25-25 July 2008 doi: 10.1109/CSNDSP.2008.4610732

[5] Salkintzis, A.K.; Hong Nie; Mathiopoulos, P.T., "ADC and DSP challenges in the development of software radio base stations," Personal Communications, IEEE , vol.6, no.4, pp.47,55, Aug 1999, doi: 10.1109/98.788215

[6] Mehendale, M., "Challenges in the design of embedded real-time DSP SoCs," VLSI Design, 2004. Proceedings. 17th International Conference on , vol., no., pp.507,511, 2004 doi: 10.1109/ICVD.2004.1260971

[7] Mitra, B., "Consumer digitization: accelerating DSP applications, growing VLSI design challenges," Design Automation Conference, 2002. Proceedings of ASP-DAC 2002. 7th Asia and South Pacific and the 15th International Conference on VLSI Design. Proceedings. , vol., no., pp.3,4, 2002, doi: 10.1109/ASPDAC.2002.994869

[8] Ogboi, F.L.; Tasker, P.J.; Akmal, M.; Lees, J.; Benedikt, J.; Bensmida, S.; Morris, K.; Beach, M.; McGeehan, J., "A LSNA configured to perform baseband engineering for device linearity investigations under modulated excitations," Microwave Conference (EuMC), 2013 European , vol., no., pp.684,687, 6-10 Oct. 2013

High bandwidth investigations of a baseband linearization approach formulated in the envelope domain under modulated stimulus

F.L. Ogboi, P.J. Tasker, M. Akmal, J. Lees, J. Benedikt
Centre for High Frequency Engineering
Cardiff University
Cardiff, United Kingdom
ogboifl2@cardiff.ac.uk

S. Bensmida, K. Morris, M. Beach, J. McGeehan
Centre for Communications Research
University of Bristol
Bristol, United Kingdom

***Abstract*— Baseband injection provides a useful approach for use in linearizing power amplifiers. The challenge is the determination of the required baseband signal. In [6] a generalized formulation quantifying the baseband voltage signal, injected at the output bias port, to linearize the device behavior was introduced. This envelope domain based solution requires the determination of only a small number of linearizing coefficients. More importantly these coefficients should be stimulus, hence bandwidth independent. This property has been experimentally investigated using a 10W Cree GaN HEMT device under a 3-tone modulated stimulus at 1.5dB of compression. It will be shown that the linearization coefficients were invariant when varying the modulation bandwidth from 2MHz to 20MHz.**

Keywords—bandwidth; modulation; independence; distortion

I. INTRODUCTION

The non-linear behavior of transistors used in wireless communication systems, power amplifiers, degrades system performance by generating out-of-band intermodulation distortion products. The third and fifth order terms typically dominate. Thus to meet the systems spectral mask requirements power amplifiers must be linearized. A number of approaches have been suggested and used e.g. analog pre-distortion, digital pre-distortion, feed-forward techniques and others described in [1-5]. Linearization can also be achieved by injecting an appropriately engineered baseband signal at the output bias port. System architectures that integrated modulation of the output bias port are presently being robustly investigated and developed, envelope-tracking systems, mainly focused on improving efficiency.

In [6] a mathematical description of the required output baseband signal necessary to linearize the transistor was presented and validated. It defines the baseband envelope as a function of the input carrier signal envelope. Linearization just requires the determination of a small number of linearization coefficients. A key implication is that these coefficients should be independent of the modulation envelope and bandwidth.

This work is supported by EPSRC (grant EP/F033702/1). We also thank CREE for supplying devices and specifically Simon Wood, Ryan Baker and Ray Pengelly.

This paper confirms the bandwidth independence of this formulation, when used with baseband injection to linearize a transistor when the modulation bandwidth is varied from 2MHz to 20MHz.

II. BANDWIDTH CONSIDERATIONS

Consider now, a RF modulated system with a modulated envelope given by E(t) having a bandwidth $\Delta\omega$. In this investigation we will consider a 3-tone modulated stimulus with δ tone spacing, hence $\Delta\omega = 2\delta$. Signals produced by odd order intermodulation distortion (IMD) not only distort the in-band signal but also generate out of band components. The m^{th} odd order IMD term will increase the bandwidth to $m\Delta\omega$. If these terms are to be removed, cancelled, using pre-distortion, analogue or digital, the modulation bandwidth of the signal must now increase significantly and also become $m\Delta\omega$. So for a modulation signal of 20MHz bandwidth and considering distortion only up to 5^{th} order, this would require the pre-distorter and the power amplifier to have a modulation bandwidth of at least 100MHz.

In the case of baseband linearization the bandwidth of the RF modulated signal remains unchanged, however a modulated baseband signal is required. In [6] it was determined that this signal can be computed using the following expression;

$$\hat{V}_{2,bb}(t) = \sum_{p=1}^{q} \beta_{2p} |E(t)|^{2p} \quad (1)$$

The bandwidth of this signal is given by $2q\Delta\omega$. So for a modulation signal of 20MHz bandwidth and considering distortion only up to 5^{th} order, hence linearization can be achieved with q=2, a baseband signal with only an 80MHz is required. This reduced bandwidth requirement for baseband linearization compared to pre-distortion could become very significant in future communication systems requiring high modulation bandwidths >20MHz.

III. LINEARITY INVESTIGATIONS

To investigate the scaling up of baseband linearization to higher modulation bandwidths, the waveform measurement system described in [7] is utilized. This fully vector-error corrected measurement system is capable of measuring multiple-complex modulated voltage and current waveforms while 'engineering' and injecting intelligent baseband voltage signals into the device. This system has a 100MHz RF modulation bandwidth, but since the baseband bandwidth is also limited to 100MHz, linearization investigations are limited to RF modulated signal with bandwidths less than 25MHz.

In this investigation the modulation bandwidth of a 3-tone signal was varied from 2MHz to 20MHz in 2MHz steps. In all cases the PAPR of the 3-tone excitation was 4.77dB, the RF excitation was centered at 2GHz, while maintaining a constant peak envelope power of approximately 38dBm. This ensured that the device under test, a10W, CREE HFET, was driven to a compression level of approximately 1.5dB. The GaN device was biased in class AB, with RF fundamental and all harmonic frequencies terminated into a passive 50Ω. The drain and gate bias voltages of 28V and -2.08V respectively were used, giving a quiescent drain current of approximately 12% I_{DSS}, for each modulation bandwidth.

A. Baseband short circuit reference state results

Initially the non-linear behavior of the transistor is characterized in to a reference baseband output voltage envelope. The reference state is the classical, ideal, baseband short circuit condition. Results achieved are shown in Fig. 1, Fig. 2 and Fig. 3, for the 4MHz, 8MHz and 16MHz 3-tone stimuli respectively.

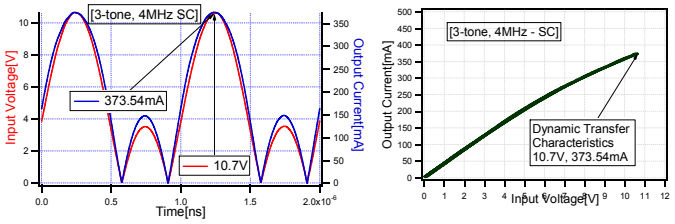

Fig. 1, Measured 4 MHz bandwidth 3-tone fundamental RF input voltage/output current envelopes and the determined, measured, 3-tone RF fundamental dynamic envelope transfer characteristic for the short circuit reference state.

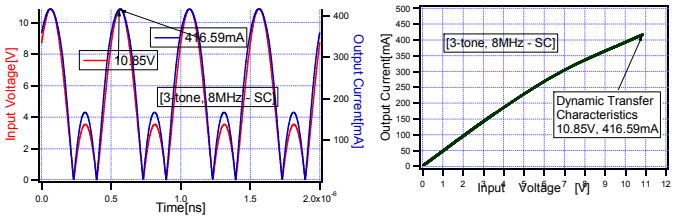

Fig. 2, Measured 8 MHz bandwidth 3-tone fundamental RF input voltage/output current envelopes and the determined, measured, 3-tone RF fundamental dynamic envelope transfer characteristic for the short circuit reference state.

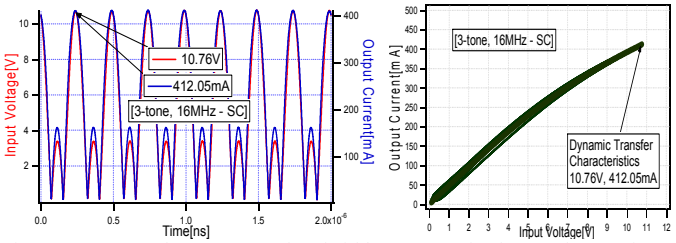

Fig. 3, Measured 16 MHz bandwidth 3-tone fundamental RF input voltage/output current envelopes and the determined, measured, 3-tone RF fundamental dynamic envelope transfer characteristic for the short circuit reference state.

The dynamic envelope transfer characteristic is modeled as follows:

$$\hat{I}_{2,rf}(t) = \sum_{n=0}^{m} \alpha_{2n+1} |E(t)|^{2n} E(t). \quad (2)$$

where α_1 represents the linear gain of the system, α_3 quantifies the level of third order intermodulation distortion, α_5 quantifies the level of fifth order intermodulation distortion, and so on, up to the desired maximum order m. In this case m=3 is sufficient, distortion up to fifth order, to fit the measured behavior and the coefficient values, α_{2n+1}, extracted are given in table 1.

Bandwidth	α_1	α_3	α_5
4MHz	44.47	-0.104	0.0002
8MHz	48.55	-0.122	0.0003
16MHz	48.67	-0.128	0.0003

TABLE 1. Coefficients describing the non-linearity of the observed dynamic envelope transfer characteristic measured as a function of increasing modulation bandwidth; baseband short circuit reference state.

These results clearly highlight, certainly over this bandwidth that the non-linear behavior of the transistor is modulation bandwidth invariant, this is consistent with our previous investigations [8]. This confirms the advantage of the formulations introduced in [6]. If the envelope transfer characteristic is stimulus invariant so should the linearizing baseband voltage envelope (1) coefficients be stimulus invariant.

B. Application of baseband linearization

The two, β_2 and β_4, optimized linearization coefficient, required to compute the necessary output baseband stimulus using (1), to linearize the transistor were now determined as in [6]. The values determined are summaries in table 2.

Bandwidth	β_2	β_4
4MHz	0.0178	-8.7e-5
8MHz	0.018	-9e-5
16MHz	0.018	-9e-5

TABLE 2. Optimized linearization coefficients determined as a function of increasing modulation bandwidth.

Fig. 4, Fig. 5 and Fig. 6, show the linearized performance achieved. In all cases the device has been successfully linearized. The dynamic envelope transfer characteristics becoming a straight line through the origin

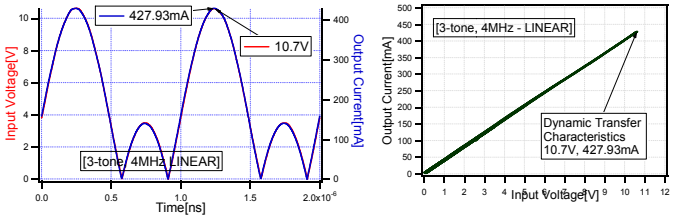

Fig. 4, Measured 4 MHz 3-tone fundamental RF input voltage/output current envelops achieved and linear, measured, 3-tone RF fundamental dynamic envelope transfer characteristic achieved using output baseband injection to linearize the system

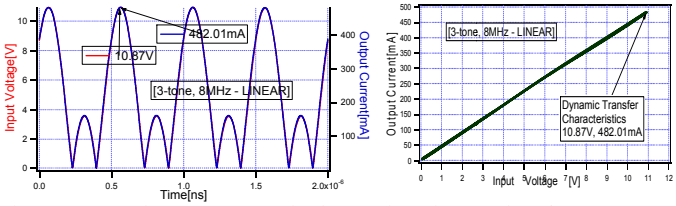

Fig. 5, Measured 8 MHz 3-tone fundamental RF input voltage/output current envelops achieved and linear, measured, 3-tone RF fundamental dynamic envelope transfer characteristic achieved using output baseband injection to linearize the system

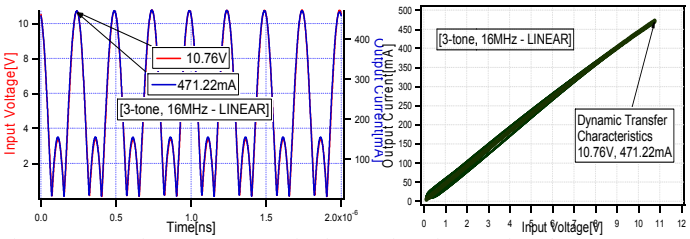

Fig. 6, Measured 16 MHz 3-tone fundamental RF input voltage/output current envelops achieved and linear, measured, 3-tone RF fundamental dynamic envelope transfer characteristic achieved using output baseband injection to linearize the system

This linearized performance was achieved for the entire 20MHz bandwidth investigated. Fig. 7 shows that the two, β_2 and β_4, optimized linearization coefficient, determined to achieve this level of linearization were basically constant over the entire 20MHz bandwidth.

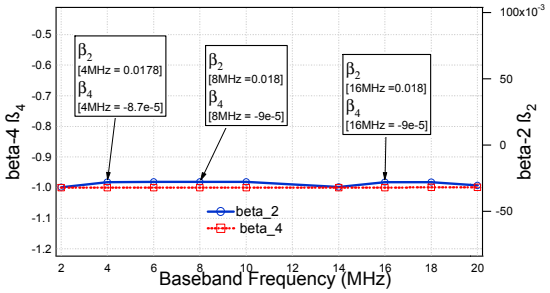

Fig. 7.Measured linearizing coefficients values over 20MHz bandwidth

C. *Spectral analysis*

More traditional this performance improvement is presented in terms of the minimizing the spectral regrowth.

Fig. 8, Fig. 9 and Fig. 10 show spectral performance improvements achieved in the case of 4MHz, 8MHz and 16MHz 3-tone stimulus respectively.

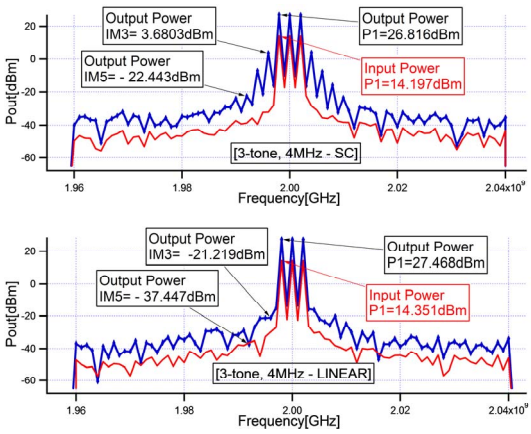

Fig. 8, Measured 4MHz 3-tone Spectrum before (a) and after (b) applying baseband linearization.

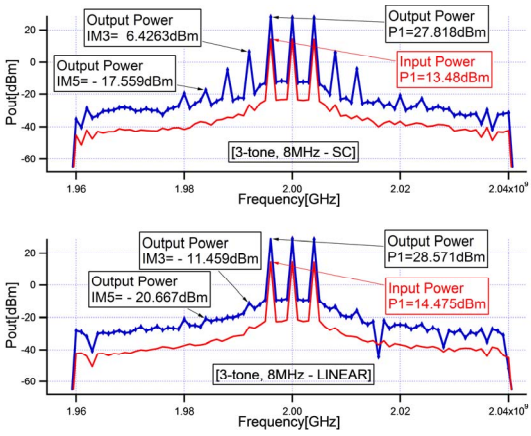

Fig. 9, Measured 8MHz 3-tone Spectrum before (a) and after (b) applying baseband linearization.

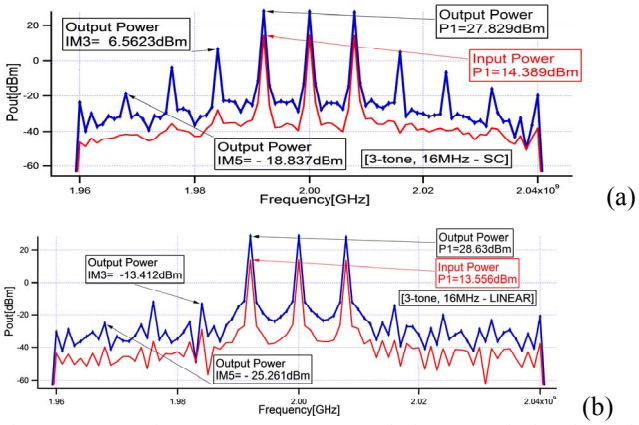

Fig. 10, Measured 16MHz 3-tone Spectrum before (a) and after (b) applying baseband linearization.

In all cases a very similar level of improvement is observed. Distortion in all cases is reduced to a level around -40dB, a value we believed is limited more by the dynamic range of the measurement system than the ability of the optimized baseband enveloped derived signal to linearize, eliminated the AM/AM distortion

A summary of the linearization and suppression achieved over the entire 20MHz bandwidth is shown in Fig. 11. In all cases the IM3 suppression was approximately 20dBc across-board. IM5 was successfully suppressed to the noise-floor of the measurement system.

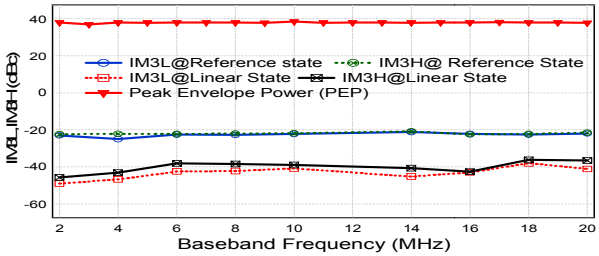

Fig. 11. Measured 20dBc suppression in IM3 over 20MHz tone spacing over the reference baseband short circuit state.

IV. BASEBAND LINEARIZATION AT HIGH BANDWIDTH

Fig. 12 shows that even in the case where the modulation bandwidth is 20MHz, hence the linearization bandwidth is now 80MHz, approaching the bandwidth of the measurement system harmonic suppression of down to -30dBc was still achieved.

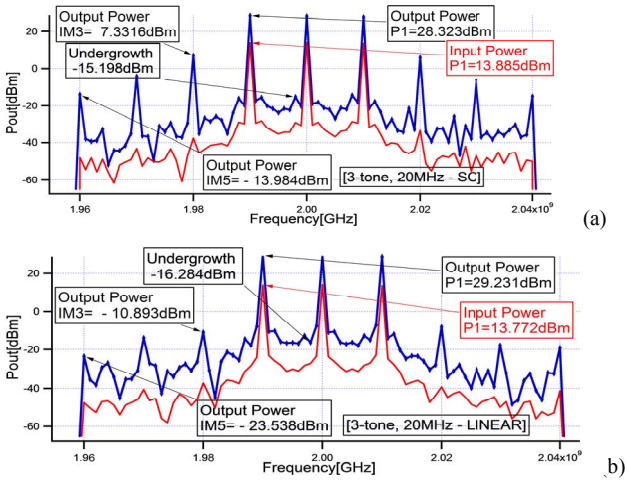

Fig. 12, Measured 20MHz 3-tone Spectrum before (a) and after (b) applying baseband linearization.

This shows that this technique could be important for wide-bandwidth applications like WCDMA, and LTE in minimizing the impact of AM/AM distortion. This concept when coupled with pre-distortion solution could then also address the AM/PM distortion component.

V. CONCLUSION

It has been shown that correctly formulated and implemented baseband injection can provide a solution for linearizing power amplifiers that is insensitive to modulation bandwidth. This has been achieved using a baseband linearization signal to be injected at the output bias port which is computed, irrespective of the complexity of the stimulus signal, using a formulation, generalized in the envelope domain. In this approach the number of linearization coefficient required is small, typical only two, and they are modulation bandwidth invariant. This property was validated in this paper by performing baseband linearization investigations, using just two-linearization coefficients, on a 10W Cree GaN HEMT device driven 1.5 dB into compression with 3-tone modulated signals with increasing modulation bandwidth ranging from 2MHz to 20MHz. However, similar results have been achieved with more complex stimulus up to 9-tone. In all cases distortion was reduced to around -40dB a value very close to the dynamic range of the measurement system. We believe that the technique can be applied to any modulation bandwidth.

REFERENCES

[1] Andrei Grebennikov, “RF and Microwave Power Amplifier Design”. McGraw-Hill ISBN 0-07-144493-9

[2] McIntosh, P.M.; Snowden, C.M., "The effect of a variation in tone spacing on the intermodulation performance of Class A and Class AB HBT power amplifiers," *Microwave Symposium Digest, 1997., IEEE MTT-S International* , vol.2, no., pp.371,374 vol.2, 8-13 June 1997 doi: 10.1109/MWSYM.1997.602811.

[3] John Wood, David E. Root, “Fundamentals of nonlinear behavioral modeling for RF and microwave design”. Artech House, 2005.

[4] J. C. Pedro, N. B. Carvalho, “Intermodulation Distortion in Microwave and Wireless Circuits” Artech House, 2003.

[5] Suadet, A.; Kasemsuwan, V., "A 0.5 V quasi-floating-gate (QFG) inverter-based class-AB gain-bandwidth independent amplifier," *Computer Applications and Industrial Electronics (ICCAIE), 2011 IEEE International Conference on* , vol., no., pp.245,249, 4-7 Dec. 2011, doi: 10.1109/ICCAIE.2011.6162139.

[6] Ogboi, F.L.; et al.; "A LSNA configured to perform baseband engineering for device linearity investigations under modulated excitations," *Microwave Conference (EuMC), 2013 European* , vol., no., pp.684,687, 6-10 Oct. 2013

[7] Akmal, M.; et al.; , "An enhanced modulated waveform measurement system for robust characterization of microwave devices under modulated excitation," *Microwave Integrated Circuits Conference (EuMIC), 2011 European,*vol.,no.,pp.180-183, 10-11 Oct. 2011.

[8] Akmal, M.; et al.; , "Linearity enhancement of GaN HEMT’s under complex modulated excitation by optimizing the baseband impedance environment," *Microwave Symposium Digest(MTT), 2011 IEEE MTT-S International,*vol.,no.,pp.1,4,5-10June, 2011doi:10.1109/MWSYM.2011.5972833

[9] Lees, J.; Williams, T.; Woodington, S.; McGovern, P.; Cripps, S.; Benedikt, J.; Tasker, P., "Demystifying Device related Memory Effects using Waveform Engineering and Envelope Domain Analysis," Microwave Conference, 2008. EuMC 2008. 38th European , vol., no., pp.753,756, 27-31 Oct. 2008, doi: 10.1109/EUMC.2008.4751562.

†Investigation of various envelope complexity linearity under modulated stimulus using a new envelope formulation approach

†F.L. Ogboi, †P.J. Tasker, †M. Akmal, †J. Lees, †J. Benedikt, *S. Bensmida, *K. Morris, *M. Beach, *J. McGeehan

†Centre for High Frequency Engineering, Cardiff University, Cardiff, United Kingdom
*Centre for Communications Research, University of Bristol, Bristol, United Kingdom

Ogboifl2@cardiff.ac.uk

***Abstract* — In [1] a new formulation for quantifying the linearizing baseband voltage signal, injected at the output bias port, to linearize a device behavior was introduced. A key feature of this approach is that since it is formulated in the envelope domain the number of linearization coefficient required is independent of the envelope shape, complexity. This property is validated by performing baseband linearization investigations on a 10W Cree GaN HEMT device. Modulated signals with increasing complexity 3, 5, and 9-tone modulated stimulus, at 1.5dB of compression, were utilized. In all cases just two-linearization coefficients needed to be determined in order to compute the output baseband signal envelope necessary. Intermodulation distortion was reduced to around -50dBc, a value very close to the dynamic range limit of the measurement system.**

***Index Terms* — Distortion, envelope, modulation, waveform engineering, power amplifiers.**

I. Introduction

The linearity behavior of wireless communications systems are usually performance degraded by in-band intermodulation distortion products, namely third and fifth order terms, generated in the active devices used such as transistors (DUT). This is largely due to the non-linear behavior of the DUT as a result of its physics, environment, and connected circuits in its response to both previously and presently applied stimulus. A number of approaches and publications [4, 8] have been suggested and used to suppress/eliminate these with considerable success. In our earlier work [5], baseband investigation focused on 'engineering' the output baseband impedance environment. Such solutions involved presenting constant broadband baseband impedances, targeted at specific IMD components contained in the baseband IMD envelope.

Such solution proved successful for signals with a small number of tones and limited IMD components like the 2-tone case, shown in Fig. 1.

However, as the number of tones in the modulation scale up, 9-tone case is shown in Fig. 2, so does the number of baseband and IMD components with each component resulting in an increasing number of impedances requirements, and hence increasing number of variables to control.

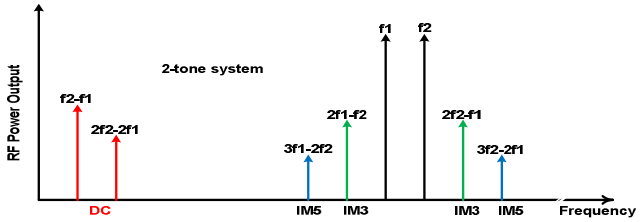

Fig. 1. 2-tone system

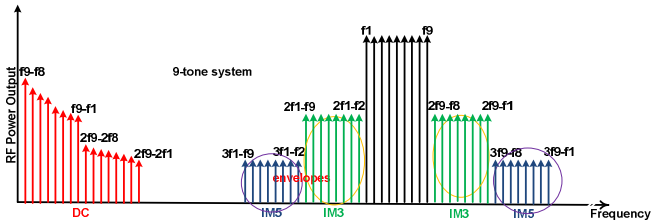

Fig. 2. 9-tone system

The alternative approach introduced in [1], however involves computing the output baseband signal envelope $\hat{V}_{2,bb}$, when targeting the suppression/elimination of the carrier IMD components, using the following equation;

$$\hat{V}_{2,bb}(t) = \sum_{p=1}^{q} \beta_{2p} \left|\hat{V}_{1,rf}(t)\right|^{2p} \quad (1)$$

The advantage of this approach is that it has only a few variables, β_{2p} to control and the number is independent of the RF input envelope shape, $\hat{V}_{1,rf}(t)$. Hence, predicting no increased complexity in the iterative process for determining the optimum linearizing output baseband voltage when moving from the simple 3-tone to the complex 9-tone is expected. This paper validates this envelope complexity insensitivity.

978-1-4799-3622-9/14/$31.00 ©2014 IEEE

II. Measurement System

To investigate this concept, the baseband measurement system described in [1], and shown in Fig. 3, capable of measuring multiple-complex modulated voltage and current waveforms while 'engineering' and injecting intelligent baseband voltage signals into the device, was utilized. For this investigation, a 75W, 10KHz-250MHz wideband baseband amplifier from "Amplifier Research" Model 75A250, was used to engineer the injected baseband voltage. The advantage of this is that we are able to precisely engineer and absolutely control the baseband components associated with this system. The modulated RF time domain terminal voltage and current waveforms were also captured by the measurement system. Hence, it was possible to measure all the necessary dynamic voltage and current envelope behavior at baseband, RF and harmonic frequencies.

This measurement system was vector calibrated to the device package plane using a custom built 50 TRL test fixture, over, precisely 50MHz baseband bandwidth and 100MHz RF bandwidth, for each of the first three harmonics. Stimuli with increasing complexities were measured, using equally spaced tones on a 0.5MHz grid. Using this tone spacing of 0.5MHz, peak to average power ratio (PAPR) for the 3-tone, 5-tone and 9-tone are 4.77dB, 6.99dB and 9.54dB respectively. The fundamental excitation was centered at 2GHz, while delivering a peak envelope power (PEP) of approximately 38dBm for each of the modulation type. The input signal was adjusted in each case to maintain approximately 1.5dB compression and an approximately constant input envelope dynamic voltage swing. The transistor, a 10W Cree GaN HEMT, was biased in class AB, with RF fundamental and all harmonic frequencies terminated into a passive 50 .

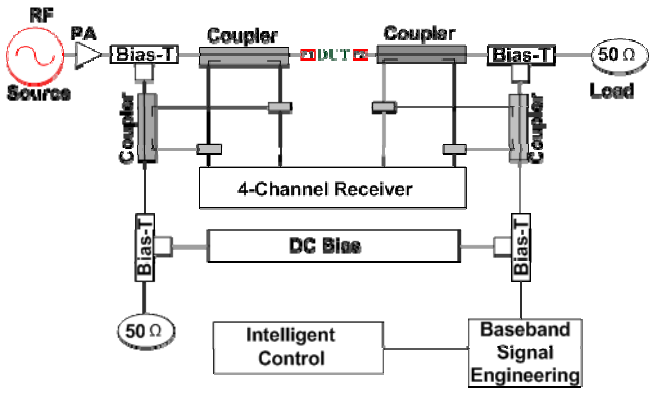

Fig. 3. Baseband waveform engineering and modulated RF measurement system (LSNA).

The drain and gate bias voltages of +28V and -2.08V were used, giving a quiescent drain current of approximately 12% I_{DSS}, for each modulation type. The load condition, although not quite optimal, was considered sufficiently close for this investigation.

III. Linearization Investigation

The transistor inherent non-linearity is observed and measured using the baseband short circuit condition. The RF fundamental dynamic envelope transfer characteristic and the input voltage output current envelopes measured are shown below for the various envelope complexities.

A. Observed transistor inherent non-linearity

Results achieved are shown in Fig. 4, Fig. 5 and Fig. 6, for the 3-tone, 5-tone and 9-tone stimuli. They show considerable distortion produced, as evident in the observed compressed dynamic envelope transfer characteristics.

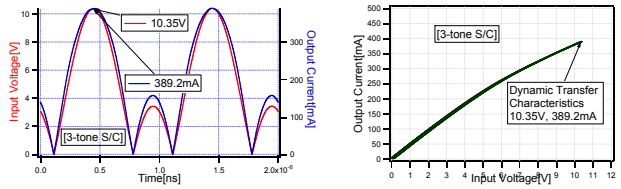

Fig. 4, Measured 3-tone fundamental RF input voltage/output current envelopes and the determined, measured, 3-tone RF fundamental dynamic envelope transfer characteristic for the baseband short circuit condition.

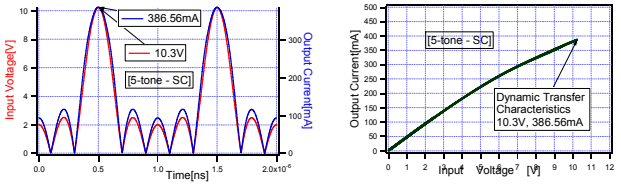

Fig. 5, Measured 5-tone fundamental RF input voltage/output current envelopes and the determined, measured, 5-tone RF fundamental dynamic envelope transfer characteristic for the baseband short circuit condition.

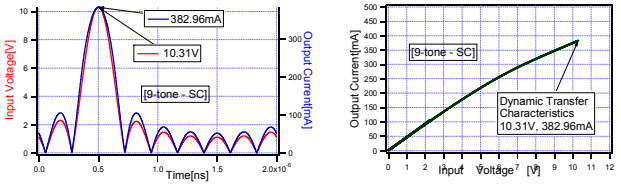

Fig. 6, Measured 9-tone fundamental RF input voltage/output current envelopes and the determined, measured, 9-tone RF fundamental dynamic envelope transfer characteristic for the baseband short circuit condition.

Note that the observed dynamic envelope transfer characteristic can be modeled as follows:

$$\hat{I}_{2,rf}(t) = \sum_{n=0}^{m} \alpha_{2n+1} \left|\hat{V}_{1,rf}(t)\right|^{2n} \hat{V}_{1,rf}(t). \quad (2)$$

where α_1 represents the linear gain of the system, α_3 quantifies the level of third order intermodulation distortion (IMD), α_5 quantifies the level of fifth order intermodulation distortion (IMD), and so on, up to the desired maximum order m. In this case distortion up to fifth order is observed; hence only three terms in (2) are required. Note the insensitivity of these envelope transfer characteristic to the varying stimulus modulation complexity.

B. Applying Baseband Linearization

The formulation, being demonstrated in this paper, and detailed in [1] was now used to 'engineer' the required output baseband stimulus to linearize the transistors dynamic RF transfer characteristic. In this case just two coefficients, β_2 and β_4, need to be optimized to compute the necessary output baseband linearizing stimulus using equation (1). Fig. 7, Fig. 8 and Fig. 9, show the linearized performance achieved. In all cases the device has been successfully linearized. The dynamic envelope transfer characteristics now becoming a straight line through the origin.

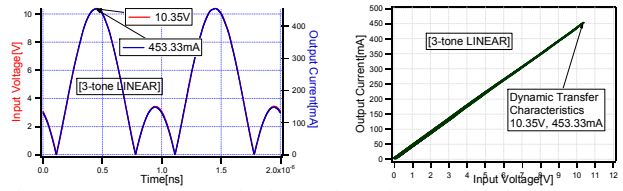

Fig. 7, Measured 3-tone fundamental RF input voltage/output current envelopes confirming that a linear, measured, 3-tone RF fundamental dynamic envelope transfer characteristic can be achieved using an optimized output baseband injection signal.

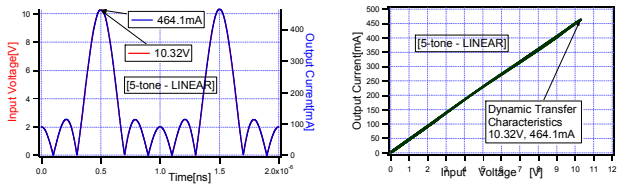

Fig. 8, Measured 5-tone fundamental RF input voltage/output current envelopes confirming that a linear, measured, 5-tone RF fundamental dynamic envelope transfer characteristic can be achieved using an optimized output baseband injection signal.

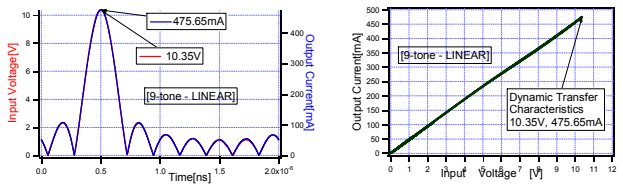

Fig. 9, Measured 9-tone fundamental RF input voltage/output current envelopes confirming that a linear, measured, 9-tone RF fundamental dynamic envelope transfer characteristic can be achieved using an optimized output baseband injection signal..

It is important to note, that in all cases, independent of signal complexity, the determination of the optimized output baseband signal necessary to achieve this linear performance required the determination of just two linearization coefficients, β_2 and β_4. In fact the values of these components was also insensitive to varying stimulus modulation complexity.

IV. Envelope Independence

More traditionally this performance improvement is presented and observed in terms of the elimination of spectral regrowth.

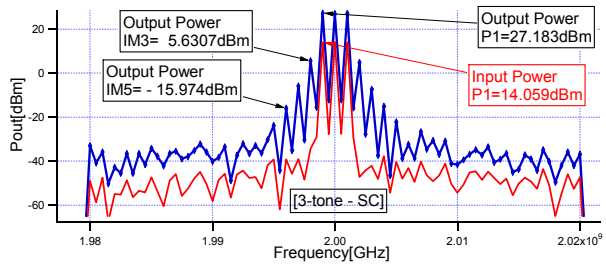

(a)

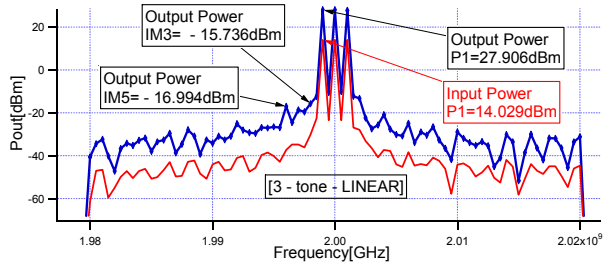

(b)

Fig. 10, Measured 3-tone Spectrum before (a) and after (b) applying baseband linearization.

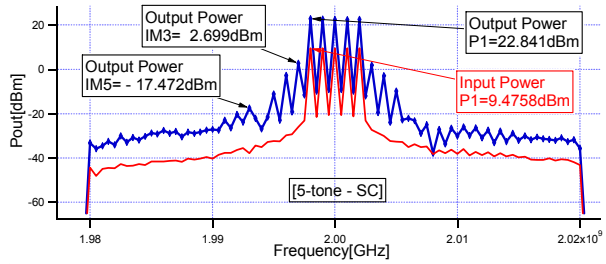

(a)

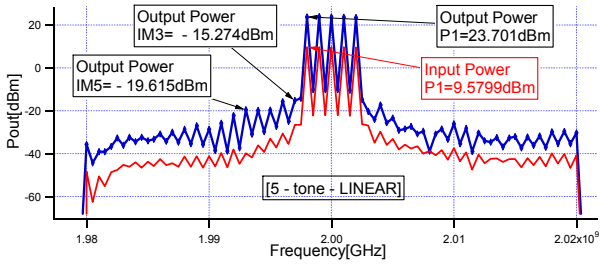

(b)

Fig. 11, Measured 5-tone Spectrum before (a) and after (b) applying baseband linearization.

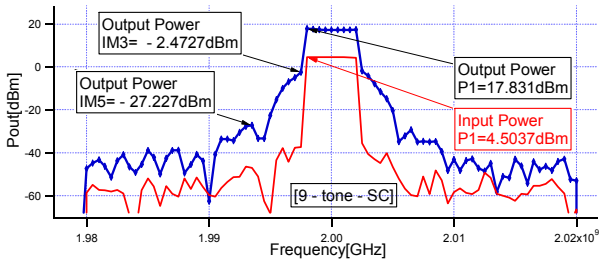

(a)

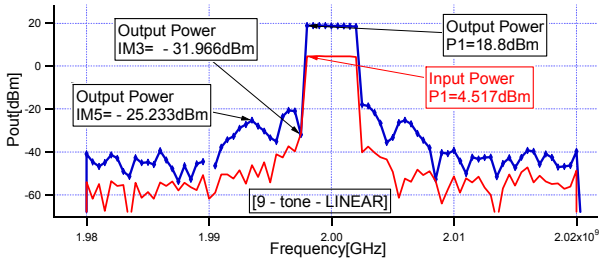

(b)

Fig. 12, Measured 9-tone Spectrum before (a) and after (b) applying baseband linearization.

Fig. 10, Fig. 11 and Fig. 12 show the spectral performance improvements achieved in the case of 3-tone, 5-tone and 9-tone stimulus respectively as a result of linearizing the envelope transfer characteristic.

In all cases a very similar level of improvement is observed. Spectral regrowth, distortion, in all cases is simultaneously reduced to a level around -50dBc, a value we believed is limited more by the dynamic range of the measurement system than the ability of the optimized baseband enveloped derived signal to linearize, and eliminated the AM/AM distortion.

VII. Conclusion

The linearization of the transistor dynamic transfer characteristic via the injection of a correctly formulated baseband signals at the output bias port has been demonstrated. Since the formulation for this signal is defined in the envelope domain it ensures that the number of linearization coefficients are independent of the complexity of the modulated signal. This property was validated with modulated signals of increasing complexity of 3, 5, and 9-tones. In each case a 10W Cree GaN HEMT device was driven 1.5dB into compression generating non-linear behavior up to 5th order system. Irrespective of the signal complexity the device was successfully linearized using just two-linearization coefficients. Distortion was reduced to around -50dBc a value very close to the dynamic range of the measurement system. More work is now planned to use this approach on a real communication signal.

Acknowledgment

This work is supported by EPSRC (grant EP/F033702/1). We also thank CREE for supplying devices and specifically Simon Wood, Ryan Baker and Ray Pengelly.

References

[1] Ogboi, F.L.; Tasker, P.J.; Akmal, M.; Lees, J.; Benedikt, J.; Bensmida, S.; Morris, K.; Beach, M.; McGeehan, J., "A LSNA configured to perform baseband engineering for device linearity investigations under modulated excitations," *Microwave Conference (EuMC), 2013 European* , vol., no., pp.684,687, 6-10 Oct. 2013

[2] Andrei Grebennikov, "RF and Microwave Power Amplifier Design". McGraw-Hill ISBN 0-07-144493-9

[3] Joel Vuolevi and Timo Rahkonen," Distortion in RF Power Amplifiers", Norwood, MA: Artech House, 2003.

[4] Chi-Shuen Leung, Kwok-Keung, M. Cheng, "A new approach to amplifier linearization by the generalized baseband signal injection method," IEEE microwave and wireless components letters, vol. 12, no.9, September, 2002.

[5] Akmal, M.; ,et al "Linearity enhancement of GaN HEMTs under complex modulated excitations by optimizing the baseband impedance environment," *Microwave Symposium Digest (MTT), 2011 IEEE MTT-S International* , vol., no., pp.1,1, 5-10 June 2011, doi: 10.1109/MWSYM.2011.5973183.

[6] Akmal, M.; Ogboi, F.L.; Yusoff, Z.; Lees, J.; Carrubba, V.; Choi, H.; Bensmida, S.; Morris, K.; Beach, M.; McGeehan, J.; Benedikt, J.; Tasker, P.J., "Characterization of electrical memory effects for complex multi-tone excitations using broadband active baseband load-pull," *Microwave Conference (EuMC), 2012 42nd European* , vol., no., pp.1265,1268, Oct. 29 2012-Nov. 1 2012

[7] Yusoff, Z.; Lees, J.; Benedikt, J.; Tasker, P.J.; Cripps, S.C., "Linearity improvement in RF power amplifier system using integrated Auxiliary Envelope Tracking system," *Microwave Symposium Digest (MTT), 2011 IEEE MTT-S International* , vol., no.,pp.1,4,5-10June2011doi: 10.1109/MWSYM.2011.5972769

[8] Reynolds, J., "Nonlinear distortions and their cancellation in transistors," Electron Devices, IEEE Transactions on , vol.12, no.11, pp.595,599, Nov 1965, doi: 10.1109/T-ED.1965.15615

Characterization of Electrical Memory Effects for Complex Multi-tone Excitations using Broadband Active Baseband Load-pull

M. Akmal[†], F. L. Ogboi[†], Z. Yusoff[†], J. Lees[†], V. Carrubba[†], H. Choi[†], S. Bensmida[*], K. Morris[*], M. Beach[*], J. McGeehan[*], J. Benedikt[†], P. J. Tasker[†]

[†]Cardiff School of Engineering, University of Cardiff, The Parade, Cardiff, CF24 3AA, Wales, UK

AkmalM1@Cardiff.ac.uk

[*]Centre for Communications Research, University of Bristol, Woodland Rd, Bristol, BS8 1UB, UK

Abstract— **This paper focuses on multi-tone characterization of baseband (IF) electrical memory effects and their reduction through the application of complex-signal, active baseband load-pull. This system has been implemented to allow the precise evaluation of intrinsic nonlinearity in high-power microwave devices for wideband applications. The developed active baseband load-pull capability allows a constant, frequency independent baseband load environment to be presented across wide modulation bandwidths, and this capability is important in allowing the effects of baseband impedance variation on the performance of nonlinear microwave devices, when driven by broadband multi-tone stimuli, to be fully understood. The experimental investigations were carried out using a 10 W GaN HEMT device, under 9-carrier complex modulated excitation. These confirmed that presenting a wideband baseband short circuit was essential for maximum ACPR suppression together with the minimization of ACPR asymmetry, confirming the importance of proper termination of baseband frequency components when designing DC bias networks.**

***Index Terms*—Active load-pull, baseband, memory effects, adjacent channel power ratio, power amplifiers.**

I. INTRODUCTION

The linearity and specifically the adjacent channel power ratio (ACPR) of a power amplifier (PA) is affected, not only by the impedance presented to the device at the fundamental and higher harmonic frequencies, but also at baseband frequencies [1-3]. In this work, the baseband frequencies are defined as those associated with the modulating signals and, in the case of a system excited by a multi-tone stimulus, the frequency difference between the individual excitation tones. The impedances presented to the device at these 'difference' frequencies, hereafter will be referred to as baseband or IF impedances, and in a practical PA, these are usually determined by the bias insertion and video by-pass networks. Non-ideal behavior in these physical circuits create time constants that are much larger than the period of the microwave frequencies being amplified and these in turn result in increased and frequency dependent distortion in microwave power devices [4]. Non-ideal baseband impedance significantly affects the level of ACPR, and invariably causes asymmetry between the upper and lower ACPR levels. These phenomena are attributable to the baseband memory effect, which is one of the major contributors to electrical memory effects [4-7]. For example, in a typical PA, the ACPR levels measured with a modulation frequency of 10 MHz can be significantly different from those measured with a modulation frequency of 100 kHz. The ability to successfully design PAs for future wireless communication systems that minimize the effects of such distortion sources relies largely on accurate characterization of microwave power devices under realistic multi-sine stimulus. In reality, and in response to a multi-tone stimulus, the baseband frequency spectrum will consists of not only the significant baseband components IF1 (the modulation frequency) and IF2 (twice the modulation frequency), but also the higher baseband components IF3 and IF4, etc. If these higher-order baseband current components are uncontrolled and allowed to terminate into arbitrary impedances, significant baseband voltage ripple will result, and device linearity measurements will become difficult to interpret. This presents a serious measurement issue when investigating bandwidth dependent baseband electrical memory effects as it is not sufficient to suppress only the significant baseband components but also the higher components. This is indeed critical for realistic modulated excitations, which will result in baseband components that will extend from DC to many tens of MHz. It also highlights that bandwidth dependent baseband electrical memory is an important problem that needs investigation, in order to pave the way for the development of future communication systems with much increasing modulation bandwidths.

To quantify the persistent influence of baseband electrical memory effects on the ACPR performance of microwave device, the baseband impedance environment needs to be optimized in a controlled way, and is achieved in this work through the application of broadband active IF load-pull. This paper demonstrates the application of the multi-tone measurement system reported in [8] that has accelerated device characterization through the adoption of new measurement technique referred to as "Time Domain Partitioning". This paper also details an improved baseband load-pull architecture that has, for the first time been employed in achieving a broadband baseband impedance termination in response to a complex, 9-tone modulated excitation. Furthermore, the importance of reducing baseband electrical memory effects is demonstrated by controlling the significant baseband components (IF1 and IF2) as well as the higher baseband components (IF3 and IF4) in response to the

multi-sine stimulus. Through measurements, a link has been established that shows how higher baseband components, if not suitably terminated in addition to significant baseband components, are instrumental in the generation of bandwidth dependent baseband electrical memory effects.

II. Broadband Baseband Load-pull Capability

In order to characterize and understand bandwidth dependent electrical memory effects, a measurement system was developed [9-11], capable of presenting specific baseband impedances to a limited number, in this case two, of the most significant baseband components (IF1 and IF2), generated as a result of 2-tone excitation. In order to limit the number of baseband tones generated, the device was driven only moderately, remaining in a relatively linear region of its characteristic, 1dB below the 1dB compression point. When the device was driven more deeply into compression, significantly more mixing terms were generated resulting in significantly more baseband frequency components, and these, when terminated into uncontrolled impedances, significantly degraded the measurement accuracy. In order to overcome this problem, and achieve a sufficiently broadband IF termination, significant modification of the baseband load-pull measurement system was required to both accurately account for higher baseband harmonics, as well as allow the device to be driven into higher, representative levels of compression. This additional functionality is now achieved in the time domain, using a single arbitrary waveform generator (AWG) to synthesize the necessary waveforms to allow a constant and specific baseband impedance environment to be maintained across a wide bandwidth. In response to multi-tone excitation, the AWG generates baseband components that are multiples of the baseband fundamental frequency.

The instrument configuration used to generate the necessary arbitrary waveforms is shown in Fig. 1, and illustrates the triggering arrangement, and how the 10 MHz reference synchronization is employed. A separate triggering AWG is used which is necessary because without the external trigger, the AWG loses phase coherence between the modulation and the other baseband signals when it is re-initiated to generate the arbitrary waveform. This then allows the AWG to generate the precise arbitrary waveform with the required amplitude and 'shape' and for this waveform to be aligned in phase with the modulation envelope. The simple equation (1) is used to generate the resultant arbitrary waveform containing all the frequency components at baseband frequencies.

$$V(t) = A_n \sum_{n=1}^{\infty} \mathrm{Cos}(2\pi f_c nt + n\varphi) . \qquad (1)$$

Where A is the amplitude in volts, 'n' refers to the harmonic of the fundamental baseband component (IF1), 't' is time in seconds (the horizontal axis), 'V' is the voltage (the vertical axis), and 'f_c' is the frequency in Hz, 'φ' is the phase of the individual harmonics. The magnitude and relative phase for these will change when different baseband components are load-pulled to different loads. To create an arbitrary waveform of the highest resolution, it is critical to use the entire vertical dynamic range of the AWG in defining amplitude. The desired relative magnitude and phase of the individual baseband components are firstly defined in the frequency domain, and then converted to the time domain using an inverse Fourier transform (IFFT). The amplitude of the resulting synthesized waveform (not the individual tones) is then scaled to ensure that when it is downloaded to the AWG, it occupies all of the available vertical resolution. The fundamental frequency of the AWG is then set and the trigger derived from triggering AWG. Load-pull is then achieved by careful manipulation of the magnitude and phase of each individual baseband components, and this is achieved by repeating the above process and retriggering. For example, the synthesized arbitrary waveform that results when all the baseband frequency components have the same magnitude and phase is shown in Fig. 2. This waveform is downloaded to the volatile memory of the AWG through a GPIB bus.

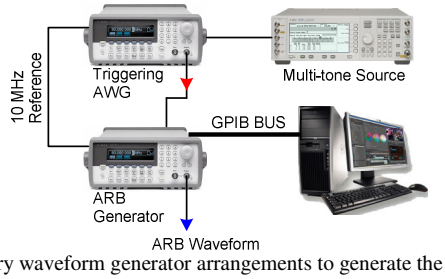

Fig. 1 Arbitrary waveform generator arrangements to generate the IF signal.

The AWG will always replicate the finite-length time record to produce a periodic version of the data in the waveform memory and play it continuously. Care needs to be taken however, as it is possible that the shape and phase of a signal may be such that a discontinuity may be introduced at the end of one cycle. When the wave shape is repeated continuously, this end-point discontinuity will introduce leakage errors in the frequency domain because many spectral terms are required to describe the discontinuity. It is important to create arbitrary waveforms as a single period or as multiple periods and avoid a discontinuity.

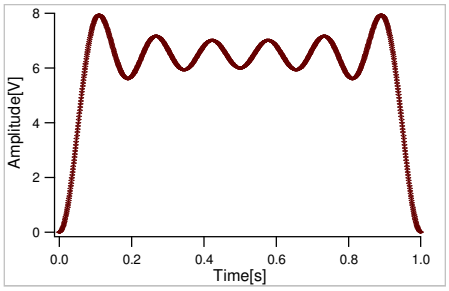

Fig. 2 An example of the AWG synthesized time domain signal used to load-pull the first four baseband components.

The maximum output frequency is typically limited by the bandwidth of the AWG. The AWG outputs the entire arbitrary waveform at the specified rate, synchronized to the modulated waveform being generated by the modulated microwave source. When a downloaded arbitrary waveform contains harmonics of the fundamental IF1 component, care has to be taken to ensure the actual output frequency content does not exceed the maximum for the AWG used. For instance, if a waveform is defined as 10 cycles of a sine wave and is output at a fundamental frequency of 2 MHz, the actual frequency will be 20 MHz, 2 MHz above the maximum frequency of the

AWG. To combat this problem, an anti-aliasing filter is used to smooth the voltage quantization steps and to create the final waveform. When using multiple cycles in an arbitrary waveform, especially at high frequencies, the final result may be attenuated. The example time domain signal depicted in Fig. 2 is used to drive a suitable baseband PA to load-pull the increased amplitude baseband components that are generated when a power device is driven into deep compression.

III. Multi-Tone Measurements and Investigations

The following measurements were carried out to demonstrate the capability of the enhanced active IF load-pull system, using a CREE CGH40010 discrete 10 W GaN HEMT device, characterized at center frequency of 2 GHz with a 2 MHz modulation frequency. The system was fully vector-error corrected and can therefore account for any errors introduced due to losses, mismatches, imperfect directivities and delay in the system, thus allowing the measurement of the complete modulated voltage and current waveforms and impedances that are presented at the input and output of the DUT. The device was class AB biased at a drain voltage of 28 V and a gate voltage of -2.5 V, resulting in a quiescent current of 250 mA. The RF components were terminated into a nominal 50Ω, close to the optimum impedance for this device. The input stimulus composed of nine equally spaced tones with peak-to-average power ratio of 9.54 dB, all of equal amplitude but random phases to emulate to some extent, a realistic wideband signal [12]. During measurements, this 10W device delivered 39.5 dBm peak envelope power (PEP) when driven approximately 1.5 dB into compression and active IF load-pull was used to present the constant baseband impedance to IF1 through IF4.

The contours of $ACPR_L$ and $ACPR_H$ were found to be identical and here only contours of $ACPR_L$ are plotted for simplicity. Fig. 3 depicts the contours of $ACPR_L$ that result when the baseband impedance is swept (all impedance components together) over a well defined grid, to find the optimum impedance for reduction of memory effects, This is obviously important as the linearizability of memory-less device is much better than the devices with memory [12-13]. The significant observation to note is that there are pronounced ACPR variations around the measurement grid. These measurements suggest that the optimum baseband load for minimum asymmetry is located at the short circuit, at point-A, where an approximate 12 dB improvement in ACPR is observed in comparison with point-B. This observation confirms, perhaps unsurprisingly the strong dependence of ACPR on the baseband impedance termination. Fig. 4 shows the output spectra observed by the measurement system, for both point-A and point-B. Terminating the baseband components at point-B emulates a large degree of electrical memory, causing a significant ripple to appear on the DC drain voltage present at the device output plane, which effectively results in a re-modulation of the RF signal. This, then, leads to the change in the ACPR levels and it can be seen that this enforced memory effect results in more than 6 dB of ACPR asymmetry between upper and lower ACPR products, as well as significant distortion of the in-band tones. For the case when the optimum short circuit impedance is maintained constant and presented to the baseband components, at modulation frequency of 1 MHz, there is no baseband electrical memory effect, so the spectral regrowth around in-band components shows no asymmetry.

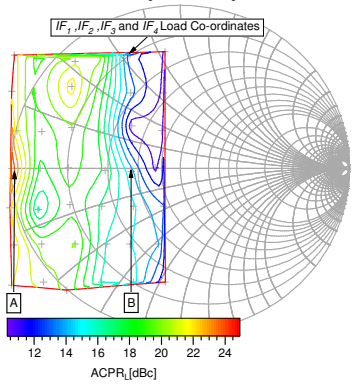

Fig. 3 Baseband load-pull characterization of 10 W GaN HEMT under multi-tone stimulus for optimum $ACPR_L$ as a function of baseband impedance.

The measured output RF voltage envelopes obtained for the two baseband impedance conditions, are shown in Fig. 5. In the case of baseband impedance at point-B, an asymmetrical envelope is clearly observed, and this in turn results in asymmetrical ACPR products. Whilst terminating the baseband components at point-A, which has been demonstrated to be the optimum load termination, an undistorted output envelope is produced.

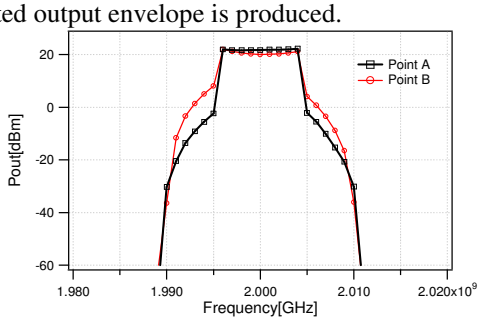

Fig. 4 Measured output spectrum, when different impedances were provided to baseband components with nominal 50 Ω RF termination.

The dynamic transfer characteristics obtained for the two cases of Γ_{IF} are depicted in Fig.6. In the case where the baseband impedance presented to the transistor's output is not a short circuit, the output RF current envelope becomes asymmetrical, and when plotted against the input voltage, appears as hysteresis in the V_{in}-I_{out} dynamic transfer characteristic. However, when short circuit impedance (Γ_{IF} =1∠180°) was maintained, then negligible hysteresis was observed. The broadband, baseband short circuit impedance termination was thus utilized as shown in Fig. 7, for modulation frequency ranging from 0.5 MHz to 7 MHz, in order to achieve the symmetrical ACPR response. The magnitude of the IF reflection coefficient could not be brought precisely to a short circuit for frequency components above 10 MHz due to the bandwidth limitations of baseband load-pull PA. For example, the third harmonic of 6 MHz at 18 MHz could not be adequately controlled, resulting in the dispersed load observed in the following Smith chart. Figure 8 shows

how the fundamental output power remains constant and independent of the modulation frequency. With regard to the ACPR distortion $ACPR_L$ and $ACPR_H$, it is clear that the symmetry level of ACPR is degraded at a higher modulation frequency after 5 MHz and this is due to impedance variations in higher baseband components (IF3 and IF4), as shown in Fig. 8. It is important to note that the observed variations in $ACPR_L$ and $ACPR_H$ magnitude observed below 1 MHz are not related to variations in baseband impedance and attributable to other sources of memory.

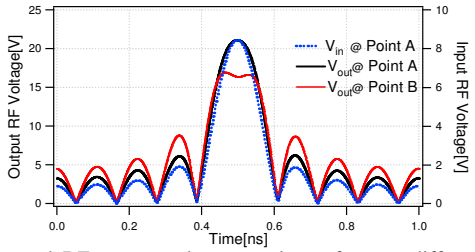

Fig. 5 Measured RF output voltage envelopes for two different baseband impedance environment at 2 MHz modulation frequency.

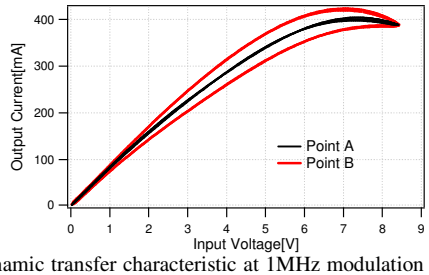

Fig. 6 Dynamic transfer characteristic at 1MHz modulation frequency for the two different baseband loads (Γ_{IF}) identified in Fig. 3.

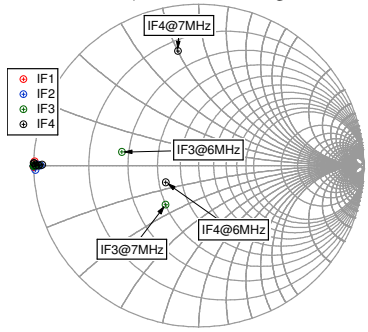

Fig. 7 Measured IF1, IF2, IF3 and IF4 for modulation frequency ranging from 0.5 MHz to 7 MHz.

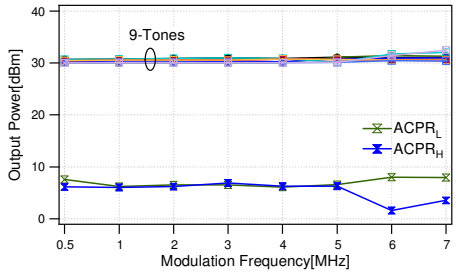

Fig. 8 Measured fundamentals and ACPR power for different modulation frequencies.

IV. CONCLUSION

This paper has detailed the implementation of a broadband active IF load-pull capability for the robust characterization of bandwidth dependent memory effects. This capability, when integrated with the enhanced waveform measurement system [8] has enabled the measurement and characterization of baseband electrical memory effects under complex, multi-tone stimuli. The 9-tone measurements noticeably show the effect of the baseband impedance variations on the behavior of a 10 W GaN HEMTs, in terms of ACPR behavior and induced ACPR asymmetry. The suppression of baseband electrical memory has been achieved by simultaneously engineering the impedance presented to the most significant IF components (IF1 and IF2) and higher order IF components (IF3 and IF4) which emphasizes the fact that, in order to achieve the frequency independent response and complete suppression of electrical memory effects, the baseband impedance environment needs to be engineered to accommodate termination of frequency components of at least eight times of the modulation frequency. The results also highlight optimum IF impedance terminations that minimize overall in-band distortion. This important observation then in turn enables an accurate design of PA bias networks, as well as an understanding of the effects they can cause.

REFERENCES

[1] S. C. Cripps, RF Power Amplifier for Wireless Communication, 2nd edition, Artech House Publishers, 2006.

[2] Alghanim, A;Less, J.; Williams, T.; Benedikt, J.; Tasker, P. "Reduction of electrical base-band memory effects in high-power LDMOS Devices Using Optimum Termination for IMD3 and IMD5 using active load-pull", in Proc., IEEE International Microwave Symposium, June2008.

[3] M. D. LeFevre, D. W. Runton, C. T. Burns, M. K. Mellor, "Digital Predistortion from an RF Perspective", 2010 IEEE Topical Symposium on Power Amplifiers for Wireless Communications, September 2010.

[4] Joel Vuolevi and Timo Rahkonen, "Distortion in RF Power Amplifiers," Norwood, MA: Artech House, 2003.

[5] J. Vuolevi, J. Manninen, T. Rahkonen, "Cancelling the memory effects in RF power amplifiers", in IEEE International Circuits and Systems Symposium, 2001, pp. 57–60.

[6] J. F. Sevic, K. L. Burger, M. B. Steer, "A Novel Envelope Termination Load-pull Method for ACPR Optimization of RF/Microwave Power Amplifiers", in IEEE MTT-S International Microwave Symposium Digest, 1998, pp. 723–726.

[7] N. B. de Carvalho, J. C. Pedro, "A comprehensive explanation of distortion sideband asymmetries," IEEE Trans. Microwave Theory Techniques, September 2002, vol. 50, pages. 2090–2101.

[8] M. Akmal, et al, "An Enhanced Modulated Waveform Measurement System for Robust Characterisation of Microwave Devices under Modulated Excitation", in Proc. of 41st European Microwave Conference (EuMC), October 2011.

[9] A. Alghanim, J. Lees,T. Williams, J. Benedikt, P.J. Tasker, P "Using active IF load-pull to investigate electrical base-band induced memory effects in high-power LDMOS transistors," in Proc. Asia-Pacific Microwave Conference, 2007, 11-14 Dec. 2007 Page(s):1 - 4.

[10] M. Akmal, et al, "The Impact of Baseband Electrical Memory Effects on the Dynamic Transfer Characteristics of Microwave Power Transistors", in Proc. of 4th International Nonlinear Microwave Monolithic Integrated Circuit(INMMIC), April 2010, pages: 148 - 151.

[11] J. Lees, et al, "Demystifying Device Related Memory Effects Using Waveform Engineering and Envelope Domain Analysis", in Proc. 38th European Microwave Conference, October 2008, pages:753-756.

[12] M.Akmal, "An Enhanced Modulated Waveform Measurement System" Ph.D. thesis, Cardiff University, November 2011.

[13] J. P. Martins, P. M. Cabral, N. B. Carvalho,J. C. Pedro, "A Metric for the Quantification of Memory Effects in Power Amplifiers", Microwave Theory and Techniques, IEEE Transactions on Microwave Theory and Techniques, December 2006, vol.54, pages: 4432-4439.